



All Theses and Dissertations

2017-08-01

Electrophilic Catalysis Using Heterobimetallic Complexes

Whitney Kaye Walker
Brigham Young University

Follow this and additional works at: <https://scholarsarchive.byu.edu/etd>

 Part of the [Chemistry Commons](#)

BYU ScholarsArchive Citation

Walker, Whitney Kaye, "Electrophilic Catalysis Using Heterobimetallic Complexes" (2017). *All Theses and Dissertations*. 6962.
<https://scholarsarchive.byu.edu/etd/6962>

This Dissertation is brought to you for free and open access by BYU ScholarsArchive. It has been accepted for inclusion in All Theses and Dissertations by an authorized administrator of BYU ScholarsArchive. For more information, please contact scholarsarchive@byu.edu, ellen_amatangelo@byu.edu.

Electrophilic Catalysis Using Heterobimetallic Complexes

Whitney Kaye Walker

A dissertation submitted to the faculty of
Brigham Young University
in partial fulfillment of the requirements for the degree of

Doctor of Philosophy

David J. Michaelis, Chair
Merritt B. Andrus
Matthew C. Asplund
Daniel H. Ess
Roger G. Harrison

Department of Chemistry and Biochemistry

Brigham Young University

Copyright © 2017 Whitney Kaye Walker

All Rights Reserved

ABSTRACT

Electrophilic Catalysis Using Heterobimetallic Complexes

Whitney Kaye Walker

Department of Chemistry and Biochemistry, BYU

Doctor of Philosophy

Conventional ligand design in transition metal catalysis capitalizes on the ability of phosphorous, nitrogen, carbon, oxygen, and sulfur-based donors to modify the steric and electronic properties of a reactive metal center. Heterobimetallic transition metal complexes that contain a dative metal-metal bond provide a unique approach to ligand design where the reactivity of the metal center can be modified by metal-metal electronic communication. Our laboratory is interested in using the unique properties of heterobimetallic complexes to address significant limitations in current transition metal catalysis.

My PhD work has focused on the ability of early/late transition metal heterobimetallic complexes to facilitate catalysis by speeding up reductive processes that occur at the late transition metal center. My initial studies were aimed at understanding the importance of the metal-metal interaction to catalysis in allylic amination reactions catalyzed by Pd-Ti heterobimetallic complexes and the potential of these catalysts to enable reactivity with challenging nitrogen nucleophiles.

We also explored the substrate scope of the allylic amination with a variety of hindered amines and allylic chloride substrates under mild conditions. Aminations of this type have previously been shown to require harsh reaction conditions and tend to give low yields. A variety of sterically hindered secondary amine nucleophiles were able to readily undergo allylic substitution. Many of these aminations were complete within ten minutes. A series of allylic electrophiles were also shown to undergo the reaction. We have also looked at the ability of hindered amines to undergo intramolecular cyclizations to produce pyrrolidine and piperidine products.

My continuing efforts in the laboratory are focused on developing chiral titanium-phosphinoamide ligands for enantioselective heterobimetallic catalysis. We have synthesized a series of chiral diamine-based phosphinoamide-titanium ligands in order to investigate enantioselective intramolecular aminations. Importantly, each of these new Ti-ligands enables room temperature catalysis in intramolecular aminations with hindered amines, suggesting contributions by the Ti center. Similar reactivity has not been achieved with monometallic chiral Pd catalysts in our lab. Importantly, many of these ligands enable modest enantioselectivity in the allylic aminations.

Keywords: heterobimetallic, catalysis, allylic aminations, enantioselective

ACKNOWLEDGEMENTS

I am very thankful for all of the support and encouragement that I have received during my time at Brigham Young University, especially from my advisor Dr. Michaelis, who was always willing to help and push me to do my best. I am grateful for the help given to me by my committee members and for all of their patience. I am also grateful to my coworkers in the Michaelis lab, particularly Ryjul Stokes and Mike Talley for always keeping me on my toes. I also appreciate all of the computational work that members of the Ess lab provided. Most of all I am thankful for all of the love and support I have received from my family.

TABLE OF CONTENTS

TITLEPAGE.....	i
ABSTRACT.....	ii
ACKNOWLEDGEMENTS.....	iii
TABLE OF CONTENTS.....	iv
LIST OF TABLES.....	vii
LIST OF FIGURES.....	viii
Chapter 1.....	1
1.1 INTRODUCTION.....	1
1.2 METAL-METAL BONDS USED IN REDOX PROCESSES.....	3
1.2.1 Oxidative Reactions That Break the Metal-Metal Bond.....	4
1.2.2 Metal-Metal Bond Formation From Oxidative Addition.....	5
1.2.3 Oxidative Additions at a Metal-Metal Multiple Bond.....	6
1.2.4 Oxidative Addition at a Metal-Metal Bond with Redox Activity at the Ligand.....	7
1.3 REACTIONS INVOLVING EACH DISTINCT METAL CENTER.....	8
1.3.1 Ru/Mn Complex for Carbon-Carbon Bond Formation.....	8
1.3.2 Zr/Ru Complex for Dehydrogenation of Dimethylamine-Borane.....	9
1.3.3 Zr/M Complex for Ethylene Polymerization.....	10
1.3.4 Ti/Rh Complex for Hydroacylation.....	11
1.4 CATALYSTS WITH METAL-METAL BONDS THAT REMAIN INTACT.....	12
1.4.1 Carbene Transfer Reaction with a Dirhodium Catalyst.....	12
1.4.2 Ru ₂ Allenylidene Intermediates for Propargylic Substitution.....	13
1.4.3 Alkene Hydrogenation with Early/Late Heterobimetallic Catalyst.....	14
1.4.4 Allylic Substitution with Pd/Ti Heterobimetallic Complex.....	15
1.4.5 Nickel Catalyzed Hydrogenation Utilizing Dative Interactions.....	16
1.4.6 Zr/Co Catalyzed Hydrosilylation.....	17
1.5 CONCLUSION.....	18
1.6 REFERENCES.....	20
Chapter 2.....	24
2.1 INTRODUCTION.....	24
2.2 RESULTS AND DISCUSSION.....	26

2.2.1 Optimization Studies of Allylic Aminations with Hindered Amine Nucleophiles	26
2.2.2 In Situ Formation of Heterobimetallic Complex	28
2.2.3 Synthesis and Reactions of Titanium Phosphinoamide Ligands	29
2.2.4 Substrate Scope and Reactivity of Secondary Hindered Amines	31
2.2.5 Intramolecular Aminations	33
2.3 CONCLUSION	33
2.4 REFERENCES	35
Chapter 3	40
3.1 INTRODUCTION	40
3.2 RESULTS AND DISCUSSION	42
3.2.1 Computational Assessment of Heterobimetallic Pd-Ti Complex 1 and Mechanism for Allylic Amination	42
3.2.2 Experimental and Computational Evaluation of the Impact of Replacing TiCl ₂ to Remove the Pd-Ti Interaction	48
3.2.3 Impact of Coordination Angle and Electronic Effects on Catalysis	50
3.2.4 Testing the Limits of the Pd-Ti Interaction	52
3.3 CONCLUSION	55
3.4 REFERENCES	56
Chapter 4	65
4.1 INTRODUCTION	65
4.2 RESULTS AND DISCUSSION	66
4.2.1 Optimization of Pt-catalyzed Cycloisomerizations	66
4.2.2 Substrate scope for Pt-catalyzed cycloisomerization reactions	70
4.2.3 Influence of reaction selectivity by ligand modification	72
4.3 CONCLUSION	73
4.4 REFERENCES	75
Chapter 5	78
5.1 INTRODUCTION	78
5.2 RESULTS AND DISCUSSION	80
5.2.1 Synthesis of Chiral Titanium Ligands	80
5.2.2 Enantioselective Intramolecular Aminations	82
5.3 CONCLUSION	83
5.4 REFERENCES	84

Chapter 6.....	85
6.1 SUPPORTING INFORMATION FOR CHAPTER 2	85
6.1.1 General Information	85
6.1.2 Intramolecular Allylic Aminations with Ti-Pd Complex 1	86
6.1.3 Control Studies	93
6.1.4 Synthesis of Titanium-containing Ligands 12 and 13	94
6.1.5 Synthesis of Alcohol Substrates for Intramolecular Aminations	96
6.1.6 Intramolecular Amination Reactions.....	99
6.1.7 Spectral Images.....	105
6.2 SUPPORTING INFORMATION FOR CHAPTER 3	132
6.2.1 General Information	132
6.2.2 Synthesis of Bisphosphinepalladium methyl triflate Complexes	133
6.2.3 Allylic Amination Rate Studies.....	139
6.2.4 Observation of Catalytic Intermediates	141
6.2.5 XYZ Coordinates and Absolute Energies	142
6.2.6 Spectral Images.....	142
6.3 SUPPORTING INFORMATION FOR CHAPTER 4	161
6.3.1 General Information	161
6.3.2 Synthesis of Trichlorotitanium N-tert-butyl(diphenylphosphino)amide.....	161
6.3.3 Experimental Procedures	162
6.3.4 ³¹ P NMR Studies	165

LIST OF TABLES

Table 2.1: Optimization Studies of Allylic Aminations with 3	27
Table 2.2. Substrate Scope with Hindered Amines	32
Table 3.1. Reactivity Comparison for Monometallic Pd-Catalyzed Allylic Aminations	51
Table 3.2. Reactivity of Sterically Hindered Amine 13.....	53
Table 4.1. Optimization of Pt-catalyzed Cycloisomerization.....	69
Table 4.2. Substrate Scope for Pt-catalyzed Cycloisomerization.....	71
Table 4.3. Optimization of Product Selectivity	73

LIST OF FIGURES

Figure 1.1. Bimetallic active sites of oxygen activation enzymes.....	2
Figure 1.2. Electron withdrawing effects of a second metal center.....	3
Figure 1.3. Oxidative addition reactions across a Zr-Ir metal-metal bond.....	4
Figure 1.4. Binuclear oxidative addition across a Fe-Cu metal-metal bond.....	5
Figure 1.5. Metal-metal bond formation through oxidative addition.....	6
Figure 1.6. Multiple metal-metal bonds undergo oxidative addition.....	7
Figure 1.7. Ni(I)-Ni(I) complex with ligand-centered redox activity.....	8
Figure 1.8. Proposed Ru/Mn mechanism for epoxide/CO ₂ coupling.....	9
Figure 1.9. Proposed mechanism for the Zr/Ru catalyzed amine-borane dehydrogenation.....	10
Figure 1.10. Polymerization catalyst containing Zr/M.....	11
Figure 1.11. Ti/Rh catalyst used in the hydroacylation.....	11
Figure 1.12. Rh ₂ and Rh/Bi catalysts used for styrene cyclopropanation.....	13
Figure 1.13. Ru ₂ (allenylidene) intermediate used for propargylic substitution.....	14
Figure 1.14. Proposed mechanism of a Ta/Ir catalyzed ethylene hydrogenation.....	15
Figure 1.15. Catalytic activity of a Pd/Ti complex and its monometallic analogue.....	16
Figure 1.16. Ni-catalyzed hydrogenation of styrene.....	17
Figure 1.17. Ketone hydrosilylation catalyzed by a Zr/Co complex.....	18
Figure 2.1. Stoichiometric allylic amination with complex 1 and monometallic Pd analogue....	25
Figure 2.2. <i>In situ</i> formation of heterobimetallic catalyst 1.....	29
Figure 2.3. Novel titanium-containing ligands. Hydrogens omitted for clarity.....	29
Figure 2.4. Allylic aminations using different Ti ligands.....	30
Figure 2.5. Intramolecular aminations for heterocycle synthesis.....	33
Figure 3.1. Amination of methallyl chloride using catalyst 1.....	41
Figure 3.2. Stochastic Studies Previously Reported for Reductive Amine Addition.....	41

Figure 3.3. Calculated mechanism for allylic amination catalyzed by 1 (kcal/mol)	43
Figure 3.4. (Left) M06 free energy landscape for Et ₂ NH reductive addition and methallyl chloride-induced Pd ⁰ to Pd ^{II} oxidation. ωB97X-D free energy values given in parentheses. Free energies in kcal/mol. (Right) Transition-state structures. Bond lengths reported in Å.	44
Figure 3.5. Possible alternative species involved in catalysis	45
Figure 3.6. Boat and flat conformations of catalyst 1	46
Figure 3.7. Comparison of allylic amination M06 free energy landscapes catalyzed by 1 (boat) and 1 (flat) (kcal/mol)	47
Figure 3.8. Comparison of ground-state boat conformations and corresponding reactivity for <i>N</i> - ^t Bu and <i>N</i> -Me	48
Figure 3.9. Ethylene bridged bidentate phosphinoamine Pd-Ti complex.....	49
Figure 3.10. Reactivity of complex 1 and 6 in the allylic amination reaction.....	49
Figure 3.11. Allylic amination using allyl acetates and 13 catalyzed by 1.....	55
Figure 4.1. Ligands used for Pt-catalyzed cycloisomerization reactions.....	66
Figure 5.1. Intramolecular aminations for heterocycle synthesis.....	79
Figure 5.2. Chiral Ti ligands and crystal structures.....	81
Figure 5.3. Reaction scheme for BINAM-derived Ti ligand.....	82
Figure 5.4. Intramolecular aminations using chiral titanium ligands.....	83

Chapter 1

Utilizing Metal-Metal Bonds in Organic Transformations

1.1 INTRODUCTION

The field of homogeneous transition metal catalysis has been extremely successful within the last fifty years. This success is due to the ability of supporting ligands to tune the steric and electronic properties of the metal. The reactivity of these organometallic complexes is often facilitated by the ligands ability to σ -donate and π -accept electrons. In recent years we have seen the emergence of “inorganic ligands” which introduce a second transition metal within the first coordination sphere of the catalytic metal and enhance the electronic tuning of the metal center.

Metal-metal interaction within a bimetallic complex can provide unique properties that are not observed in their monometallic counterparts. For example, having a second metal can decrease the reduction potential of the first metal. This is done by withdrawing electron density from the first metal. Oxidative processes can also be accelerated by having an electron rich metal present to share the burden of oxidation state change.¹ Another possible benefit of bimetallic complexes is the ability of the second metal to act as a reservoir for reactive intermediates and enable unique cooperative mechanisms.²

Metal-metal interactions are often observed in nature’s enzymes as a way to tune the electronic and catalytic properties of metals. The activation of dioxygen is an example of an important biological transformation that uses bimetallic cooperativity (Figure 1.1). The enzyme hemocyanin has two copper atoms that each bind to dioxygen by donating a single electron to form complex **1** (Figure 1.1a). The hemerythrin enzyme also has two iron atoms that share the

burden of oxidation state change. In this example, the molecule of oxygen only binds to a single iron atom, but both metal centers are oxidized by one electron, forming complex **2** (Figure 1.1b).

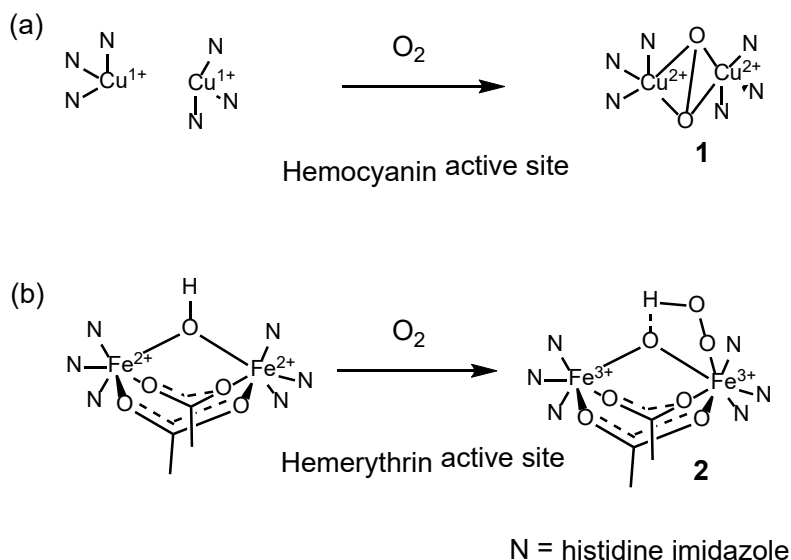


Figure 1.1. Bimetallic active sites of oxygen activation enzymes

One way to facilitate and utilize metal-metal interactions is by placing two different metals into close proximity with each other through a ligand scaffold or a direct metal-metal bond. The two metal's differing electronic properties can provide unique reactivity due to electron-sharing. If an electron deficient early transition metal is paired with an electron rich late transition metal an electron withdrawing dative interaction is formed, which will change the reactivity of the two metals³ (Figure 1.2). The dative interaction formed between the Lewis-acidic early transition metal and an electron-rich late metal withdraws electrons from the late metal, and helps these complexes achieve reactivity not seen in their monometallic analogues. The electron rich late transition metal becomes more electrophilic, which can increase the rate of nucleophilic addition, reductive elimination, and reductive addition steps in catalytic cycles. Also, changing the

structure of the supporting ligands on either metal center can be useful for improving reaction selectivity without decreasing reactivity in these complexes.

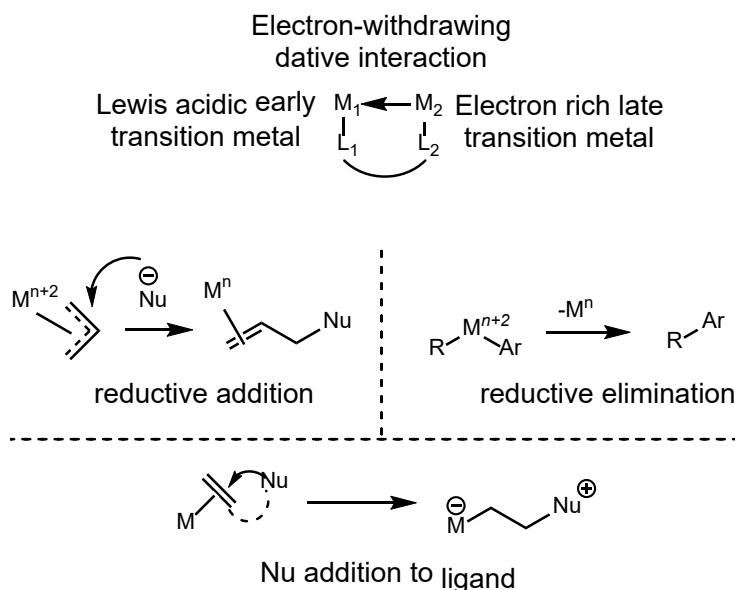


Figure 1.2. Electron withdrawing effects of a second metal center

The following section reviews catalytic applications of bimetallic complexes where the presence of two metals is essential for the reactivity or the mechanism in small molecule transformations.^{4,5,6} Specifically, we will first review a series of redox processes that are facilitated by the presence of two metal centers. Next we will look at complexes that cooperatively use two metals in their catalytic cycle. Lastly, we will cover complexes that retain their metal-metal bond throughout catalysis.

1.2 METAL-METAL BONDS USED IN REDOX PROCESSES

Transition metals are used in a wide variety of reactions due to their ability to undergo redox processes such as oxidative addition and reductive elimination. Many powerful and broadly employed organometallic processes proceed via this cyclic process of oxidative addition and

reductive elimination, including cross couplings, hydrogenations, and hydroformylations. These transformations can often occur in the presence of metal-metal bonds and can be facilitated by metal-metal cooperativity.

1.2.1 Oxidative Reactions That Break the Metal-Metal Bond

The Bergman group reported the synthesis of a Zr/Ir bimetallic complex (**3**) that can undergo oxidative addition by breaking the metal-metal Zr-Ir bond (Figure 1.3).^{7,8} When an alcohol or aniline substrate (X-H) is added to complex **3** the metal-metal bond is broken and a hydride bridge forms between the Zr and Ir metals. The alkoxide or anilide group, however, adds only to zirconium (**4**). Even though the metal-metal bond is cleaved in this transformation, the bimetallic structure remains the same due to the bridging imido ligand. Importantly, this reaction step represents a binuclear oxidative addition mechanism, where each metal formally changes oxidation state by +1. This Zr/Ir complex is also able to undergo reversible oxidative addition with H₂. Again we see the metal-metal bond being cleaved and a hydride bridge being formed (**5**). The second hydrogen like the alkoxide or anilide ends up bonded to zirconium.

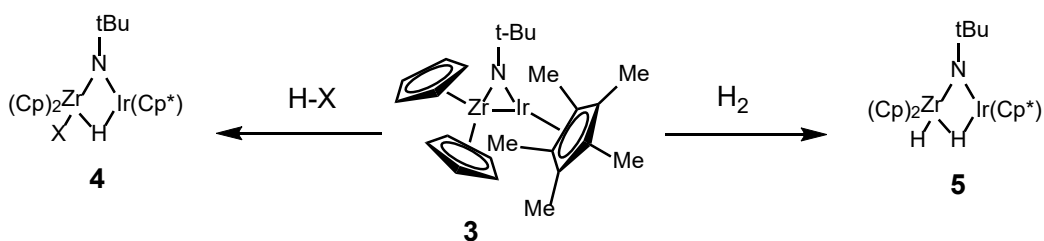


Figure 1.3. Oxidative addition reactions across a Zr-Ir metal-metal bond

The Mankad group reported the synthesis of a Fp-Cu(IPr) complex (**6**) that contains an unsupported Fe-Cu bond (Figure 1.4). They demonstrated that **6** will react with organic

electrophiles in such a way that the Fe-Cu bond is broken forming Fp(alkyl) **7** and (IPr)CuBr **8**. The oxidative addition occurs in this way because the Fe-Cu bond is polarized. It can be regarded as an ion pair containing a nucleophilic Fp^- and an electrophilic $(\text{IPr})\text{Cu}^+$. Thus, while oxidative addition occurs across the metal-metal bond, in this case only the iron center changes oxidation state by 2+ and the Cu centers maintains a Cu(I) oxidation state. Cyclopropylmethyl bromide was used to test whether the reaction followed a radical path or a two-electron mechanism. The cyclopropane ring was not opened suggesting that a two-electron mechanism is followed in this reaction.

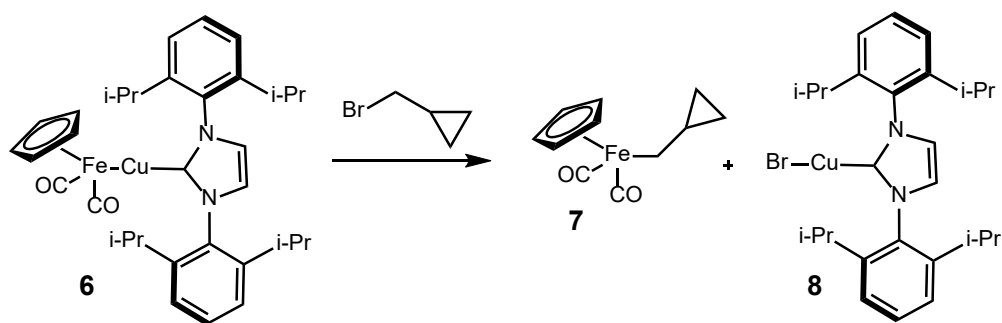


Figure 1.4. Binuclear oxidative addition across a Fe-Cu metal-metal bond

1.2.2 Metal-Metal Bond Formation From Oxidative Addition

The formation of metal-metal bonds can also be facilitated by dinuclear oxidative addition. In many bimetallic complexes, the two metals are held close together through bridging ligands. Gray¹⁰ reported the synthesis of a dirhodium(I) species using bis(isonitrile) ligands (**9**) (Figure 1.5a). A Rh(II)-Rh(II) complex (**10**) containing a metal-metal bond was rapidly formed when I_2 was added. A similar complex formed when MeI was used instead of I_2 . The mechanism is still unknown for the reaction, but it has been proposed that the addition occurs through radical

intermediates. Importantly, the formation of two Rh(II) centers containing unpaired electrons facilitates formation of the metal-metal bond due to the driving force for the two unpaired electrons on the two rhodium centers to pair. Fackler¹¹ obtained a similar result using Au₂ complex **11**. Upon oxidative addition of either I₂ or MeI a metal-metal bond was formed, changing the Au(I)/Au(I) complex to a Au(II)/Au(II) species (**12**) (Figure 1.5b).

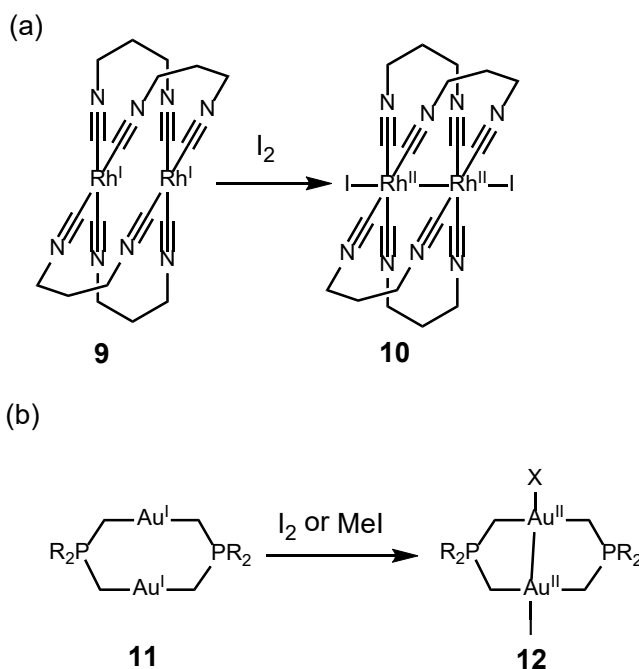


Figure 1.5. Metal-metal bond formation through oxidative addition

1.2.3 Oxidative Additions at a Metal-Metal Multiple Bond

Oxidative addition reactions can use either the sigma- or pi- electrons of a metal-metal bond when there are multiple metal-metal bonds in a complex.^{12, 13} This is observed in the oxidative addition of diisopropylperoxide to (*i*-PrO)₆Mo₂ complex **13** to form complex **14** (Figure 1.6). A formal one-electron oxidation is observed for each Mo atom. This decreases the Mo-Mo bond number from three down to two. When 2 equivalents of Cl₂ are added to complex **13** a

tetrachloro complex (**15**) is formed, which contains a single Mo-Mo bond. When multiple metal bonds are present, oxidative addition can happen without complete dissociation of the complex, which often happens when only single metal-metal bonds are present.

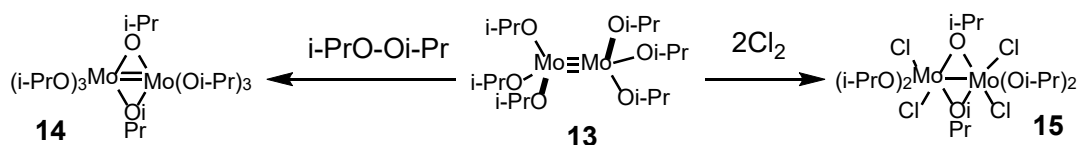


Figure 1.6. Multiple metal-metal bonds undergo oxidative addition

1.2.4 Oxidative Addition at a Metal-Metal Bond with Redox Activity at the Ligand

When redox-active ligands are bound to the metal center two electron processes can occur without changing the electronics of the metal-metal bond. The Uyeda group recently reported the synthesis of a Ni₂ complex with a naphthyridine-diimine supporting ligand (**16**) (Figure 1.7). The reported crystal structure suggests that there is a single bond between the two Ni(I) metals, and that the naphthyridine-diimine ligand has a dianionic charge. The electrons on the ligand are therefore available to participate in oxidative addition. When [*n*-Bu₄N]Br₃ is added to complex **16**, Ni₂Br₂ product (**17**) is formed. The Ni-Ni distance of complex **16** and complex **17** are only slightly different, which supports the idea that the redox reaction is occurring because of the dianionic ligand and not the nickel. The same electronic effects are observed in the oxidative coupling of enyne **18** to form complex **19**.¹⁵

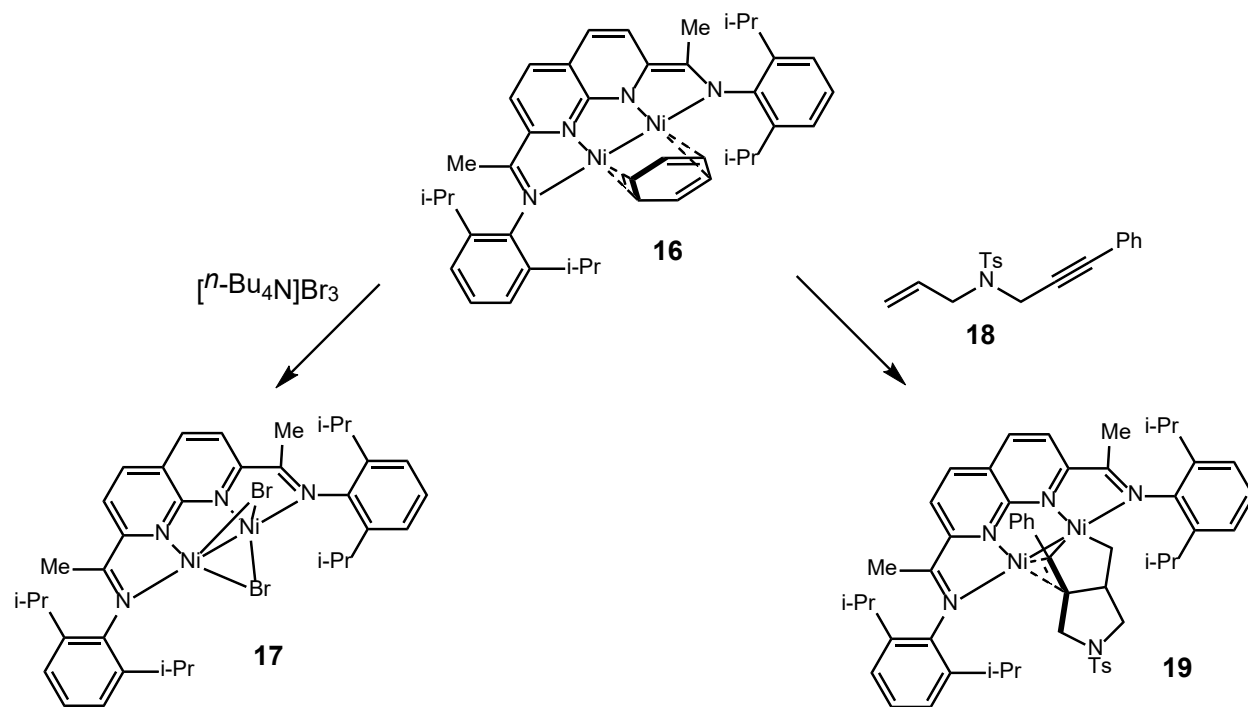


Figure 1.7. Ni(I)-Ni(I) complex with ligand-centered redox activity

1.3 REACTIONS INVOLVING EACH DISTINCT METAL CENTER

There are certain complexes that require each metal to play a distinct role for catalysis to occur. This section will look at how the two metals participate separately in each mechanism discussed. In most cases the bimetallic complex enables catalysis that was unable to occur in monometallic systems.

1.3.1 Ru/Mn Complex for Carbon-Carbon Bond Formation

Lau¹⁶ recently reported the use of a Ru/Mn complex in the catalytic coupling of CO₂ and epoxides (Figure 1.8). The Mn(-I) and the Ru(II) metal centers are linked by a 1,1-bis(diphenylphosphino)methane (dppm) ligand, which allows the two metals to stay between 2.85 Å and 2.87 Å apart. For catalysis to begin the metal-metal bond is broken which results in

two electronically different metals that are held in close proximity to each other. The electrophilic Ru then binds to the epoxide, followed by ring opening by the adjacent Mn, leading to formation of a C-Mn bond. CO₂ insertion is then followed by reductive elimination to generate the carbonate product and reforms the Ru-Mn bond. Each metal center is necessary in this mechanism in order to drive the catalysis forward. They also showed that a Mn monometallic complex was less active, and that when a monometallic Ru complex was used no reaction occurred.

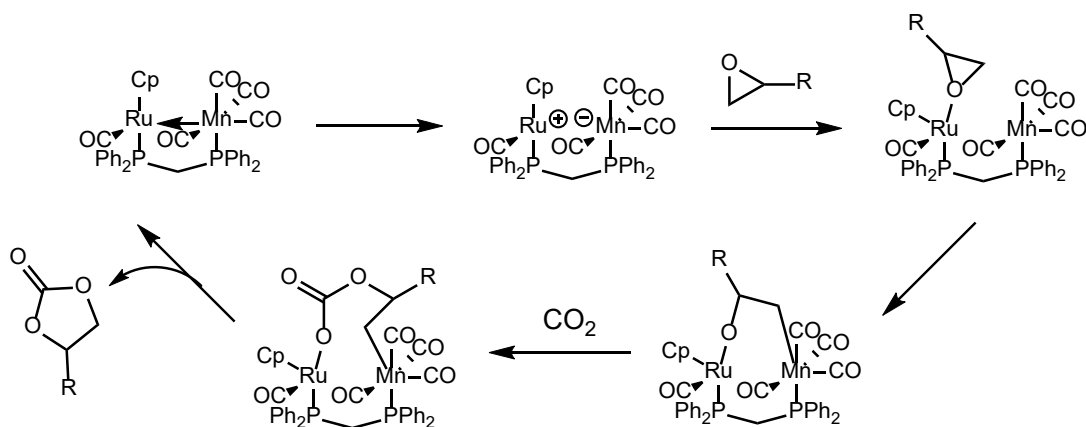


Figure 1.8. Proposed Ru/Mn mechanism for epoxide/CO₂ coupling

1.3.2 Zr/Ru Complex for Dehydrogenation of Dimethylamine-Borane

A series of group 4/group 8 bimetallic complexes have been used in the dehydrogenation of dimethylamine-borane including Zr/Ru, Hf/Ru, and Zr/Fe complexes.¹⁷ Each of these bimetallic complexes were very active, whereas the monometallic Zr and Hf complexes were inactive and the monometallic Ru complex only showed slight reactivity. The proposed mechanism suggests that each metal plays a role in the reaction (Figure 1.9). To begin, the amine-borane oxidatively adds to the Zr/Ru complex breaking the bond between the Zr center and the bridging hydrogen.

A binuclear reductive elimination then ensues, releasing dihydrogen and forming a new Zr-Ru bond. The B-H bond of the amine-borane complex is then added across the metal-metal bond to reform the bridging hydride species, release the product and reform the catalyst.

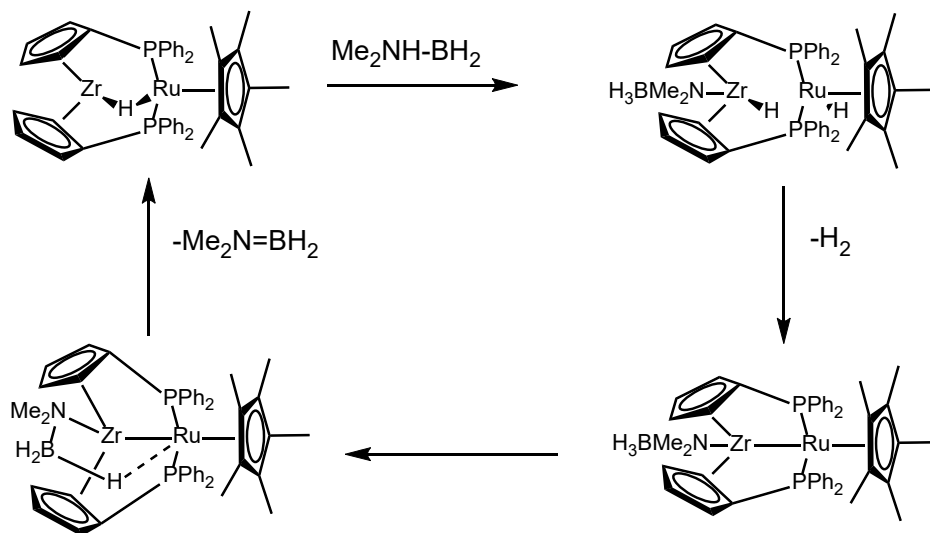


Figure 1.9. Proposed mechanism for the Zr/Ru catalyzed amine-borane dehydrogenation

1.3.3 Zr/M Complex for Ethylene Polymerization

The Osakada group¹⁸ successfully used transition metal Zr/Pd, Zr/Co, and Zr/Ni complexes to polymerize ethylene (Figure 1.10). Polymers with different properties were synthesized depending on which metal was used with zirconium. For example, when nickel was used as the second metal, highly branched polymers were observed. While the Zr center was responsible for ethylene polymerization, the Ni center simultaneously formed ethylene oligomers that would insert themselves into the growing chain.

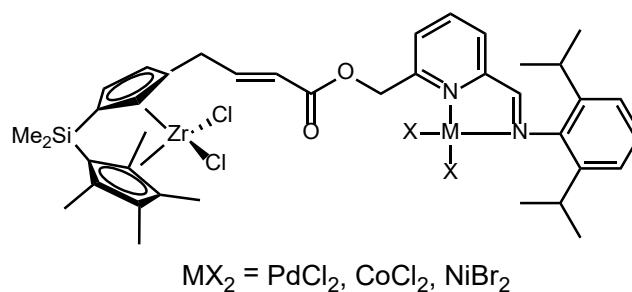


Figure 1.10. Polymerization catalyst containing Zr/M

1.3.4 Ti/Rh Complex for Hydroacylation

Slaughter and Wolczanski^{19,20} reported a Ti/Rh complex capable of the hydroacylation of 3-phenyl-4-pentenal and styrene. In this example, the Ti(IV) and Rh(I) centers are linked by an alkoxy-phosphine bridge (Figure 1.11). It was shown that monometallic analogues were inactive in this hydroacylation reaction, whereas complex **20** was able to complete the transformation in 11 hrs. It is believed that this exceptional reactivity is due to the ability of the Ti to act as an anchor for the aldehyde oxygen, which aids in the C-H insertion at Rh by bringing the Rh center into close proximity with the C-H bond.

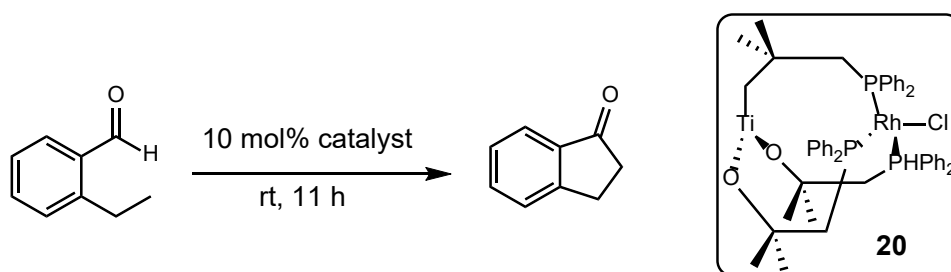


Figure 1.11. Ti/Rh catalyst used in the hydroacylation

1.4 CATALYSTS WITH METAL-METAL BONDS THAT REMAIN INTACT

Recently there has been a surge in the design of metal-metal bonded catalysts that retain their structure during the entire catalytic cycle. This is done by designing a ligand structure that is able to support the different metals and keep them in a position that favors bonding. This section will give examples of catalysts that retain their metal-metal bond and act as a single functional site during the transformation. The substrate will bind to one metal center, while the other acts as ligand to support catalysis.

1.4.1 Carbene Transfer Reaction with a Dirhodium Catalyst

Carbene transfer reactions using dirhodium catalysts are believed to go through a $\text{Rh}=\text{CR}_2$ intermediate in which the second Rh acts as a metalloligand.²¹ Davies and Dikarev did a study where they compared a Rh_2 catalyst (**21**) and a Rh/Bi catalyst (**22**) in order to help determine the role of the second Rh metal center (Figure 1.12).²² Each catalyst was able to successfully cyclopropanate styrene with methyl phenyldiazoacetate, but the Rh_2 catalyst was 1600 times faster. Through computational studies they determined that the rate determining step using the Rh/Bi complex was 3.2 kcal/mol higher in energy than with the Rh_2 complex. They rationalized this difference in energy was due to the difference in orbital overlap. The Rh-Bi interaction was significantly weaker than the Rh-Rh interaction.

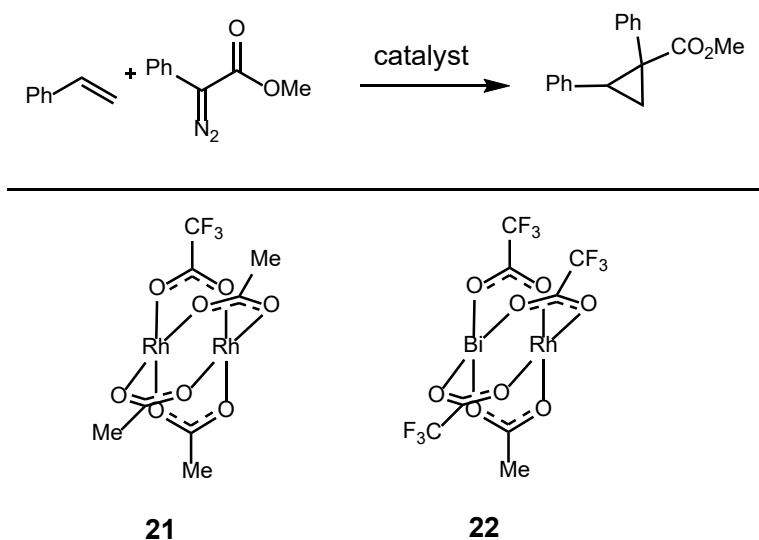


Figure 1.12. Rh₂ and Rh/Bi catalysts used for styrene cyclopropanation

1.4.2 Ru₂ Allenylidene Intermediates for Propargylic Substitution

Hidai and Nishibayashi used a stable Ru₂(allenylidene) intermediate to perform substitution reactions with propargyl alcohols.^{23,24} By treating complex **23** with tertiary propargyl alcohol **24** and NH₄BF₄, cationic complex **25** was formed and isolated as a crystalline solid (Figure 1.13). When ethanol was stoichiometrically added to complex **25** the propargyl ether **26** was formed. A series of monometallic Ru(II) complexes were used in the reaction, but did not give the substitution product. The activity of the Ru₂(III) complex **25** is thought to come from two things. First, the Ru-Ru bond is able to help stabilize the intermediate formed when the product dissociates. Second, the second Ru metal is cationic, which allows it to have an electron withdrawing effect on the Ru that is participating in the ligand exchange step.

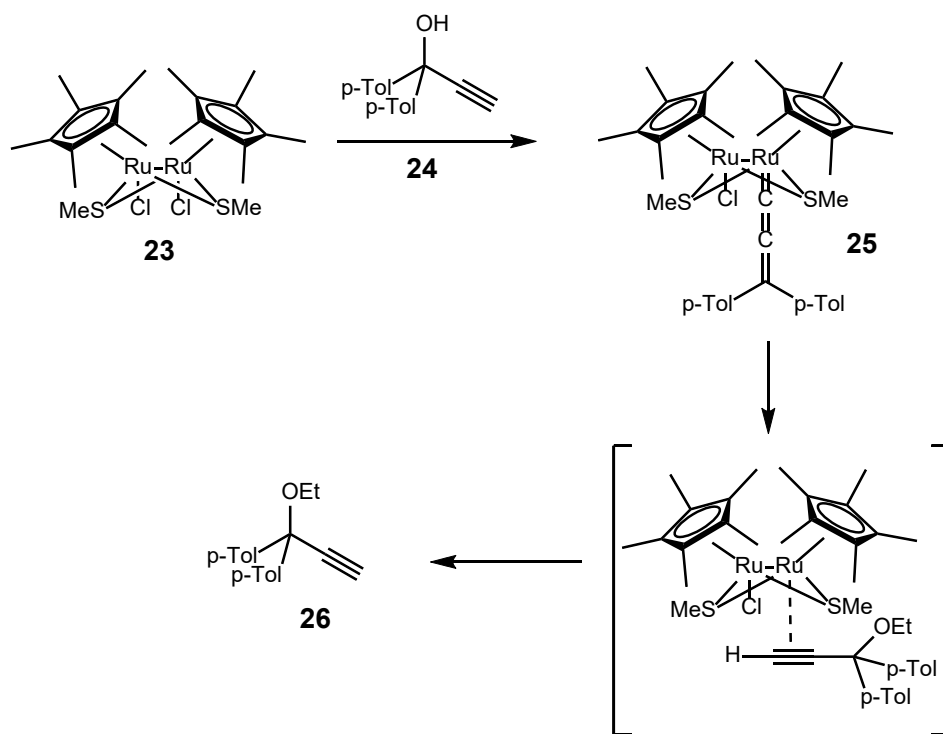


Figure 1.13. Ru_2 (allynylidene) intermediate used for propargylic substitution

1.4.3 Alkene Hydrogenation with Early/Late Heterobimetallic Catalyst

Bergman reported a Ta/Ir complex that can be used for hydrosilylation, alkene isomerization, and hydrogenation reactions.²⁵ Complex **26** was shown to be especially efficient for ethylene hydrogenation (Figure 1.14). When the monometallic complex $\text{Ph}_2\text{P}(\text{CH}_2)_2\text{Ir}(\text{PPh}_3)\text{CO}$ (**27**) was used, the reaction proceeded 150 times slower than when complex **26** was used.^{26a} Deuterium studies showed that complex **26** underwent reversible C-H reductive elimination at the bridging CH_2 group, but complex **27** did not show any deuterium in its ethylene bridge. This led them to believe that the two complexes were undergoing different catalytic mechanisms.

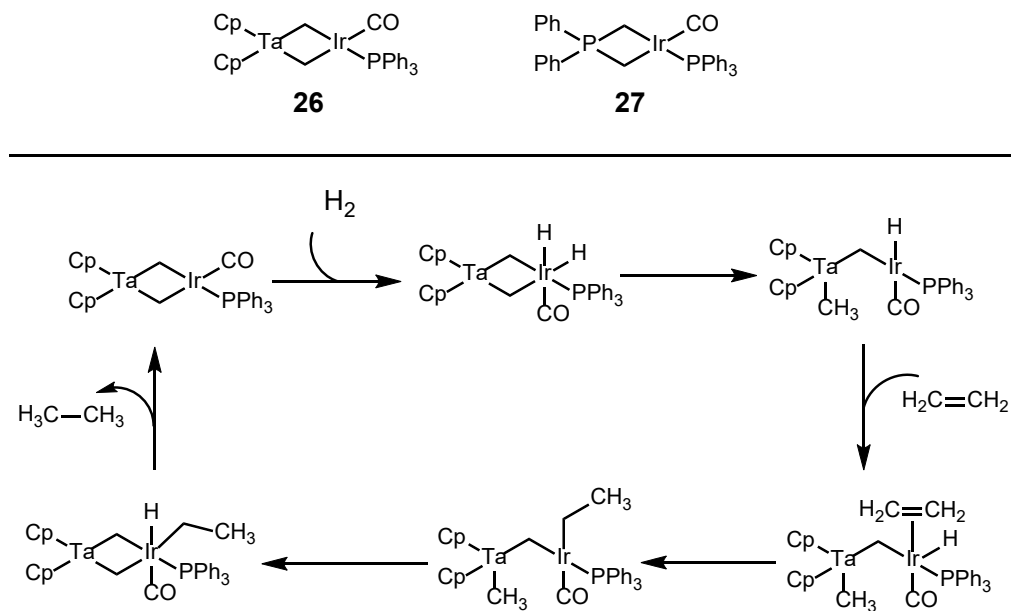


Figure 1.14. Proposed mechanism of a Ta/Ir catalyzed ethylene hydrogenation

The Ess group performed calculations that supported that these catalysts operate by different mechanisms.^{26b} Complex **26** follows the mechanism shown in Figure 1.14, whereas complex **27** does not undergo reductive elimination because the activation barrier is significantly higher in energy.

1.4.4 Allylic Substitution with Pd/Ti Heterobimetallic Complex

Nagashima reported the use of a Pd/Ti in an allylic substitution reaction.²⁷ When Pd/Ti catalyst **28** was added stoichiometrically with diethylamine complete conversion to the methallyl amine was observed at room temperature within 5 mins (Figure 1.15). When the monometallic Pd(dppp) catalyst (**29**) was used no reaction was observed within 2 hrs. The change in catalytic activity is attributed to the ability of the Ti and Pd to datively bond making the Pd more electrophilic.

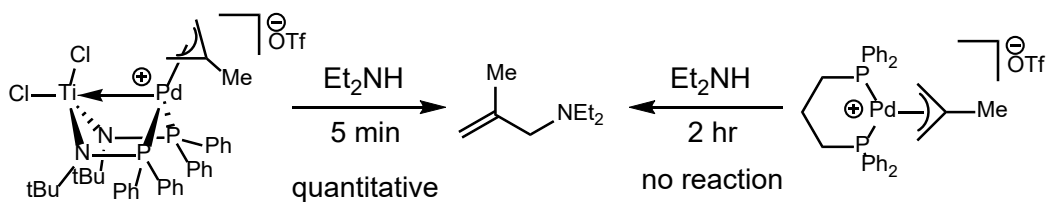


Figure 1.15. Catalytic activity of a Pd/Ti complex and its monometallic analogue

The Michaelis and Ess groups in a combined computational and experimental study examined the origin of the Pd-Ti interaction on catalysis, and if these catalysts could enable new reactivity in allylic amination reactions.²⁸ Their studies showed that certain monometallic analogues could efficiently catalyze aminations using diethylamine, but when sterically hindered amines were used the Pd/Ti interaction was essential for catalysis.²⁹ In addition, these Pd/Ti catalysts proved to be highly effective catalysts for allylic aminations with a variety of hindered amine nucleophiles. These studies will be extensively discussed in chapters 2 and 3.

1.4.5 Nickel Catalyzed Hydrogenation Utilizing Dative Interactions

Lu and coworkers recently studied the effect of different Lewis acidic metals in hydrogenation reactions catalyzed by heterobimetallic Ni-M catalysts. In these complexes, the Lewis acidic metal forms a dative interaction with the Ni center.³⁰ The metals studied were Al, Ga, and In (Figure 1.16). It was observed that the larger cations were able to have a stronger dative interaction with nickel due to the increase of orbital overlap. Monometallic complex **30** and complex **31-Al** were not reactive in hydrogenation reactions because they are unable to bind H₂. Complex **31-In** was only slightly reactive even though it was able to bind H₂. However, when 5 mol % of complex **31-Ga** was used the hydrogenation of styrene yielded >99% of ethylbenzene

after 24 hrs. These results show the ability to control reactivity based on different Ni-Lewis acid interactions.

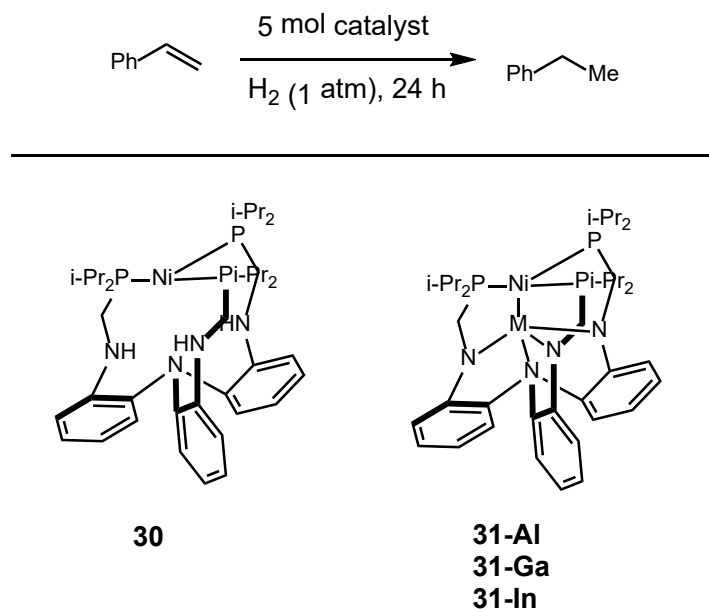


Figure 1.16. Ni-catalyzed hydrogenation of styrene

1.4.6 Zr/Co Catalyzed Hydrosilylation

Thomas³¹ showed that a Zr/Co complex (**32**) can be used to efficiently catalyze the hydrosilylation of ketones (Figure 1.17). When **32** is treated with benzophenone, complex **33** is formed. Thomas proposed a mechanism in which the substrate binds only to Zr, but the charge is distributed between both metals. In a monometallic catalyst the Zr(III)/Zr(IV) catalytic cycle is unfavorable, but is made possible by the electron donating effect of the second metal in the bimetallic catalyst.

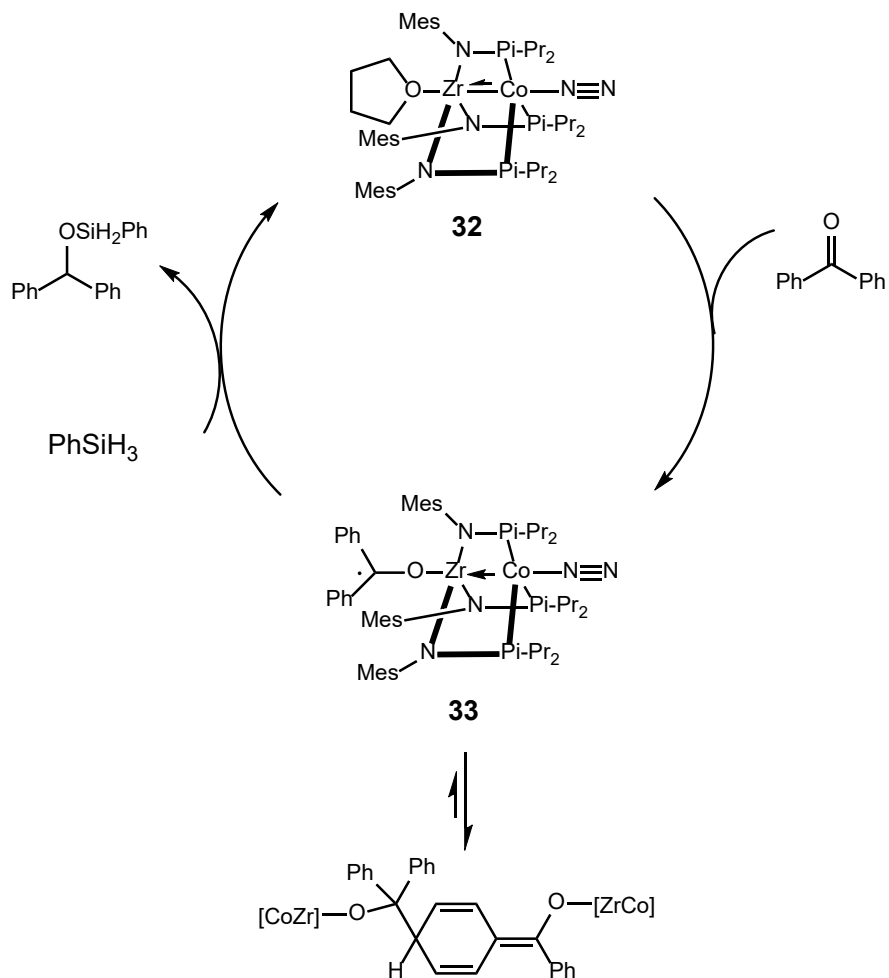


Figure 1.17. Ketone hydrosilylation catalyzed by a Zr/Co complex

1.5 CONCLUSION

Metal-metal bonds provide a unique way to increase reactivity in various organic transformations. Redox processes can be facilitated by the presence of metal-metal bonds. In some of these examples, the reaction proceeds by breaking the metal-metal bond. In others, the formation of a metal-metal bond is needed for the transformation to proceed. Cooperativity between the two metals can facilitate reductive or ring opening processes that were previously unachievable by monometallic analogues. Other cases utilize the second metal as a ligand which

can change the reactivity of the first metal. This can occur by simply changing the ligand environment or changing the reaction mechanism. In some cases the presence of a metal-metal bond reduces the reactivity due to the strong interaction between the metals. There are numerous variables that still need to be analyzed in order to fully understand the significance of metal-metal bonds in catalysis.

These recent examples of metal-metal cooperativity demonstrate the potential impact of utilizing bimetallic complexes for the development of novel catalytic transformations. Thus efforts to design and synthesize bimetallic complexes and apply them to catalytic reactions will continue to impact the area of transition metal catalysis in the coming years.

1.6 REFERENCES

- (1) (a) Powers, D. C.; Benitez, D.; Tkatchouk, E.; Goddard, William A. III.; Ritter, T., Bimetallic Reductive Elimination from Dinuclear Pd(III) Complexes. *J. Am. Chem. Soc.* **2010**, *132*, 14092-14103.
- (b) Bosnich, B., Cooperative Bimetallic Redox Reactivity. *Inorg. Chem.* **1999**, *38*, 2554-2562.
- (2) (a) Broussard, M. E.; Juma, B.; Train, S. G.; Peng, W. -J.; Laneman, S. A.; Stanley, G. G., A Bimetallic Hydroformylation Catalyst: High Regioselectivity and Reactivity Through Homobimetallic Cooperativity. *Science* **1993**, *260*, 1784-1788.
- (b) Baxter, S. M.; Ferguson, G. S.; Wolczanski, P. T., Mechanistic Investigation of the ZrMe/PtMe Exchange in Cp*ZrMe(μ -OCH₂Ph₂P)₂PtMe₂. *J. Am. Chem. Soc.* **1988**, *110*, 4231-4241.
- (3) Zhang, Y.; Roberts, S. P.; Bergman, R. G.; Ess, D. H., Mechanism and Catalytic Impact of Ir-Ta Heterobimetallic and Ir-P Transition Metal/Main Group Interactions on Alkene Hydrogenation. *ACS Catal.* **2015**, *5*, 1840-1849.
- (4) Powers, I. G.; Uyeda, C., Metal-Metal Bonds in Catalysis. *ACS Catal.* **2017**, *7*, 936-958.
- (5) Thomas, C., Metal-Metal Multiple Bonds in Early/Late Heterobimetallic Complexes: Applications Toward Small Molecule Activation and Catalysis. *Comments on Inorganic Chemistry*, **2011**, *32*, 14-38.
- (6) Cooper, B. G.; Napoline, J. W.; Thomas, C. M., Catalytic Applications of Early/Late Heterobimetallic Complexes. *Catal. Rev. Sci. Eng.* **2012**, *54*, 1-40.
- (7) Baranger, A. M.; Bergman, R. G., Cooperative Reactivity in the Interactions of X-H Bonds with a Zirconium-Iridium Bridging Imido Complex. *J. Am. Chem. Soc.* **1994**, *116*, 3822-3835.
- (8) Kuwabara, J.; Takeuchi, D.; Osakada, K., Early-Late Heterobimetallic Complexes as Initiator for Ethylene Polymerization. Cooperative Effect of Two Metal Centers to Afford Highly Branched Polyethylene. *Chem. Commun.* **2006**, 3815-3817.
- (9) Karunananda, M. K.; Parmelee, S. R.; Waldhart, G. W.; Mankad, N. P., Experimental and Computational Characterization of the Transition State for C-X Bimetallic Oxidative Addition at a Cu-Fe Reaction Center. *Organometallics* **2015**, *34*, 3857-3864.
- (10) Lewis, N. S.; Mann, K. R.; Gordon, J. G.; Gray, H. B., Oligomerization and two-center oxidative addition reactions of a dimeric rhodium(I) complex. *J. Am. Chem. Soc.* **1976**, *98*, 7461-7463.
- (11) Fackler, J. P.; Basil, J. D., Oxidative addition of methyl iodide to a dinuclear gold(I) complex. The x-ray crystal structure of bis[μ -(dimethyldimethylenephosphoranyl-C,C)]-

iodomethyldigold(II)(Au-Au), Au₂[(CH₂)₂P(CH₃)₂]₂(CH₃)I. *Organometallics* **1982**, *1*, 871-873.

(12) (a) Chisholm, M. H., Interconverting multiple bonds between molybdenum and tungsten atoms: oxidative-additions and reductive-eliminations from dinuclear centers. *Polyhedron* **1986**, *5*, 25-30.

(b) Chisholm, M. H., The $\sigma^2\pi^4$ Triple Bond between Molybdenum and Tungsten Atoms: Developing the Chemistry of an Inorganic Functional Group. *Angew. Chem., Int. Ed.* **1986**, *25*, 21-30.

(13) Chisholm, M. H.; Kirkpatrick, C. C.; Huffman, J. C., Reactions of metal-metal multiple bonds. 7. Addition of the halogens chlorine bromine and iodine and diisopropyl peroxide to hexaisopropoxydimolybdenum. Dinuclear Oxidative-Addition Reactions Accompanied by Metal-Metal Bond-Order Changes from 3 to 2 to 1. *Inorg. Chem.* **1981**, *20*, 871-876.

(14) Zhou, Y. -Y.; Hartline, D. R.; Steiman, T. J.; Fanwick, P. E.; Uyeda, C., Dinuclear Nickel Complexes in Five States of Oxidation Using a Redox-Active Ligand. *Inorg. Chem.* **2014**, *53*, 11770-11777.

(15) Hartline, D. R.; Zeller, M.; Uyeda, C., Well-Defined Models for the Elusive Dinuclear Intermediates of the Pauson-Khand Reaction. *Angew. Chem., Int. Ed.* **2016**, *55*, 6084-6087.

(16) Man, M. L.; Zhou, Z. Y.; Ng, S. M.; Lau, C. P., Synthesis, characterization and reactivity of heterobimetallic complexes (η^5 -C₅R₅)Ru(CO)(μ -dppm)M(CO)₂(η^5 -C₅H₅) (R=H, CH₃; M=Mo, W). Interconversion of hydrogen/carbon dioxide and formic acid by these complexes. *Dalton Trans.* **2003**, 3727-3735.

(17) Miyazaki, T.; Tanabe, Y.; Yuki, M.; Miyake, Y.; Nishibayashi, Y., Synthesis of Group IV (Zr, Hf)-Group VIII (Fe, Ru) Heterobimetallic Complexes Bearing Metallocenyl Diphosphine Moieties and Their Application to Catalytic Dehydrogenation of Amine-Boranes. *Organometallics* **2011**, *30*, 2394-2404.

(18) Kuwabara, J.; Takeuchi, D.; Osakada, K. Early-late heterobimetallic complexes as initiator for ethylene polymerization. Cooperative effect of two metal centers to afford highly branched polyethylene. *Chem. Commun.* **2006**, 3815-3817.

(19) Slaughter, L. M.; Wolaczanski, P. T., Ti(μ : η^1 , η^1 -OCMe₂CH₂PPh₂)₃Rh has a cylindrically symmetric triple bond. *Chem. Commun.* **1997**, 2109-2110.

(20) Wheatley, N.; Kalck, P. Structure and Reactivity of Early-Late Heterobimetallic Complexes. *Chem. Rev.* **1999**, *99*, 3379-3420.

(21) (a) Davies, H. M. L.; Manning, J. R., Catalytic C-H functionalization by metal carbenoid and nitrenoid insertion. *Nature* **2008**, *451*, 417-424.

(b) Ford, A.; Miel, H.; Ring, A.; Slattery, C. N.; Maguire, A. R.; McKervey, M. A., Modern Organic Synthesis with α -Diazocarbonyl Compounds. *Chem. Rev.* **2015**, *115*, 9981-10080.

- (22) Hansen, J. R.; Li, B.; Dikarev, E.; Autschbach, J.; Davies, H. M. L., Combined Experimental and Computational Studies of Heterobimetallic Bi-Rh Paddlewheel Carboxylates as Catalysts for Metal Carbenoid Transformations. *J. Org. Chem.* **2009**, *74*, 6564-6571.
- (23) (a) Nishibayashi, Y.; Wakiji, I.; Hidai, M., Novel Propargylic Substitution Reactions Catalyzed by Thiolate-Bridged Diruthenium Complexes via Allenylidene Intermediates. *J. Am. Chem. Soc.* **2000**, *122*, 11019-11020.
- (b) Miyake, Y.; Uemura, S.; Nishibayashi, Y., Catalytic Propargylic Substitution Reactions. *ChemCatChem* **2009**, *1*, 342-356.
- (24) Takagi, Y.; Matsuzaka, H.; Ishii, Y.; Hidai, M., Synthesis and Reactivities of Cationic Diruthenium Complexes with Terminal Vinylidene Ligands. Hydration and Novel Cyclization of Acetylenes on the Diruthenium Center. *Organometallics*, **1997**, *16*, 4445-4452.
- (25) (a) Hostetler, M. J.; Bergman, R. G., Synthesis and reactivity of Cp₂Ta(CH₂)₂Ir(CO)₂: an early-late heterobimetallic complex that catalytically hydrogenates, isomerizes and hydrosilates alkenes. *J. Am. Chem. Soc.* **1990**, *112*, 8621-8623.
- (b) Hostetler, M. J.; Butts, M. D.; Bergman, R. G., Rate and equilibrium study of the reversible oxidative addition of silanes to the iridium center in Cp₂Ta(μ-CH₂)₂Ir(CO)₂ and of alkene hydrosilylation/isomerization catalyzed by this system. *Organometallics*, **1993**, *12*, 65-75.
- (26) (a) Hostetler, M. J.; Butts, M. D.; Bergman, R. G., Scope and mechanism of alkene hydrogenation/isomerization catalyzed by complexes of the type R₂E(CH₂)₂M(CO)(L) (R=Cp, Me, Ph; E=phosphorus, tantalum; M=rhodium, iridium; L=CO, PPh₃). *J. Am. Chem. Soc.* **1993**, *115*, 2743-2753.
- (b) Zhang, Y.; Roberts, S. P.; Bergman, R. G.; Ess, D. H., Mechanism and Catalytic Impact of Ir-Ta Heterobimetallic and Ir-P Transition Metal/Main Group Interactions on Alkene Hydrogenation. *ACS Catal.* **2015**, *5*, 1840-1849.
- (27) Tsutsumi, H.; Sunada, Y.; Shiota, Y.; Yoshizawa, K.; Nagashima, H., Nickel(II), Palladium(II), and Platinum(II) η³-Allyl Complexes Bearing a Bidentate Titanium(IV) Phosphinoamide Ligand: A Ti-M₂ Dative Bond Enhances the Electrophilicity of the π-Allyl Moiety. *Organometallics* **2009**, *28*, 1988-1991.
- (28) Walker, W. K.; Kay, B. M.; Michaelis, S. A.; Anderson, D. L.; Smith, S. J.; Ess, D. H.; Michaelis, D. J., Origin of Fast Catalysis in Allylic Amination Reactions Catalyzed by Pd-Ti Heterobimetallic Complexes. *J. Am. Chem. Soc.* **2015**, *137*, 7371-7378.
- (29) Walker, W. K.; Anderson, D. L.; Stokes, R. W.; Smith, S. J.; Michaelis, D. J., Allylic Aminations with Hindered Secondary Amine Nucleophiles Catalyzed by Heterobimetallic Pd-Ti Complexes. *Org. Lett.* **2015**, *17*, 752-755.
- (30) (a) Rudd, P. A.; Liu, S.; Gagliardi, L.; Young, V. G.; Lu, C. C., Metal-Alane Adducts with Zero-Valent Nickel, Cobalt, and Iron. *J. Am. Chem. Soc.* **2011**, *133*, 20724-20727.

(b) Cammarota, R. C.; Lu, C. C., Tuning Nickel with Lewis Acidic Group 13 Metalloligands for Catalytic Olefin Hydrogenation. *J. Am. Chem. Soc.* **2015**, *137*, 12486-12489.

(31) Greenwood, B. P.; Rowe, G. T.; Chen, C. -H.; Foxman, B. M.; Thomas, C. M., Metal-Metal Multiple Bonds in Early/Late Heterobimetallics Support Unusual Trigonal Monopyramidal Geometries at both Zr and Co. *J. Am. Chem. Soc.* **2010**, *132*, 44-45.

Chapter 2

Heterobimetallic Pd-Ti Complexes for Catalysis in Allylic Aminations with Hindered Secondary Amine Nucleophiles

Portions of this work have been previously published:

Walker, W. K.; Anderson, D. L.; Stokes, R. W.; Smith, S. J.; Michaelis, D. J., Allylic Aminations with Hindered Secondary Amine Nucleophiles Catalyzed by Heterobimetallic Pd-Ti Complexes. *Org. Lett.* **2015**, *17*, 752-755.

2.1 INTRODUCTION

Heterobimetallic transition-metal complexes have the potential to be highly useful catalysts. The metal-metal interaction can be used to directly influence the rate of catalysis. By placing two electronically different metals within close proximity of each other the electronic properties of the catalytically active metal can be altered through the formation of a dative bond. The second metal center can also be used to provide ligand support and electronic effects to the catalytically active metal that are difficult to achieve with existing organic ligands.¹ Early/late transition metal heterobimetallic complexes have been shown to form strong metal-metal interactions. This happens when the electron-rich late transition metal donates electron density to the early, electron poor transition metal. Recently there has been an increase in reports on the design and synthesis of heterobimetallic complexes², but the use of these complexes in catalytic applications where the metal-metal cooperativity is used to facilitate novel reactivity is still rare.^{1a} We have been interested in how these heterobimetallic complexes can be used to address limitations in current transition-metal catalyzed reactions. This chapter will focus on our efforts to accelerate allylic aminations with hindered secondary amine substrates using heterobimetallic Pd-Ti catalysts.

Basic, *N*-alkyl substituted amines are found in many bioactive molecules, which make them important to various pharmaceutical processes. Naturally occurring alkaloids also contain sterically

hindered amine functional groups. The high basicity and low nucleophilicity of these hindered amines make them difficult to incorporate in organic synthesis. Another challenge is their potential to bind to and deactivate transition metal catalysts. To overcome these obstacles, C-N bonds are often generated using electron-withdrawing amine protecting groups.³ We proposed that the application of heterobimetallic Pd-Ti complexes in allylic aminations could speed up catalysis and provide high reactivity with traditionally unreactive hindered amine nucleophiles. The formation of a Pd to Ti dative interaction would generate a highly electrophilic palladium center, which would increase the rate of the turnover limiting reductive addition step.

Recently, the Nagashima group⁷ reported the catalytic activity of a Pd-Ti heterobimetallic complex (**1**) in the allylic amination of methallyl chloride and diethylamine. The complex consists of a phosphinoamide scaffold that brings the titanium and palladium together, which enables the metals to form a dative bond. They proposed that this interaction enabled the electron rich palladium to donate electron density to the electron poor titanium. The resulting electrophilic palladium was then able to facilitate the catalysis. They found that within 5 mins diethylamine completely added to the palladium bound methallyl ligand at room temperature (Figure 2.1). They also reported the synthesis of a monometallic palladium analogue that gave no product, even after 2 hr. This result supported their hypothesis that the dative interaction between the two metals enables this allylic amination by accelerating the rate of the amine addition.

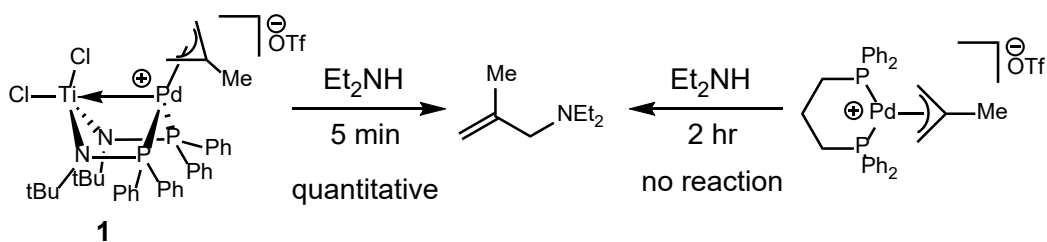


Figure 2.1. Stoichiometric allylic amination with complex 1 and monometallic Pd analogue

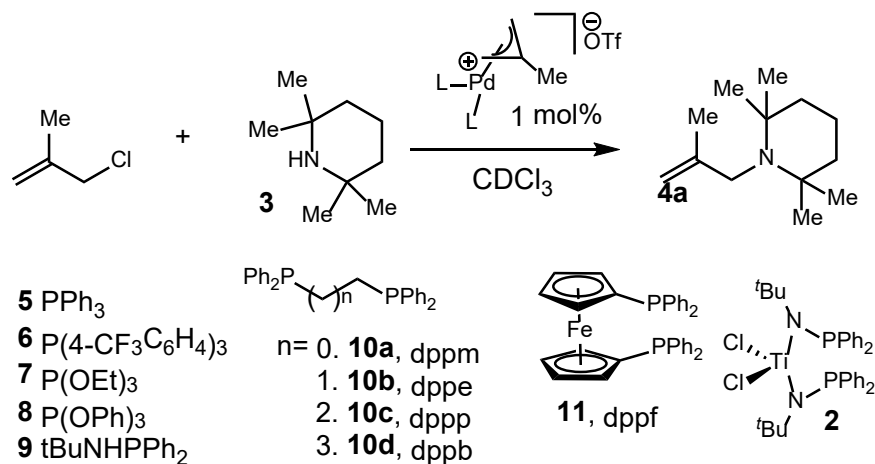
Our group wanted to determine whether these Pd-Ti catalysts could be used in transformations that traditional palladium ligands are unable to perform, as well as expand the nucleophiles that can be used in allylic aminations. We wanted to determine how the reactivity of Pd-Ti complexes compared to the reactivity of known bisphosphine ligands. We also wanted to determine if these complexes could form *in situ*, avoiding the need to synthesize the bimetallic complex. We also probed how the titanium ligand structure affected catalysis.

2.2 RESULTS AND DISCUSSION

2.2.1 *Optimization Studies of Allylic Aminations with Hindered Amine Nucleophiles*

Our lab was interested in the potential of bimetallic complexes to enable novel catalysis, so we focused on hindered secondary amines, which cannot currently be used in allylic aminations. We began our catalytic studies with the reaction of 2,2,6,6-tetramethylpiperidine (**3**) and methallyl chloride (Table 2.1). Using complex **1**, we saw rapid formation of the desired amination product in 35 minutes at room temperature (entry 1). No allylation product was observed when bis(triphenylphosphine) complex **5** was used at room temperature (entry 2). When we heated the reaction for 24 hours (90°C) we were able to observe a small amount of the desired product (entry 3). We found that when the reaction was heated modest product formation was achieved with phosphite ligands (entries 5 and 6). Palladium complexes that contained phosphinoamide ligands without titanium provided poor conversion to product (entry 7). We also investigated other bis(phosphine) ligands, but were unable to see product formation in these cases (entries 8-12). These results demonstrate that heterobimetallic complex **1** is able to efficiently catalyze allylic aminations with hindered amine nucleophiles under mild reaction conditions.

Table 2.1: Optimization Studies of Allylic Aminations with **3**



entry ^a	ligand	Temp	time	% conv. ^b
1	2	r.t.	35 min	100
2	5	r.t.	24 hr	N.R.
3	5	90 °C	24 hr	7
4	6	90 °C	24 hr	6
5	7	90 °C	24 hr	14
6	8	90 °C	24 hr	67
7	9	90 °C	24 hr	<5
8	10a	90 °C	24 hr	11
9	10b	90 °C	24 hr	<5
10	10c	90 °C	24 hr	<5
11	10d	90 °C	24 hr	<5
12	11	90 °C	24 hr	<5

^aReactions performed using 1 mmol of methallyl chloride, 2.2 equiv of **3**, and 0.05 mmol of the indicated allyl complex formed in situ (0.025 mmol [Pd(methallyl)Cl]₂, 0.05 mmol of AgOTf. And either 0.05 mmol of bisphosphine or 0.10 mmol of monophosphine) in CDCl₃ (1M) for the indicated time. ^bDetermined by ¹H NMR.

Several control experiments also were performed to verify the need for the phosphinoamide scaffold. When titanium tetrachloride was added to phosphite ligand **8**, conversion was very low (~20%, 24 h). When TiCl_2 was added to phosphinoamine ligand **9** no product formation was detected. Also when $[\text{Pd}(\text{methallyl})\text{Cl}]_2$ was used by itself or with the addition of silver triflate, no amination product was formed. These control studies suggest that the catalysis only works when the titanium phosphinoamide structure is present in the active catalyst.

2.2.2 *In Situ* Formation of Heterobimetallic Complex

After having established the high reactivity of complex **1** with hindered amine nucleophiles, we next explored the possibility of generating the active heterobimetallic catalyst *in situ* from a titanium-containing ligand precursor. This would allow us to avoid presynthesizing and purifying the heterobimetallic complex. Formation of the complex was done by combining 0.5 mol% $[\text{Pd}(\text{methallyl})\text{Cl}]_2$, 1 mol% silver triflate⁹ and 1 mol% of the titanium-containing ligand (**2**). The formation of the complex was followed by ^1H and ^{31}P NMR, and characteristic peaks from the bimetallic Pd-Ti complex were observed.¹⁰ When the complex was formed in the presence of the substrates, the reaction exhibited essentially the same reactivity as when bimetallic catalyst **2** was employed, achieving full conversion within 20 mins at room temperature (Figure 2.2). This result suggests that the complex can be formed in the reaction mixture without losing any of its reactivity. Ligand **2** is relatively stable in the solid state, and can be synthesized using standard air-free Schlenk line techniques reported in the literature.²¹ Therefore, the ligand can be used in reactions set up on the benchtop as long as it is stored under argon and the solvents and reagents used are dried prior to use. This eliminates the need to use a glovebox.

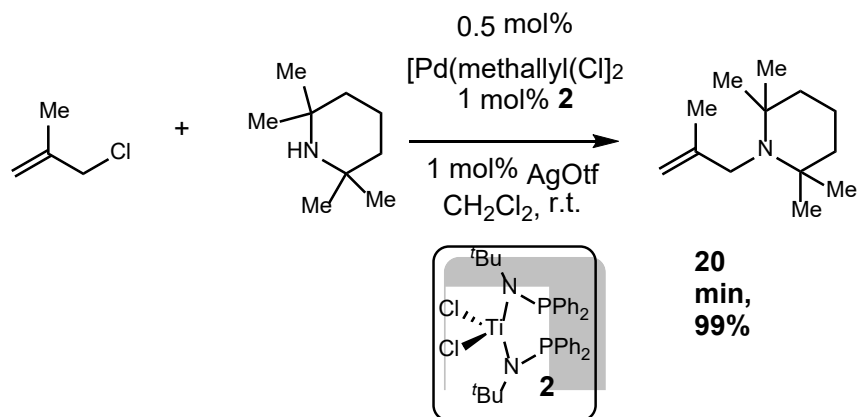


Figure 2.2. *In situ* formation of heterobimetallic catalyst **1**

2.2.3 Synthesis and Reactions of Titanium Phosphinoamide Ligands

Next we wanted to see how the structure of the titanium ligand would affect the catalysis. We began by synthesizing complexes **12** and **13** by changing the stoichiometry and reaction conditions used in the formation of **2**. As far as we know these ligands have never been synthesized before. We were able to confirm their structure with single crystal X-ray analysis (Figure 2.3).

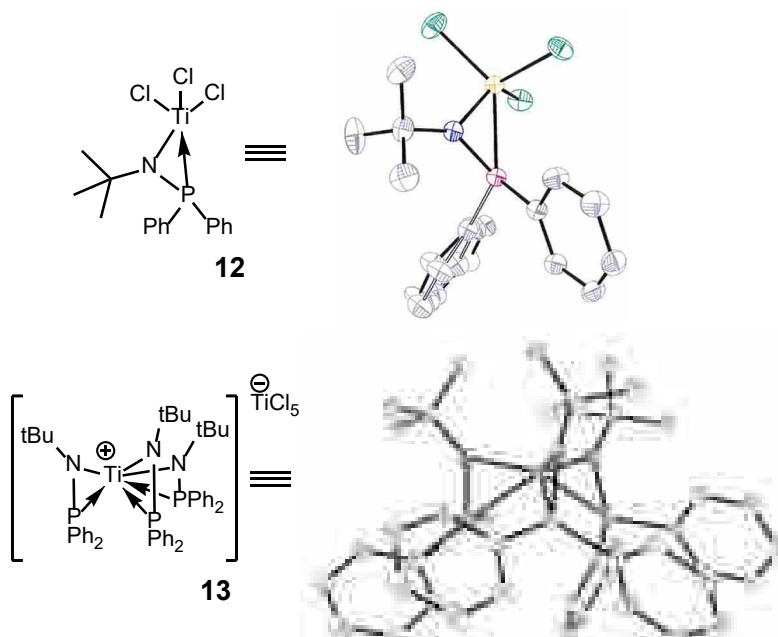


Figure 2.3. Novel titanium-containing ligands. Hydrogens omitted for clarity.

Phosphinoamide ligands like these contain a dynamic titanium-phosphorous bond.¹¹ This allows the phosphorous to break its coordination to titanium, enabling it to capture a palladium atom from solution and generate a bimetallic complex that contains a Pd-Ti dative interaction. With this dynamic titanium-phosphorous bond in mind, we combined [Pd(methallyl)Cl]₂, silver triflate, and ligand **12**. We were able to monitor the formation of the palladium-phosphorous bond by ³¹P NMR. The spectra showed the titanium-phosphorous peak (-11.0 ppm) disappear as the palladium-phosphorous peak (-2.6 ppm) appeared. To date, we have been unsuccessful in our attempts to isolate heterobimetallic complexes with ligands **12** and **13**, but we believe the ³¹P experiments provide strong evidence that these ligands are able to form heterobimetallic complexes *in situ*. We used ligands **12** and **13** in the allylic amination of methallyl chloride and **3** in the presence of [Pd(methallyl)Cl]₂ and silver triflate and found that each ligand provided quantitative yields of the amination product **4a** after 2.5 h (Figure 2.4). Importantly, we have not found a monometallic Pd catalyst capable of performing this allylic amination at room temperature, suggesting the importance of the titanium atom in each of these ligands. This result also helps show that titanium-phosphinoamide ligands are very useful in enabling catalysis in allylic aminations with hindered secondary amines. The formation of the metal-metal dative interaction allows electron density to transfer to titanium making the catalytically active palladium more electrophilic.

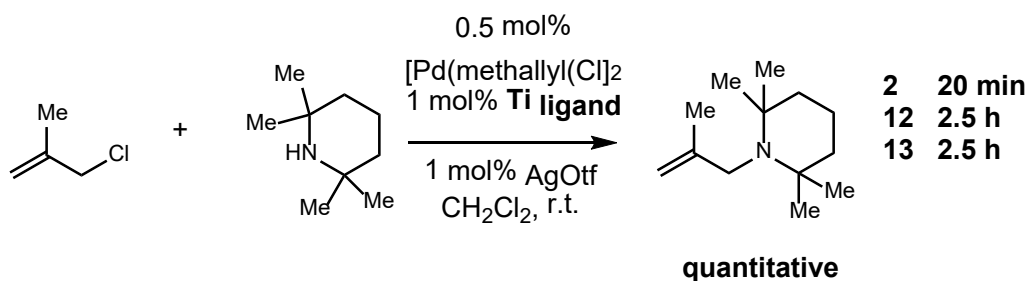
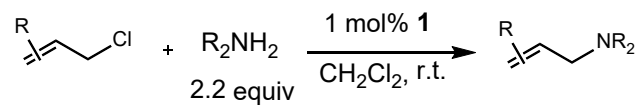


Figure 2.4. Allylic aminations using different Ti ligands

2.2.4 Substrate Scope and Reactivity of Secondary Hindered Amines

We then began looking at the substrate scope that can be used in the allylic chloride amination reaction by varying the amine as well as the allylic chloride (Table 2.2). A variety of sterically hindered secondary amine nucleophiles were able to readily undergo allylic substitution with methallyl chloride (entries 1-7). Many of these aminations were complete within ten minutes. The bis(trimethylsilyl)amine was able to undergo the reaction at room temperature, but took 4.5 hours to go to completion. The only substrate that failed to react was tert-amyl-tert-butylamine. A series of allylic electrophiles were also shown to undergo the reaction. These included crotyl, cinnamyl, and allyl chlorides. Each of these chlorides reacted in high yields at room temperature (entries 8-10). Allyl acetates and allyl carbonates gave low yields in the allylic amination reaction, which we believe is due to the formation of Lewis basic acetate or alkoxide byproducts that can lead to catalyst decompositions. (entries 11 and 12).

Table 2.2. Substrate Scope with Hindered Amines



entry ^a	amine	chloride	4	yield ^b
1 ^c			4a	99%
2			4b	72%
3			4c	98%
4			4d	99%
5			4e	82%
6 ^d			4f	99% ^e
7			4g	<5%
8 ^c			4h	97% ^{f,g}
9 ^c			4i	87% ^f
10 ^c			4j	85%
11 ^d			4j	5% ^e
12 ^d			4i	33% ^e
13 ^c			4h	78% ^{f,h}

^aReactions run with 1 mmol of allyl chloride, 2.2 mmol of amine, and 0.01 mmol of **1** (or 0.005 mmol of [Pd(methallyl)Cl]₂, 0.01 mmol of **2**, and 0.01 mmol of AgOTf in CDCl₃ or CH₂Cl₂ (1M) for 10 min at room temperature. ^bIsolated yields. ^cRun for 20 min. ^dRun for 4.5 h. ^eInternal standard yield. ^fLinear product only. ^g5:1 *trans/cis*. ^h1.3:1 *trans/cis*. C-Hex = cyclohexyl

2.2.5 Intramolecular Aminations

We also looked at the ability of hindered amines to undergo intramolecular cyclizations to produce pyrrolidine and piperidine products. It has been previously shown that these types of cyclizations with hindered amines require long reaction times and harsh conditions, and with some substrates failing altogether. However using heterobimetallic complex **1** we have been able to get these intramolecular aminations to occur at room temperature within 10 min, and with high yields (Figure 2.5). The reaction formed both 5- and 6-membered heterocycles (**14** and **15** respectively) in high yields. We were also able to form a morpholine heterocycle (**16**) in good yield.

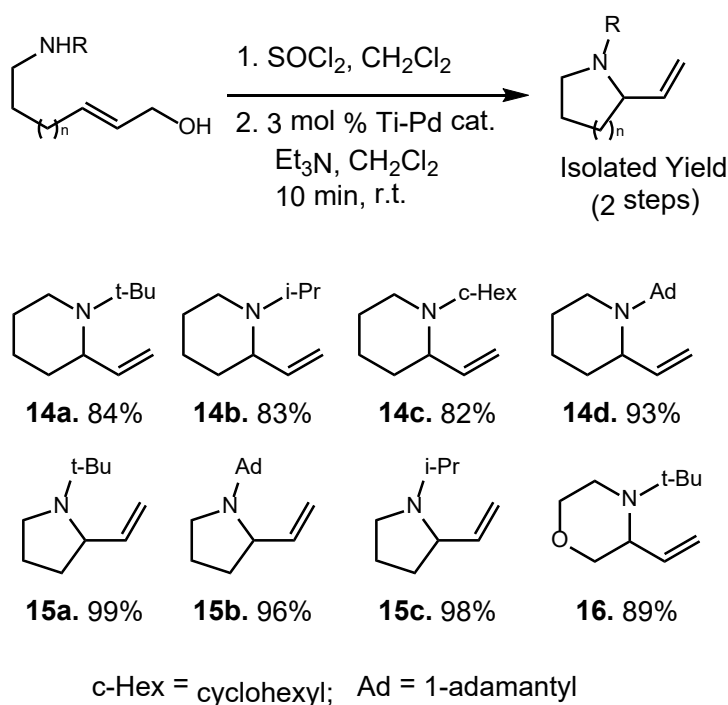


Figure 2.5. Intramolecular aminations for heterocycle synthesis

2.3 CONCLUSION

In conclusion, we have established that Pd-Ti heterobimetallic complexes can efficiently catalyze allylic aminations, including aminations with hindered secondary amine nucleophiles at room

temperature. Various titanium ligands were used in these aminations by forming a dative titanium palladium bond *in situ*. These catalysts can be used with various hindered secondary amines and in the formation of pyrrolidines and piperidines by intramolecular cyclizations. These results show the potential that heterobimetallic complexes have in enabling a variety of transformations in organic synthesis.

2.4 REFERENCES

(1) For reviews, see:

(a) Cooper, B. G.; Napoline, J. W.; Thomas, C. M., Catalytic Applications of Early/Late Heterobimetallic Complexes. *Catal. Rev.* **2012**, *54*, 1.

(b) Oelkers, B.; Butovskii, M. V.; Kempe, R., f-Element-Metal Bonding and the Use of the Bond Polarity to Build Molecular Intermetalloids. *Chem. Eur. J.* **2012**, *18*, 13566.

(c) Mandal, S. K.; Roesky, H. W., Assembling Heterometals through Oxygen: An Efficient Way to Design Homogeneous Catalysts. *Acc. Chem. Res.* **2010**, *43*, 248.

(d) Ritleng, V.; Chetcuti, M. J., Hydrocarbyl Ligand Transformations on Heterobimetallic Complexes. *Chem. Rev.* **2007**, *107*, 797.

(e) Collman, J. P.; Boulatav, R., Heterodinuclear Transition-Metal Complexes with Multiple Metal-Metal Bonds. *Angew. Chem., Int. Ed.* **2002**, *41*, 3948.

(f) Gade, L. H., Highly Polar Metal-Metal Bonds in “Early-Late” Heterodimetallic Complexes. *Angew. Chem., Int. Ed.* **2000**, *39*, 2658.

(g) Wheatley, N.; Kalck, P., Structure and Reactivity of Early-Late Heterobimetallic Complexes. *Chem. Rev.* **1999**, *99*, 3379.

(2) For selected recent examples, see:

(a) Tereniak, S. J.; Carlson, R. K.; Clouston, L. J.; Young, V. G., Jr.; Bill, E.; Maurice, R.; Chen, Y.-S.; Kim, H. J.; Gagliardi, L.; Lu, C. C., Role of the Metal in the Bonding and Properties of Bimetallic Complexes Involving Manganese, Iron, and Cobalt. *J. Am. Chem. Soc.* **2014**, *136*, 1842.

(b) Clouston, L. J.; Siedschlag, R. B.; Rudd, P. A.; Planas, N.; Hu, S.; Miller, A. D.; Gagliardi, L.; Lu, C. C., Systematic Variation of Metal-Metal Bond Order in Metal-Chromium Complexes. *J. Am. Chem. Soc.* **2013**, *135*, 13142.

(c) Cooper, B. G.; Fafard, C. M.; Foxman, B. M.; Thomas, C. M., Electronic Factors Affecting Metal-Metal Interactions in Early/Late Heterobimetallics: Substituent Effects in Zirconium/Platinum Bis(phosphinoamide) Complexes. *Organometallics* **2010**, *29*, 5179.

(d) Greenwood, B. P.; Forman, S. L.; Rowe, G. T.; Chen, C.-H.; Foxman, B. M.; Thomas, C. M., Multielectron Redox Activity Facilitated by Metal-Metal Interactions in Early/Late

Heterobimetallics: Co/Zr Complexes Supported by Phosphinoamide Ligands. *Inorg. Chem.* **2009**, *48*, 6251.

(e) Nippe, M.; Berry, J. F., Introducing a Metal-Metal Multiply Bonded Group as an “Axial Ligand” to Iron: Synthetic Design of a Linear Cr-Cr-Fe Framework. *J. Am. Chem. Soc.* **2007**, *129*, 12684.

(f) Nagashima, H.; Sue, T.; Oda, T.; Kanemitsu, A.; Matsumoto, T.; Motoyama, Y.; Sunada, Y., Dynamic Titanium Phosphinoamides as Unique Bidentate Phosphorus Ligands for Platinum. *Organometallics*, **2006**, *25*, 1987.

(3) (a) Bariwal, J.; Van der Eycken, E., C-N bond forming cross-coupling reactions: an overview. *Chem. Soc. Rev.* **2013**, *42*, 9283.

(b) *Science of Synthesis, Cross Coupling and Heck-Type Reactions*, Vol. 2; Molander, G. A., Wolfe, J. P., Larhed, M., Eds.; Thieme: Stuttgart, **2013**.

(c) McDonald, R. I.; Liu, G.; Stahl, S. S., Palladium(II)-Catalyzed Alkene Functionalization via Nucleopalladation: Stereochemical Pathways and Enantioselective Catalytic Applications. *Chem. Rev.* **2011**, *111*, 2981.

(d) Wolfe, J. P., Synthesis of Heterocycles via Metal-Catalyzed Reactions that Generate One or More Carbon-Heteroatom Bonds. *Top. Heterocycl. Chem.* **2013**, *32*, 1.

(e) Schultz, D. M.; Wolfe, J. P., Recent Developments in Palladium-Catalyzed Alkene Aminoarylation Reactions for the Synthesis of Nitrogen Heterocycles. *Synthesis*, **2012**, *44*, 351.

(4) (a) Trost, B. M.; Lee, C. *In Catalytic Asymmetric Synthesis*, 2nd Ed.; Wiley-VCH: New York, **2010**; pp 593-649.

(b) Dieguez, M.; Pamies, O., Biaryl Phosphites: New Efficient Adaptive Ligands for Pd-Catalyzed Asymmetric Allylic Substitution Reactions. *Acc. Chem. Res.* **2010**, *43*, 312.

(c) Lu, Z.; Ma, S., Metal-Catalyzed Enantioselective Allylation in Asymmetric Synthesis. *Angew. Chem., Int. Ed.* **2008**, *47*, 258.

(d) Trost, B. M.; Machacek, M. R.; Aponick, A., Predicting the Stereochemistry of Diphenylphosphino Benzoic Acid (DPPBA)-Based Palladium-Catalyzed Asymmetric Allylic Alkylation Reactions: A Working Model. *Acc. Chem. Res.* **2006**, *39*, 747.

(e) Dai, L.-X.; Tu, T.; You, S.-L.; Deng, W.-P.; Hou, X.-L., Asymmetric Catalysis with Chiral Ferrocene Ligands. *Acc. Chem. Res.* **2003**, *36*, 659.

(f) Helmchen, G.; Pfaltz, A., Phosphinooxazolines – A New Class of Versatile, Modular P,N-Ligands for Asymmetric Catalysis. *Acc. Chem. Res.* **2000**, *33*, 336.

(g) Johannsen, M.; Jorgensen, K. A., Allylic Amination. *Chem. Rev.* **1998**, *98*, 1689.

(5) (a) Tosatti, P.; Nelson, A.; Marsden, S. P., Recent advances and applications of iridium-catalysed asymmetric allylic substitution. *Org. Biomol. Chem.* **2012**, *10*, 3147.

(b) Milhau, L.; Guiry, P. J., Palladium-Catalyzed Enantioselective Allylic Substitution. *Top. Organomet. Chem.* **2011**, *38*, 95.

(c) Hartwig, J. F.; Stanley, L. M., Mechanistically Driven Development of Iridium Catalysts for Asymmetric Allylic Substitution. *Acc. Chem. Res.* **2010**, *43*, 1461.

(d) Helmchen, G.; Dahnz, A.; Dubon, P.; Schelwies, M.; Weihofen, R., Iridium-catalysed asymmetric allylic substitutions. *Chem. Commun.* **2007**, 675.

(e) Helmchen, G. *In Asymmetric Synthesis*; Christman, M., Brase, S., Eds.; Wiley-VHC: Weinheim, **2007**; pp 95-99.

(f) Miyabe, H.; Takemoto, Y., Regio- and Stereocontrolled Palladium- or Iridium-Catalyzed Allylation. *Synlett* **2005**, *11*, 1641.

(6) For recent selected examples, see:

(a) Kawatsure, M.; Terasaki, S.; Minakawa, M.; Hirakawa, T.; Ikeda, K.; Itoh, T., Enantioselective Allylic Amination of Trifluoromethyl Group Substituted Racemic and Unsymmetrical 1,3-Disubstituted Allylic Esters by Palladium Catalysts. *Org. Lett.* **2014**, *16*, 2442.

(b) Kawatsura, M.; Uchida, K.; Terasaki, S.; Tsuji, H.; Minakawa, M.; Itoh, T., Ruthenium-Catalyzed Regio- and Enantioselective Allylic Amination of Racemic 1-Arylallyl Esters. *Org. Lett.* **2014**, *16*, 1470.

(c) Boualy, B.; Harrad, M.; El Houssame, S.; El Firdoussi, L.; Ait Ali, M.; Karim, A., Copper(II) catalyzed allylic amination of terpenic chloride in water. *Catal. Commun.* **2012**, *19*, 46.

(d) Touchet, S.; Carreaux, F.; Molander, G. A.; Carboni, B.; Bouillon, A., Iridium-Catalyzed Allylic Amination Route to α -Aminoboronates: Illustration of the Decisive Role of Boron Substituents. *Adv. Synth. Catal.* **2011**, *353*, 3391.

(e) Tosatti, P.; Horn, J.; Campbell, A. J.; House, D.; Nelson, A.; Marsden, S. P., Iridium-Catalyzed Asymmetric Allylic Amination with Polar Amines: Access to Building Blocks with Lead-Like Molecular Properties. *Adv. Synth. Catal.* **2010**, *352*, 3153.

- (f) Defieber, C.; Ariger, M. A.; Moriel, P.; Carreira, E. M., Iridium-Catalyzed Synthesis of Primary Allylic Amines from Allylic Alcohols: Sulfamic Acid as Ammonia Equivalent. *Angew. Chem., Int. Ed.* **2007**, *46*, 3139.
- (g) Roggen, M.; Carreira, E. M., Stereospecific Substitution of Allylic Alcohols To Give Optically Active Primary Allylic Amines: Unique Reactivity of a (P,alkene)Ir Complex Modulated by Iodide. *J. Am. Chem. Soc.* **2010**, *132*, 11917.
- (h) Pouy, M. J.; Stanley, L. M.; Hartwig, J. F., Enantioselective, Iridium-Catalyzed Monoallylation of Ammonia. *J. Am. Chem. Soc.* **2009**, *131*, 11312.
- (i) Adak, L.; Chattopadhyay, K.; Ranu, B. C., Palladium Nanoparticle-Catalyzed C-N Bond Formation. A Highly Regio- and Stereoselective Allylic Amination by Allyl Acetates. *J. Org. Chem.* **2009**, *74*, 3982.
- (j) Nagano, T.; Kobayashi, S., Palladium-Catalyzed Allylic Amination Using Aqueous Ammonia for the Synthesis of Primary Amines. *J. Am. Chem. Soc.* **2009**, *131*, 4200.
- (k) Kawatsura, M.; Ata, F.; Hirakawa, T.; Hayase, S.; Itoh, T., Ruthenium-catalyzed linear selective allylic aminations of monosubstituted allyl acetates. *Tetrahedron Lett.* **2008**, *49*, 4873.
- (l) Dubovyk, I.; Watson, I. D. G.; Yudin, A. K., Chasing the Proton Culprit from Palladium-Catalyzed Allylic Amination. *J. Am. Chem. Soc.* **2007**, *129*, 14172.
- (m) Takeuchi, R.; Ue, N.; Tanabe, K.; Yamashita, K.; Shiga, N., Iridium Complex-Catalyzed Allylic Amination of Allylic Esters. *J. Am. Chem. Soc.* **2001**, *123*, 9525.
- (7) Tsutsumi, H.; Sunada, Y.; Shiota, Y.; Yoshizawa, K.; Nagashima, H., Nickel(II), Palladium(II), and Platinum(II) η^3 -Allyl Complexes Bearing a Bidentate Titanium(IV) Phosphinoamide Ligand: A Ti-M₂ Dative Bond Enhances the Electrophilicity of the π -Allyl Moiety. *Organometallics*, **2009**, *28*, 1988.
- (8) Cationic bis(triphenylphosphine)(η -allyl)palladium complexes are among the most active catalysts for allylic aminations. See: Canovese, L.; Visentin, F.; Levi, C.; Dolmella, A., Synthesis, characterization, dynamics and reactivity toward amination of η^3 -allyl palladium complexes bearing mixed ancillary ligands. Evaluation of the electronic characteristics of the ligands from kinetic data. *Dalton Trans.* **2011**, *40*, 966.
- (9) Silver triflate led to faster reaction kinetics in the *in situ* formation protocol, but its omission still provided full conversion in 1 h.
- (10) ³¹P NMR of the *in situ* formed catalyst solution shows a characteristic shift from -17.2 ppm for ligand **2** to +9.08 ppm for complex **1**.

(11) (a) Sue, T.; Sunada, Y.; Nagashima, H., Zirconium(IV) Tris(phosphinoamide) Complexes as a Tripodal-Type Metalloligand: A Route to Zr-M (M=Cu, Mo, Pt) Heterobimetallic Complexes. *Eur. J. Inorg. Chem.* **2007**, 2897.

(b) Kuhl, O.; Koch, T.; Somoza, F. B., Jr.; Junk, P. C.; Hey-Hawkins, E.; Plat, D.; Eisen, M. S., Formation of elastomeric polypropylene promoted by the dynamic complexes $[\text{TiCl}_2(\text{N}(\text{PPh}_2)_2)_2]$ and $[\text{Zr}(\text{NPhPPH}_2)_4]$. *J. Organomet. Chem.* **2000**, 604, 116.

(12) Olszewska, B.; Kryczka, B.; Zawisza, A., Enantioselective synthesis of *N*-heterocycles via intramolecular Pd(0)-catalysed allylic amination. *Tetrahedron*, **2013**, 69, 9551.

Chapter 3

Origins of Fast Catalysis in Allylic Amination Reactions Catalyzed by Pd-Ti Heterobimetallic Complexes

Computational Studies were performed by Benjamin M. Kay, Scott A. Michaelis, and Diana L. Anderson. Portions of this work have been previously published:

Ellis, D. L. (2015). *A Study of Allylic Aminations as Catalyzed by Pd-Ti Heterobimetallic Complexes*. Brigham Young University, Provo, Utah.

Walker, W. K.; Kay, B. M.; Michaelis, S. A.; Anderson, D. L.; Smith, S. J.; Ess, D. H.; Michaelis, D. J., Origin of Fast Catalysis in Allylic Amination Reactions Catalyzed by Pd-Ti Heterobimetallic Complexes. *J. Am. Chem. Soc.*, **2015**, *137*, 7371-7378.

3.1 INTRODUCTION

Heterobimetallic transition-metal complexes have the potential to be extremely useful catalysts for organic transformations.¹ These complexes have the ability to have transition metal – transition metal interactions that can increase the reactivity of the reactive metal center.² We are interested in the metal-metal dative interaction that can form between late and early transition metals.³ Combining two electronically different metals through a dative interaction has the potential to change the electron density and Lewis acidity of the reactive metal.⁴

Recently, there has been significant interest in the design and synthesis of transition-metal heterobimetallic complexes that can potentially form dative metal-metal interactions.³ Even with these increased efforts, heterobimetallic catalysts are not widely used for organic synthesis. Also, there is a lack of understanding about how dative transition metal – transition metal interactions impact catalysis.⁵ If we could understand how these heterobimetallic metal-metal interactions impact the rate of catalysis then we could develop new heterobimetallic catalysts that could enhance current organic synthesis methods. With this in mind the Michaelis and Ess groups began

using computational and experimental analysis in order to identify, quantify, and test the improved catalysis of Pd-Ti heterobimetallic complexes in allylic amination reactions.⁶

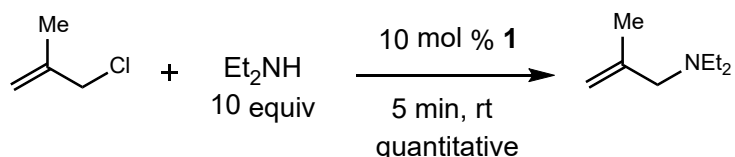


Figure 3.1. Amination of methallyl chloride using catalyst **1**

The Nagashima group recently reported the Pd-Ti heterobimetallic complex **1**, which catalyzed the allylic amination of methallyl chloride with diethylamine (Figure 3.1). They also compared the reactivity of complex **1** with a monometallic Pd catalyst (**3**) by performing a stoichiometric reaction of diethylamine with each complex (Figure 3.2). Heterobimetallic complex **1** was able to completely add diethylamine to generate allyl amine **2** in <5 min at room temperature. The monometallic Pd complex **3** was unable to undergo the amine addition after several hours.

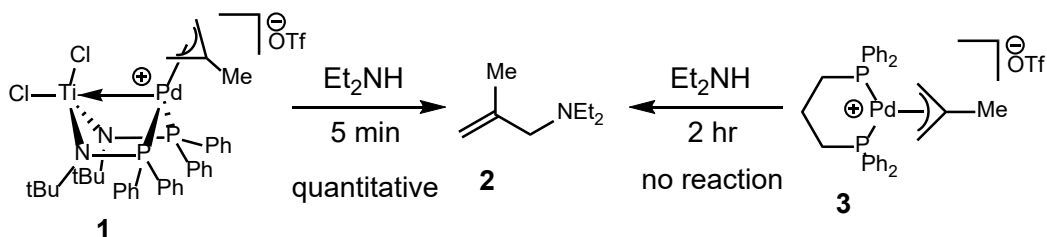


Figure 3.2. Stoichiometric Studies Previously Reported for Reductive Amine Addition

From these results, Nagashima postulated that the dative interaction between Pd and Ti in complex **1** increased the catalytic activity allowing the allylic amination to occur. However the different reactivity between complex **1** and **3** could be attributed to the different ligand composition, geometry, and electronics of the catalysts. Complex **1** has a bidentate phosphinoamide ligand structure and has a different P-Pd-P coordination angle than complex **3**. Both of these differences

could impact the catalytic reactivity significantly.⁸ These differences show that the comparison of complex **1** and **3** does not adequately measure the impact of the Pd-Ti interaction on catalysis. Therefore it still remains unclear whether ligand effects, the dative metal-metal interaction, or a combination of the two are responsible for the enhanced reactivity of complex **1** in this allylic amination reaction.

We performed experimental and computational analysis that would help determine the cause of the enhanced catalytic reactivity of complex **1**. We also wanted to quantify the impact of the Pd-Ti interaction over the P-Pd-P coordination angles as well as the ligand composition.

3.2 RESULTS AND DISCUSSION

3.2.1 *Computational Assessment of Heterobimetallic Pd-Ti Complex 1 and Mechanism for Allylic Amination*

We began by using density functional calculations in order to confirm the allylic amination mechanism when heterobimetallic complex **1** is used. We wanted to quantify how the Pd-Ti interaction affected each step in the catalytic cycle. There has been an abundance of reported studies using palladium η^3 -allyl complexes.^{9,10} After exploring a wide variety of possible mechanisms, we found that heterobimetallic complex **1** catalyzes the reaction through a similar mechanism as the studies previously reported. The lowest-energy mechanism begins with an outer-sphere amine addition then a ligand exchange (**4** to **5**) followed by an inner-sphere Pd⁰ to Pd^{II} oxidation in order to regenerate complex **1** (Figure 3.3). We were able to confirm that inner-sphere amine-allyl reductive elimination, C-Cl bond oxidative insertion, and S_N2 pathways using catalyst **1** were all higher in energy.

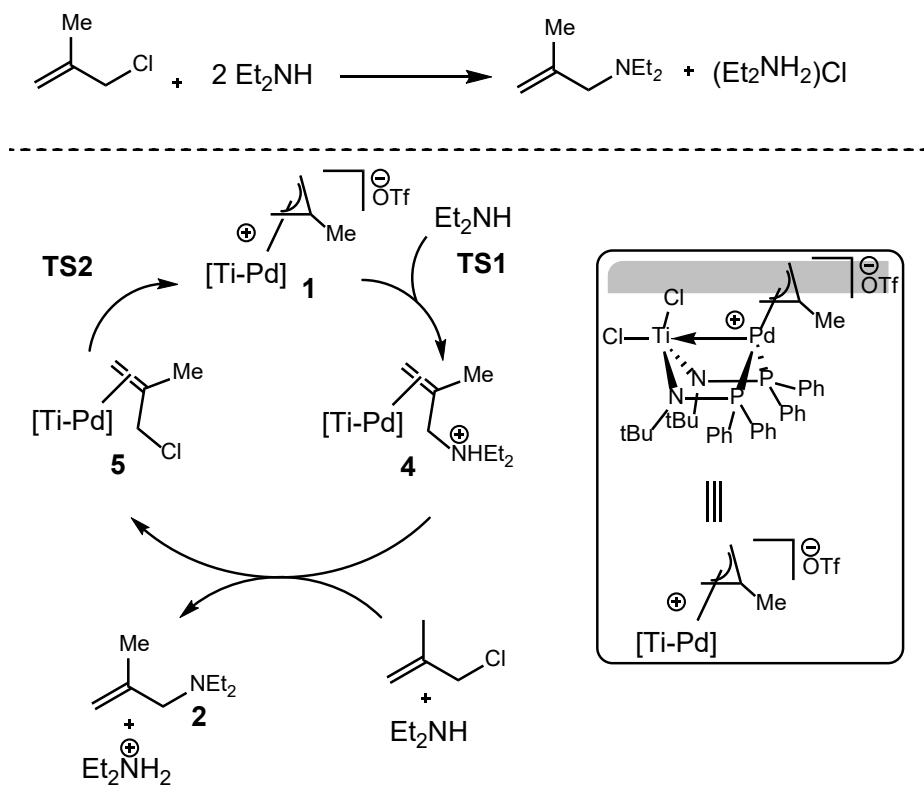


Figure 3.3. Calculated mechanism for allylic amination catalyzed by **1** (kcal/mol)

As shown in Figure 3.3, the first step in the catalytic cycle is the nucleophilic addition of diethylamine to one of the terminal η^3 -allyl carbons (**TS1**). This Pd^{II} to Pd⁰ reduction results in the formation of the Pd(η^3 -methallyl ammonium) complex **4**. The nucleophilic addition step requires $\Delta G^\ddagger = 15.8$ kcal/mol and is endergonic by 1.6 kcal/mol with respect to complex **1**, diethylamine, and methallyl chloride (Figure 3.4). It was observed that the Pd-Ti bond distance shortens as the diethylamine continues to add. The bond length went from 2.88 Å to 2.77 Å, which indicates that the interaction between the two metals increases. This bond shortening suggests that stabilization is occurring due to the ability of titanium to withdraw electron density from the newly forming electron rich palladium center.

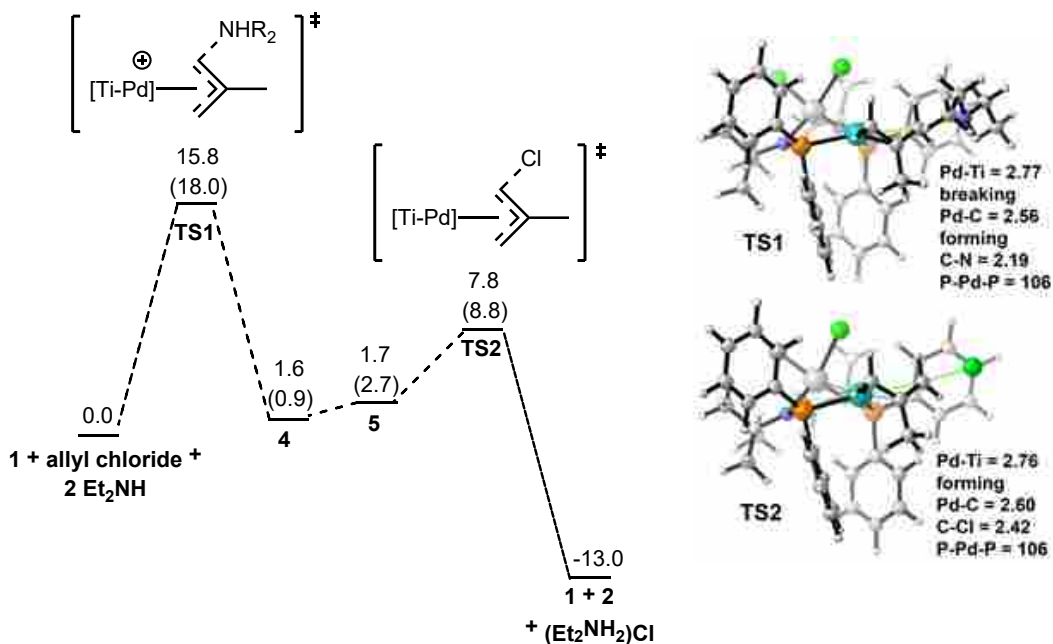


Figure 3.4. (Left) M06 free energy landscape for Et₂NH reductive addition and methallyl chloride-induced Pd⁰ to Pd^{II} oxidation. ωB97X-D free energy values given in parentheses. Free energies in kcal/mol. (Right) Transition-state structures. Bond lengths reported in Å.

The next step in the cycle is a ligand exchange where the allyl ammonium intermediate dissociates and allyl chloride coordinates to the palladium (**4** to **5**, Figure 3.3). The heterobimetallic catalyst **1** is regenerated by an intramolecular substitution reaction in which **5** forms a Pd-C bond on the backside of the C-Cl bond at the same time as the chloride is ejected (**TS2**, Figure 3.4). One potential problem for future organic transformations is the possible overstabilization of the Pd⁰ intermediate from the Pd-Ti interaction, which would raise the barrier for oxidative addition. While we see an increase in the barrier of oxidative addition, it is not enough to cause the Pd⁰ to Pd^{II} step to become rate limiting. This transition step (**TS2**) requires $\Delta G^\ddagger = 7.8$ kcal/mol and is 8.0 kcal/mol lower than **TS1**. These calculations showed **TS1** is rate determining, therefore to improve catalysis the barrier for reductive addition needs to be lowered.

So far our experiments have assumed that the metal-metal dative bond of complex **1** is responsible for the catalysis. There are several possible transformations that could occur in which the active catalyst does not have a dative interaction. Some of the possible transformations that we looked at are shown in Figure 3.5. A more electron deficient Pd intermediate could form from the dissociation of one phosphine from Pd and coordination to Ti. This could lead to faster catalysis where there isn't a Pd-Ti interaction present (**1-slip**). The ΔG^\ddagger for amine addition for **1-slip** is 25.5 kcal/mol, which is significantly higher than **TS1**. When a phosphine ligand slips to Ti the coordination of the chloride or diethylamine to Pd also have higher ΔG^\ddagger values than **TS1** for amine addition. There is a large buildup of chlorine as the reaction progresses, so we looked at the possible coordination of chloride to the Ti and Pd metal centers (**1-Cl**). We found that chloride coordination to Ti dissolves the Pd-Ti interaction and the amine addition has a $\Delta G^\ddagger = 22.7$ kcal/mol. Therefore when the chloride concentration is high chloride dissociation occurs and catalysis follows the reaction pathway shown in Figure 3.3.

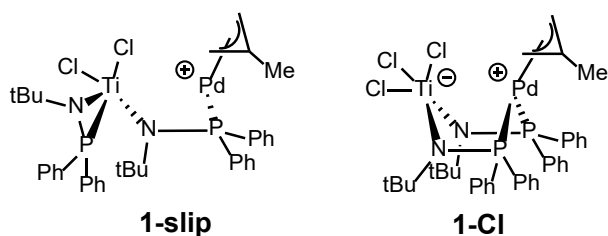


Figure 3.5. Possible alternative species involved in catalysis

Moving forward, we were confident that the catalytically active complex **1** had an intact Pd-Ti interaction during allylic amination. We then wanted to quantify the significance of the Pd-Ti interaction. In order to do this we compared the catalytic free energies using the **1 (flat)** and **1 (boat)** conformations (Figure 3.6 and 3.7). In the **1(flat)** conformation the Pd-Ti interaction has been severed. The amine addition barrier of this conformation increased to 20.3 kcal/mol, and the oxidative addition of the methallyl chloride increased to 10.2 kcal/mol. This result shows that the Pd-Ti interaction has a stabilization effect of 4.5 kcal/mol, which increases the rate by 10^3 . This rate enhancement is due to the Pd-Ti interaction stabilizing the Pd^0 as it is forming.

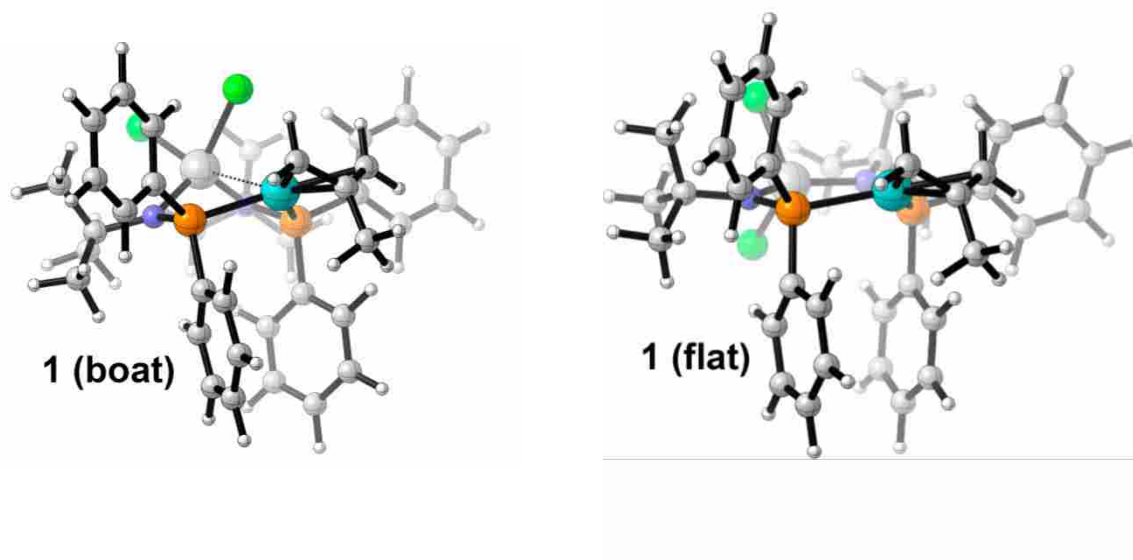


Figure 3.6. Boat and flat conformations of catalyst **1**

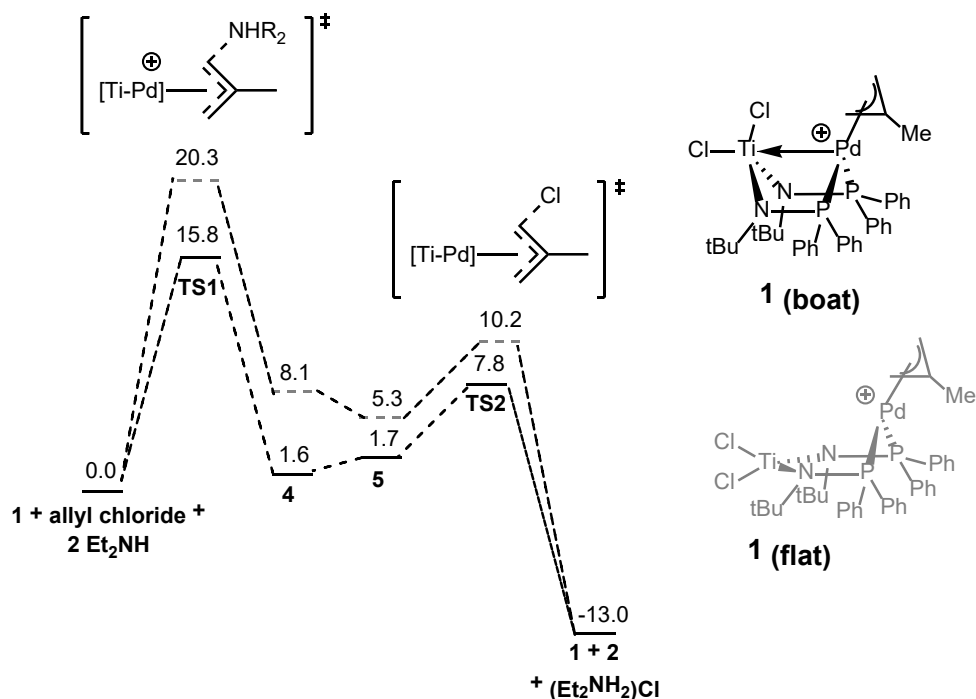


Figure 3.7. Comparison of allylic amination M06 free energy landscapes catalyzed by **1 (boat)** and **1 (flat)** (kcal/mol)

We next looked at whether the Pd-Ti interaction formed because it was electronically favorable or was due to the ligand structure forcing the two metals into close proximity. To determine the effect of the ligand structure we replaced the *tert*-butyl groups on the nitrogen in the phosphinoamide framework with methyl groups (Figure 3.8). We determined that the boat structure was retained but the bond length between palladium and titanium increased from 2.88 Å to 3.38 Å. This would indicate that the Pd-Ti interaction has been lost. Therefore the *tert*-butyl groups are necessary for the formation of the Pd-Ti interaction, which in turn is needed to lower the barrier for reductive addition. When the amine addition transition state was calculated for the methylated boat complex the Pd-Ti bond length increased by 0.08 Å when compared to **TS1**. The increase in bond length was enough to inhibit the stabilization effect gained by the Pd-Ti interaction, which slowed down the addition of amine.

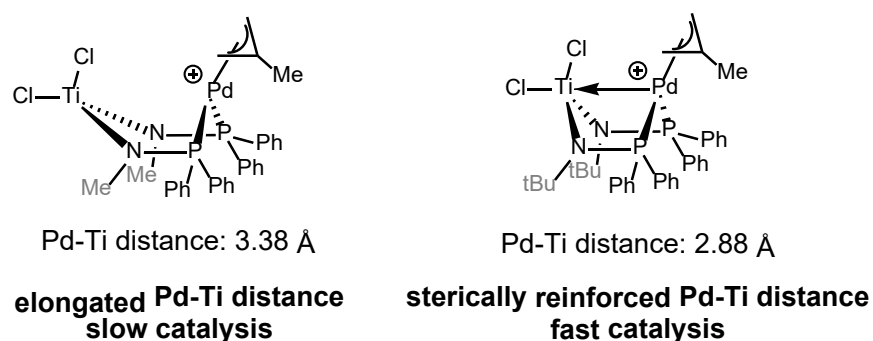


Figure 3.8. Comparison of ground-state boat conformations and corresponding reactivity for *N*-^tBu and *N*-Me

3.2.2 Experimental and Computational Evaluation of the Impact of Replacing TiCl_2 to Remove the *Pd-Ti* Interaction

Wanting to find another way to evaluate the effect of the Pd-Ti interaction in allylic aminations we designed, synthesized and characterized complex **6** (Figure 3.9). Complex **6** was computationally and experimentally designed to mimic the structure and electronics of complex **1** by maintaining the phosphinoamide scaffold minus the titanium. The TiCl_2 group was replaced with an ethylene bridge between the nitrogen atoms. Single crystal X-ray analysis confirmed that complex **6** retains the boat conformation found in complex **1**. The P-Pd-P coordination angle of **6** was found to be 103.8° which only slightly differs from complex **1** (104.3°). Unlike complex **1**, complex **6** only had a modest amount of catalytic activity when used in the allylic amination with diethylamine (Figure 3.10). Complex **6** gave ~50% conversion after 3 h (~TOF=17), whereas complex **1** provided complete amination within <1 min (~TOF>1200). This result shows that the titanium is needed in order to significantly increase the rate of allylic amination independently of the phosphinoamide ligand.

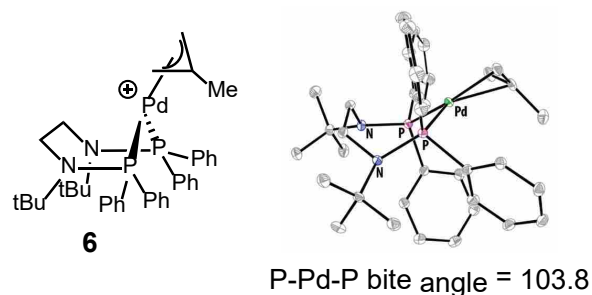


Figure 3.9. Ethylene bridged bidentate phosphinoamine Pd-Ti complex

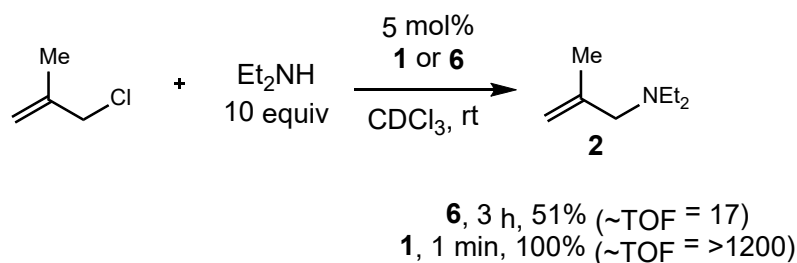


Figure 3.10. Reactivity of complex **1** and **6** in the allylic amination reaction

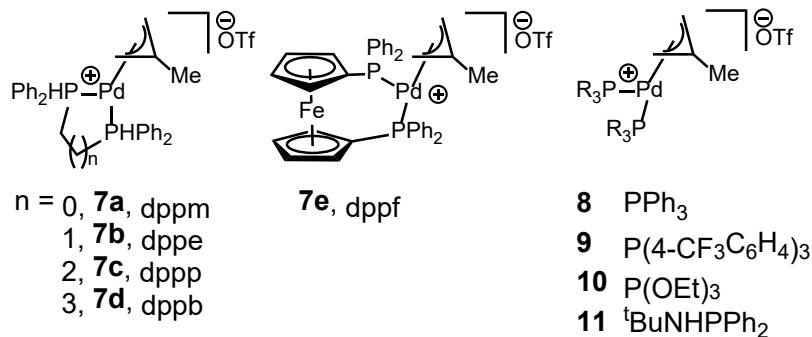
We next examined the catalytic cycle of allylic amination using complex **6** computationally. Our calculations showed that the transition state geometries of complex **1** and **6** are similar, but the diethylamine addition to complex **6** was $\Delta G^\ddagger = 23.8$ kcal/mol. This is about 8.0 kcal/mol higher than the barrier for diethylamine addition with complex **1**. This difference in energy corresponds to $\sim 10^5$ decrease in rate which resembles the results seen in Figure 3.10.

The computational and experimental results we found support the need of the Pd-Ti interaction found in complex **1** in order to see an enhanced rate catalytic allylic amination reactions. We determined that the turnover-limiting reductive addition of diethylamine is lowered when there is a

Pd-Ti interaction present. Finally, we determined that the Pd-Ti interaction is dependent upon the *tert*-butyl groups sterically forcing a boat confirmation in the ground and transition states of the catalytic cycle.

3.2.3 Impact of Coordination Angle and Electronic Effects on Catalysis

We have been able to show the importance of the Pd-Ti interaction for fast catalysis using complex **1**, but this does not necessarily mean that a monometallic Pd catalyst would be able to react just as fast, if not faster. The comparison of complex **1** and complex **2** does not take into account the ligand structure and geometries of each catalyst. Therefore we designed and synthesized a series of monometallic Pd catalysts that would help us determine the significance of ligand structure and electronics of the catalyst (Table 3.1).

Table 3.1. Reactivity Comparison for Monometallic Pd-Catalyzed Allylic Aminations

entry ^a	complex	P-Pd-P angle	time	% conv. ^b	~TOF ^c
1	1	104°	<1 min	100	>1200
2	7a	72°	1 min	48	576
3	7b	86°	12 h	45	0.75
4	7c	95°	12 h	73	1.2
5	7d	99°	1 h	46	9.1
6	7e	101°	6 h	78	2.6
7	8		<1 min	100	>1200
8	9		<1 min	100	>1200
9	10		15 min	71	57
10	11		3 h	50	3.3

^aReactions performed using 1 mmol methallyl chloride, 10 equiv of diethylamine, and 0.05 mmol of the indicated preformed allyl complex in CDCl₃ (1 M) for indicated time. ^bDetermined by ¹H NMR analysis of the crude reaction mixture. ^cReported in (mmol product/mmol catalyst)/h.

Each catalyst was used in the allylic amination of diethylamine and methallyl chloride. Heterobimetallic complex **1** provided 100% conversion in 1 min with a catalyst loading of 5 mol% (entry 1). Other bis(phosphine) allyl complexes were catalytically active, but many had significantly lower TOFs (entries 2-6). The Bis(diphenylphosphino)methane catalyst **7a** had the

fastest catalytic rate of the bis(phosphine) ligands tested. This confirms the need for a particular P-Pd-P bite angle in order to increase the rate of allylic amination.^{14,15}

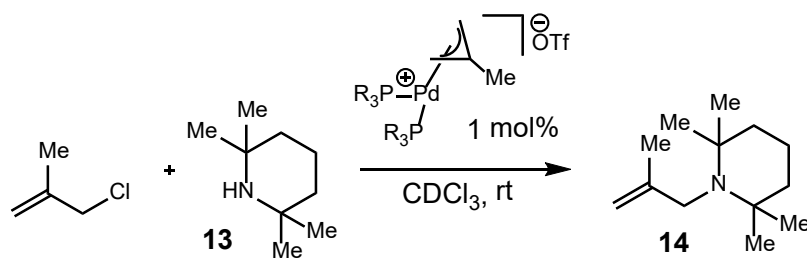
We also looked at different bis(monophosphine) palladium catalysts and found that certain complexes displayed similar reactivity to that of complex **1** (entries 8-11). The bis(triphenylphosphine) complex **8** (entry 7) had catalytic activity that was indistinguishable from complex **1**. The reported P-Pd-P coordination angle of complex **8** is 105.4°^{16,17}, which is very similar to complex **1** (104.3°). This suggests that a certain coordination angle is needed for the catalytic activity seen. The electron-deficient bis(triarylphosphine) complex **9** had a rate comparable to **8** (entry 8), but the triethylphosphite complex **10** and bis(phosphinoamine) complex **11** had slower rates (entries 9 and 11).

Since the reactivity of heterobimetallic complex **1** and complex **8** were so similar in the allylic amination reaction we calculated the activation barrier for the reductive addition of the amine for each complex. The diethylamine addition (**TS1**) to complex **8** had a $\Delta G^\ddagger = 21.3$ kcal/mol, which is not as low as the activation barrier for complex **1**. We believe that the similar turnover numbers for complex **1** and complex **8** are due to the inability to measure the kinetics of the reaction. We lowered the catalyst loading to 1 mol% and saw that catalyst **1** still provided 100% conversion in 1 min. However catalyst **8** only produced 28% of the product within 3 mins. This is further evidence that catalyst **1** is far superior than the other catalyst tested in the allylic amination reaction.

3.2.4 Testing the Limits of the Pd-Ti Interaction

We have previously shown that heterobimetallic complex **1** is able to efficiently catalyze the allylic amination of sterically hindered secondary amines.¹⁸ By using sterically strained 2,2,6,6-tetramethylpiperidine (TMP) (**13**) we are able to slow down the allylic amination which allowed us to distinguish the catalytic activity of **1** and **8**. Using 1 mol% catalyst loading of catalyst **1** we were able to get 85% conversion to product **14** within 15 min at room temperature (Table 3.2, entry 1). When catalyst **8** was used at room temperature no product formation was observed within 24 h (entry 2). When the reaction was heated to 90 °C for 24 h, complex **8** only gave 17% yield of the product (entry 3).

Table 3.2. Reactivity of Sterically Hindered Amine **13**



entry	complex	time	temp	%conv. ^b	~TOF ^c
1	1	15 min	r.t.	85%	340
2	8	24 h	r.t.	N.R.	-
3 ^d	8	24 h	90 °C	17%	0.7
4 ^d	9	24 h	90 °C	6%	0.2

^aReactions performed using 1 mmol of methyl allyl chloride, 2.2 equiv of amine, and 0.01 mmol of the indicated preformed allyl complex in CDCl₃ (0.1 M). ^bDetermined by ¹H NMR analysis. ^cReported in (mmol product/mmol catalyst)/h. ^dReaction run at 90 °C in a sealed vial. N.R. = No Reaction

We calculated the ΔG^\ddagger for addition of TMP to complex **1** to be 18.5 kcal/mol. This is ~3kcal/mol higher in energy than when diethylamine is added. When TMP is added to complex **8** the $\Delta G^\ddagger = 26.0$ kcal/mol. This energy is 4kcal/mol higher than the addition of diethylamine to complex **8** and 7.5 kcal/mol higher than for **1**. The Pd-Ti interaction in complex **1** stabilizes the Pd⁰ intermediate which makes the catalyst less sensitive to the bulkiness of the amine nucleophile. This allows fast catalysis even when hindered secondary amines are used. The ability to use normally unreactive substrates is a unique trait of this heterobimetallic complex and can possibly be used in future catalyst design.

In our previous work we showed that when allylic acetates were used in the allylic amination with **13**, complex **1** provided low yields.¹⁸ We believe that Lewis basic byproducts are formed which cause the catalyst to decompose or can deactivate the titanium by coordination to it. Another explanation is that the acetate is a poor leaving group compared to chloride, which would cause the turnover-limiting step to become the oxidative addition. When methallyl acetate (**15**) was used in the allylic amination with TMP only 16% conversion was observed before the reaction stalled (Figure 11). We calculated that the ΔG^\ddagger for **TS2** in this system was 16.0 kcal/mol higher than for methallyl chloride. This shows that the stabilization the Pd-Ti interaction gives to the Pd⁰ catalyst can be detrimental when the limiting step is the oxidation of Pd⁰. However when allylic trifluoroacetates are used the reaction proceeds quickly. This is most likely due to the ability of the stable trifluoroacetate leaving group, which allows the Pd⁰ oxidation to easily happen.



Figure 3.11. Allylic amination using allyl acetates and **13** catalyzed by **1**

3.3 CONCLUSION

Through combined experimental and computational results we have determined that the fast catalysis observed with complex **1** is due to the electron-withdrawing dative interaction between Pd and Ti. The catalysis is independent of the electronic properties found in the phosphinoamide ligand scaffold. The *tert*-butyl groups are able to force a boat conformation which allows the dative Pd-Ti interaction to occur.

This Pd-Ti interaction is able to efficiently catalyze allylic aminations using hindered amine nucleophiles under mild reaction conditions.¹⁸ These results show that highly reactive metal complexes can be formed by utilizing transition metal-transition metal interactions. These interactions could have an impact on catalyst design used in organic synthesis.

3.4 REFERENCES

(1) (a) Buchwalter, P.; Rose, J.; Braustein, P., Multimetallic Catalysis Based on Heterometallic Complexes and Clusters. *Chem. Rev.* **2015**, *115*, 28.

(b) Cooper, B. G.; Napoline, J. W.; Thomas, C. M., Catalytic Applications of Early/Late Heterobimetallic Complexes. *Catal. Rev. Sci. Eng.* **2012**, *54*, 1.

(c) Thomas, C. M., Metal-Metal Multiple Bonds in Early/Late Heterobimetallic Complexes: Applications Toward Small Molecule Activation and Catalysis. *Comments Inorg. Chem.* **2011**, *32*, 14.

(2) For reviews see:

(a) Oelkers, B.; Butovskii, M. V.; Kempe, R., f-Element-Metal Bonding and the Use of the Bond Polarity To Build Molecular Intermetalloids. *Chem. Eur. J.* **2012**, *18*, 13566.

(b) Mandal, S. K.; Roesky, H. W., Assembling Heterometals through Oxygen: An Efficient Way to Design Homogenous Catalysts. *Acc. Chem. Res.* **2010**, *43*, 248.

(c) Ritleng, V.; Chetcuti, M. J., Hydrocarbyl Ligand Transformations on Heterobimetallic Complexes. *Chem. Rev.* **2007**, *107*, 797.

(d) Collman, J. P.; Boulatav, R., Heterodinuclear Transition-Metal Complexes with Multiple Metal-Metal Bonds. *Angew. Chem., Int. Ed.* **2002**, *41*, 3948.

(e) Gade, L. H., Highly Polar Metal-Metal Bonds in “Early-Late” Heterodimetallic Complexes. *Angew. Chem., Int. Ed.* **2000**, *39*, 2658.

(f) Wheatley, N.; Kalck, P., Structure and Reactivity of Early-Late Heterobimetallic Complexes. *Chem. Rev.* **1999**, *99*, 3379.

(g) Stephan, D. W., Early-late heterobimetallics. *Coord. Chem. Rev.* **1989**, *95*, 41.

(3) Zhang, Y.; Roberts, S. P.; Bergman, R. G.; Ess, D. H., Mechanism and Catalytic Impact of Ir-Ta Heterobimetallic and Ir-P Transition Metal/Main Group Interactions on Alkene Hydrogenation. *ACS Catal.* **2015**, *5*, 1840.

(4) For selected recent examples, see:

(a) Kuppuswamy, S.; Cass, T. R.; Bezpalko, M. W.; Foxman, B. M.; Thomas, C. M., Synthesis and investigation of the metal-metal interactions in heterobimetallic Cr/Rh and Cr/Ir complexes. *Inorg. Chim. Acta.* **2014**, *424*, 167.

- (b) Tereniak, S. J.; Carlson, R. K.; Clouston, L. J.; Young, V. G., Jr.; Bill, E.; Maurice, R.; Chen, Y.-S.; Kim, H. J.; Gagliardi, L.; Lu, C. C., Role of the Metal in the Bonding and Properties of Bimetallic Complexes Involving Manganese, Iron, and Cobalt. *J. Am. Chem. Soc.* **2014**, *136*, 1842.
- (c) Clouston, L. J.; Siedschlag, R. B.; Rudd, P. A.; Planas, N.; Hu, S.; Miller, A. D.; Gagliardi, L.; Lu, C. C., Systematic Variation of Metal-Metal Bond Order in Metal-Chromium Complexes. *J. Am. Chem. Soc.* **2013**, *135*, 13142.
- (d) Cooper, B. G.; Fafard, C. M.; Foxman, B. M.; Thomas, C. M., Electronic Factors Affecting Metal-Metal Interactions in Early/Late Heterobimetallics: Substituent Effects in Zirconium/Platinum Bis(phosphinoamide) Complexes. *Organometallics*, **2010**, *29*, 5179.
- (e) Greenwood, B. P.; Forman, S. I.; Rowe, G. T.; Chen, C.-H.; Foxman, B. M.; Thomas, C. M., Multielectron Redox Activity Facilitated by Metal-Metal Interactions in Early/Late Heterobimetallics: Co/Zr Complexes Supported by Phosphinoamide Ligands. *Inorg. Chem.* **2009**, *48*, 6251.
- (f) Nippe, M.; Berry, J. F., Introducing a Metal-Metal Multiply Bonded Group as an “Axial Ligand” to Iron: Synthetic Design of a Linear Cr-Cr-Fe Framework. *J. Am. Chem. Soc.* **2007**, *129*, 12684.
- (g) Nagashima, H.; Sue, T.; Oda, T.; Kanemitsu, A.; Matsumoto, T.; Motoyama, Y.; Sunada, Y., Dynamic Titanium Phosphinoamides as Unique Bidentate Phosphorus Ligands for Platinum. *Organometallics*, **2006**, *25*, 1987.
- (h) Uyeda, C.; Peters, J., Access to formally Ni(I) states in a heterobimetallic NiZn system. *Chem. Sci.* **2013**, *4*, 157.
- (i) Curley, J. J.; Bergman, R. G.; Tilley, T. D., Preparation and physical properties of early-late heterobimetallic compounds featuring Ir-M bonds (M=Ti, Zr, Hf). *Dalton Trans.* **2012**, *41*, 192-200.
- (j) Hansen, J.; Li, B.; Dikarev, E.; Autschbach, J.; Davies, H. M. L., Combined Experimental and Computational Studies of Heterobimetallic Bi-Rh Paddlewheel Carboxylates as Catalysts for Metal Carbenoid Transformations. *J. Org. Chem.* **2009**, *74*, 6564.
- (k) Hostetler, M. J.; Bergman, R. G., Synthesis and reactivity of Cp₂Ta(CH₂)₂Ir(CO)₂: an early-late heterobimetallic complex that catalytically hydrogenates, isomerizes and hydrosilates alkenes. *J. Am. Chem. Soc.* **1990**, *112*, 8621-8623.
- (l) Baxter, S. M.; Ferguson, G. S.; Wolczanski, P. T., Mechanistic investigation of the ZrMe/PtMe exchange in Cp*ZrMe(μ-OCH₂PPh₂)₂PtMe₂. *J. Am. Chem. Soc.* **1988**, *110*, 4231.

- (m) Casey, C. P.; Rutter, E. W.; Haller, K. J., Synthesis of a heterobimetallic dihydride by the addition of a rhenium dihydride to a platinum(0) complex. *J. Am. Chem. Soc.* **1987**, *109*, 6886-6887.
- (5) (a) Zhou, W.; Saper, N. I.; Krogman, J. P.; Foxman, B. M.; Thomas, C. M., Effect of ligand modification on the reactivity of phosphinoamide-bridged heterobimetallic Zr/Co complexes. *Dalton Trans.* **2014**, *43*, 1984.
- (b) Zhou, W.; Marquard, S. L.; Bezpalko, M. W.; Foxman, B. M.; Thomas, C. M., Catalytic Hydrosilylation of Ketones Using a Co/Zr Heterobimetallic Complex: Evidence for an Unusual Mechanism Involving Ketyl Radicals. *Organometallics*, **2013**, *32*, 1766.
- (c) Zhou, W.; Napoline, J. W.; Thomas, C. M., A Catalytic Application of Co/Zr Heterobimetallic Complexes: Kumada Coupling of Unactivated Alkyl Halides with Alkyl Grignard Reagents. *Eur. J. Inorg. Chem.* **2011**, 2029.
- (6) (a) Trost, B. M.; Lee, C. *In Catalytic Asymmetric Synthesis*; Ojima, L., Ed.; Wiley-VCH: New York, **2010**; pp 593-649.
- (b) Dieguez, M.; Pamies, O., Biaryl Phosphites: New Efficient Adaptive Ligands for Pd-Catalyzed Asymmetric Allylic Substitution Reactions. *Acc. Chem. Res.* **2010**, *43*, 312.
- (c) Lu, Z.; Ma, S., Metal-Catalyzed Enantioselective Allylation in Asymmetric Synthesis. *Angew. Chem., Int. Ed.* **2008**, *47*, 258.
- (d) Trost, B. M.; Machacek, M. R.; Aponick, A., Predicting the Stereochemistry of Diphenylphosphino Benzoic Acid (DPPBA)-Based Palladium-Catalyzed Asymmetric Allylic Alkylation Reactions: A Working Model. *Acc. Chem. Res.* **2006**, *39*, 747.
- (e) Dai, L.-X.; Tu, T.; You, S.-L.; Deng, W.-P.; Hou, X.-L., Asymmetric Catalysis with Chiral Ferrocene Ligands. *Acc. Chem. Res.* **2003**, *36*, 659.
- (f) Helmchen, G.; Pfaltz, A., Phosphinooxazolines- A New Class of Versatile, Modular P,N-Ligands for Asymmetric Catalysis. *Acc. Chem. Res.* **2000**, *33*, 336.
- (g) Johannsen, M.; Jorgensen, K. A., Allylic Amination. *Chem. Rev.* **1998**, *98*, 1689.
- (7) Tsutsumi, H.; Sunada, Y.; Shiota, Y.; Yoshizawa, K.; Nagashima, H., Nickel(II), Palladium(II), and Platinum(II) η^3 -Allyl Complexes Bearing a Bidentate Titanium(IV) Phosphinoamide Ligand: A Ti-M₂ Dative Bond Enhances the Electrophilicity of the π -Allyl Moiety. *Organometallics*, **2009**, *28*, 1988.
- (8) (a) Tolman, C. A., Steric effects of phosphorus ligands in organometallic chemistry and homogeneous catalysis. *Chem. Rev.* **1977**, *77*, 313.

(b) van Leeuwen, P. W. N. M.; Kamer, P.C.J.; Reek, J. N. H.; Dierkes, P., Ligand Bite Angle Effects in Metal-catalyzed C-C Bond Formation. *Chem. Rev.* **2000**, *100*, 2741.

(c) Canovese, L.; Visentin, F.; Levi, C.; Dolmella, A., Synthesis, characterization, dynamics and reactivity toward amination of η^3 -allyl palladium complexes bearing mixed ancillary ligands. Evaluation of the electronic characteristics of the ligands from kinetic data. *Dalton Trans.* **2011**, *40*, 966.

(9) For reports of amine addition transition states to Pd-allyl complexes, see:

(a) Blochl, P. E.; Togni, A., First-Principles Investigation of Enantioselective Catalysis: Asymmetric Allylic Amination with Pd Complexes Bearing P,N-Ligands. *Organometallics*, **1996**, *15*, 4125.

(b) Hagelin, H.; Akermark, B.; Norrby, P.-O., A Solvated Transition State for the Nucleophilic Attack on Cationic η^3 -Allylpalladium Complexes. *Chem Eur. J.* **1999**, *5*, 902.

(c) Macsari, I.; Szabo, K. J., Nature of the Interactions between the β -Silyl Substituent and Allyl Moiety in (η^3 -Allyl)palladium Complexes. A Combined Experimental and Theoretical Study. *Organometallics*, **1999**, *18*, 701.

(d) Branchadell, V.; Moreno-Manas, M.; Pajuelo, F.; Pleixats, R., Density Functional Study on the Regioselectivity of Nucleophilic Attack in 1,3-Disubstituted (Diphosphino)(η^3 -allyl)palladium Cations. *Organometallics*, **1999**, *18*, 4934.

(e) Delbecq, F.; Lapouge, C. *Organometallics*, **2000**, *19*, 2716.

(f) Branchadell, V.; Moreno-Manas, M.; Pleixats, R., Theoretical Study on the Regioselectivity of Nucleophilic Attack in Silyl-Substituted (Diphosphino)(η^3 -allyl)palladium Cations. *Organometallics*, **2002**, *21*, 2407.

(g) Piechaczyk, O.; Thoumazet, C.; Jean, Y.; le Floch, P., DFT Study on the Palladium-Catalyzed Allylation of Primary Amines by Allylic Alcohol. *J. Am. Chem. Soc.* **2006**, *128*, 14306.

(h) De luliis, M. Z.; Watson, I. D. G.; Yudin, A. K.; Morris, R. H., A DFT investigation into the origin of regioselectivity in palladium-catalyzed allylic amination. *Can. J. Chem.* **2009**, *87*, 54.

(10) For general computational reports of nucleophile addition to Pd-allyl complexes, see:

(a) Schilling, B. E. R.; Hoffmann, R.; Faller, J. W., Effect of ligand asymmetry on the structure and reactivity of CpMLL'(allyl) (Cp=cyclopentadienyl, M=metal, L=ligand) and π -(ethylene) complexes. *J. Am. Chem. Soc.* **1979**, *101*, 592.

- (b) Sakaki, S.; Nishikawa, M.; Ohyoshi, A., A palladium-catalyzed reaction of a π -allyl ligand with a nucleophile. An MO study about a feature of the reaction and a ligand effect on the reactivity. *J. Am. Chem. Soc.* **1980**, *102*, 4062.
- (c) Curtis, M. D.; Eisenstein, O., A molecular orbital analysis of the regioselectivity of nucleophilic addition to η^3 -allyl complexes and the conformation of the η^3 -allyl ligand in $L_3(CO)_2(\eta^3-C_3H_5)Mo(II)$ complexes. *Organometallics*, **1984**, *3*, 887.
- (d) Bigot, B.; Delbecq, F., Catalysis of nucleophilic substitution on α -allylic and allylic derivatives by palladium(0) complexes: a theoretical study. *New J. Chem.* **1990**, *14*, 659.
- (e) Sjogern, M.; Hansson, S.; Norby, P.-O.; Akermark, B.; Cucciolito, M. E.; Vitagliano, A., Selective stabilization of the anti isomer of (η^3 -allyl)palladium and platinum complexes. *Organometallics*, **1992**, *11*, 3954.
- (f) Blochl, P. E.; Togni, A., First-Principles Investigation of Enantioselective Catalysis: Asymmetric Allylic Amination with Pd Complexes Bearing P,N-Ligands. *Organometallics*, **1996**, *15*, 4125.
- (g) Ward, T. R., Regioselectivity of Nucleophilic Attack on [Pd(allyl)(phosphine)(imine)] Complexes: A Theoretical Study. *Organometallics*, **1996**, *15*, 2836.
- (h) Sakaki, S.; Takeuchi, K.; Sugimoto, M., Geometries, Bonding Nature, and Relative Stabilities of Dinuclear Palladium(I) π -Allyl and Mononuclear Palladium(II) π -Allyl Complexes. A Theoretical Study. *Organometallics*, **1997**, *16*, 2995.
- (i) Lloyd-Jones, G. C.; Stephen, S. C., Memory Effects in Pd-Catalysed Allylic Alkylation: Stereochemical Labeling through Isotopic Desymmetrization. *Chem. Eur. J.* **1998**, *4*, 2539.
- (j) Dedieu, A., Theoretical Studies in Palladium and Platinum Molecular Chemistry. *Chem. Rev.* **2000**, *100*, 543.
- (k) Solin, N.; Szabo, K. J., Mechanism of the η^3 - η^1 - η^3 Isomerization in Allylpalladium Complexes: Solvent Coordination, Ligand, and Substituent Effects. *Organometallics*, **2001**, *20*, 5464.
- (l) Szabo, K. J., Nature of the interaction between β -substituents and the allyl moiety in (η^3 -allyl)palladium complexes. *Chem. Soc. Rev.* **2001**, *30*, 136.
- (m) Fristrup, P.; Jensen, T.; Hoppe, J.; Norby, P.-O., Deconvoluting the Memory Effect in Pd-Catalyzed Allylic Alkylation: Effect of Leaving Group and Added Chloride. *Chem. Eur. J.* **2006**, *12*, 5352.
- (n) Ariafard, A.; Lin, Z., DFT Studies on the Mechanism of Allylative Dearomatization Catalyzed by Palladium. *J. Am. Chem. Soc.* **2006**, *128*, 13010.
- (o) Fristrup, P.; Ahlquist, M.; Tanner, D.; Norby, P.-O., On the Nature of the Intermediates and the Role of Chloride Ions in Pd-Catalyzed Allylic Alkylations: Added Insight from Density Functional Theory. *J. Phys. Chem. A*, **2008**, *112*, 12862.

(p) Kazmaier, U.; Stolz, D.; Kraemer, K.; Zumpe, F. L., Influences on the Regioselectivity of Palladium-Catalyzed Allylic Alkylations. *Chem. Eur. J.* **2008**, *14*, 1322.

(q) Marinho, V. R.; Ramalho, J. P. P.; Rodrigues, A. I.; Burke, A. J., A Comparison of (R,R)-Me-DUPHOS and (R,R)-DUPHOS-*i*Pr Ligands in the Pd⁰-Catalyzed Asymmetric Allylic Alkylation Reaction: Stereochemical and Kinetic Considerations. *Eur. J. Org. Chem.* **2009**, 6311.

(r) Kleimark, J.; Johansson, C.; Olsson, S.; Hakansson, M.; Hansson, S.; Akermark, B.; Norby, P.-O., Sterically Governed Selectivity in Palladium-Assisted Allylic Alkylation. *Organometallics*, **2011**, *30*, 230.

(s) Ortiz, D.; Blug, M.; Le Goff, X.-F.; Le Floch, P.; Mezailles, N.; Maitre, P., Mechanistic Investigation of the Generation of a Palladium(0) Catalyst from a Palladium(II) Allyl Complex: A Combined Experimental and DFT Study. *Organometallics*, **2012**, *31*, 5975.

(11) Indeed, when tetrabutylammonium chloride is added to catalyst **1**, a new species is seen to reversibly form, as observed by ³¹P NMR (see Supporting Information).

(12) In **1 (boat)** there are weak direct through-space orbital interactions between the Pd filled d_{yz} and d_{x²-y²} orbitals with the TiCl₂ vacant d_{x²-y²} and p orbitals. A gross fragment orbital population analysis in the Amsterdam Density Functional program (Baerends, E. J.; et al. *ADF2013.01*; SCM, Theoretical Chemistry, Vrije Universiteit: Amsterdam, 2013; See: www.scm.com) suggests that in **1 (boat)** the Pd-Ti bonding molecular orbital is composed of ~35% contribution from the Pd orbitals and only ~3% from the TiCl₂ orbitals. This small contribution from the TiCl₂ orbitals is why the previous NBO analysis by Nagashima was inconclusive (ref7). As indicated in the main text, the most important impact of the TiCl₂ fragment is on the Pd-C allyl π* vacant orbitals, which are stabilized by the Pd-Ti interaction.

(13) There are two different boat conformations with N-Me groups. The 2.2 kcal/mol higher energy boat conformation has a slightly shorter Pd-Ti distance of 3.15 Å.

(14) (a) Birkholz, M.-N.; Freixa, Z.; van Leeuwen, P. W. N. M., Bite angle effects of diphosphines in C-C and C-X bond forming cross coupling reactions. *Chem. Soc. Rev.* **2009**, *38*, 1099.

(b) Jones, A. M.; Tye, J. W.; Hartwig, J. F., Relative Rates for the Amination of η³-Allyl and η³-Benzyl Complexes of Palladium. *J. Am. Chem. Soc.* **2006**, *128*, 16010.

(15) Hughes, A. N., Bis(diphenylphosphino)methane in Organometallic Synthesis. *ACS Symp. Ser.* **1992**, *486*, 173.

(16) General phosphine bite angle references:

(a) Dierkes, P.; van Leeuwen, P. W. N. M., The bite angle makes the difference: a practical ligand parameter for diphosphine ligands. *J. Chem. Soc., Dalton Trans.* **1999**, 1519.

(b) van Leeuwen, P. W. N. M.; Kamer, P. C. J.; Reek, J. N. H.; Dierkes, P., Ligand Bite Angle Effects in Metal-catalyzed C-C Bond Formation. *Chem. Rev.* **2000**, *100*, 2741.

(17) Specific phosphine bite angle references for Pd complexes:

(a) Sjorgen, M. P. T.; Hansson, S.; Akermark, B.; Vitagliano, A., Stereo- and Regiocontrol in Palladium-Catalyzed Allylic Alkylation Using 1,10-Phenanthrolines as Ligands. *Organometallics*, **1994**, *13*, 1963.

(b) Szabo, K. J., Effects of the Ancillary Ligands on Palladium-Carbon Bonding in (η^3 -Allyl)palladium Complexes. Implications for Nucleophilic Attack at the Allylic Carbons. *Organometallics*, **1996**, *15*, 1128.

(c) Aranyos, A.; Szabo, K. J.; Castano, A. M.; Backvall, J.-E., Central versus Terminal Attack in Nucleophilic Addition to (π -Allyl)palladium Complexes. Ligand Effects and Mechanism. *Organometallics*, **1997**, *16*, 1058.

(d) van Haaren, R. J.; Oevering, H.; Coussens, B.; van Strijdonck, G. P. F.; Reek, J. N. H.; Kamer, P. C. J.; van Leeuwen, P. W. N. M., On the Influence of the Bite Angle of Bidentate Phosphane Ligands on the Regioselectivity in Allylic Alkylation. *Eur. J. Inorg. Chem.* **1999**, 1237.

(e) van Haaren, R. J.; Drujven, C. J. M.; van Strijdonck, G. P. F.; Oevering, H.; Reek, J. N. H.; Kamer, P. J. C.; van Leeuwen, P. W. N. M., Bite angle effect of bidentate P-N ligands in palladium catalyzed allylic alkylation. *J. Chem. Soc., Dalton Trans.* **2000**, *10*, 1549.

(f) Delbecq, F.; Lapouge, C., Regioselectivity of the Nucleophilic Addition to (η^3 -allyl) Palladium Complexes. A Theoretical Study. *Organometallics*, **2000**, *19*, 2716.

(g) van Haaren, R. J.; Goubitz, K.; Fraanje, J.; van Strijdonck, G. P. F.; Oevering, H.; Coussens, B.; Reek, J. N. H.; Kamer, P. C. J.; van Leeuwen, P. W. N. M., An X-ray Study of the Effect of the Bite Angle of Chelating Ligands on the Geometry of Palladium(allyl) Complexes: Implications for the Regioselectivity in the Allylic Alkylation. *Inorg. Chem.* **2001**, *40*, 3363.

(h) Tromp, M.; van Bokhoven, J. A.; van Haaren, R. J.; van Strijdonck, G. P. F.; van der Eerden, A. M. J.; van Leeuwen, P. W. N. M.; Koningsberger, D. C., Structure-Performance Relations in Homogeneous Pd Catalysis by In Situ EXAFS Spectroscopy. *J. Am. Chem. Soc.* **2002**, *124*, 14814.

(18) Walker, W. K.; Anderson, D. L.; Stokes, R. W.; Smith, S. J.; Michaelis, D. J., Allylic Aminations with Hindered Secondary Amine Nucleophiles Catalyzed by Heterobimetallic Pd-Ti Complexes. *Org. Lett.* **2015**, *17*, 752.

(19) These results are consistent with the reported rates of allylic amination of **13** with *in situ* generated complexes **8** and **9**. See ref 16.

(20) Frisch, M. J.; Trucks, G. W.; Schlegel, H. B.; Scuseria, G. E.; Robb, M. A.; Cheeseman, J. R.; Scalmani, G.; Barone, V.; Mennucci, B.; Petersson, G. A.; Nakatsuji, H.; Caricato, M.; Li, X.; Hratchian, H. P.; Izmaylov, A. F.; Bloino, J.; Zheng, G.; Sonnenberg, J. L.; Hada, M.; Ehara, M.; Toyota, K.; Fukuda, R.; Hasegawa, J.; Ishida, M.; Nakajima, T.; Honda, Y.; Kitao, O.; Nakai, H.; Vreven, T.; Montgomery, J. A., Jr.; Peralta, J. E.; Ogliaro, F.; Bearpark, M.; Heyd, J. J.; Brothers, E.; Kudin, K. N.; Staroverov, V. N.; Kobayashi, R.; Normand, J.; Raghavachari, K.; Rendell, A.; Burant, J. C.; Iyengar, S. S.; Tomasi, J.; Cossi, M.; Rega, N.; Millam, M. J.; Klene, M.; Knox, J. E.; Cross, J. B.; Bakken, V.; Adamo, C.; Jaramillo, J.; Gomperts, R.; Stratmann, R. E.; Yazyev, O.; Austin, A. J.; Cammi, R.; Pomelli, C.; Ochterski, J. W.; Martin, R. L.; Morokuma, K.; Zakrzewski, V. G.; Voth, G. A.; Salvador, P.; Dannenberg, J. J.; Dapprich, S.; Daniels, A. D.; Farkas, O.; Foresman, J. B.; Ortiz, J. V.; Cioslowski, J.; Fox, D. J. *Gaussian 09*, Revision B.01; Gaussian, Inc.: Wallingford, CT, 2009.

(21) Zhao, Y.; Truhlar, D. G., The Mo6 suite of density functionals for main group thermochemistry, thermochemical kinetics, noncovalent interactions, excited states, and transition elements: two new functionals and systematic testing of four Mo6-class functionals and 12 other functionals. *Theor. Chem. Acc.* **2008**, *120*, 215.

(22) (a) Ditchfield, R.; Hehre, W. J.; Pople, J. A., Self-Consistent Molecular-Orbital Methods. IX. An Extended Gaussian-Type Basis for Molecular-Orbital Studies of Organic Molecules. *J. Chem. Phys.* **1971**, *54*, 724.

(b) Hehre, W. J.; Ditchfield, R.; Pople, J. A., Self-Consistent Molecular Orbital Methods. XII. Further Extensions of Gaussian-Type Basis Sets for Use in Molecular Orbital Studies of Organic Molecules. *Chem. Phys.* **1972**, *56*, 2257.

(c) Francl, M. M.; Pietro, W. J.; Hehre, W. J.; Binkley, J. S.; Gordon, M. S.; DeFrees, D. J.; Pople, J. A., Self-consistent molecular orbital methods. XXIII. A polarization-type basis set for second-row elements. *J. Chem. Phys.* **1982**, *77*, 3654.

(d) Frisch, M. J.; Pople, J. A.; Binkley, J. S., Self-consistent molecular orbital methods 25. Supplementary functions for Gaussian basis sets. *J. Chem. Phys.* **1984**, *80*, 3265.

(e) Rassolov, V. A.; Pople, J. A.; Ratner, M. A.; Windus, T. L., 6-31G* basis set for atoms K through Zn. *J. Chem. Phys.* **1998**, *109*, 1223.

(f) Rassolov, V. A.; Ratner, M. A.; Pople, J. A.; Redfern, P. C.; Curtiss, L. A., 6-31G* basis set for third-row atoms. *J. Comput. Chem.* **2001**, *22*, 976.

(23) (a) Dunning, T. H., Jr.; Hay, P. J. *In Modern Theoretical Chemistry*; Schaefer, H. F., III, Ed.; Plenum, New York, 1977; Vol. 3, pp 1-28.

(b) Hay, P. J.; Wadt, W. R., *Ab initio* effective core potentials for molecular calculations. Potentials for the transition metal atoms Sc to Hg. *J. Chem. Phys.* **1985**, *82*, 270.

(c) Wadt, W. R.; Hay, P. J., *Ab initio* effective core potentials for molecular calculations. Potentials for main group elements Na to Bi. *J. Chem. Phys.* **1985**, *82*, 284.

(d) Hay, P. J.; Wadt, W. R., *Ab initio* effective core potentials for molecular calculations. Potentials for K to Au including the outermost core orbitals. *J. Chem. Phys.* **1985**, *82*, 299.

(24) Marenich, A. V.; Cramer, C. J.; Truhlar, D. G., Universal Solvation Model Based on Solute Electron Density and on a Continuum Model of the Solvent Defined by the Bulk Dielectric Constant and Atomic Surface Tensions. *J. Phys. Chem. B*, **2009**, *113*, 6378.

(25) (a) The LANL2TZ(f) basis set for Pd and Ti was obtained from the EMSL Basis Set Exchange; see: <https://bse.pnl.gov/bse/portal>; accessed on Jan 1, 2014.

(b) Hay, P. J.; Wadt, W. R., *Ab initio* effective core potentials for molecular calculations. Potentials for the transition metal atoms Sc to Hg. *J. Chem. Phys.* **1985**, *82*, 270.

(c) Hay, P. J.; Wadt, W. R., *Ab initio* effective core potentials for molecular calculations. Potentials for main group elements Na to Bi. *J. Chem. Phys.* **1985**, *82*, 284.

(d) Hay, P. J.; Wadt, W. R., *Ab initio* effective core potentials for molecular calculations. Potentials for K to Au including the outermost core orbitals. *J. Chem. Phys.* **1985**, *82*, 299.

Chapter 4

Electrophilic Activation of Alkynes for Enyne Cycloisomerization Reactions with *in situ* Generated Early/Late Heterobimetallic Pt-Ti Catalysts

Portions of this work have been previously published:

Talley, M. R.; Stokes, R. W.; Walker, W. K.; Michaelis, D. J., Electrophilic activation of alkynes for enyne cycloisomerization reactions with *in situ* generated early/late heterobimetallic Pt-Ti catalysts. *Dalton Trans.* **2016**, *45*, 9770-9773.

4.1 INTRODUCTION

In recent years, highly atom economical processes that utilize Lewis acidic late transition metals have become a popular area of study. The Lewis acidic late transition metal is used to activate olefins and alkynes in order to facilitate nucleophilic addition reactions.¹⁻⁶ Electron-accepting ligands are used to accelerate the nucleophilic addition to the alkene/alkyne bound to the metal.⁷ The nucleophilic addition is the turn-over limiting step, which means the ability to make the C-C multiple bond more electrophilic is key when designing the active metal catalyst. Diphosphinidene-cyclobutenes,⁸ cyclopropenium-substituted phosphines,⁹ and phosphine ligands with Z-type botane ligands¹⁰⁻¹² have been reported to produce highly active catalysts for alkyne activation reactions (Figure 4.1). Nagashima showed that phosphine based ligands containing Lewis acidic early transition metals can form highly electrophilic late transition metal centers through the formation of a metal-metal dative interaction.^{13,14} Michaelis and Ess recently demonstrated that turnover-limiting reductive addition steps in allylic amination reactions are enhanced by the formation of a Pd-Ti dative interaction.¹⁵ The formation of the Pd-Ti dative interaction can also be used to facilitate allylic aminations using traditionally unreactive hindered amines.¹⁶ In this chapter, we demonstrate that the *in situ* formation of Pt-Ti heterobimetallic complexes can be used to accelerate cycloisomerizations of enyne substrates and achieve high reactivity at room temperature.

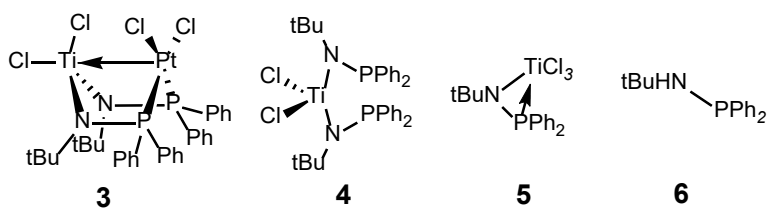


Figure 4.1. Ligands used for Pt-catalyzed cycloisomerization reactions

Heterobimetallic transition metal complexes have the potential to become useful catalysts for organic transformations.¹⁷⁻¹⁹ Metal-metal bonds formed by having two metals in close proximity on a ligand scaffold can facilitate new reaction mechanisms.²⁰⁻²³ The second metal can also effect the selectivity of the product. This selectivity arises from the ability of the second metal to coordinate intermediates,²⁴ induce bimetallic cooperativity,²⁵ or by holding onto reactive intermediates.^{26,27} We are interested in changing the nucleophilicity or electrophilicity of the reactive metal center by forming dative metal-metal interactions.²⁸⁻³¹ In this chapter, we demonstrate that phosphine-based ligands that contain a Lewis acidic titanium atom combined with platinum catalysts are able to perform room temperature enyne cycloisomerization reactions at an enhanced rate.

4.2 RESULTS AND DISCUSSION

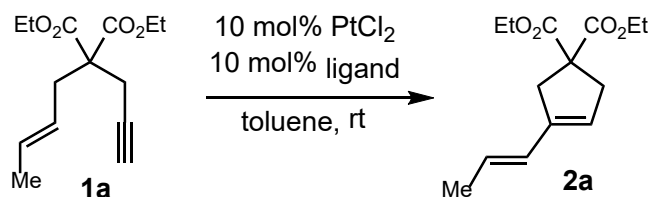
4.2.1 *Optimization of Pt-catalyzed Cycloisomerizations*

Cyclic intermediates in natural product and pharmaceuticals are often made through cycloisomerization reactions of enynes.³² The most common catalysts for these reactions are platinum(II) and gold(I) complexes.³³ PtCl₂ without any additional ligands added is typically used to facilitate cycloisomerizations.³² Aromatic solvents and elevated temperatures are often needed. These reaction conditions are useful for a wide variety of substrates used in cycloisomerization reactions, but the absence of a ligand limits the ability to optimize the reactions for reactivity and

selectivity. There are several π -accepting ligands^{9,12} and cationic Pt complexes^{1,33-35} that have been used to catalyze cycloisomerization reactions. We believe that by using a titanium-containing phosphinamide ligand a Pt-Ti dative interaction would form, which would make the platinum highly electrophilic. The electrophilic platinum center could be used as a highly active catalysts in alkyne activation reactions.

We began by looking at the cycloisomerization of enyne substrate **1a** to produce diene product **2a** (Table 4.1). When platinum chloride is used **2a** is formed in high yield after 12 h at 80 °C (entry 1). However, when conducted at room temperature, the reaction proceeded slowly and required a longer reaction time (entry 2). No reaction was observed at room temperature when heterobimetallic Pt-Ti complex **3**¹⁴ was used as the catalyst (entry 3). However when PtCl₂ was mixed with bisphosphinoamide-titanium ligand **4**¹³ after 12 h a small amount of product was seen (entry 4). We believe that titanium ligand **4** yielded little product due to its bidentate nature. There are only two open coordination sites on platinum, and both were occupied by ligand **4**. We believe that the small amount of reactivity is due to the partial formation of a monophosphinoamide platinum intermediate during the *in situ* formation of complex **3**. We next used monophosphinamide titanium ligand **5**¹⁶ in order to avoid the formation of an unreactive bis(phosphinoamide) platinum catalyst. Complete conversion to the product **2a** was seen within 2 h (entry 5, 99% isolate yield). When two equivalents of ligand **5** were added to the reaction we observed a decrease in the rate of product formation (entry 6), which supports our theory that a bidentate ligand produces low reactivity. When phosphinoamine ligand **6** was used no reaction was observed after 12 h (entry 7). Since ligand **6** does not contain the Lewis acidic titanium, this result shows that simple phosphinoamine ligands do not produce an active platinum catalyst. When ligand **5** is used in the reaction without PtCl₂ no product is observed (entry 8). Addition of trace amounts of water to the reaction resulted in almost no product is formation (entry 9). When TiCl₄ was added

to platinum chloride the reactivity was not much improved from the reaction with platinum chloride alone (entry 10). Similar reactivity was also observed when TiCl_4 was combined with phosphinoamine **6** and PtCl_2 (entry 11). These results suggest that the *in situ* formation of a heterobimetallic complex containing a dative Pt-Ti interaction was needed for fast catalysis.¹⁵ When common mono- and bis-phosphine ligands were used no product was observed (entries 12 and 13). These studies suggest that the enhanced rate is not due to the titanium phosphinoamide ligand **5** simply breaking the PtCl_2 polymer, increasing platinum solubility, or decomposing the platinum phosphinoamide into a more reactive catalyst. Unfortunately, all efforts to isolate and characterize the monodentate $(\text{tBuNPPH}_2)\text{TiCl}_3\text{-PtCl}_2$ complex have been unsuccessful.

Table 4.1. Optimization of Pt-catalyzed Cycloisomerization

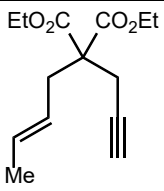
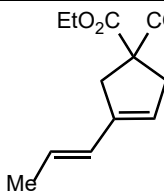
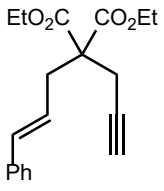
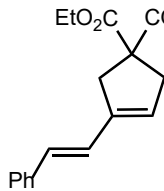
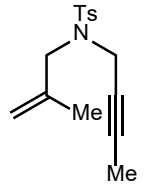
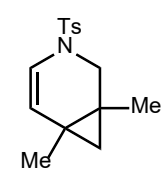
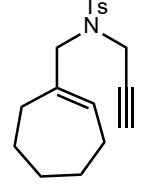
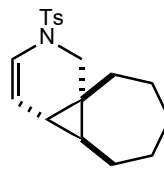
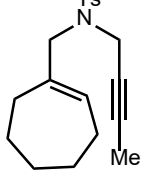
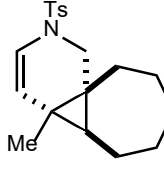
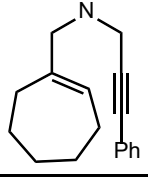
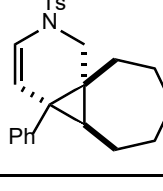
Entry ^a	Ligand	Time	% Conversion ^b
1	None (80 °C)	12 h	100
2	None	12 h	50
3	Complex 3 instead of PtCl ₂	12 h	0
4	4	12 h	12
5	5	2 h	100 (99)
6	5 (20 mol%)	2 h	90
7	6	12 h	0
8	5 (no PtCl ₂)	12 h	0
9	5 + H ₂ O (10 mol%)	12 h	6
10	TiCl ₄ (10 mol%)	12 h	57
11	6 + TiCl ₄ (10 mol%)	12 h	26
12	PPh ₃	12 h	0
13	dppe	12 h	0

^aReactions performed using 0.2 or 0.04 mmol enyne **1a**, 10 mol% PtCl₂, 10 mol% ligand in toluene (0.2 M) at room temperature for the indicated time unless otherwise noted. ^bDetermined by ¹H NMR analysis of the crude reaction mixture, isolated yield in parentheses. dppe = 1,2-bis(diphenylphosphine)ethane.

4.2.2 Substrate scope for Pt-catalyzed cycloisomerization reactions

Once we discovered a highly active Pt-Ti catalyst for enyne cycloisomerizations we began to explore the reactivity of different enyne substrates. Malonate substrates that were substituted at the alkene reacted efficiently at room temperature (Table 4.2, entries 1 and 2). *N*-tosyl bridged substrates produced heterocyclic cyclopropane products³⁶ instead of the diene product in good yield (entries 3-6). These cyclization reactions worked with substituents on either the alkene (entries 3 and 4) or the terminal end of the alkyne (entries 4-6).

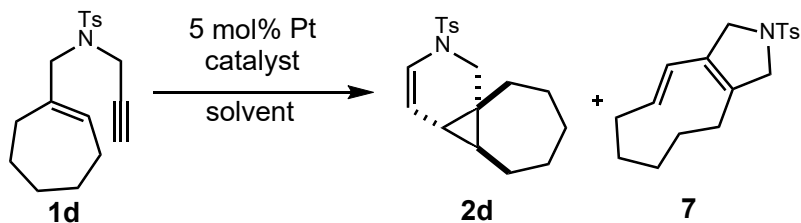
Table 4.2. Substrate Scope for Pt-catalyzed Cycloisomerization

Entry ^a	Substrate	Product	Yield ^b
1	 1a	 2a	99%
2	 1b	 2b	58%
3	 1c	 2c	99%
4	 1d	 2d	96% ^c
5	 1e	 2e	87%
6	 1f	 2f	90%

^aConditions: reactions performed using 0.2 mmol substrate, 10 mol% PtCl₂, 10 mol% ligand **5** in toluene (0.2 M) at room temperature for 2.48 h. ^bIsolated yield. ^cIsolated as a 1 : 1.3 mixture of cyclopropane ; diene product.

4.2.3 Influence of reaction selectivity by ligand modification

Using supporting ligands for transition metal catalysis opens up the possibility to influence the reaction selectivity by changing the ligand structure. Pt-catalyzed enyne cycloisomerizations often show poor selectivity for the different possible products. These products include the cyclopropane and diene products we observed for different enyne substrates. When PtCl₂ is used to catalyze the enyne cycloisomerization of substrate **1d** a 1:2 mixture of cyclopropane and diene product was produced (Table 4.3, entry 1). In this reaction ligand **4** produced almost no product (entry 2), but ligand **5** produced the product in high yield with a slight preference for the cyclopropane product **2d** (entry 3). However when bisphosphine ligands **4** or **5** were mixed with Pt(cod)Cl₂ at a slightly elevated temperature (35 °C) the selectivity for the cyclopropane product increased significantly (entries 5-8). When chloroform was used as the solvent bisphosphine ligand **4** gave 96% yield of cyclopropane product **2d** and gave a selectivity of 10:1 (entry 6). When Pt(cod)Cl₂ is used without the presence of ligand no product is observed even when the reaction is heated to 80 °C (entry 4). We are unsure of the role cod has in the reaction mechanism, but when used the rate of reaction is reduced whether ligand is present (entry 3 vs. 7) or not (entry 1 vs. 4). These results indicate that the cod remains bound to the platinum to some extent throughout the reaction. In summary we have been able to show that ligand structure has an impact on product selectivity and that titanium-containing ligands are able to facilitate rapid catalysis and optimize the product selectivity in cycloisomerization reactions.

Table 4.3. Optimization of Product Selectivity

Entry ^a	Ligand	Temp.	Time	% Yield ^b	2d : 7 ^c
1	PtCl ₂	80 °C	12 h	96	1 : 2
2	PtCl ₂ + 4	rt	12 h	3	-
3	PtCl ₂ + 5	rt	17 h	96	1 : 1
4	Pt(cod)Cl ₂	80 °C	24 h	0	-
5	Pt(cod)Cl ₂ + 4	35 °C	24 h	53	5 : 1
6 ^d	Pt(cod)Cl ₂ + 4	35 °C	24 h	96	10 : 1
7	Pt(cod)Cl ₂ + 5	35 °C	24 h	41	13 : 1
8 ^d	Pt(cod)Cl ₂ + 5	35 °C	24 h	20	8 : 1

^aConditions: reactions performed using 0.1 mmol substrate, 5 mol% PtCl₂ or Pt(cod)Cl₂, and 5 mol% ligand (when indicated) in toluene or CHCl₃ (0.1 M). ^bIsolated yield. ^cDetermined by ¹H NMR of the reaction mixture. ^dRun in CHCl₃.

4.3 CONCLUSION

We have successfully shown that cycloisomerization reactions can be done at room temperature when titanium-containing phosphinoamide ligands are combined with platinum(II) catalysts. We believe this is possible through the formation of an electron-withdrawing Pt to Ti dative interaction which increases the electrophilicity of the Pt(II) center. This increased electrophilicity enables fast

cycloisomerization of enyne substrates. We obtained high yields with a variety of enynes, including heterocyclic cyclopropane products. Ligand optimization studies were performed to enhance the selectivity of cyclopropane product formation. These results have the potential to expand the applications of heterobimetallic complexes in organic synthesis.

4.4 REFERENCES

- (1) Furstner, A.; Davies, P. W., Catalytic Carbophilic Activation: Catalysis by Platinum and Gold π Acids. *Angew. Chem., Int. Ed.*, **2007**, *46*, 3410-3449.
- (2) Chianese, A. R.; Lee, S. J.; Gagne, M. R., Electrophilic Activation of Alkenes by Platinum(II): So Much More Than a Slow Version of Palladium(II). *Angew. Chem., Int. Ed.*, **2007**, *46*, 4042-4059.
- (3) de Mendoza, P.; Echavarren, A. M., Synthesis of arenes and heteroarenes by hydroarylation reactions catalyzed by electrophilic metal complexes. *Pure Appl. Chem.*, **2010**, *82*, 801-820.
- (4) Muniz, K.; Marinez, C. *In Metal-Catalyzed Cross-Coupling Reactions and More*, Ed; de Meijere, A.; Brase, S.; Oestreich, M.; Wiley-VCH: Weinheim, **2014**, pp 1259-1314.
- (5) McDonald, R. I.; Liu, G.; Stahl, S. S., Palladium(II)-Catalyzed Alkene Functionalization via Nucleopalladation: Stereochemical Pathways and Enantioselective Catalytic Applications. *Chem. Rev.* **2011**, *111*, 2981-3019.
- (6) Dorel, R.; Echavarren, A. M., Gold(I)-Catalyzed Activation of Alkynes for the Construction of Molecular Complexity. *Chem. Rev.* **2015**, *115*, 9028-9072.
- (7) Jimenez-Nunez, E.; Echavarren, A. M., Gold-Catalyzed Cycloisomerizations of Enynes: A Mechanistic Perspective. *Chem. Rev.* **2008**, *108*, 3326-3350.
- (8) Ozawa, F.; Yoshifuji, M., Catalytic applications of transition-metal complexes bearing diphosphinidene-cyclobutenes (DPCB). *Dalton Trans.* **2006**, 4987-4995.
- (9) Carreras, J.; Gopakumar, G.; Gu, L.; Gimeno, A. M.; Linowski, P.; Petuskova, J.; Thiel, W.; Alcarazo, M., Polycationic Ligands in Gold Catalysis: Synthesis and Applications of Extremely π -Acidic Catalysts. *J. Am. Chem. Soc.* **2013**, *135*, 18815-18823.
- (10) Bontemps, S.; Gornitzka, H.; Bouhadir, G.; Miqueu, K.; Bourissou, D., Rhodium(I) Complexes of a PBP Ambiphilic Ligand: Evidence for a Metal-Borane Interaction. *Angew. Chem., Int. Ed.*, **2006**, *45*, 1611-1614.
- (11) Kameo, H.; Nakazawa, H., Recent Developments in the Coordination Chemistry of Multidentate Ligands Featuring a Boron Moiety. *Chem. – Asian J.* **2013**, *8*, 1720-1734.
- (12) Inagaki, F.; Matsumoto, C.; Okada, Y.; Maruyama, N.; Mukai, C., Air-Stable Cationic Gold(I) Catalyst Featuring a Z-Type Ligand: Promoting Enyne Cyclizations. *Angew. Chem., Int. Ed.*, **2015**, *54*, 818-822.
- (13) Tsutsumi, H.; Sunada, Y.; Shiota, Y.; Yoshizawa, K.; Nagashima, H., Nickel(II), Palladium(II), and Platinum(II) η^3 -Allyl Complexes Bearing a Bidentate Titanium(IV)

Phosphinoamide Ligand: A Ti-M₂ Dative Bond Enhances the Electrophilicity of the π -Allyl Moiety. *Organometallics*, **2009**, *28*, 1988-1991.

(14) Nagashima, H.; Sue, T.; Oda, T.; Kanemitsu, A.; Matsumoto, T.; Motoyama, Y.; Sunada, Y., Dynamic Titanium Phosphinoamides as Unique Bidentate Phosphorus Ligands for Platinum. *Organometallics*, **2006**, *25*, 1987-1994.

(15) Walker, W. K.; Kay, B. M.; Michaelis, S. A.; Anderson, D. L.; Smith, S. J.; Ess, D. H.; Michaelis, D. J., Origin of Fast Catalysis in Allylic Amination Reactions Catalyzed by Pd-Ti Heterobimetallic Complexes. *J. Am. Chem. Soc.*, **2015**, *137*, 7371-7378.

(16) Walker, W. K.; Anderson, D. L.; Stokes, R. W.; Smith, S. J.; Michaelis, D. J., Allylic Aminations with Hindered Secondary Amine Nucleophiles Catalyzed by Heterobimetallic Pd-Ti Complexes. *Org. Lett.* **2015**, *17*, 752-755.

(17) Gade, L. H., Highly Polar Metal-Metal Bonds in “Early-Late” Heterodimetallic Complexes. *Angew. Chem., Int. Ed.*, **2000**, *39*, 2658-2678.

(18) Ritleng, V.; Chetcuti, M. J., Hydrocarbyl Ligand Transformations on Heterobimetallic Complexes. *Chem. Rev.* **2007**, *107*, 797-858.

(19) Cooper, B. G.; Napoline, J. W.; Thomas, C. M., Catalytic Applications of Early/Late Heterobimetallic Complexes. *Catal. Rev.*, **2012**, *54*, 1-40.

(20) Zhou, W.; Napoline, J. W.; Thomas, C. M., A Catalytic Application of Co/Zr Heterobimetallic Complexes: Kumada Coupling of Unactivated Alkyl Halides with Alkyl Grignard Reagents. *Eur. J. Inorg. Chem.*, **2011**, *2011*, 2029-2033.

(21) Karunananda, M. K.; Parmelee, S. R.; Waldhart, G. W.; Mankad, N. P., Experimental and Computational Characterization of the Transition State for C-X Bimetallic Oxidative Addition at a Cu-Fe Reaction Center. *Organometallics*, **2015**, *34*, 3857-3864.

(22) Mazzacano, T. J.; Mankad, N. P., Base Metal Catalysts for Photochemical C-H Borylation That Utilize Metal-Metal Cooperativity. *J. Am. Chem. Soc.*, **2013**, *135*, 17258-17261.

(23) Powers, D. C.; Benitez, D.; Tkatchouk, E.; Goddard, W. A., III; Ritter, T., Bimetallic Reductive Elimination from Dinuclear Pd(III) Complexes. *J. Am. Chem. Soc.* **2010**, *132*, 14092-14103.

(24) Pal, S.; Uyeda, C., Evaluating the Effect of Catalyst Nuclearity in Ni-Catalyzed Alkyne Cyclotrimerizations. *J. Am. Chem. Soc.* **2015**, *137*, 8042-8045.

(25) Man, M. L.; Lam, K. C.; Sit, W. N.; Ng, S. M.; Zhou, Z.; Lin, Z.; Lau, C. P., Synthesis of Heterobimetallic Ru-Mn Complexes and the Coupling Reactions of Epoxides with Carbon Dioxide Catalyzed by these Complexes. *Chem. – Eur. J.* **2006**, *12*, 1004-1015.

- (26) Geoffroy, G. L., Synthesis, molecular dynamics, and reactivity of mixed-metal clusters. *Acc. Chem. Res.* **1980**, *13*, 469-476.
- (27) Baxter, S. M.; Ferguson, G. S.; Wolczanski, P. T., Mechanistic investigation of the ZrMe/PtME exchange in Cp*ZrMe(μ -OCH₂PPh₂)₂PtMe₂. *J. Am. Chem. Soc.* **1988**, *110*, 4231-4241.
- (28) Cammarota, R. C.; Lu, C. C., Tuning Nickel with Lewis Acidic Group 13 Metalloligands for Catalytic Olefin Hydrogenation. *J. Am. Chem. Soc.* **2015**, *137*, 12486-12489.
- (29) Clouston, L. J.; Bernales, V.; Carlson, R. K.; Gagliardi, L.; Lu, C. C., Bimetallic Cobalt-Dinitrogen Complexes: Impact of the Supporting Metal on N₂ Activation. *Inorg. Chem.* **2015**, *54*, 9263-9270.
- (30) Nippe, M.; Berry, J. F., Introducing a Metal-Metal Multiply Bonded Group as an “Axial Ligand” to Iron: Synthetic Design of a Linear Cr-Cr-Fe Framework. *J. Am. Chem. Soc.* **2007**, *129*, 12684-12685.
- (31) Moret, M.-E., Organometallic Platinum(II) and Palladium(II) Complexes as Donor Ligands for Lewis-Acidic d¹⁰ and s² Centers. *Top. Organomet. Chem.* **2011**, *35*, 157-184.
- (32) Furstner, A., Gold and platinum catalysis – a convenient tool for generating molecular complexity. *Chem. Soc. Rev.* **2009**, *38*, 3208-3221.
- (33) Michelet, V.; *In Comprehensive Organic Synthesis II*, Ed; Knochel, P.; Molander, G. A.; Elsevier, Waltham, **2014**, vol. 5, pp 1483-1536.
- (34) Jullien, H.; Brissy, D.; Sylvain, R.; Retailleau, P.; Naubron, J.-V.; Gladiali, S.; Marinetti, A., Cyclometalated N-Heterocyclic Carbene-Platinum Catalysts for the Enantioselective Cycloisomerization of Nitrogen-Tethered 1,6-Enynes. *Adv. Synth. Catal.* **2011**, *353*, 1109-1124.
- (35) Nelsen, D. L.; Gagne, M. R., Platinum(II) Enyne Cycloisomerization Catalysis: Intermediates and Resting States. *Organometallics*, **2009**, *28*, 950-952.
- (36) Furstner, A.; Stelzer, F.; Szillat, H., Platinum-Catalyzed Cycloisomerization Reactions of Enynes. *J. Am. Chem. Soc.* **2001**, *123*, 11863-11869.

Chapter 5

Synthesis and Use of Chiral Titanium Ligands for Heterobimetallic Pd-Ti Catalyzed Allylic Aminations

5.1 INTRODUCTION

New synthetic methods provide a way to accelerate the development of drugs by enabling access to intricate and enantiopure molecules. The activation of olefins and alkynes towards nucleophilic attack is one way to obtain bioactive molecules from simple starting materials. One developing area that could be utilized is the formation of nitrogen heterocycles from the addition of nitrogen nucleophiles to olefins. A significant challenge to this method is the ability to incorporate ligand frameworks that provide the correct selectivity without diminishing the catalytic activity. Therefore the reactions often require harsh reaction conditions, and are limited by the type of nucleophile that can be used. We believe that these problems can be overcome by incorporating a metal-metal dative bond into the ligand structure. Early/late transition metal heterobimetallic complexes have been shown to form strong metal-metal interactions. When an electron rich late transition metal is placed in close proximity to a Lewis acidic early transition metal a dative metal-metal bond is formed in which the electron rich metal donates electron density to the electron poor transition metal. This electron donation increases the electrophilicity of the catalytic metal without having to significantly change the ligand structure around it. When the early transition metal becomes more electrophilic it increases the ability of weak nucleophiles to react and reduces the need for harsh reaction conditions. We recently reported the use of a Pd-Ti heterobimetallic complex (**1**) in the intramolecular cyclization of a series of pyrrolidine and piperidine products (Figure 5.1).¹ The cyclizations were done at room temperature and went to completion within 10 min. We were also

able to show that the catalyst could be generated *in situ*, which precludes the need to make and crystallize the Pd-Ti complex (**1**).

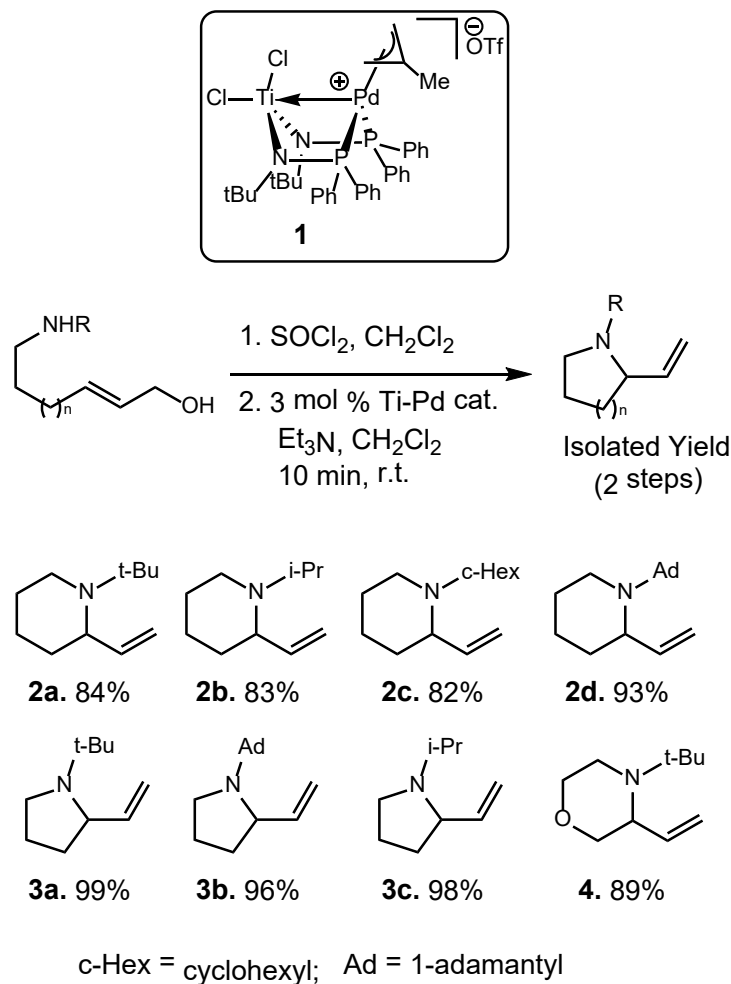


Figure 5.1. Intramolecular aminations for heterocycle synthesis

We are currently focused on developing chiral titanium-phosphinoamide ligands for enantioselective heterobimetallic catalysis. Only a single example of enantioselective heterobimetallic catalysis has been reported², and only one other example of chiral heterobimetallic complexes has been reported.³ We have synthesized a series of chiral diamine-based

phosphionoamide-titanium ligands in order to investigate enantioselective intramolecular aminations. Each of these new titanium ligands enables room temperature catalysis in intramolecular aminations with hindered amines, suggesting contribution by the Ti center. Similar reactivity has not been achieved with monometallic chiral Pd catalysts in our lab. Importantly many of these ligands enable modest enantioselectivity in the allylic aminations.

5.2 RESULTS AND DISCUSSION

5.2.1 *Synthesis of Chiral Titanium Ligands*

We have previously shown that various titanium containing ligands can form heterobimetallic complexes *in situ*, and can be used for allylic aminations and enyne cycloisomerizations.⁴ This precludes the need to isolate and purify the different Pd-Ti complexes. With this in mind we began looking at incorporating chiral ligands into our Pd-Ti scaffold. We have primarily focused on changing the groups connected to the amine. By adding a chiral group to the nitrogen the phenyls bound to phosphine are forced into a certain configuration, which forms a chiral pocket around the Pd center. A series of chiral Ti ligands have been synthesized and x-ray quality single crystals were grown for each ligand, confirming a chiral pocket can be generated by manipulating the groups connected to nitrogen in the ligand structure (Figure 5.2).

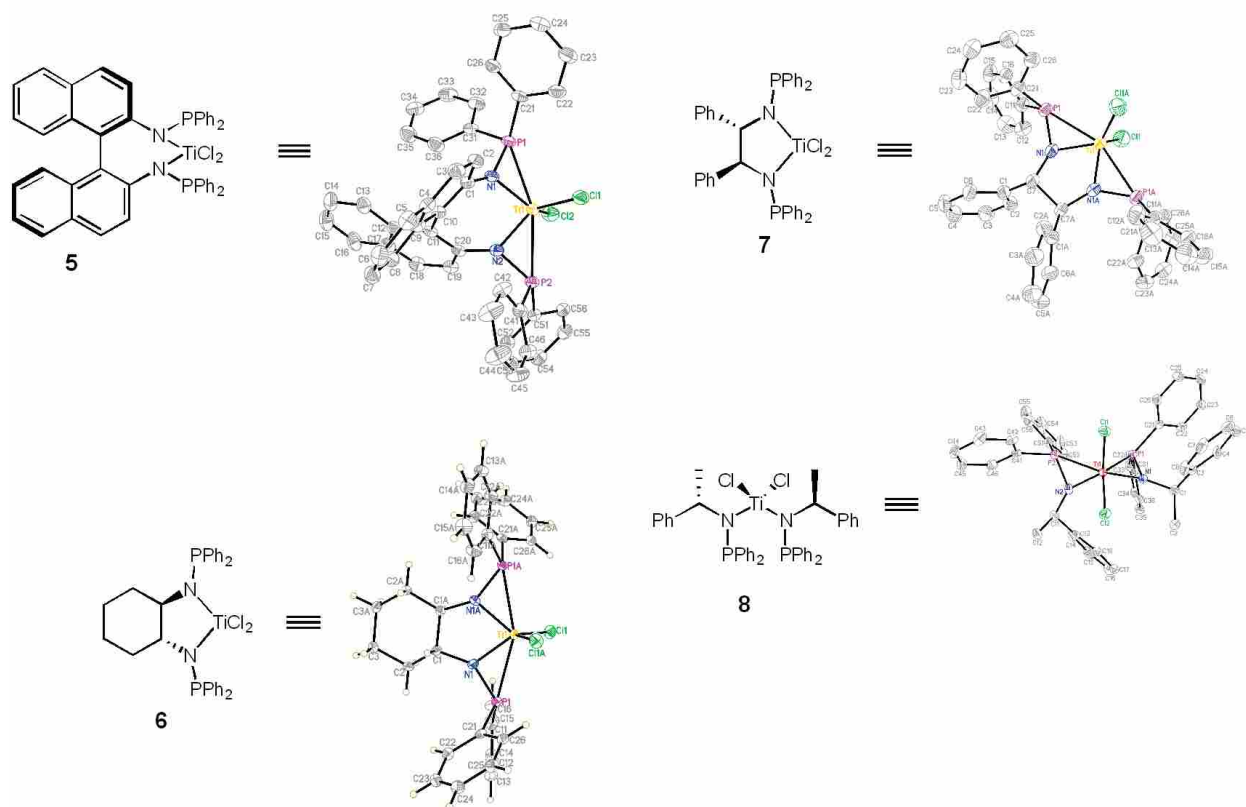


Figure 5.2 Chiral Ti ligands and crystal structures

A sample reaction scheme is shown for the BINAM-derived titanium ligand (Figure 5.3). The first step is the addition of chlorodiphenylphosphine to (R)-1,1'-binaphthyl-2,2'-diamine (**5a**) to obtain the BINAM-aminophosphine **5b**. After deprotonation of **5b** TiCl_4 is added to form the BINAM-derived titanium ligand **5**. The product is isolated by crystallization from a mixture of pentane and dichloromethane.

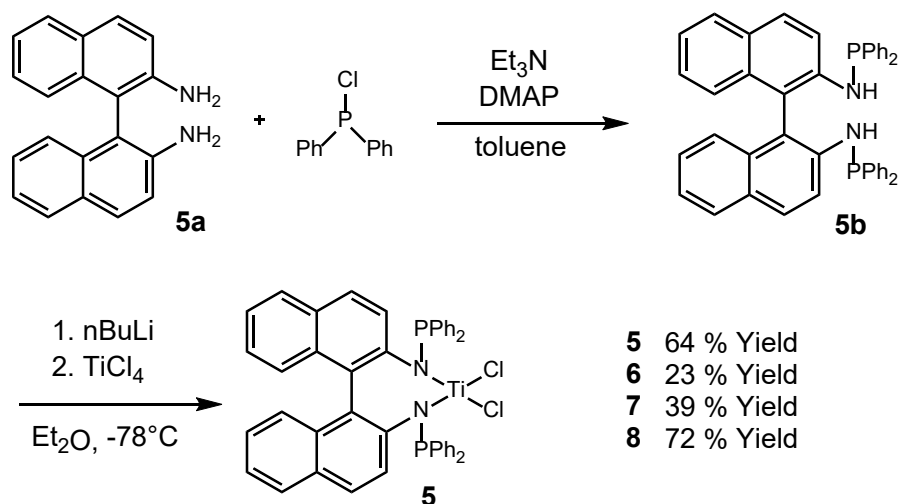


Figure 5.3 Reaction scheme for BINAM-derived Ti ligand

5.2.2 Enantioselective Intramolecular Aminations

The enantioselective synthesis of N-heterocycles is important in drug discovery due to the potential to generate a single enantiomer. Enantioselective heterobimetallic catalysts could be used in the synthesis of these molecules due to the ability to change the ligand structure without significantly changing the reactivity of the complex. We used our chiral titanium ligands in the cyclization of allylic chloride **9** to provide pyrrolidine and pyridine products **10** and **11** (Figure 5.4). The BINAM-derived ligand **5** provided an enantiomeric excess of 38% when the pyrrolidine product was formed with a 98 % isolated yield. All of the ligands were able to catalyze the reaction *in situ* within 3 hrs at room temperature. We are currently working to optimize these exciting results by modifying both the reaction conditions and the structure of the BINAM backbone in **5**.

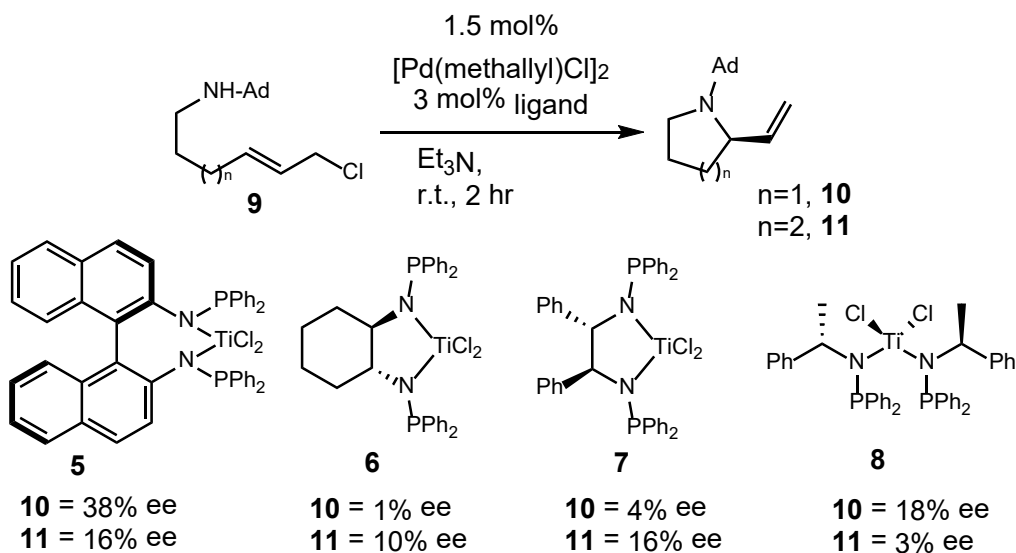


Figure 5.4. Intramolecular aminations using chiral titanium ligands

5.3 CONCLUSION

We have been able to synthesize a series of chiral Ti ligands that can form a dative titanium palladium bond *in situ*. These ligands are able to catalyze intramolecular aminations to form pyrrolidine and piperidine products at room temperature within 3 hrs. Results obtained show that these ligands could possibly provide a novel way to perform enantioselective reactions. Further optimization is being done to increase the ee obtained from each ligand.

5.4 REFERENCES

- (1) Walker, W. K.; Anderson, D. L.; Stokes, R. W.; Smith, S. J.; Michaelis, D. J., Allylic Aminations with Hindered Secondary Amine Nucleophiles Catalyzed by Heterobimetallic Pd-Ti Complexes. *Org. Lett.* **2015**, *17*, 752-755.
- (2) Hansen, J.; Li, B.; Dikarev, E.; Autschbach, J.; Davies, H. M. L., Combined Experimental and Computational Studies of Heterobimetallic Bi-Rh Paddlewheel Carboxylates as Catalysts for Metal Carbenoid Transformations. *J. Org. Chem.* **2009**, *74*, 6564-6571.
- (3) Saper, N. I.; Bezpalko, M. W.; Foxman, B. M.; Thomas, C. M., Synthesis of chiral heterobimetallic tris(phosphinoamide) Zr/Co complexes. *Polyhedron*, **2016**, *114*, 88-95.
- (4) Talley, M. R.; Stokes, R. W.; Walker, W. K.; Michaelis, D. J., Electrophilic activation of alkynes for enyne cycloisomerization reactions with *in situ* generated early/late heterobimetallic Pt-Ti catalysts. *Dalton Trans.* **2016**, *45*, 9770-9773.

Chapter 6

Supporting Information

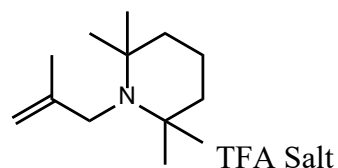
6.1 SUPPORTING INFORMATION FOR CHAPTER 2

6.1.1 *General Information*

All reactions were carried out in oven-dried glassware with magnetic stirring, unless otherwise indicated. All the reagents were used as obtained unless otherwise noted. All commercially available amines were distilled from calcium hydride under nitrogen and stored over 4Å molecular sieves for at least 12 h before use. Reactions requiring a moisture-free environment were conducted in a nitrogen atmosphere glove box (Innovative Technology, PureLab HE system, double glove box). Analytical thin-layer chromatography was performed with 0.25 mm coated commercial silica gel plates (E. Merck, DC-Plastikfolien, kieselgel 60 F254). Flash Chromatography was performed with EM Science silica gel (0.040-0.063 µm grade) Proton nuclear magnetic resonance (¹H NMR) data were acquired on a Inova 300 (300 MHz) or on a Inova-500 (500 MHz) spectrometer. Chemical shifts are reported in delta (δ) units, in parts per million (ppm) downfield from tetramethylsilane. Carbon-13 nuclear magnetic resonance (¹³C-NMR) data were acquired on a Inova 500 at 125 MHz. Signals are reported as follows: s (singlet), d (doublet), t (triplet), q (quartet), dd (doublet of doublets), qd (quartet of doublets), brs (broad singlet), m (multiplet). Coupling constants are reported in hertz (Hz). Chemical shifts are reported in ppm relative to the center line of a triplet at 77.0 ppm for chloroform-d. Mass spectral data were obtained using ESI techniques (Agilent, 6210 TOF). Commercially available ligands 5–8, 10a–10d,

and 11 were used as obtained. Heterobimetallic complex **1**¹ and titanium-ligand **2**² were synthesized as previously described. DCM= dichloromethane (CH₂Cl₂)

6.1.2 Intramolecular Allylic Aminations with Ti-Pd Complex 1

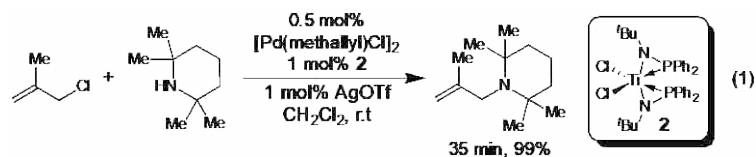


General Procedure for Intermolecular allylic aminations:

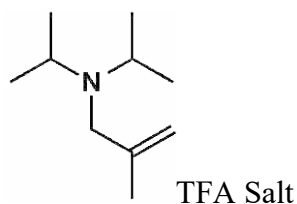
2,2,6,6-tetramethyl-1-(2-methylallyl)piperidine TFA Salt (4a): In a glove box, 9.4 mg (0.01 mmol, 1 mol%) **1** was added to a 25 ml vial and 1 ml of DCM added. 2,2,6,6-tetramethylpiperidine (311 mg, 2.2 mmol, 2.2 equiv) was then added, followed by methylallyl chloride (91 mg, 1.0 mmol). The reaction was allowed to stir for 10 minutes, removed from the glove box, diluted with 1 ml DCM and loaded directly onto a column of silica gel and eluted with 10% MeOH in DCM. Due to the volatility of the products, the fractions containing the product were combined, treated with TFA (1equiv) and the solvent removed *in vacuo*. The product TFA salt was isolated as a pale yellow oil (318mg, >99% yield). IR (film): $\nu = 3408, 2956, 1736, 1687, 1462, 1410, 1394, 1200, 1173, 1129$; ¹H-NMR (500 MHz, CDCl₃): δ (ppm) = 7.50 (bs, 1H), 5.35 (s, 1H), 5.20 (s, 1H), 3.68 (s, 2H), 2.36 (td, J=3.97 Hz, J=13.58 Hz, 2H), 1.96 (s, 3H), 1.82-1.61 (m, 4H) 1.54 (s, 6H) 1.45 (s, 6H); ¹³C-NMR (500 MHz, CDCl₃): δ (ppm) = 15.7, 21.2, 21.4, 29.9, 37.2, 53.0, 67.9, 119.1, 137.6, 160.2 (q, TFA). HRMS (ESI): C₁₃H₂₅N (M+H) calculated: 196.2065, found 196.2089.

¹ Tsutsumi, H.; Sunada, Y.; Shiota, Y.; Yoshizawa, K.; Nagashima, H. *Organometallics* **2009**, *28*, 1988–1991.

² Nagashima, H.; Sue, T.; Oda, T.; Kanemitsu, A.; Matsumoto, T.; Motoyama, Y.; Sunada, Y. *Organometallics* **2006**, *25*, 1987–1994.

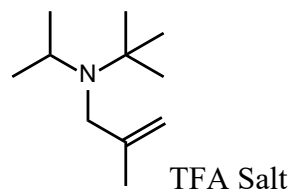


General Procedure for *in situ* formation of active bimetallic catalyst: In a glove box, into a 3 dram vial with a stir bar was weighed ligand **2** (6.3 mg, 0.01 mmol) followed by $[\text{Pd}(\text{methallyl})\text{Cl}]_2$ (2.0 mg, 0.005 mmol), and silver triflate (2.6 mg, 0.01 mmol). The mixture was then dissolved in DCM and allowed to stir for 30 minutes. 2,2,6,6-Tetramethylpiperidine (.371 ml, 2.2 mmol), followed by methallyl chloride (0.10 ml, 1.0 mmol) were then added and the reaction progress was monitored by removing a small aliquot from each reaction vial, diluting in 0.7 ml of CDCl_3 , and then by ^1H NMR analysis of the crude reaction mixture. Complete conversion to product was observed after 20 minutes.

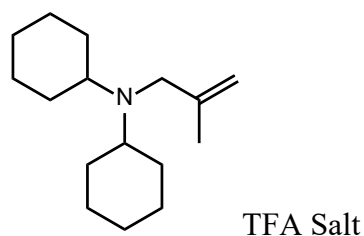


N,N-diisopropyl-2-methylprop-2-en-1-amine TFA Salt (4b): Synthesized according to the general procedure using 91 mg (1.0mmol) methallyl chloride, 223 mg (2.2mmol, 2.2 equiv) of diisopropylamine, and 9.4 mg (0.01 mmol, 1mol %) **1** and purified on silica gel with 10% MeOH in DCM as eluent. The product thus obtained was treated with TFA (1 equiv) and isolated and characterized as the TFA salt. The product was obtained as a yellow oil (161mg, 72% yield). IR (film): $\nu = 2995, 1780, 1738, 1674, 1402, 1174$; $^1\text{H-NMR}$ (500 MHz, CDCl_3): δ (ppm) = 7.80 (bs, 1H), 5.28 (s, 1H), 5.23 (s, 1H), 3.81-3.72 (m, 1H), 3.62 (d, $J=4.93$ Hz, 2H), 1.89 (s, 3H), 1.41 (t, $J=7.48$ Hz, 12H); $^{13}\text{C-NMR}$ (500 MHz, CDCl_3): δ (ppm) = 17.1, 18.4, 20.6, 53.3, 56.4, 119.3, 135.8, 160.3 (q, TFA). HRMS (ESI): $\text{C}_{10}\text{H}_{21}\text{N}$ (M+H) calculated: 156.1752, found 156.1967.

When performed using the in situ catalyst preparation method, 100% conversion to the desired product was also observed in <10 min. Spectral data matched reported values.

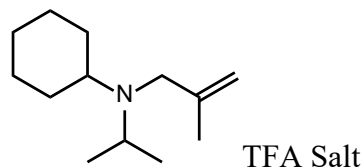


N-(*tert*-butyl)-N-isopropyl-2-methylprop-2-en-1-amine TFA Salt (4c): Synthesized according to the general procedure using 91 mg (1.0 mmol) methallyl chloride, 253 mg (2.2 mmol, 2.2 equiv) of N-isopropyl-*tert*-butylamine and 9.4 mg (0.01 mmol, 1 mol%) **1** and purified on silica gel with 10% MeOH in DCM as eluent. The product thus obtained was treated with TFA (1 equiv) and isolated and characterized as the TFA salt. The product was obtained as a yellow oil (248 mg, 98% yield). IR (film): $\nu = 3405, 2980, 2696, 1648, 1460, 1412, 1394, 1175, 1129$; $^1\text{H-NMR}$ (500 MHz, CDCl_3): δ (ppm) = 9.91 (bs, 1H), 5.46 (s, 1H), 5.22 (s, 1H), 4.28-4.17 (m, 1H), 3.68-3.52 (m, 2H), 2.20 (s, 3H), 1.74-1.38 (m, 15 H); $^{13}\text{C-NMR}$ (500 MHz, CDCl_3): δ (ppm) = 17.3, 22.1, 26.9, 50.9, 55.8, 67.9, 119.8, 138.1. HRMS (ESI): $\text{C}_{13}\text{H}_{25}\text{N}$ (M+H) calculated: 170.1903, found 170.1910.

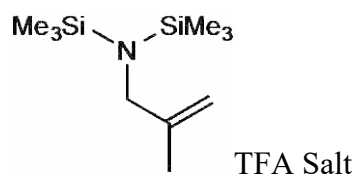


N-cyclohexyl-N-(2-methylallyl)cyclohexanamine TFA Salt (4d): Synthesized according to the general procedure using 91 mg (1.0 mmol) methallyl chloride, 400 mg (2.2 mmol, 2.2 equiv) of dicyclohexylamine, and 9.4 mg (0.01 mmol, 1 mol%) **1** and purified on silica gel with 10% MeOH in DCM as eluent. The product thus obtained was treated with TFA (1 equiv) and isolated and

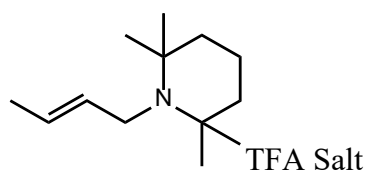
characterized as the TFA salt. The product was obtained as an orange oil (391 mg, 98% yield). IR (film): $\nu = 3405, 2935, 2858, 1454, 1270, 1031, 909$; $^1\text{H-NMR}$ (500 MHz, CDCl_3): δ (ppm) = 10.32 (bs, 1H), 5.48 (s, 1H), 5.27 (s, 1H), 3.55 (d, $J=67.27$ Hz, 2H), 2.47 (bs, 2H), 2.32-2.10 (m, 5H), 1.99-1.64 (m, 11H), 1.38-1.18 (m, 7H); $^{13}\text{C-NMR}$ (500 MHz, CDCl_3): δ (ppm) = 25.5, 27.8, 29.0, 63.9, 120.7, 138.9. HRMS (ESI): $\text{C}_{16}\text{H}_{29}\text{N}$ (M+H) calculated: 236.2373, found 236.2400.



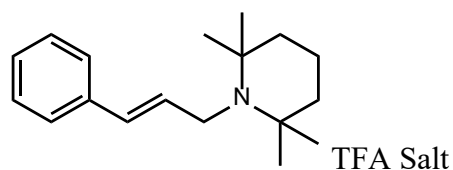
N-isopropyl-N-(2-methylallyl)cyclohexanamine TFA Salt (4e): Synthesized according to the general procedure using 91 mg (1.0 mmol) methallyl chloride, 310 mg (2.2 mmol, 2.2 equiv) of cyclohexylisopropylamine, and 9.4 mg (0.01 mmol, 1 mol%) **1** and purified on silica gel with 10% MeOH in DCM as eluent. The product thus obtained was treated with TFA (1 equiv) and isolated and characterized as the TFA salt. The product was obtained as a yellow oil (338 mg, >99% yield). IR (film): $\nu = 3406, 2933, 2858, 1445, 1119, 1031, 911$; $^1\text{H-NMR}$ (500 MHz, CDCl_3): δ (ppm) = 10.53 (bs, 1H), 5.43 (s, 1H), 5.24 (s, 1H), 3.87-3.77 (m, 1H), 3.62-3.52 (m, 2H), 3.35-3.26 (m, 1H), 2.41 (d, $J=11.92$ Hz, 1H), 2.25 (d, $J=11.93$ Hz, 1H), 2.11 (s, 3H), 1.98-1.88 (m, 1H), 1.83-1.67 (m, 3H), 1.62-1.55 (m, 6H), 1.47 (d, $J=8.52$ Hz, 3H); $^{13}\text{C-NMR}$ (500 MHz, CDCl_3): δ (ppm) = 17.5, 19.3, 22.4, 25.0, 25.5, 25.6, 27.7, 28.5, 53.6, 55.3, 64.2, 120.3, 136.7. HRMS (ESI): $\text{C}_{13}\text{H}_{25}\text{N}$ (M+H) calculated: 196.2060, found 196.2064.



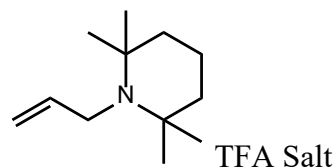
1, 1, 1-trimethyl-*N*-(2-methylallyl)-*N*-(trimethylsilyl)silanamine TFA Salt (4f): Synthesized according to the general procedure using 91 mg (1.0mmol) methallyl chloride, 474 mg (2.2mmol, 2.2 equiv) of bis(trimethylsilyl)amine, and 9.4 mg (0.01 mmol, 1mol %) **1**. Yield obtained by comparison with an internal standard (mesitylene) was >99%. The product was not isolated due to instability of TMS-amides to moisture and silica gel chromatography. ¹H-NMR (500 MHz, CDCl₃): δ (ppm) = 4.92 (s, 1H), 4.84 (s, 1H), 2.81 (s, 2H), 1.76 (s, 3H), 0.079 (s, 18H); ¹³C-NMR (500 MHz, CDCl₃): δ (ppm) = 2.4, 20.6, 60.6, 112.5, 144.0.



1-(but-2-en-1-yl)-2,2,6,6-tetramethylpiperidine TFA Salt (4h): Synthesized according to the general procedure using 91 mg (1.0 mmol) crotyl chloride, 311 mg (2.2 mmol, 2.2 equiv) of 2,2,6,6-tetramethylpiperidine, and 9.4 mg (0.01 mmol, 1 mol%) **1** and purified on silica gel with 10% MeOH in DCM as eluent. The product thus obtained was treated with TFA (1 equiv) and isolated and characterized as the TFA salt. The product TFA salt was isolated as a pale yellow oil (316mg, 97% yield). The product consisted of ~5:1 mixture of cis/trans isomers as reflected from the same ratio of isomers in the chloride starting material. IR (film): ν = 3363, 2949, 2748, 2621, 1777, 1740, 1687, 1462, 1434, 1395, 1199, 1172, 1143; ¹H-NMR (500 MHz, CDCl₃): δ (ppm) = 8.89 (bs, 1H), 5.91 (m, 1H), 5.76 (m, 1H), 3.67 (m, 2H), 2.42 (td, J=3.01 Hz, J=13.99 Hz, 2H), 1.82-1.63 (m, 7H), 1.56 (s, 6H), 1.35 (s, 6H); ¹³C-NMR (500 MHz, CDCl₃): δ (ppm) = 15.9, 17.6, 21.3, 29.3, 36.7, 49.2, 65.9, 123.9, 132.9, 160.0 (q, TFA). HRMS (ESI): C₁₃H₂₅N (M+H) calculated: 196.2065, found 196.2091.



1-cinnamyl-2,2,6,6-tetramethylpiperidine TFA Salt (4i): Synthesized according to the general procedure using 153 mg (1.0 mmol) cinnamyl chloride, 311 mg (2.2 mmol, 2.2 equiv) of 2,2,6,6-tetramethylpiperidine, and 9.4 mg (0.01 mmol, 1 mol%) **1** and purified on silica gel with 10% MeOH in DCM as eluent. The product thus obtained was treated with TFA (1 equiv) and isolated and characterized as the TFA salt. The product TFA salt was isolated as an orange oil (325mg, 87% yield). IR (film): $\nu = 3026, 2952, 1775, 1736, 1685, 1670, 1460, 1396, 1201$; $^1\text{H-NMR}$ (500 MHz, CDCl_3): δ (ppm) = 8.12 (bs, 1H), 7.42-7.28 (m, 5H), 6.64 (d, $J=15.63$ Hz, 1H), 6.50-6.43 (m, 1H), 3.92-3.89 (m, 2H), 2.19 (t, $J=13.30$ Hz, 2H), 1.85-1.66 (m, 4H), 1.57 (s, 6H), 1.45 (s, 6H); $^{13}\text{C-NMR}$ (500 MHz, CDCl_3): δ (ppm) = 15.7, 21.2, 29.6, 37.1, 49.7, 66.4, 120.8, 126.9, 128.8, 128.9, 134.8, 136.6, 160.1 (q, TFA). HRMS (ESI): $\text{C}_{18}\text{H}_{27}\text{N}$ ($\text{M}+\text{H}$) calculated: 258.222, found 258.2247.

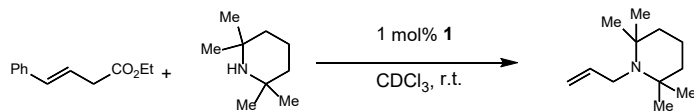


1-allyl-2,2,6,6-tetramethylpiperidine TFA Salt (4j): Synthesized according to the general procedure using 77 mg (1.0 mmol) allyl chloride, 311 mg (2.2 mmol, 2.2 equiv) of 2,2,6,6-tetramethylpiperidine, and 9.4 mg (0.01 mmol, 1 mol%) **1** and purified on silica gel with 10% MeOH in DCM as eluent. The product thus obtained was treated with TFA (1 equiv) and isolated and characterized as the TFA salt. The product TFA salt was isolated as an orange oil (247mg, 85% yield). IR (film): $\nu = 3407, 2987, 2953, 1736, 1686, 1671, 1461, 1437, 1396, 1200, 1141$; $^1\text{H-NMR}$ (500 MHz, CDCl_3): δ (ppm) = 8.09 (bs, 1H), 6.17-6.06 (m, 1H), 5.39 (d, $J=4.77$ Hz, 1H), 5.37 (s,

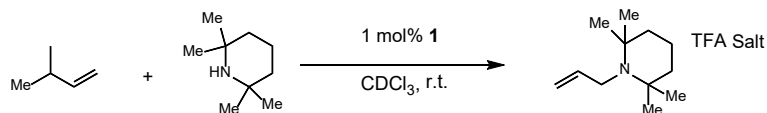
1H), 3.75-3.71 (m, 2H), 2.17 (td, J=3.18 Hz, J=13.87 Hz, 2H), 1.84-1.63 (m, 4H), 1.49 (s, 6H), 1.40 (s, 6H); ¹³C-NMR (500 MHz, CDCl₃): δ (ppm) = 15.7, 21.0, 29.3, 36.8, 49.7, 66.3, 121.9, 130.6, 160.2 (q, TFA). HRMS (ESI): C₁₂H₂₃N (M+H) calculated: 182.1909, found 182.1918.



1-allyl-2,2,6,6-tetramethylpiperidine (4j) (Table 2 Entry 11): Prepared according to general procedure I using allyl acetate (0.10 g, 1 mmol), catalyst **1** (0.0093 g, 0.01 mmol), 2,2,6,6-tetramethylpiperidine (371 μL, 2.2 mmol, 2.2 equiv), and mesitylene (internal standard, 46 μL) in 1 mL CDCl₃. The reaction was run at ambient temperature for 4.5 h and the yield (5.0%) determined by ¹H NMR analysis by comparison to an internal standard.



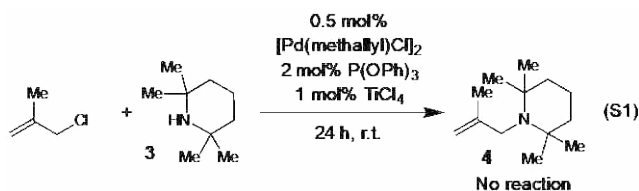
1-cinnamyl-2,2,6,6-tetramethylpiperidine (4i) (Table 2 Entry 12): Prepared according to general procedure I using ethyl cinnamylcarbonate (0.206 g, 1 mmol), catalyst **1** (0.0093 g, 0.01 mmol), 2,2,6,6-tetramethylpiperidine (371 μL, 2.2 mmol, 2.2 equiv), and mesitylene (internal standard, 46 μL) in 1 mL CDCl₃. The reaction was run at ambient temperature for 4.5 h and the yield (33.0%) determined by ¹H NMR analysis by comparison to an internal standard.



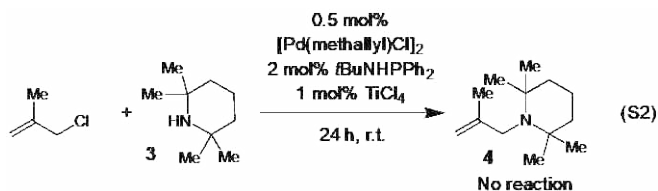
1-(but-2-en-1-yl)-2,2,6,6-tetramethylpiperidine TFA Salt (Table 2 Entry 13): Synthesized according to general procedure I using 91 mg (1.0 mmol) 3-chloro-1-butene, 311 mg (2.2 mmol, 2.2 equiv) of 2,2,6,6-tetramethylpiperidine, and 9.4 mg (0.01 mmol, 1 mol%) **1** and purified on

silica gel with 10% MeOH in DCM as eluent. The product thus obtained was treated with TFA (1 equiv) and isolated and characterized as the TFA salt. The product TFA salt was isolated as a pale yellow oil (78% yield by internal standard). The product consisted of ~1.3:1 mixture of trans/cis isomers. The product obtained was the same as in reaction **4h**.

6.1.3 Control Studies



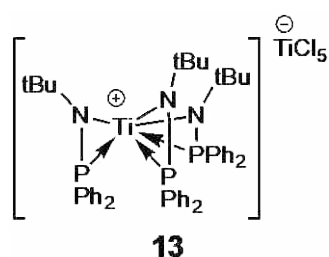
Control Study with P(OPh)₃ + TiCl₄ (Eq. S2): In a glove box, into a 3 dram vial was placed [Pd(methallyl)Cl]₂ (2.0 mg, 0.005 mmol), AgOTf (2.6 mg, 0.01 mmol), and triphenylphosphite (6.2 mg, 0.02 mmol). The mixture was dissolved in 1 ml CDCl₃, and the reaction stirred 20 min. Titanium tetrachloride (1.7 mg, 0.01 mmol) was then added and the mixture allowed to stir 5 minutes. 2,2,6,6-Tetramethylpiperidine (310 mg, 2.2 mmol) was then added, followed by methallyl chloride (92.5 mg, 1.0 mmol). The reaction mixture was then transferred to an NMR tube and the reaction progress monitored by ¹H NMR. The reaction proceeded to 22% conversion after 2 hrs and then conversion stalled, leading to no further conversion after 24 hrs.



Control Study with *t*-BuNHPPH₂ + TiCl₄: In a glove box, into a 3 dram vial was placed [Pd(methallyl)Cl]₂ (2.0 mg, 0.005 mmol), AgOTf (2.6 mg, 0.01 mmol), and *N*-*tert*-butyldiphenylphosphinoamine (2.6 mg, 0.02 mmol). The mixture was dissolved in 1 ml CDCl₃,

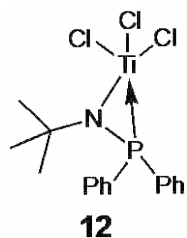
and the reaction stirred 20 min. Titanium tetrachloride (1.7 mg, 0.01 mmol) was then added and the mixture allowed to stir 5 minutes. 2,2,6,6-Tetramethylpiperidine (310 mg, 2.2 mmol) was then added, followed by methallyl chloride (92.5 mg, 1.0 mmol). The reaction mixture was then transferred to an NMR tube and the reaction progress monitored by ^1H NMR. No product formation was observed, even after 24 hrs.

6.1.4 Synthesis of Titanium-containing Ligands 12 and 13

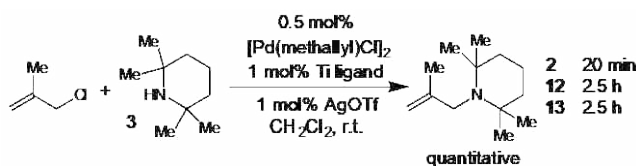


Titanium Tris(*N-tert*-butyl(diphosphino)amide) pentachlorotitanate (13): In a dry 100 ml round bottom flask 1.33 g (5.0 mmol) of phosphinoamine (Ph_2PNHtBu) was dissolved in 90 ml dry Et_2O . A hexane solution of 1.6 M *n*-BuLi (2.5 ml) was added dropwise at -78°C . The solution was warmed to room temperature and stirred for two hours. TiCl_4 (0.23 ml, 2.09 mmol) was slowly added dropwise, which caused precipitation of an orange/yellow solid. The reaction was taken into a glove box and filtered under air and moisture free conditions. The precipitate was filtered off, dissolved in 15 ml DCM in a 5 dram vial, and placed in a larger vial containing hexanes. The product was allowed to crystalize from the solution via slow vapor deposition. This process afforded the desired titanium tris(*N-tert*-butyl(diphénylphosphino)amide) as the titanium pentachloride salt. Red solid, 0.280 g, 31% yield. ^1H NMR (300 MHz, CDCl_3): δ (ppm) 7.474-7.272 (m, 9H), 7.262-7.037 (m, 9H), 6.809-6.699 (m, 6H), 6.581-6.485 (m, 6H), 1.613 (s, 27H); ^{13}C NMR (300 MHz, CDCl_3): δ (ppm) 136.393, 134.051, 132.235, 129.068, 128.084, 127.107,

126.684, 62.570, 62.422, 33.873; ^{31}P NMR (300 MHz, CDCl_3): δ (ppm) -15.919. Structure was confirmed by single Crystal X-ray analysis.



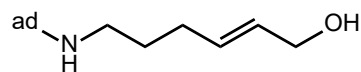
Trichlorotitanium *N*-tert-butyl(diphenylphosphino)amide (12): The red ether filtrate obtained after removal of the yellow solids above was next concentrated under vacuum in the glove box. Toluene (~50 ml) was then added to the resulting red solid, and any insoluble materials were filtered off. The toluene solution was concentrated until the volume reached about 5–7 ml. It was then layered with hexanes and placed in a $-40\text{ }^\circ\text{C}$ freezer for about 24hrs. The dark red crystals thus obtained were collected and dried under vacuum, affording trichlorotitanium *N*-tert-butyl(diphenylphosphino)amide, 0.120 g, 14% yield (45% total yield of both ligands). ^1H NMR (300 MHz, CDCl_3): δ (ppm) 7.94-7.74 (m, 4H), 7.67-7.47 (m, 6H), 1.59 (s, 9H); ^{13}C NMR (300 MHz, CDCl_3) δ (ppm) 133.738, 133.566, 132.120, 132.078, 129.270, 129.114, 32.576, 32.541; ^{31}P NMR (300 MHz, CDCl_3): δ (ppm) -10.994. Structure was confirmed by single Crystal X-ray analysis.



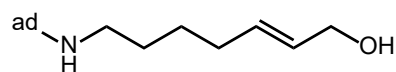
Procedure for *in situ* formation of bimetallic catalysts with ligands 2, 12, and 13. In a glove box, into a 3 dram vial with a stir bar was weighed ligand **2** (6.3 mg, 0.01 mmol), **12** (8.2 mg, 0.02 mmol) or **13** (10.4 mg, 0.01 mmol), followed by $[\text{Pd}(\text{methallyl})\text{Cl}]_2$ (2.0 mg, 0.005 mmol), and

silver triflate (2.6 mg, 0.01 mmol). The mixture was then dissolved in DCM and allowed to stir for 30 minutes. 2,2,6,6-Tetramethylpiperidine (.371 ml, 2.2 mmol), followed by methallyl chloride (0.10 ml, 1.0 mmol) were then added and the reaction progress was monitored by removing a small aliquot from each reaction vial, diluting in 0.7 ml of CDCl₃, and then by ¹H NMR analysis of the crude reaction mixture. Complete conversion to the product was observed in 20 min, 2.5 h, and 2.5 h for ligands **2**, **12**, and **13** respectively.

6.1.5 Synthesis of Alcohol Substrates for Intramolecular Aminations

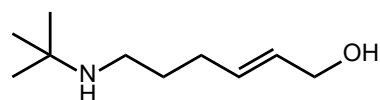


6-((adamantan-2-yl)amino)hex-2-en-1-ol (S1): General Procedure II: Into a 100 ml round bottom flask was placed 6-bromohex-2-en-1-ol (500 mg, 2.8 mmol) in 20 ml DMF. Diisopropylethylamine (1.46 ml, 8.4 mmol, 3 equiv) and 1-adamantylamine (210 mg, 14.0 mmol, 5 equiv) were then added. After stirring at room temperature for 40 hours, the solvent was removed, and the product purified on a column of silica gel. The product was eluted with 5% MeOH in DCM saturated with NH₃, and isolated as a white solid (0.335 mg, 48% yield). Melting Point: 75-80°C. IR (film): $\nu = 3246, 2902, 1451, 1024$; ¹H-NMR (500 MHz, CDCl₃): δ (ppm) = 5.72-5.61 (m, 2H), 4.07 (d, J=4.80 Hz, 2H), 2.58 (t, J=7.32, 2H), 2.12-2.03 (m, 5H), 1.69-1.51 (m, 16H); ¹³C-NMR (500 MHz, CDCl₃): δ (ppm) = 29.6, 30.2, 30.5, 36.7, 39.9, 42.7, 50.5, 63.4, 129.4, 132.5. HRMS (ESI): C₁₆H₂₇NO (M+H) calculated: 250.2171, found 250.2181.

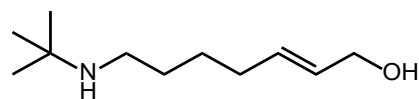


7-((adamantan-2-yl)amino)hept-2-en-1-ol (S2): Synthesized according to general procedure II using 1.5 g (7.77 mmol) 7-bromohept-2-en-1-ol, 4.06 ml (23.3 mmol, 3 equiv) of

diisopropylethylamine, and 5.88 g (38.8 mmol, 5 equiv) 1-adamantylamine and purified on silica gel with 5% MeOH in DCM saturated with NH₃ as eluent. The product was isolated as a yellow solid, 1.15 g (56% yield). (Melting Point: 69-71°C). IR (film): ν = 2905, 2848, 1452, 1098; ¹H-NMR (500 MHz, CDCl₃): δ (ppm) = 5.72-5.60 (m, 2H), 4.08 (d, J=5.07 Hz, 2H), 2.57 (t, J=7.20 Hz, 2H), 2.09-2.04 (m, 5H), 1.70-1.58 (m, 12H), 1.50, 1.38 (m, 4H); ¹³C-NMR (500 MHz, CDCl₃): δ (ppm) = 27.0, 29.6, 30.5, 32.1, 36.8, 40.2, 42.6, 42.7, 50.4, 63.6, 129.4, 132.9. HRMS (ESI): C₁₇H₂₉NO (M+H) calculated: 264.2327, found 264.2320.

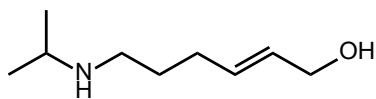


6-(*tert*-butylamino)hex-2-en-1-ol (S3): Synthesized according to general procedure II using 1.39 g (7.77 mmol) 6-bromohex-2-en-1-ol, 4.06 ml (23.3 mmol, 3 equiv) of diisopropylethylamine, and 2.84 ml (38.8 mmol, 5 equiv) *tert*-butylamine and purified on silica gel with 5% MeOH in DCM saturated with NH₃ as eluent. The product was isolated as a orange oil (1.134 g, 85.3% yield). IR (film): ν = 3273, 2966, 2931, 2856, 1456, 1364, 1215, 1092, 1020, 967; ¹H-NMR (500 MHz, CDCl₃): δ (ppm) = 5.75-5.62 (m, 2H), 4.09 (d, J=5.12 Hz, 2H), 2.55 (t, J=7.28 Hz, 2H), 2.10 (q, J=6.96 Hz, 2H), 1.55 (p, J=7.55 Hz, 2H), 1.10 (s, 9H); ¹³C-NMR (500 MHz, CDCl₃): δ (ppm) = 29.0, 30.2, 30.4, 42.1, 50.3, 63.6, 129.4, 132.6. HRMS (ESI): C₁₀H₂₁NO (M+H) calculated: 172.1701, found 172.1728.

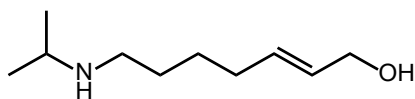


7-(*tert*-butylamino)hept-2-en-1-ol (S4): Synthesized according to general procedure II using 500 mg (2.6 mmol) 7-bromohept-2-en-1-ol, 1.4 ml (7.8 mmol, 3 equiv) of diisopropylethylamine, and 1.28 ml (13.0 mmol, 5 equiv) *tert*-butylamine and purified on silica gel with 5% MeOH in DCM

saturated with NH_3 as eluent. The product was isolated as a orange oil (414 mg, 86% yield) IR (film): $\nu = 3275, 2965, 2928, 2855, 1440, 1363, 1231, 1020, 970$; $^1\text{H-NMR}$ (500 MHz, CDCl_3): δ (ppm) = 5.70-5.59 (m, 2H), 4.06 (d, $J=4.37$ Hz, 2H), 2.56 (t, $J=7.36$ Hz, 2H), 2.52-2.35 (bs, 1H), 2.06 (q, $J=6.33$ Hz, 2H), 1.54-1.46 (m, 2H), 1.46-1.38 (m, 2H), 1.12 (s, 9H); $^{13}\text{C-NMR}$ (500 MHz, CDCl_3): δ (ppm) = 26.9, 28.6, 29.9, 32.0, 42.2, 50.9, 63.4, 129.7, 132.5. HRMS (ESI): $\text{C}_{11}\text{H}_{23}\text{NO}$ (M+H) calculated: 186.1858, found 186.1890.

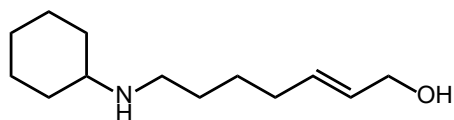


6-(isopropylamino)hex-2-en-1-ol (S5): Synthesized according to general procedure II using 1.39 g (7.77 mmol) 6-bromohex-2-en-1-ol, 4.06 ml (23.3 mmol, 3 equiv) of diisopropylethylamine, and 2.3 ml (38.8 mmol, 5 equiv) isopropylamine and purified on silica gel with 5% MeOH in DCM saturated with NH_3 as eluent. The product was isolated as a white solid (1.033 g, 85% yield). Melting Point: 28-32°C. IR (film): $\nu = 3273, 2931, 2847, 1471, 1382, 1175, 1092, 1017, 970$; $^1\text{H-NMR}$ (500 MHz, CDCl_3): δ (ppm) = 5.71-5.60 (m, 2H), 4.05 (d, $J=4.32$ Hz, 2H), 2.78 (sept, $J=6.25$ Hz, 1H), 2.59 (t, $J=7.48$ Hz, 2H), 2.08 (q, $J=6.78$ Hz, 2H), 1.57 (p, $J=7.29$ Hz, 2H), 1.05 (d, $J=6.29$ Hz, 6H); $^{13}\text{C-NMR}$ (500 Mhz, CDCl_3): δ (ppm) = 22.8, 29.6, 30.1, 46.9, 48.7, 62.8, 130.0, 131.5. HRMS (ESI): $\text{C}_9\text{H}_{19}\text{NO}$ (M+H) calculated: 158.1545, found 158.1568.



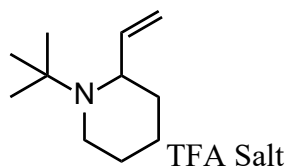
7-(isopropylamino)hept-2-en-1-ol (S6): Synthesized according to general procedure II using 500 mg (2.6 mmol) 7-bromohept-2-en-1-ol, 1.4 ml (7.8 mmol, 3 equiv) of diisopropylethylamine, and 1.12 ml (13.0 mmol, 5 equiv) isopropylamine and purified on silica gel with 5% MeOH in DCM saturated with NH_3 as eluent. The product was isolated as a white solid (395 mg, 89% yield,

Melting Point: 46-48°C). IR (film): $\nu = 3273, 2965, 2929, 2854, 1458, 1382, 1339, 1174, 1088, 1015, 970$; $^1\text{H-NMR}$ (500 MHz, CDCl_3): δ (ppm) = 5.69-5.58 (m, 2H), 4.03 (d, $J=4.37$ Hz, 2H), 2.78 (sept, $J=6.21$ Hz, 1H), 2.57 (t, $J=7.42$ Hz, 2H), 2.05 (q, $J=6.27$ Hz, 2H), 1.53-1.45 (m, 2H), 1.45-1.37 (m, 2H), 1.05 (d, $J=6.35$, 6H); $^{13}\text{C-NMR}$ (500 MHz, CDCl_3): δ (ppm) = 22.7, 26.8, 29.5, 32.0, 47.1, 48.6, 62.7, 129.9, 131.7. HRMS (ESI): $\text{C}_{10}\text{H}_{21}\text{NO}$ (M+H) calculated: 172.1701, found 172.1728.

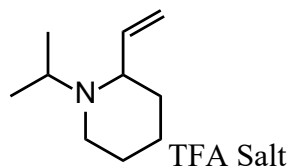


7-(cyclohexylamino)hept-2-en-1-ol (S7): Synthesized according to general procedure II using 500 mg (2.6 mmol) 7-bromohept-2-en-1-ol, 1.4 ml (7.8 mmol, 3 equiv) of diisopropylethylamine, and 1.49 ml (13.0 mmol, 5 equiv) cyclohexylamine and purified on silica gel with 5% MeOH in DCM saturated with NH_3 as eluent. The product was isolated as a white solid (519 mg, 95% yield, Melting Point: 66-69°C). IR (film): $\nu = 3255, 2963, 2928, 1260, 1090, 1021, 799$; $^1\text{H-NMR}$ (500 MHz, CDCl_3): δ (ppm) = 5.70-5.59 (m, 2H), 4.06 (d, $J=4.83$ Hz, 2H), 2.60 (t, $J=7.39$ Hz, 2H), 2.42-2.35 (m, 1H), 2.05 (q, $J=7.04$ Hz, 2H), 1.86 (d, $J=12.53$ Hz, 2H), 1.75-1.68 (m, 2H), 1.65-1.57 (m, 1H), 1.52-1.36 (m, 4H), 1.30-0.99 (m, 5H); $^{13}\text{C-NMR}$ (500 MHz, CDCl_3): δ (ppm) = 25.3, 26.3, 27.1, 30.1, 32.2, 33.8, 46.9, 57.1, 63.6, 129.7, 132.8. HRMS (ESI): $\text{C}_{13}\text{H}_{25}\text{NO}$ (M+H) calculated: 212.2014, found 212.2045.

6.1.6 Intramolecular Amination Reactions

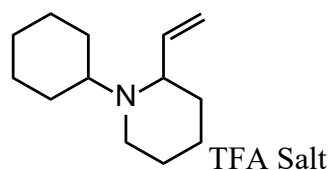


1-(*tert*-butyl)-2-vinylpiperidine TFA Salt (14a): General Procedure III. Into a 3 dram vial containing a stir bar was placed 60 mg (0.32 mmol) 7-(*tert*-butylamino)hept-2-en-1-ol in 2 ml DCM. Thionyl chloride (0.03 ml, 0.38 mmol, 1 equiv) was slowly added at 0 °C. After stirring at room temperature for 1 hour, the solvent was removed and the resulting chloride was azeotroped with benzene by adding 2 ml benzene and then removing the solvent on the rotary evaporator. The vial containing the chloride was then taken into a glovebox. Next, 8.9 mg (0.009 mmol, 3 mol%) **1** was added and the reaction mixture dissolved in 1 ml DCM. Triethylamine (0.09 ml, 0.64 mmol, 2 equiv) was then added, the reaction was allowed to stir for 10 minutes, removed from the glove box, diluted with 1 ml DCM and loaded directly onto a column of silica gel and eluted with 10% MeOH:H₂O (10:1) in DCM. Due to the volatility of the products, the fractions containing the product were combined, treated with TFA (5 equiv) and the solvent removed *in vacuo*. The product TFA salt was isolated as a yellow oil as a hydrate/TFA adduct 131 mg. The yield was determined by addition of an internal standard (mesitylene) and then via analysis of the ¹H NMR spectrum. 84% yield. IR (film): $\nu = 2962, 1672, 1260, 1091, 1021, 799$; ¹H-NMR (500 MHz, CDCl₃): δ (ppm) = 8.98 (bs, 1H), 6.37-6.27 (m, 1H), 5.51-5.44 (m, 2H), 4.48 (d, J=8.17 Hz, 1H), 3.46 (d, J=12.10 Hz, 1H), 3.10 (q, J=12.22 Hz, 1H), 2.51 (tt, J=4.33 Hz, J=14.18 Hz, 1H), 2.20-2.06 (m, 1H), 1.97 (d, J=14.48 Hz, 1H), 1.77-1.55 (m, 3H), 1.45 (s, 9H); ¹³C-NMR (500 MHz, CDCl₃): δ (ppm) = 17.3, 23.5, 25.4, 32.1, 43.1, 60.8, 65.6, 121.9, 130.4. HRMS (ESI): C₁₁H₂₁N (M+H) calculated: 168.1752, found 168.1776.



1-isopropyl-2-vinylpiperidine TFA Salt (14b): Synthesized according to general procedure III using 60 mg (0.35 mmol) 7-(isopropylamino)hept-2-en-1-ol, 0.03 ml (0.35 mmol, 1 equiv) thionyl chloride, 8.9 mg (.009 mmol, 3 mol%) of **1**, and 0.09 ml (0.63 mmol, 2 equiv) triethylamine and purified on silica gel with 9:1 MeOH:H₂O in DCM. Due to the volatility of the products, the fractions containing the product were combined, treated with TFA (5 equiv) and the solvent removed *in vacuo*. The product TFA salt was isolated as a yellow oil as a hydrate/TFA adduct 168 mg. The yield was determined by addition of an internal standard (mesitylene) and then via analysis of the ¹H NMR spectrum. 83% yield. IR (film): ν = 2992, 2953, 1739, 1671, 1201, 1173, 1142; ¹H-NMR (500 MHz, CDCl₃): δ (ppm) = 13.60 (bs, 1H), 10.24 (bs, 1H), 6.20-6.09 (m, 1H), 5.42-5.35 (m, 2H), 3.83 (p, J=6.51 Hz, 1H), 3.53-3.37 (m, 2H), 2.62 (q, J=11.18 Hz, 1H), 2.17-2.05 (m, 2H), 1.97-1.88 (m, 2H), 1.84 (d, J=14.37 Hz, 1H), 1.54-1.44 (m, 1H), 1.41 (d, J=6.63 Hz, 3H), 1.17 (d, J=6.70 Hz, 3H); ¹³C-NMR (500 MHz, CDCl₃): δ (ppm) = 13.2, 18.1, 22.5, 22.5, 30.7, 44.8, 53.6, 66.8, 121.4, 133.2. HRMS (ESI): C₁₀H₁₉N (M+H) calculated: 154.1596, found 154.1614.

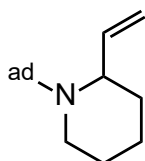
When this same reaction protocol was performed with the *in situ* generated catalyst, complete consumption of the starting material was also observed in <10 min.



1-cyclohexyl-2-vinylpiperidine TFA Salt (14c): Synthesized according to general procedure III using 60 mg (0.28 mmol) 7-(cyclohexylamino)hept-2-en-1-ol, 0.02 ml (0.28 mmol, 1 equiv) thionyl chloride, 7.4 mg (.008 mmol, 3 mol%) of **1**, and 0.07 ml (0.52 mmol, 2 equiv) triethylamine and purified on silica gel with 9:1 MeOH:H₂O in DCM. Due to the volatility of the products, the

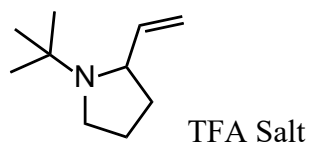
fractions containing the product were combined, treated with TFA (5 equiv) and the solvent removed *in vacuo*. The product TFA salt was isolated as a yellow oil as a hydrate/TFA adduct 125 mg. The yield was determined by addition of an internal standard (mesitylene) and then via analysis of the ^1H NMR spectrum. 82% yield. IR (film): $\nu = 2945, 2863, 1670, 1456, 1200, 1177, 1142, 910, 733$; ^1H -NMR (500 MHz, CDCl_3): δ (ppm) = 10.07 (bs, 1H), 6.21-6.12 (m, 1H), 5.43-5.32 (m, 2H), 3.60-3.39 (m, 3H), 2.65 (q, $J=11.91$ Hz, 1H), 2.22-2.08 (m, 3H), 1.92-1.86 (m, 4H), 1.70 (d, $J=13.29$ Hz, 1H), 1.53-1.09 (m, 8H); ^{13}C -NMR (500 MHz, CDCl_3): δ (ppm) = 22.5, 22.7, 23.8, 25.0, 25.3, 28.1, 30.7, 46.8, 61.9, 66.3, 121.3, 133.4. HRMS (ESI): $\text{C}_{13}\text{H}_{23}\text{N}$ (M+H) calculated: 194.1909, found 194.1924.

When this same reaction protocol was performed with the *in situ* generated catalyst, complete consumption of the starting material was also observed in <10 min.

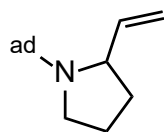


1-(adamantan-2-yl)-2-vinylpiperidine (14d): Synthesized according to general procedure III (see below) using 130 mg (0.50 mmol) 7-((adamantan-2-yl)amino)hex-2-en-1-ol, 0.04 ml (0.50 mmol, 1 equiv) thionyl chloride, 8.5 mg (.009 mmol, 2 mol%) of **1**, and 0.13 ml (0.92 mmol, 2 equiv) triethylamine and purified on silica gel with 5% MeOH in DCM saturated with NH_3 as eluent. The product was isolated as an orange solid (106 mg, 93% yield. When this same reaction protocol was performed with the *in situ* generated catalyst, complete consumption of the starting material was also observed in <10 min. Melting Point: 61-65°C). IR (film): $\nu = 2929, 2905, 2849, 1260, 1099, 1021$; ^1H -NMR (500 MHz, CDCl_3): δ (ppm) = 6.55-6.46 (m, 1H), 5.08-5.00 (m, 2H), 3.86-3.81 (m, 1H), 2.87 (d, $J=12.12$, 1H), 2.69-2.62 (m, 1H), 2.03 (s, 3H), 1.87-1.41 (m, 18H); ^{13}C -NMR (500

MHz, CDCl₃): δ (ppm) = 20.5, 27.4, 29.9, 34.8, 36.9, 39.0, 40.1, 54.7, 55.7, 113.3, 140.1. HRMS (ESI): C₁₇H₂₇N (M+H) calculated: 246.2222, found 246.2238.

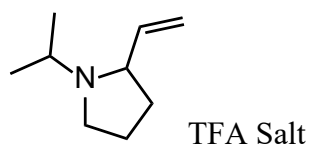


1-(*tert*-butyl)-2-vinylpyrrolidine TFA Salt (15a): Synthesized according to general procedure III using 60 mg (0.35 mmol) 6-(*tert*-butylamino)hex-2-en-1-ol, 0.03 ml (0.35 mmol, 1 equiv) thionyl chloride, 8.9 mg (.009 mmol, 3 mol%) of **1**, and 0.09 ml (0.63 mmol, 2 equiv) triethylamine and purified on silica gel with 9:1 MeOH:H₂O in DCM. Due to the volatility of the product, the fractions containing the product were combined, treated with TFA (5 equiv) and the solvent removed *in vacuo*. The product TFA salt was isolated as a yellow oil as a hydrate/TFA adduct 158 mg. The yield was determined by addition of an internal standard (mesitylene) and then via analysis of the ¹H NMR spectrum. : 99% yield. IR (film): ν = 2963, 1673, 1260, 1092, 1020, 799; ¹H-NMR (500 MHz, CDCl₃): δ (ppm) = 13.24 (bs, 1H), 10.47 (bs, 1H), 6.32-6.22 (m, 1H), 5.36-5.30 (m, 2H), 4.00 (p, J=7.82 Hz, 1H), 3.84 (h, J=6.10 Hz, 1H), 3.17-3.08 (m, 1H), 2.25-1.92 (m, 4H), 1.44 (s, 9H); ¹³C-NMR (500 MHz, CDCl₃): δ (ppm) = 23.3, 25.6, 32.9, 50.1, 63.0, 66.5, 119.9, 134.4. HRMS (ESI): C₁₀H₁₉N (M+H) calculated: 154.1596, found 154.1620.



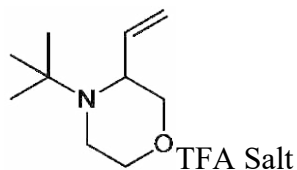
1-(adamantan-2-yl)-2-vinylpyrrolidine (15b): General Procedure III: Into a 3 dram vial containing a stir bar was placed 6-((adamantan-2-yl)amino)hex-2-en-1-ol (95 mg, 0.38 mmol) in 2 ml DCM. Thionyl chloride (0.03 ml, 0.38 mmol, 1 equiv) was slowly added at 0 °C. After stirring at room temperature for 1 hour, the solvent was removed and the resulting chloride was azeotroped

with benzene by adding 2 ml benzene and then removing the solvent on the rotary evaporator. The vial containing the chloride was then taken into a glovebox. Next, 10 mg (0.01 mmol, 3 mol%) **1** was added and the reaction mixture dissolved in 1 ml DCM. Triethylamine (0.10 ml, 0.71 mmol, 2 equiv) was then added, the reaction was allowed to stir for 10 minutes, removed from the glove box, diluted with 1 ml DCM and loaded directly onto a column of silica gel and eluted with 5% MeOH in DCM saturated with NH₃. The product was isolated was an orange oil (79 mg, 96% yield). IR (film): ν = 2904, 2849, 1638, 1450, 1359, 1309, 994; ¹H-NMR (500 MHz, CDCl₃): δ (ppm) = 5.89 (p, J=8.55 Hz, 1H), 5.06 (d, J=17.03 Hz, 1H), 4.88 (d, J=10.09 Hz, 1H), 3.59 (s, 1H), 2.94 (s, 1H), 2.78 (q, J=8.75 Hz, 1H), 2.05 (s, 3H), 1.82-1.55 (m, 16H); ¹³C-NMR (500 MHz, CDCl₃): δ (ppm) = 23.9, 29.6, 33.3, 37.0, 40.0, 46.1, 58.2, 111.5, 146.1. HRMS (ESI): C₁₆H₂₅N (M+H) calculated: 232.2065, found 232.2080.



1-isopropyl-2-vinylpyrrolidine TFA Salt (15c): Synthesized according to general procedure III using 24.5 mg (0.155 mmol) 7-(*iso*-propylamino)hept-2-en-1-ol, 0.012 ml (0.155 mmol, 1 equiv) thionyl chloride, 4.4 mg (.0047 mmol, 3 mol%) of **1**, and 0.043 ml (0.32 mmol, 2 equiv) triethylamine and purified on silica gel with 9:1 MeOH:H₂O in DCM. Due to the volatility of the products, the fractions containing the product were combined, treated with TFA (5 equiv) and the solvent removed *in vacuo*. The product TFA salt was isolated as a yellow oil as a hydrate/TFA adduct 45.9 mg. The yield was determined by addition of an internal standard (mesitylene) and then via analysis of the ¹H NMR spectrum. 98% yield (92% yield obtained using 0.06 g starting material alcohol). IR (film): ν = 2990, 2917, 1670, 1200, 1139; ¹H-NMR (500 MHz, CDCl₃): δ (ppm) = 10.06 (bs, 1H), 6.09-5.99 (m, 1H), 5.50-5.42 (m, 2H), 3.78-3.60 (m, 3H), 3.10-3.00 (m,

1H), 2.27-2.16 (m, 2H), 2.13-1.92 (m, 2H), 1.38 (d, J=6.64 Hz, 3H), 1.27 (d, J=6.62 Hz, 3H); ¹³C-NMR (500 MHz, CDCl₃): δ (ppm) = 14.9, 19.0, 21.5, 30.5, 46.8, 52.6, 67.8, 123.5, 131.3. HRMS (ESI): C₉H₁₇N (M+H) calculated: 140.1439, found 140.1457.



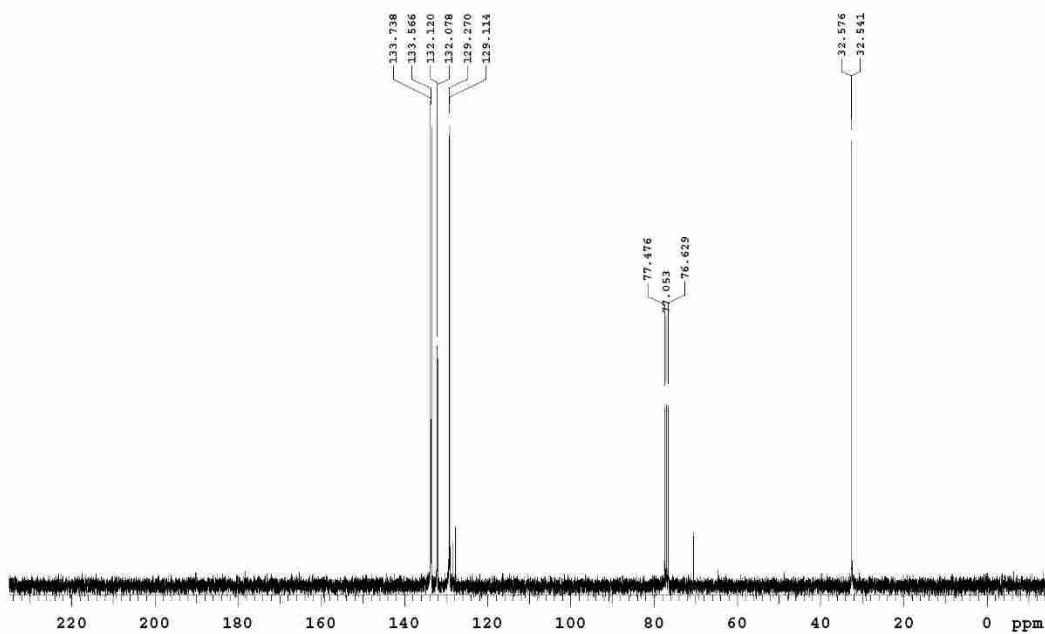
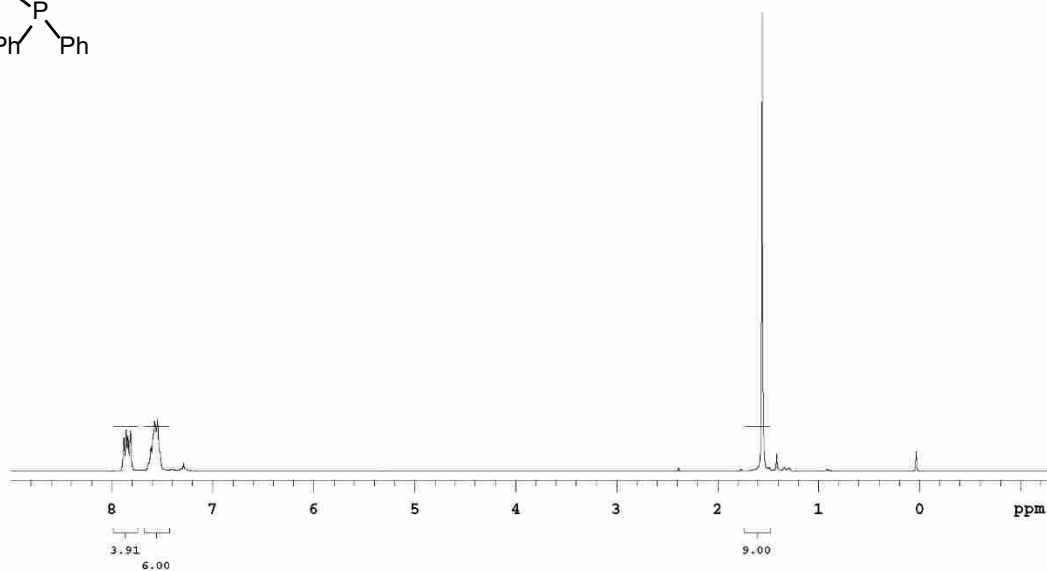
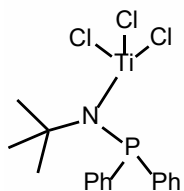
4-(tert-butyl)morpholine TFA Salt (16): Synthesized from the corresponding chloride as follows:

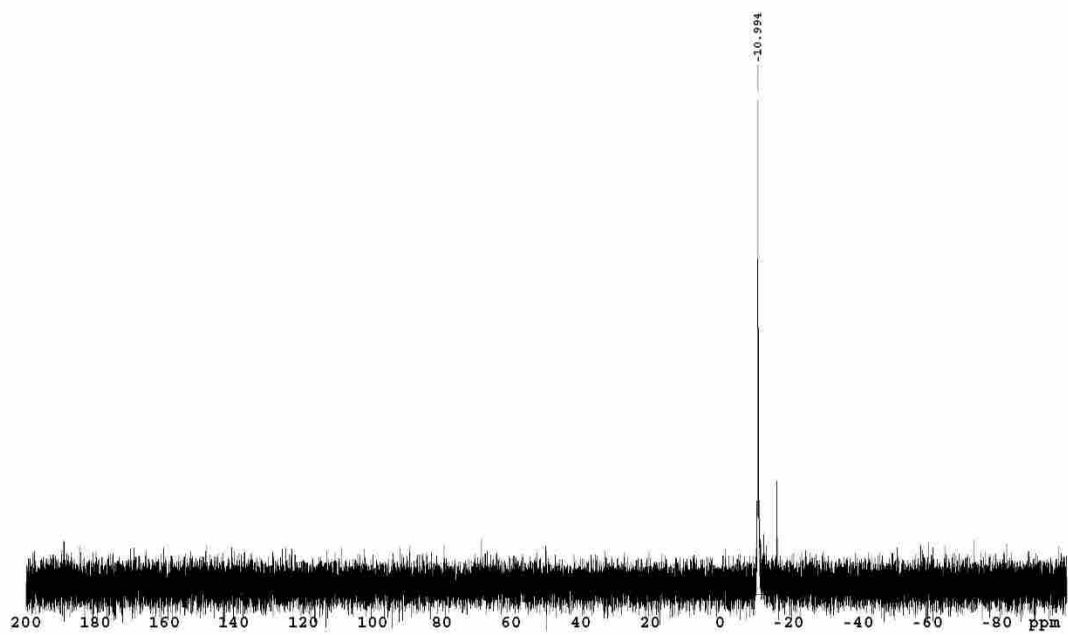
In a glove box, into a 3 dram vial was placed 50 mg (0.24 mmol) N-(2-((4-chlorobut-2-en-1-yl)oxy)ethyl)-2-methylpropan-2-amine,³ 6.9 mg (.007 mmol, 3 mol%) of **1**, 1 ml DCM, and finally 0.07 ml (0.48 mmol, 2 equiv) triethylamine. The reaction was stirred for 10 minutes, removed from the glove box, diluted with 1 ml DCM, and loaded directly onto a column of silica gel. The product was eluted with 9:1 MeOH:H₂O in DCM. Due to the volatility of the products, the fractions containing the product were combined, treated with TFA (5 equiv) and the solvent removed *in vacuo*. The product TFA salt was isolated as a yellow oil as a hydrate/TFA adduct 104 mg. The yield was determined by addition of an internal standard (mesitylene) and then via analysis of the ¹H NMR spectrum. 89% yield. IR (film): ν = 2988, 2918, 2877, 2768, 2636, 1671, 1383, 1202, 1136; ¹H-NMR (500 MHz, CDCl₃): δ (ppm) = 10.65 (bs, 1H), 6.43-6.34 (m, 1H), 5.65-5.56 (m, 2H), 4.32 (d, J=10.10 Hz, 1H), 4.24 (d, J=13.07 Hz, 1H), 4.13-4.07 (m, 2H), 3.82 (d, J=13.00 Hz, 1H), 3.41-3.28 (m, 2H), 1.46 (s, 9H); ¹³C-NMR (500 MHz, CDCl₃): δ (ppm) = 25.1, 26.3, 42.1, 60.1, 64.6, 71.6, 123.3, 129.9. HRMS (ESI): C₁₃H₂₃N (M+H) calculated: 170.1545, found 170.1565.

6.1.7 Spectral Images

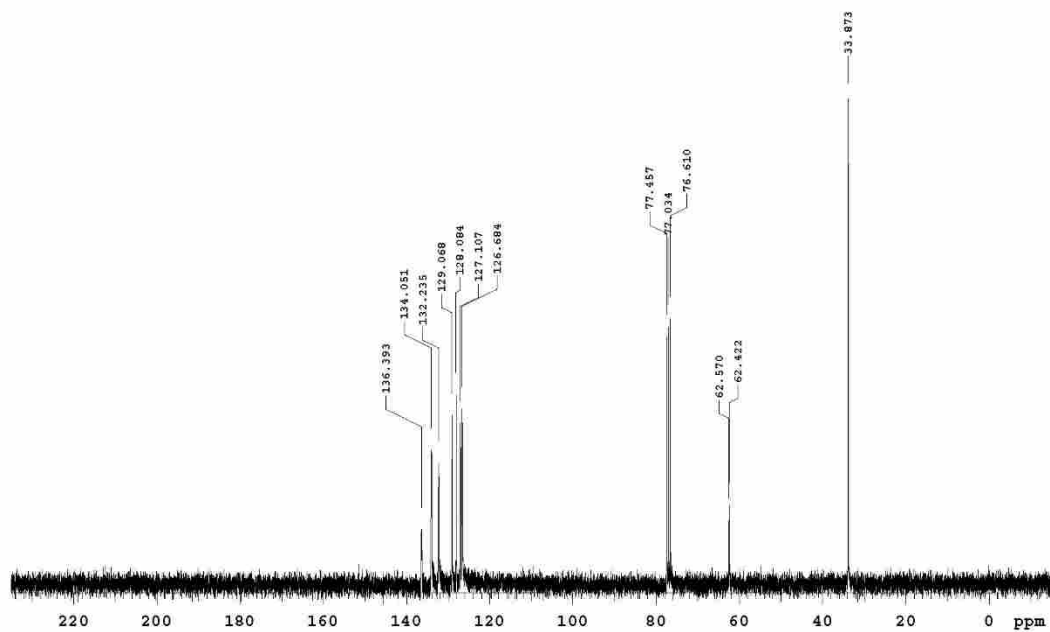
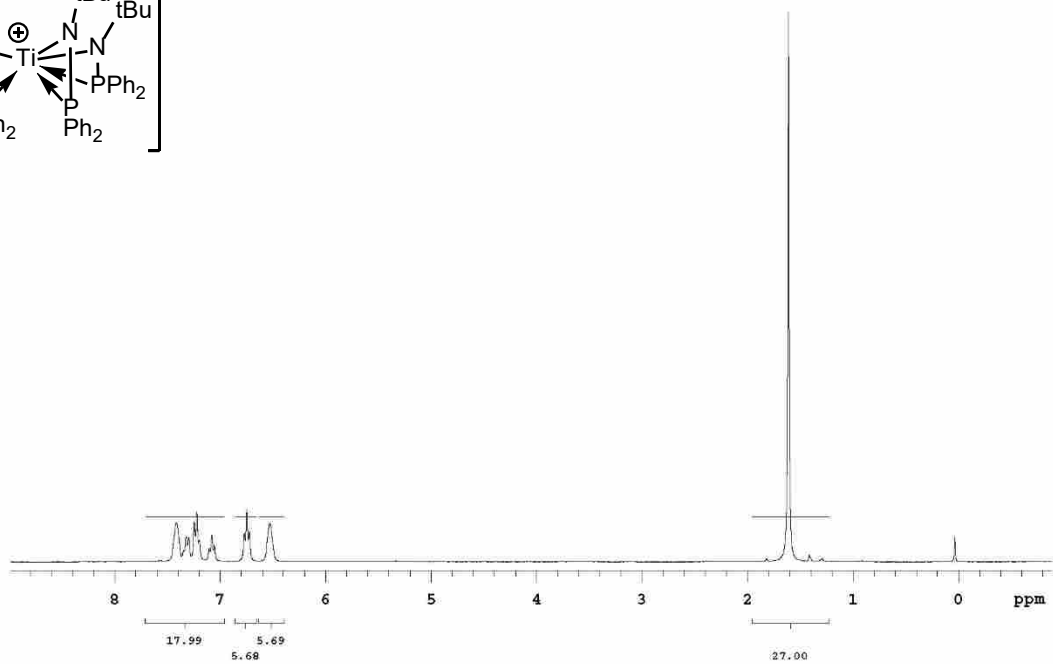
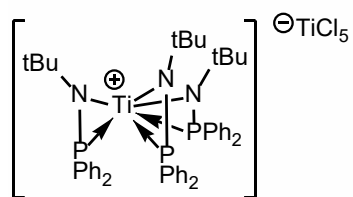
³ Synthesized from N-tert-butylaminoethanol based on the following precedent: Arisawa, M.; Kato, C.; Kaneko, H.; Nishida, A.; Nakagawa, M. *J. Chem. Soc., Perkin Trans. 1*, **2000**, 12 1873.

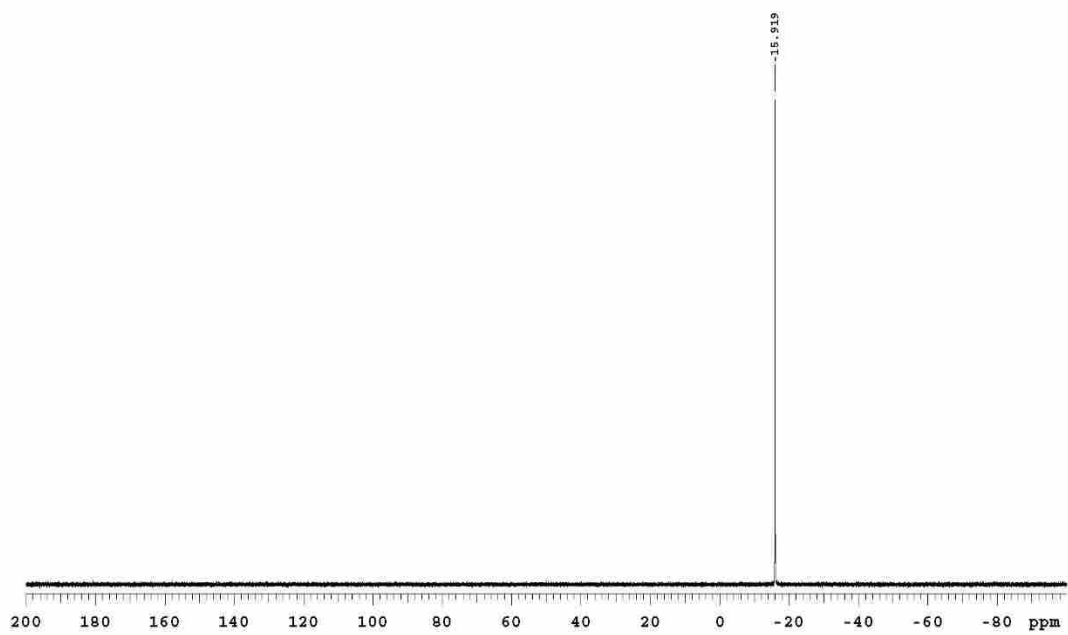
(*tert*-butyl(diphenylphosphanyl)amino)titanium(IV) trichloride (**12**):



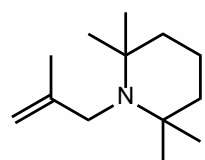


Titanium Tris(*N*-*tert*-butyl-diphenylphosphinoamide) pentachlorotitanate (**13**):

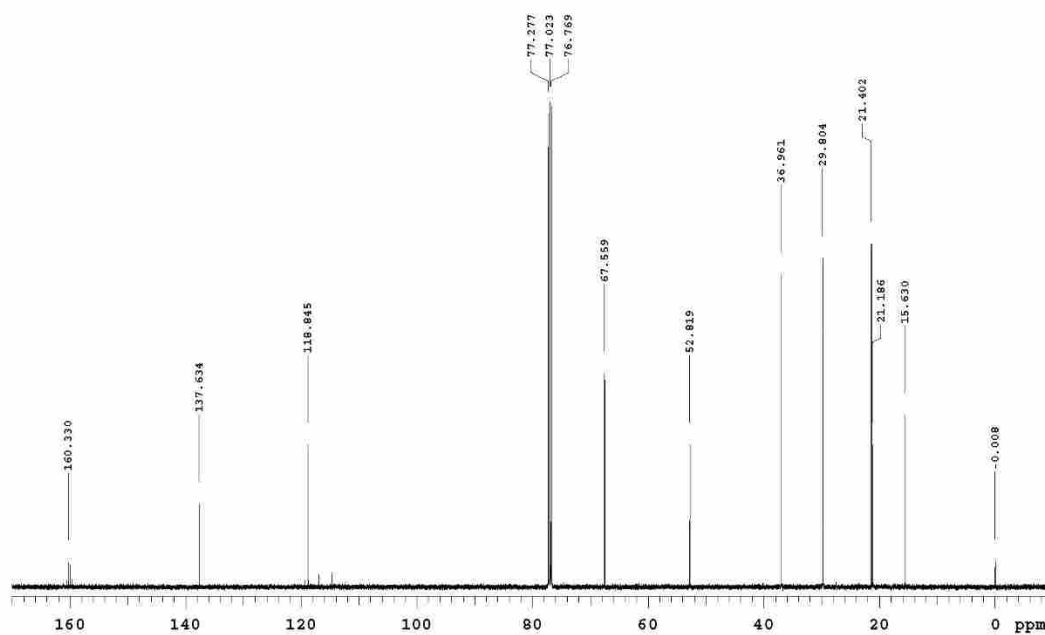
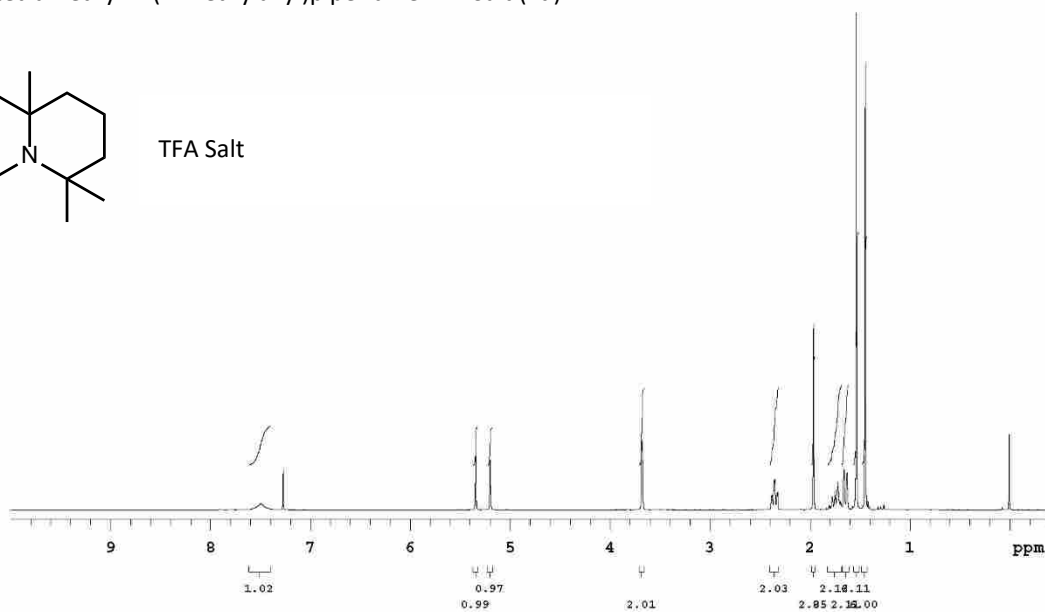




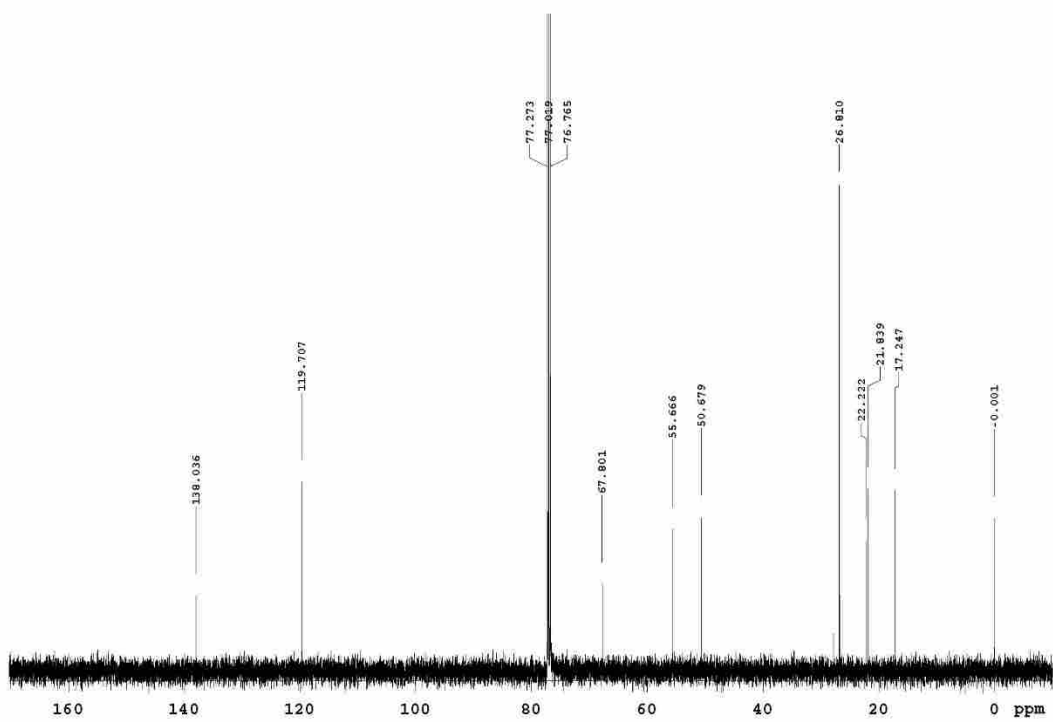
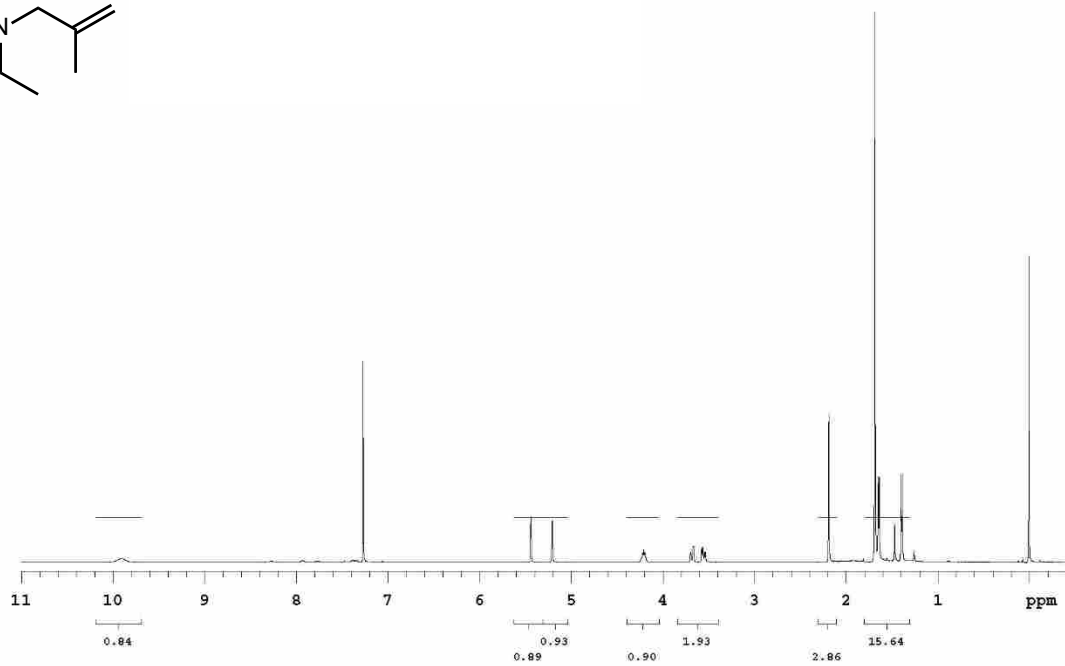
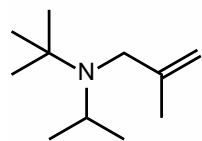
2,2,6,6-tetramethyl-1-(2-methylallyl)piperidine TFA Salt (**4a**):



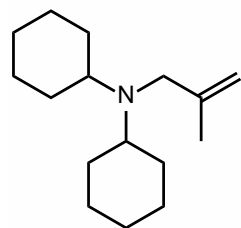
TFA Salt



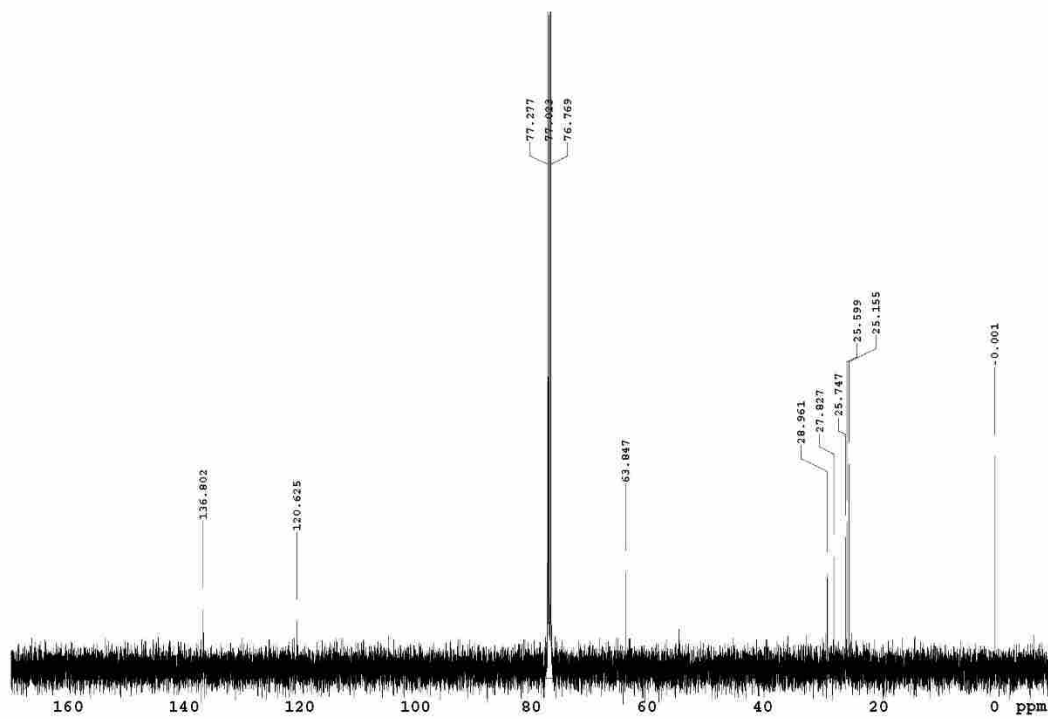
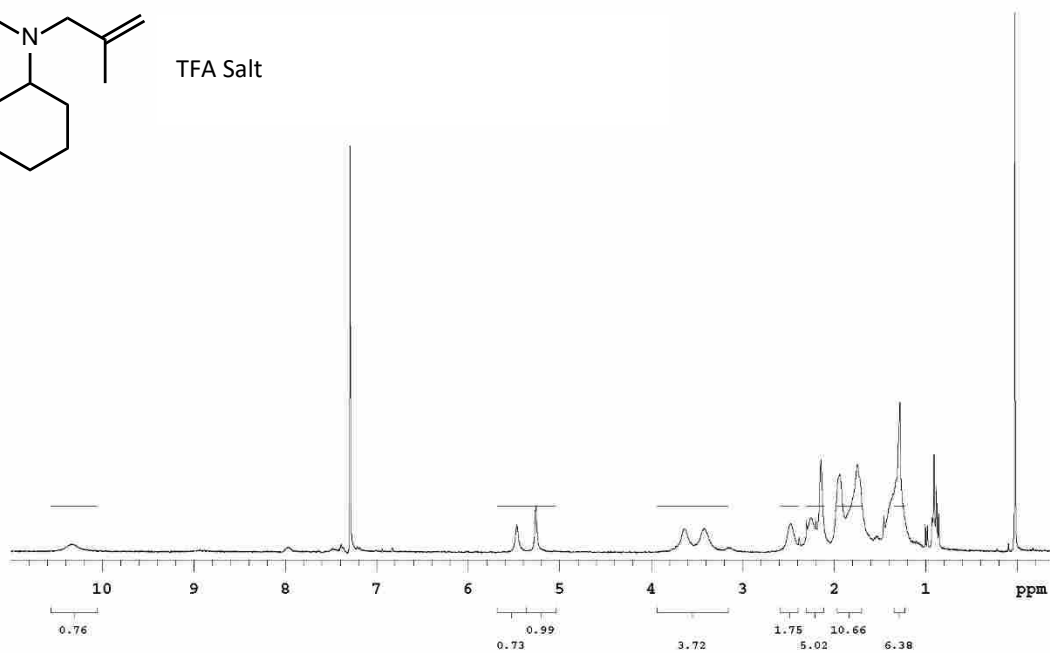
N-(*tert*-butyl)-N-isopropyl-2-methylprop-2-en-1-amine TFA Salt (**4c**):



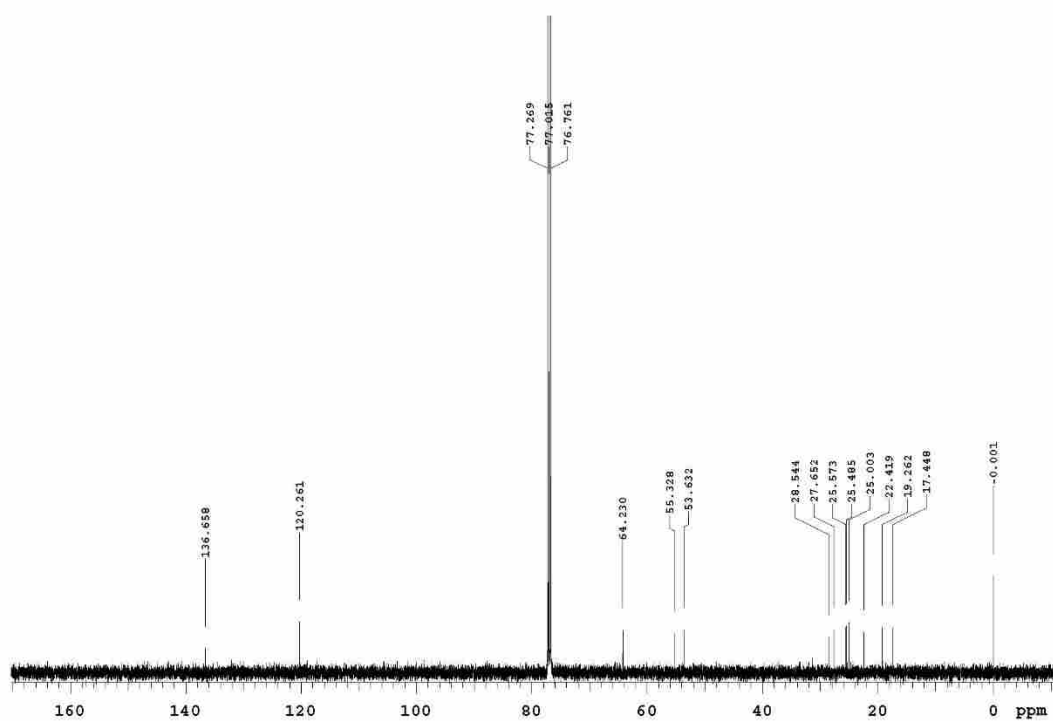
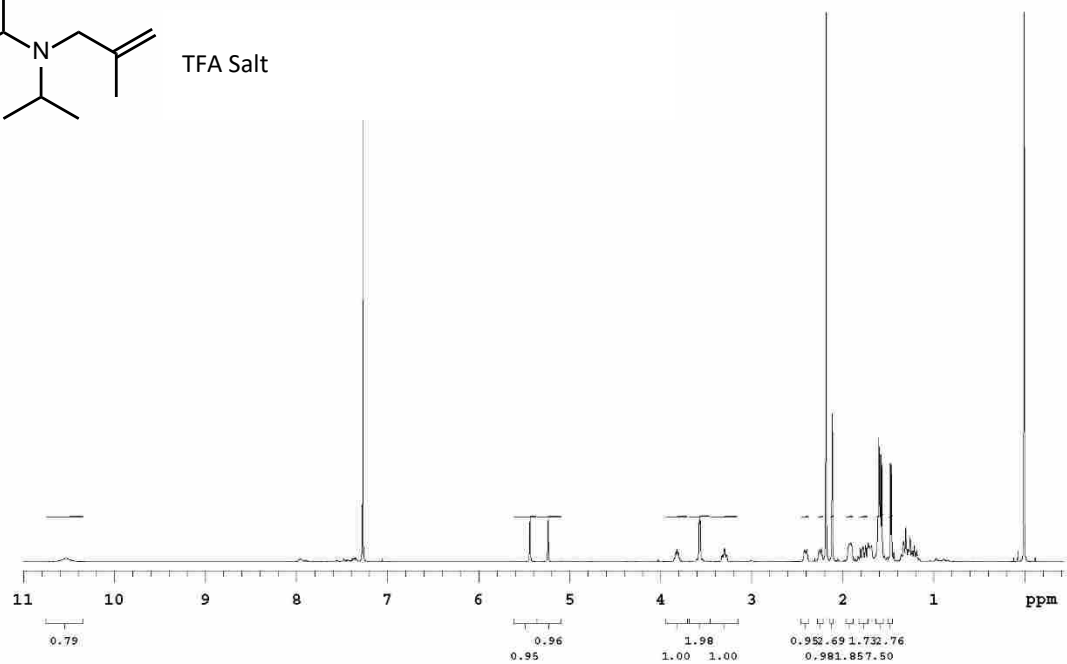
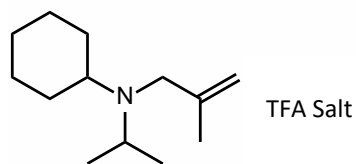
N-cyclohexyl-N-(2-methylallyl)cyclohexanamine TFA Salt (**4d**):



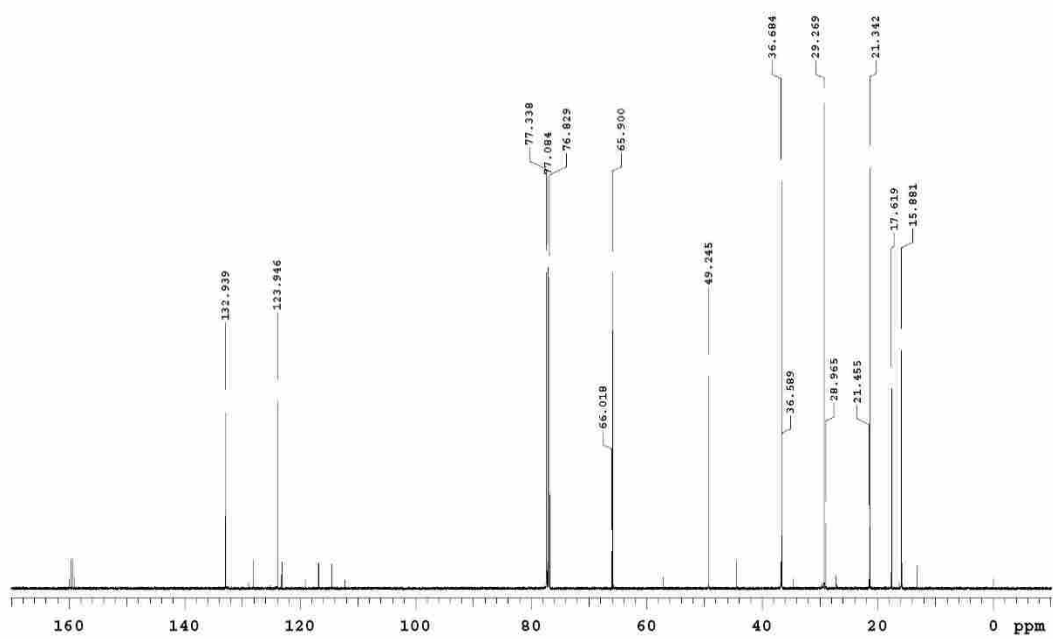
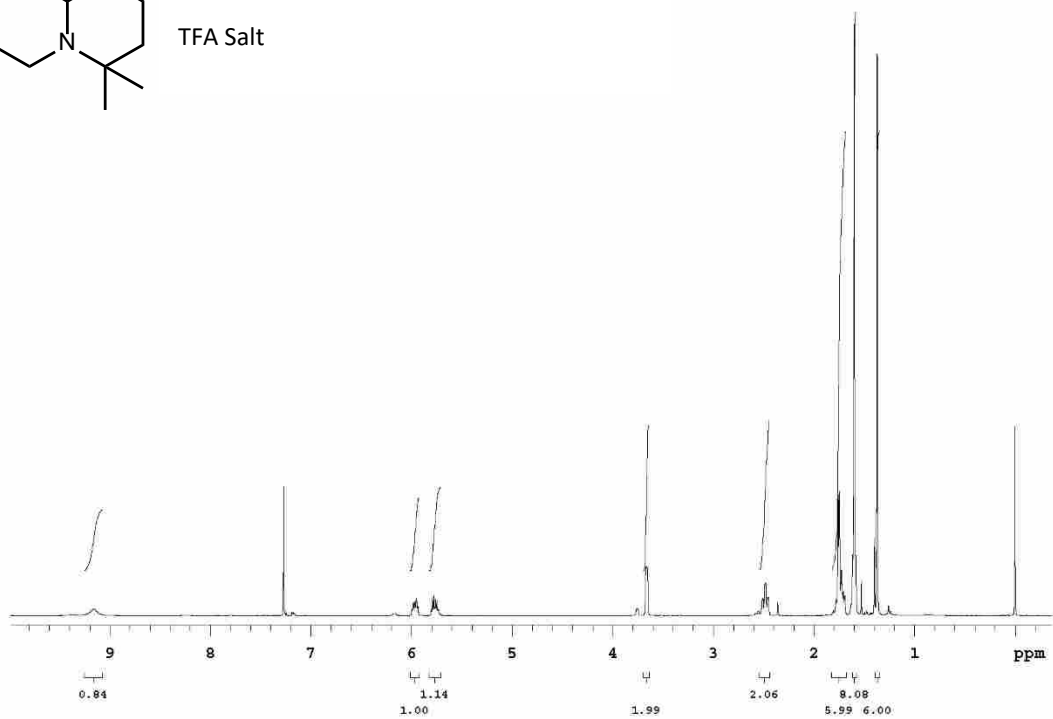
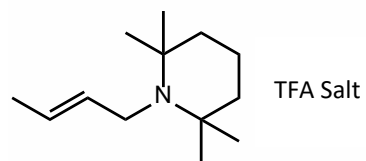
TFA Salt



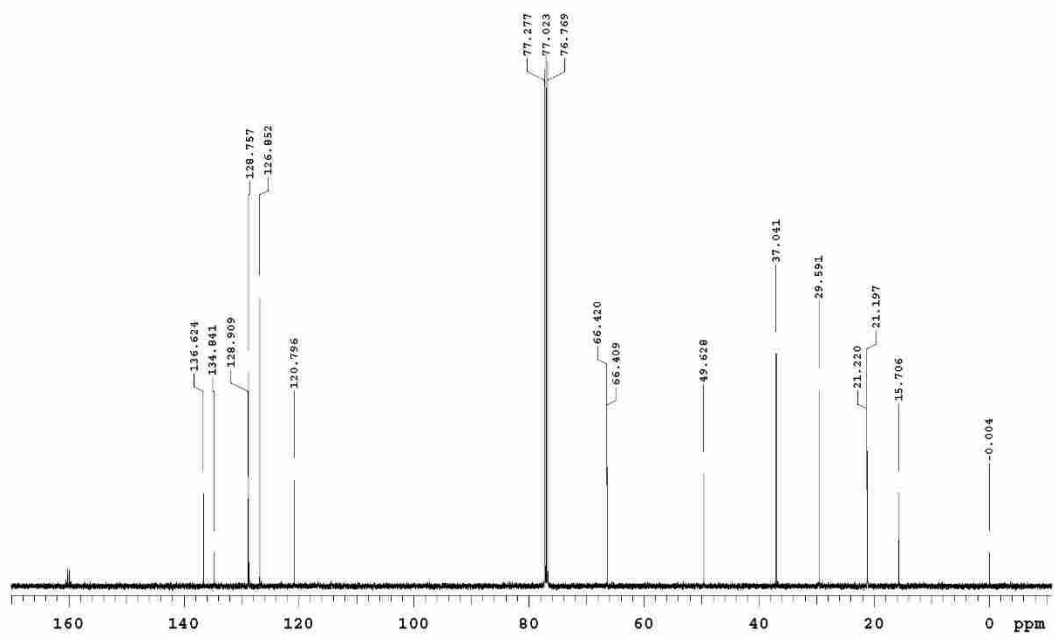
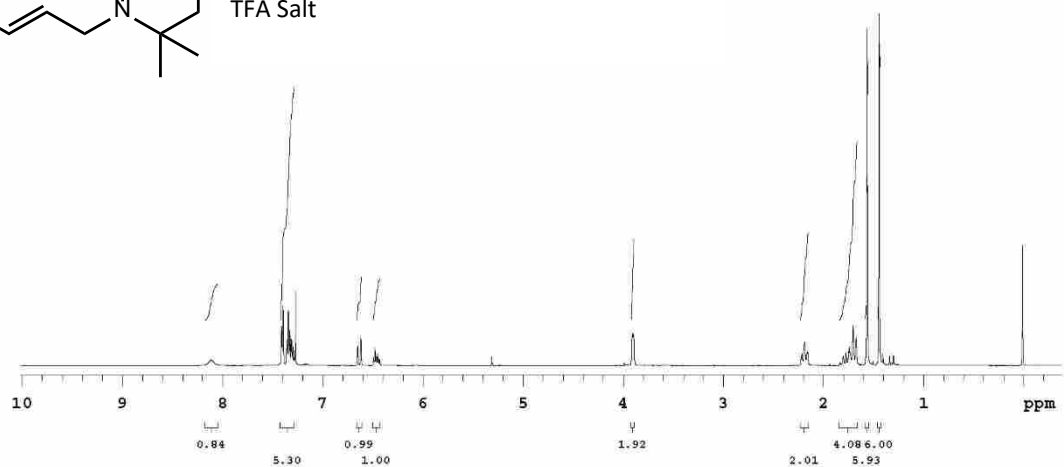
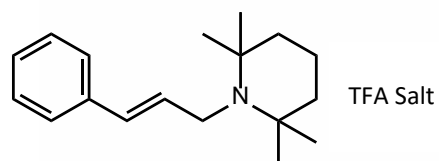
N-isopropyl-N-(2-methylallyl)cyclohexanamine TFA Salt (**4e**):



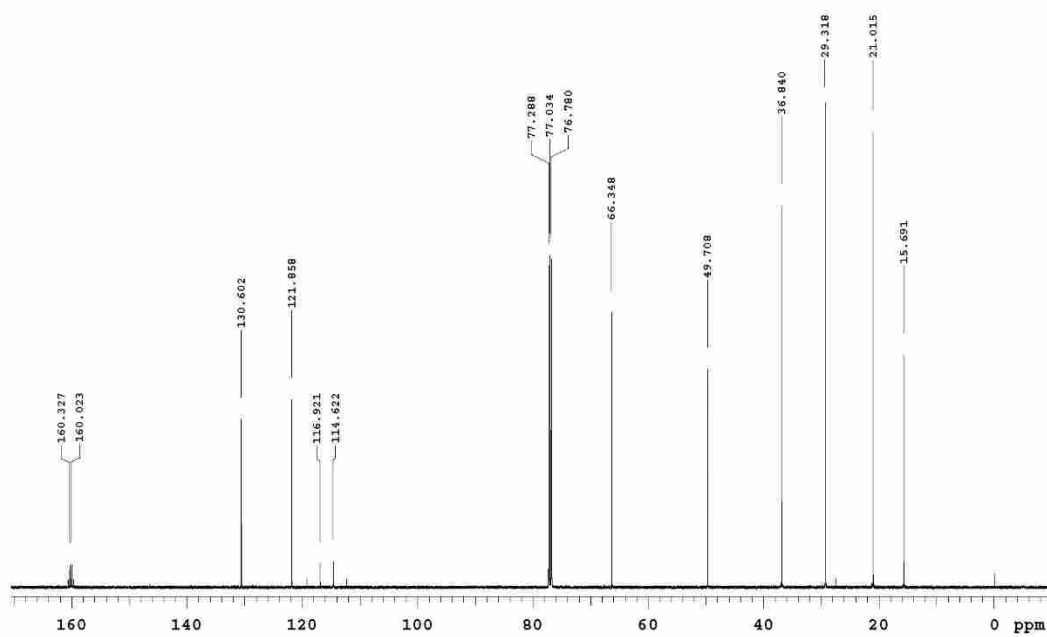
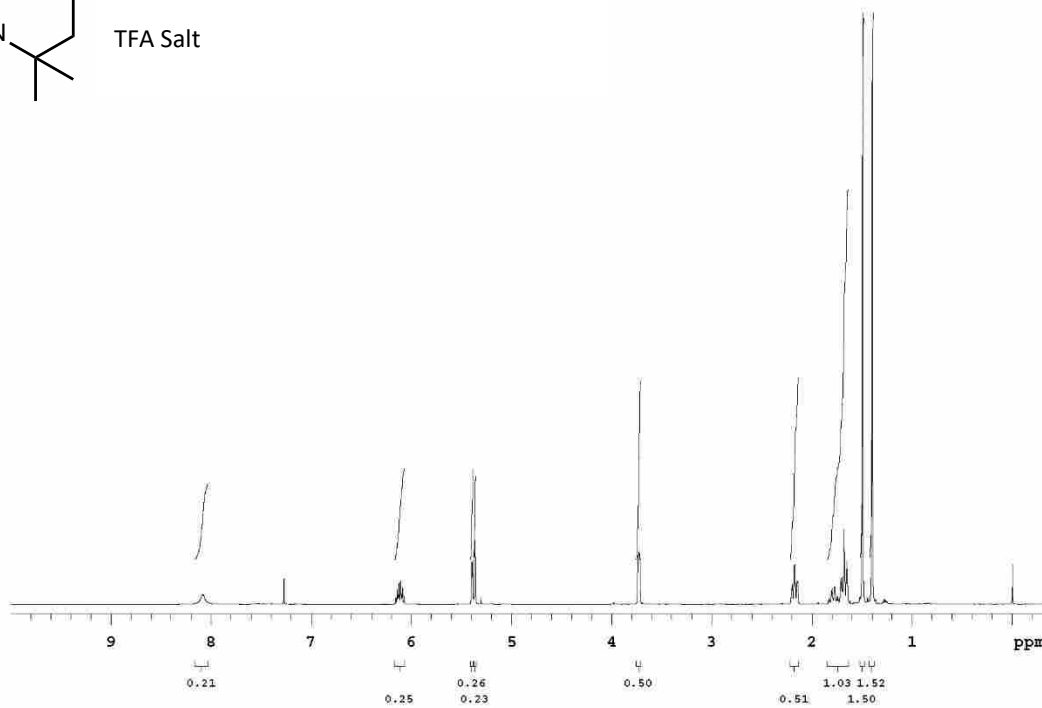
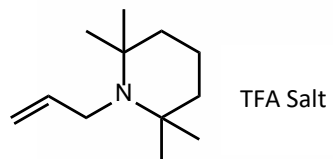
1-(but-2-en-1-yl)-2,2,6,6-tetramethylpiperidine TFA Salt (**4h**):



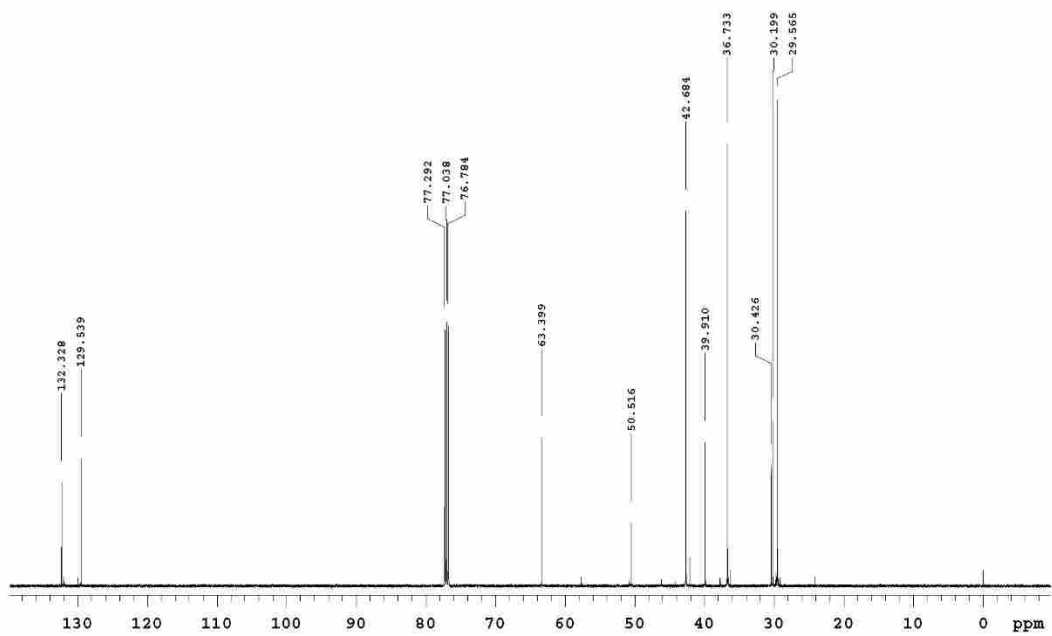
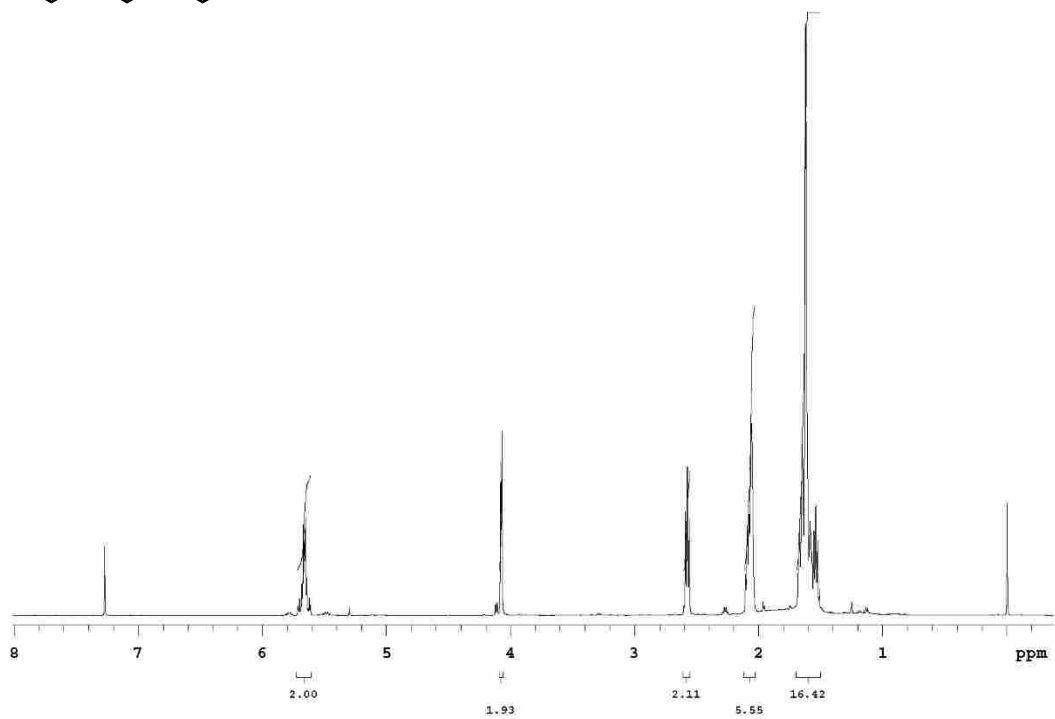
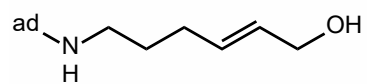
1-cinnamyl-2,2,6,6-tetramethylpiperidine TFA Salt (**4i**):



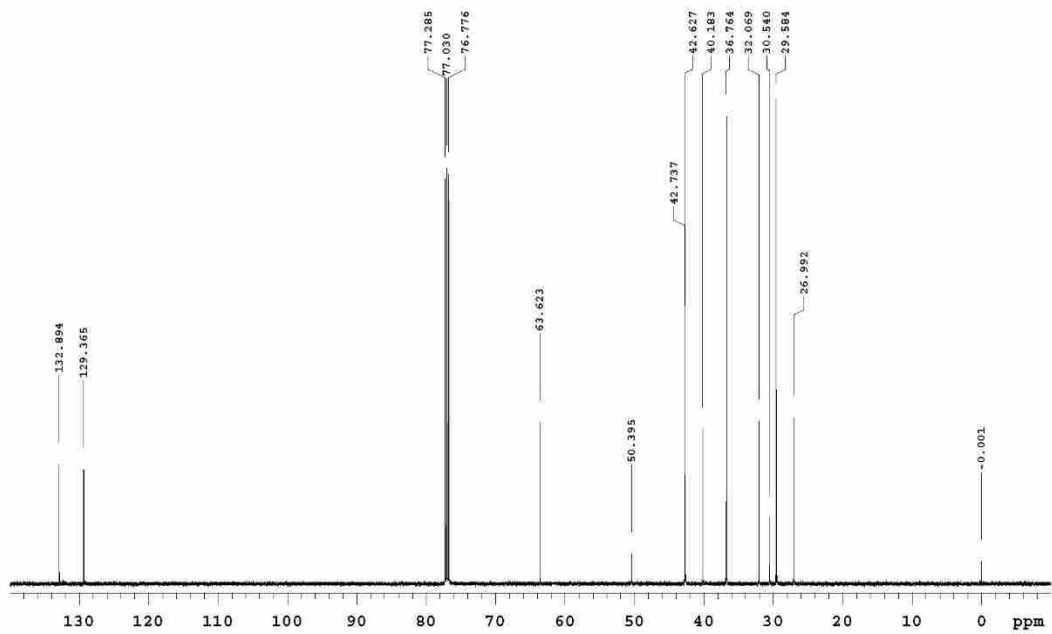
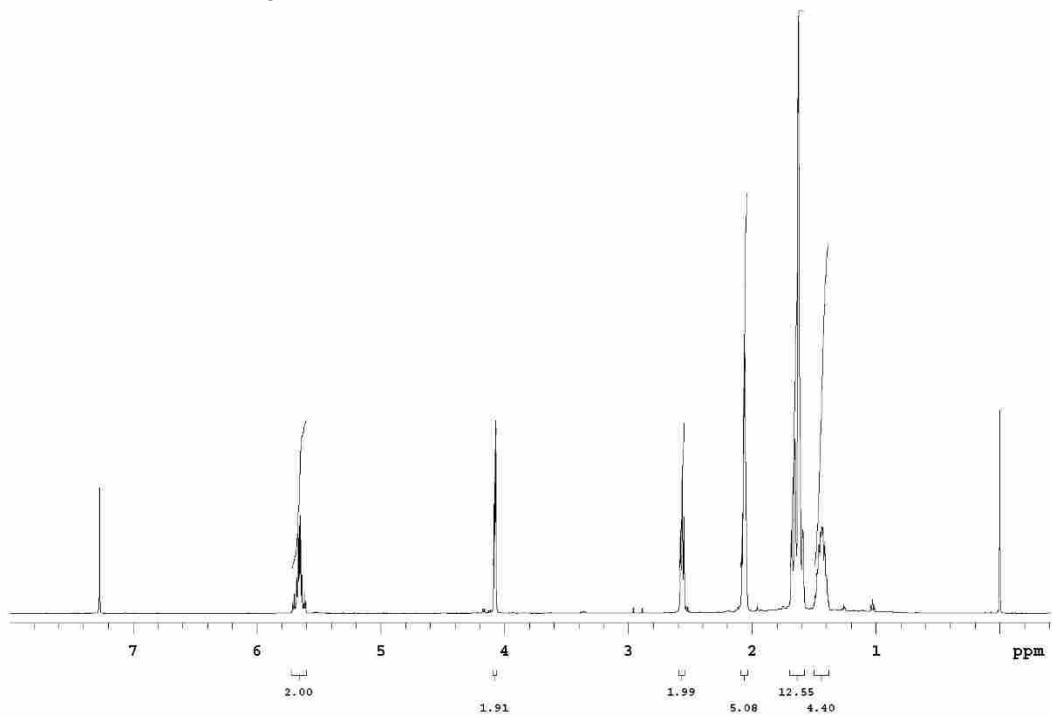
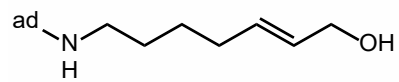
1-allyl-2,2,6,6-tetramethylpiperidine TFA Salt (**4j**):



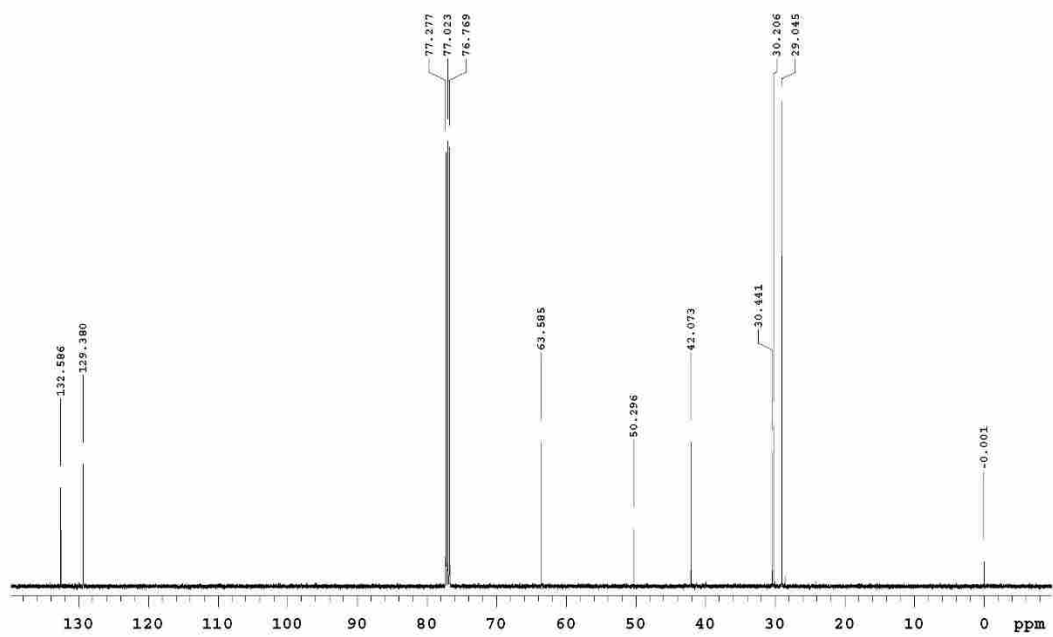
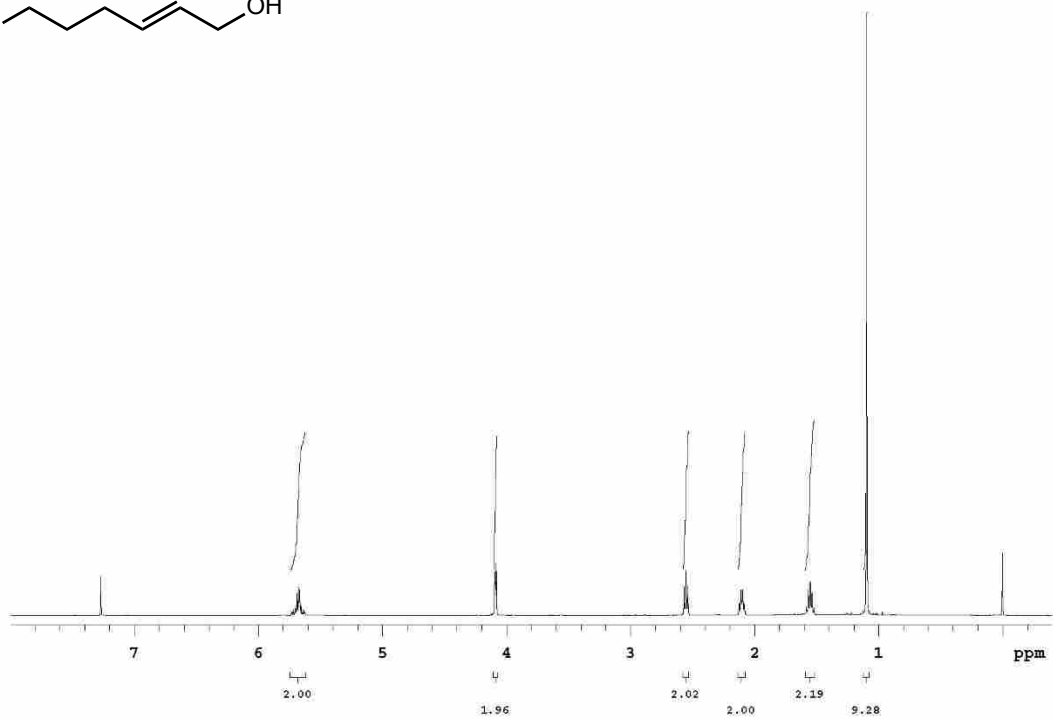
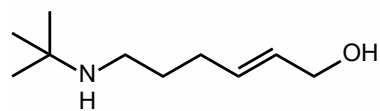
6-((adamantan-2-yl)amino)hex-2-en-1-ol (S1):



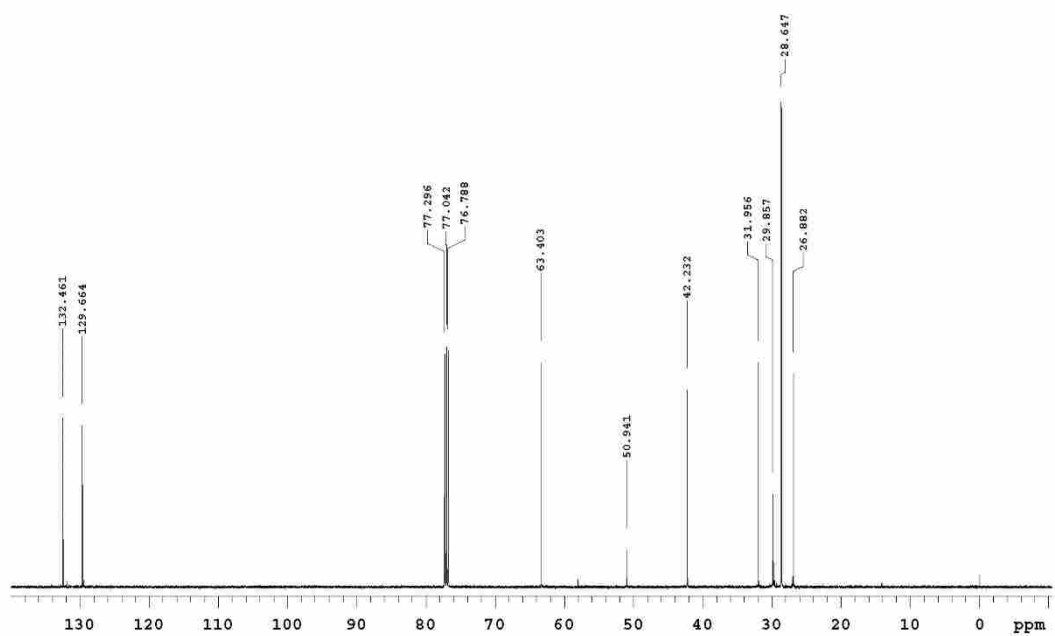
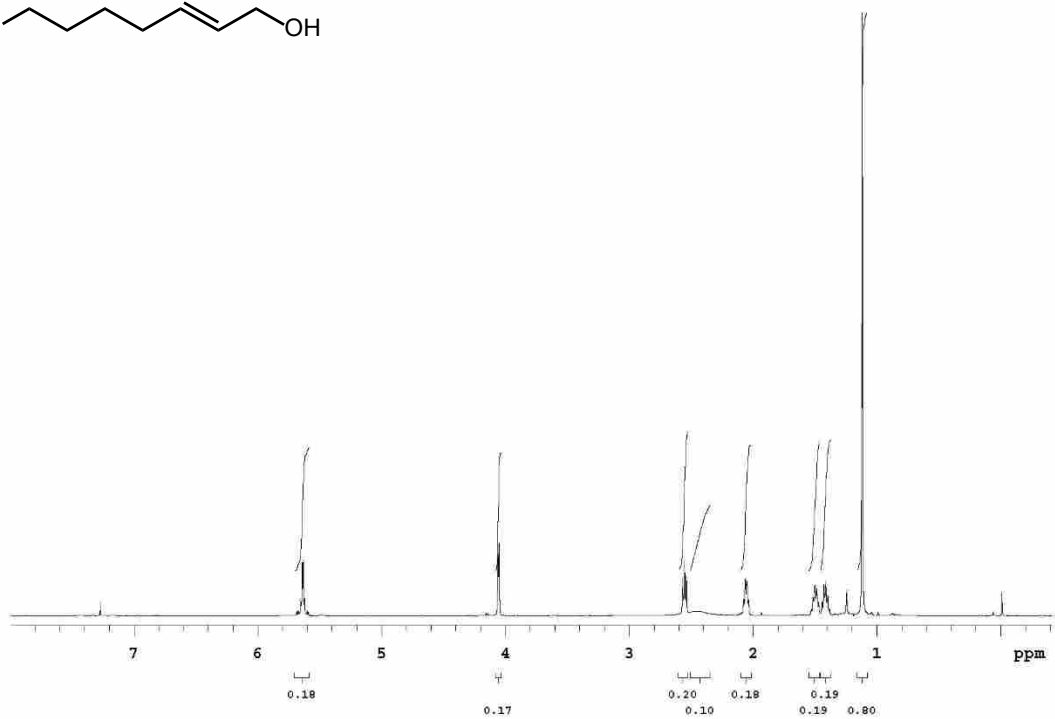
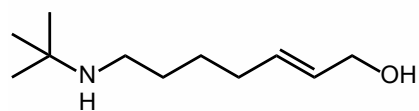
7-((adamantan-2-yl)amino)hex-2-en-1-ol (S2):



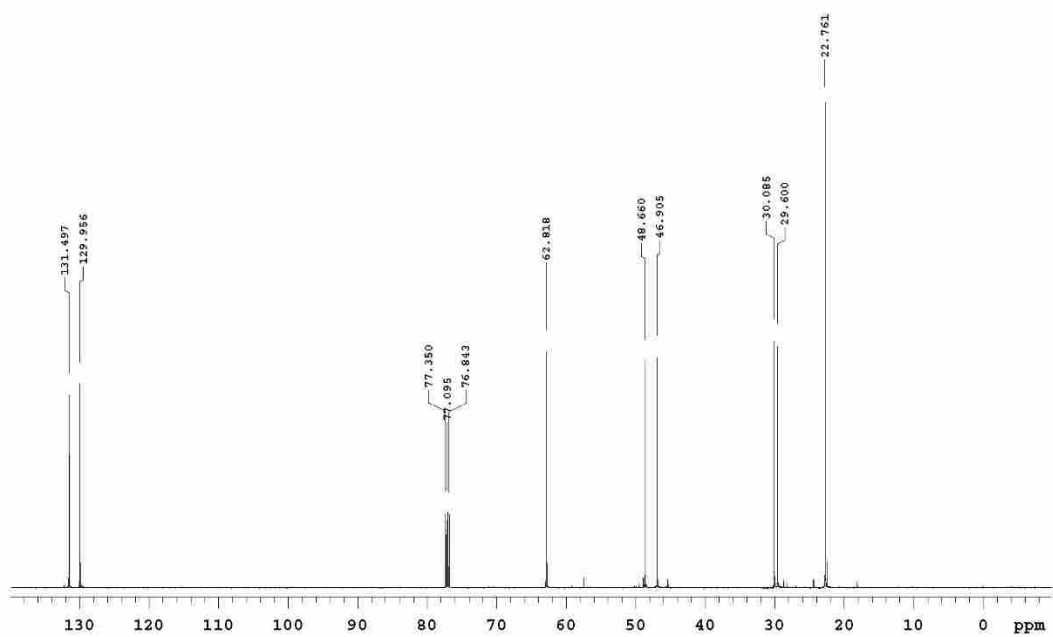
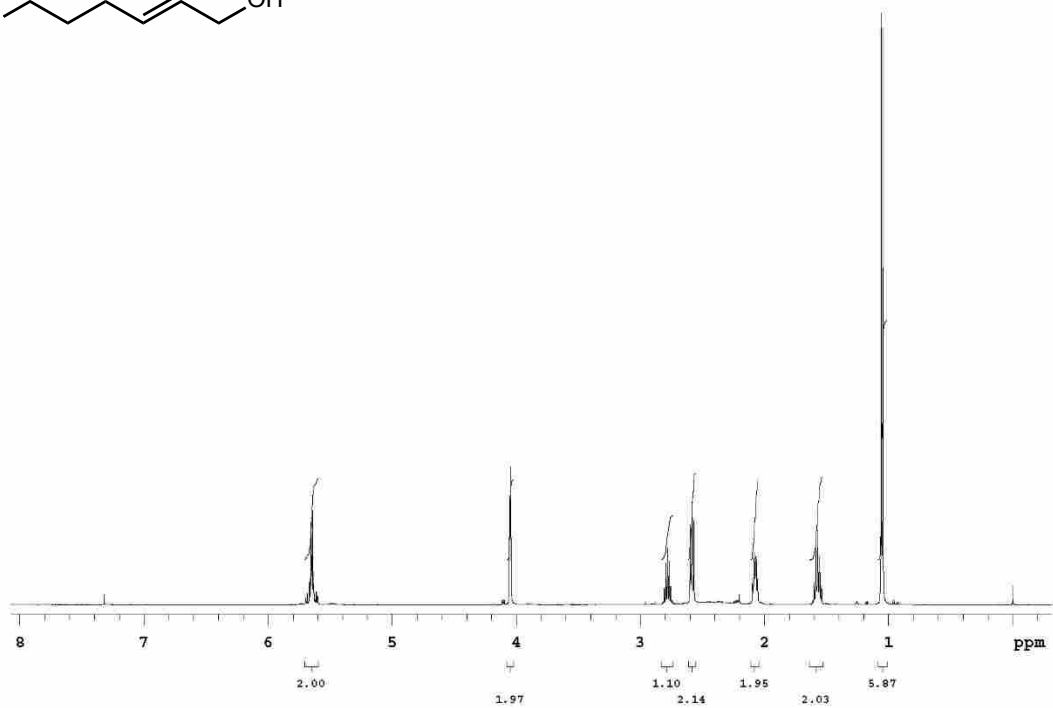
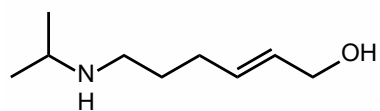
6-(*tert*-butylamino)hex-2-en-1-ol (**S3**):



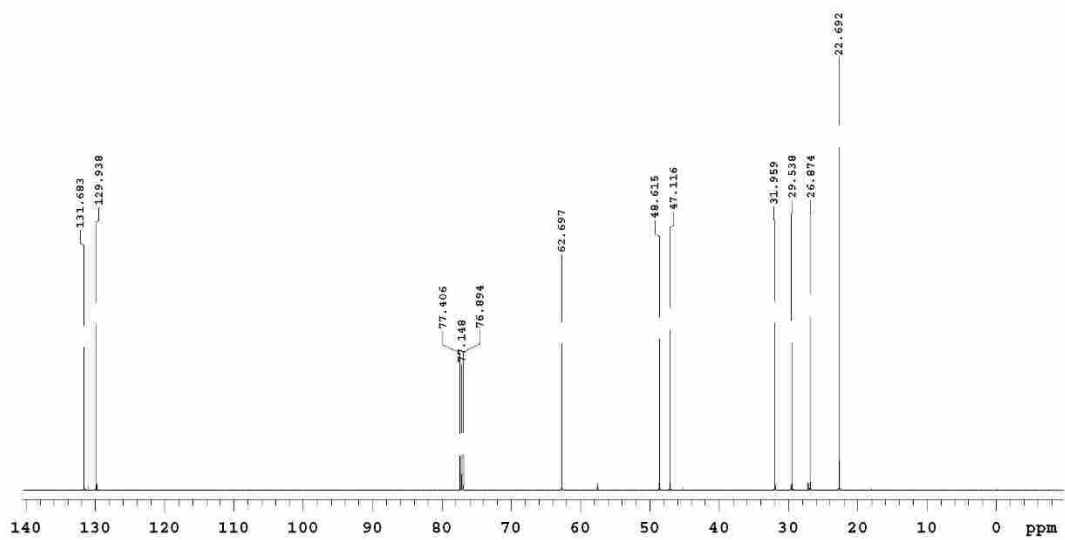
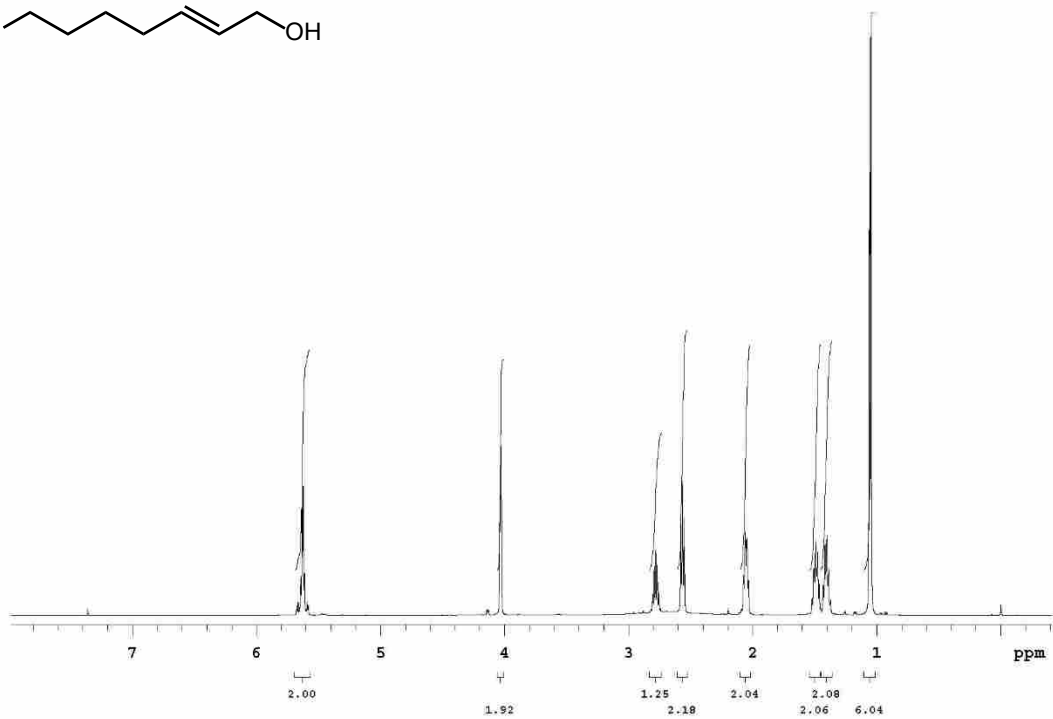
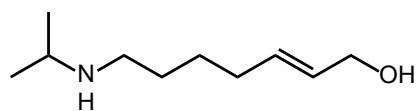
7-(*tert*-butylamino)hept-2-en-1-ol (**S4**):



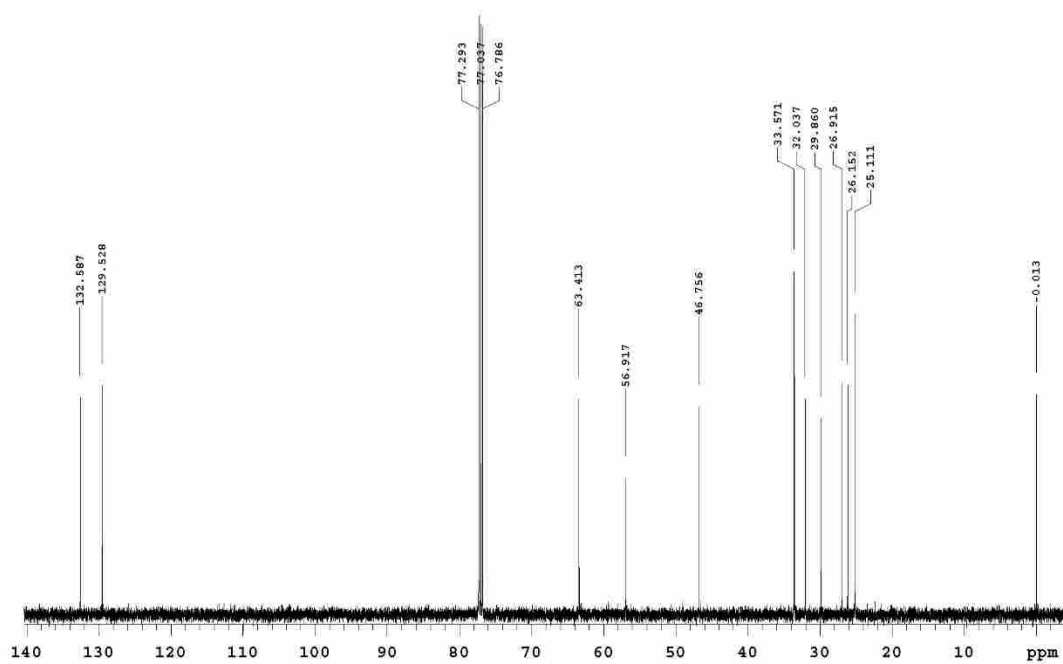
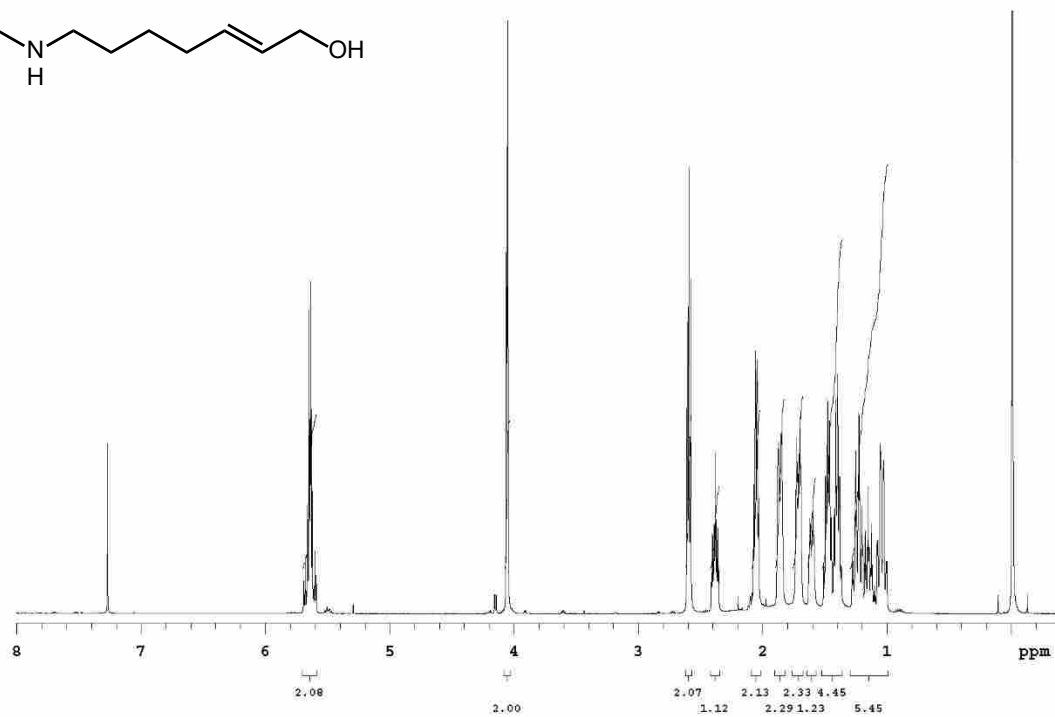
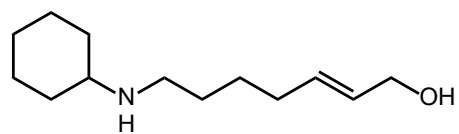
6-(isopropylamino)hex-2-en-1-ol (**S5**):



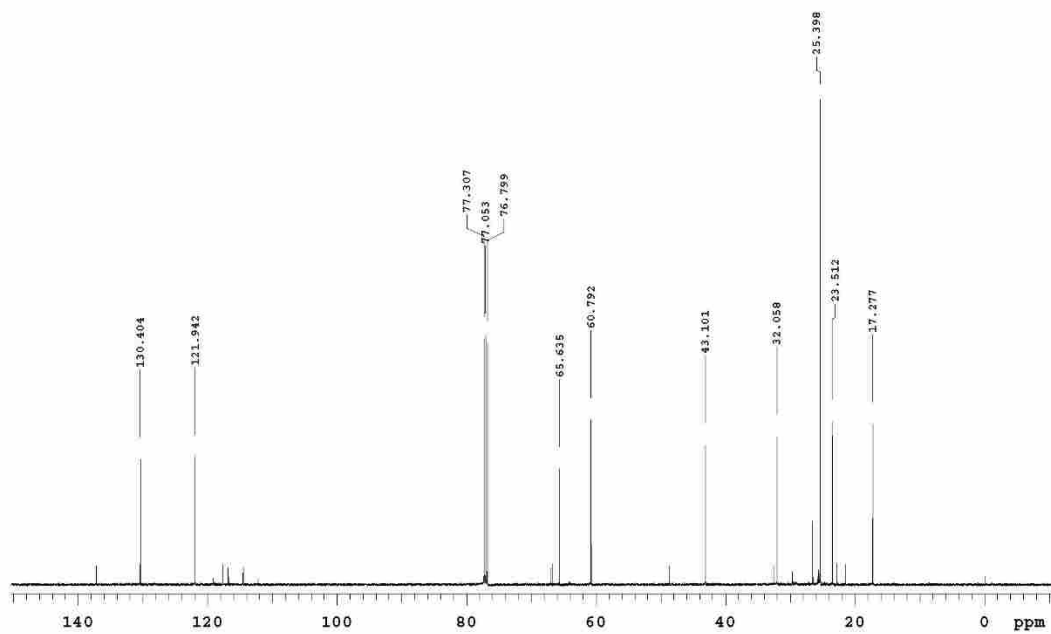
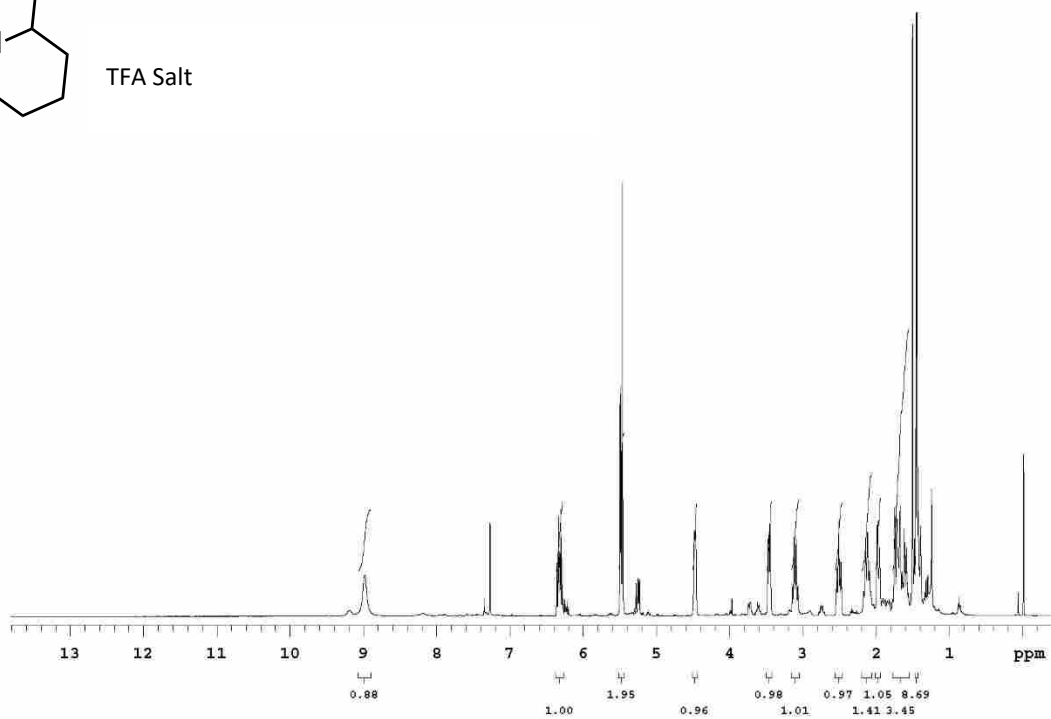
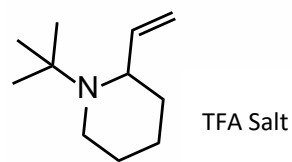
7-(isopropylamino)hept-2-en-1-ol (**S6**):



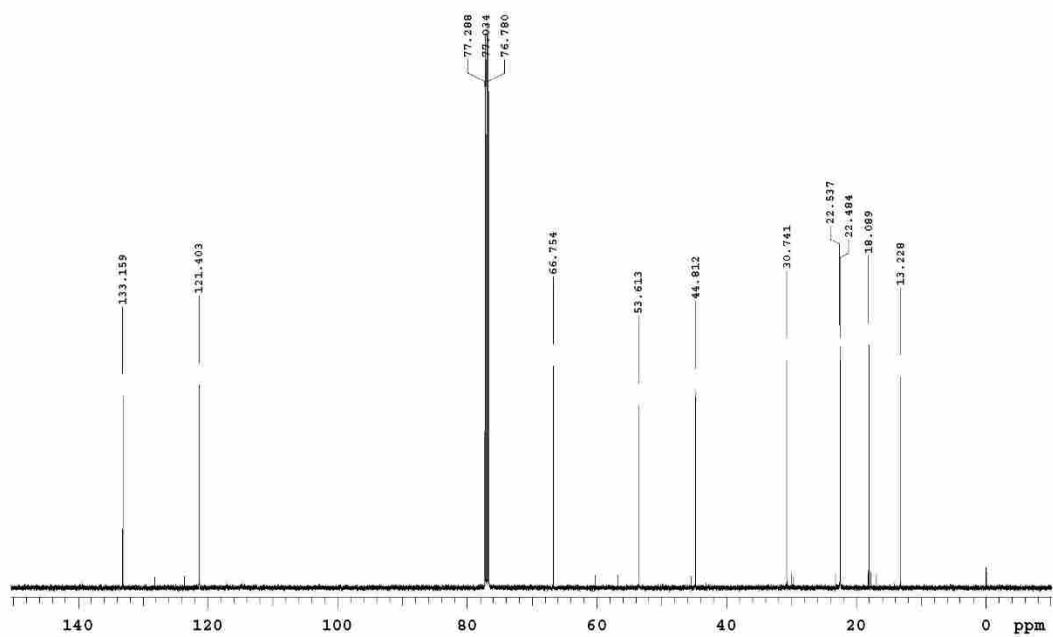
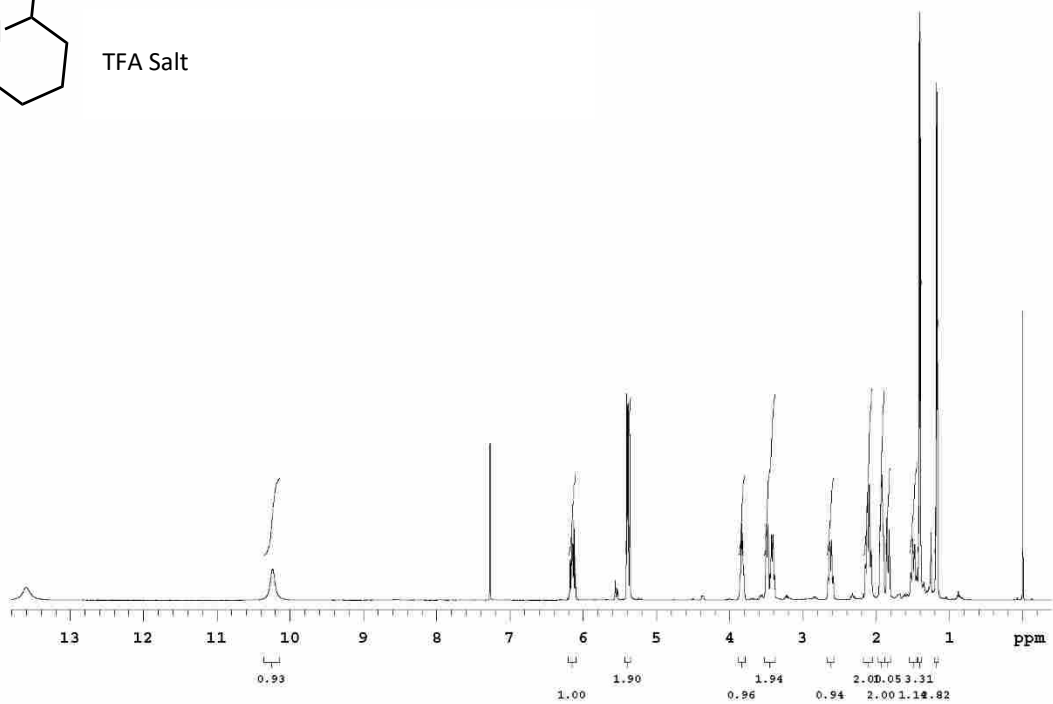
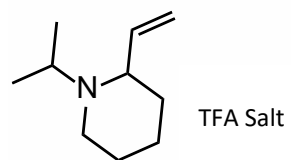
7-(cyclohexylamino)hept-2-en-1-ol (S7):



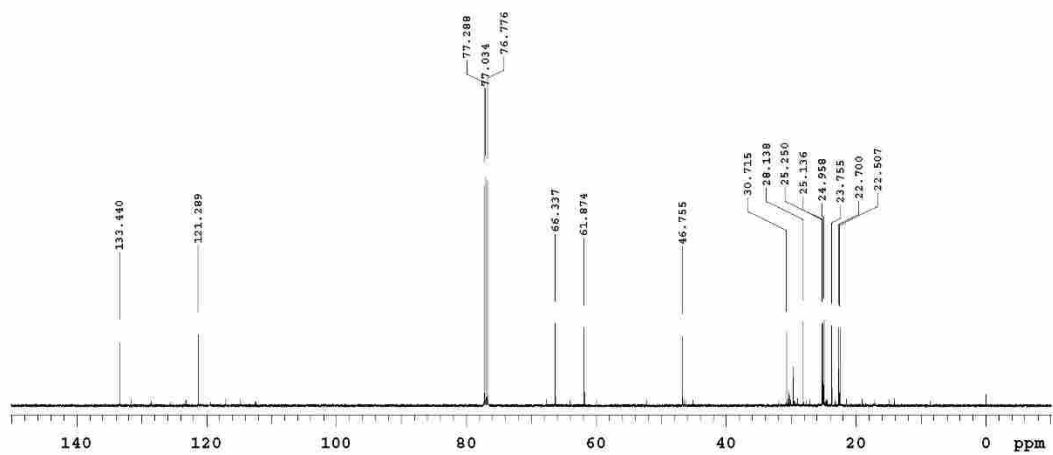
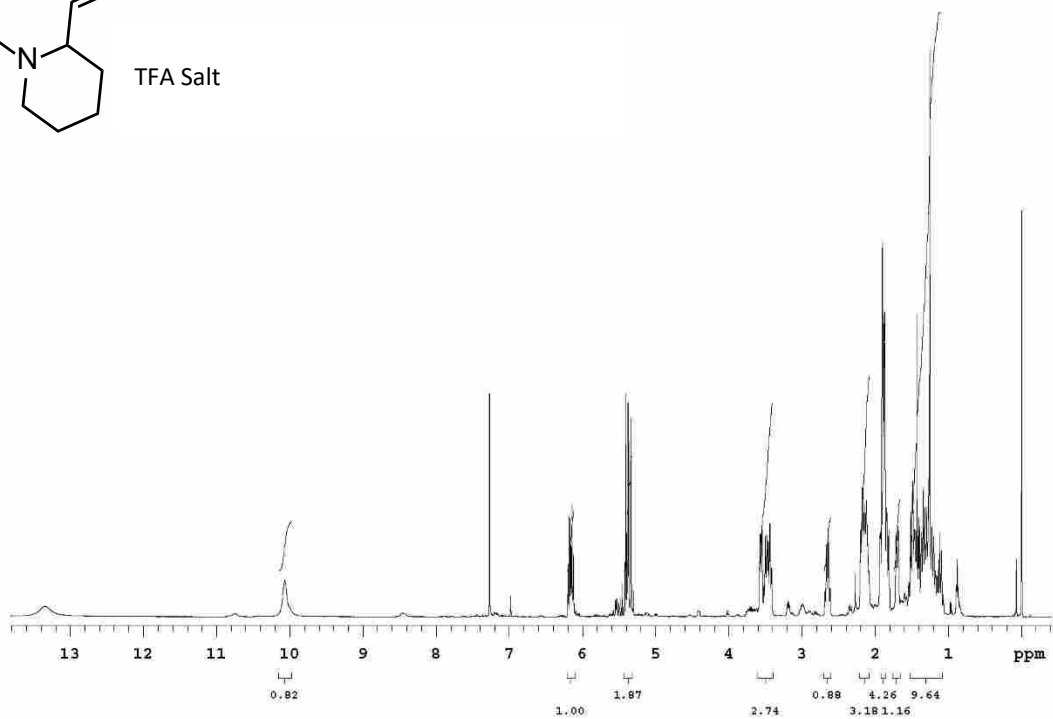
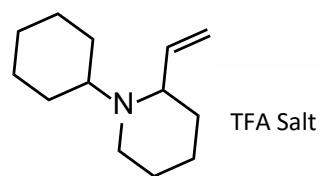
1-(*tert*-butyl)-2-vinylpiperidine TFA Salt (**14a**):



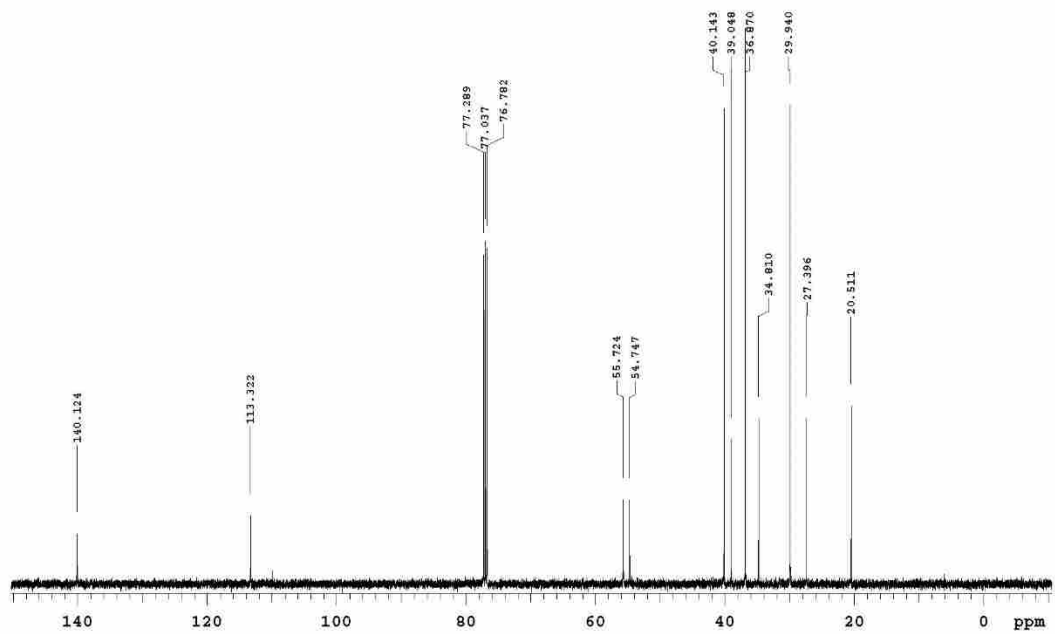
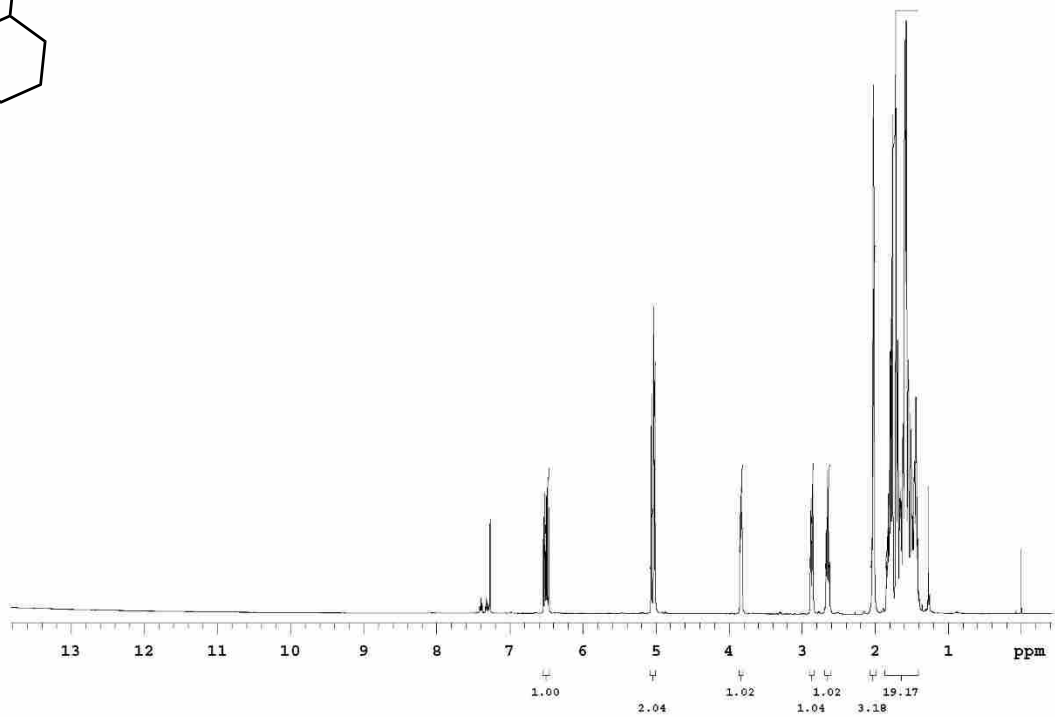
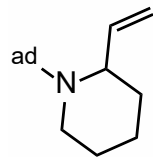
1-isopropyl-2-vinylpiperidine TFA Salt (**14b**):



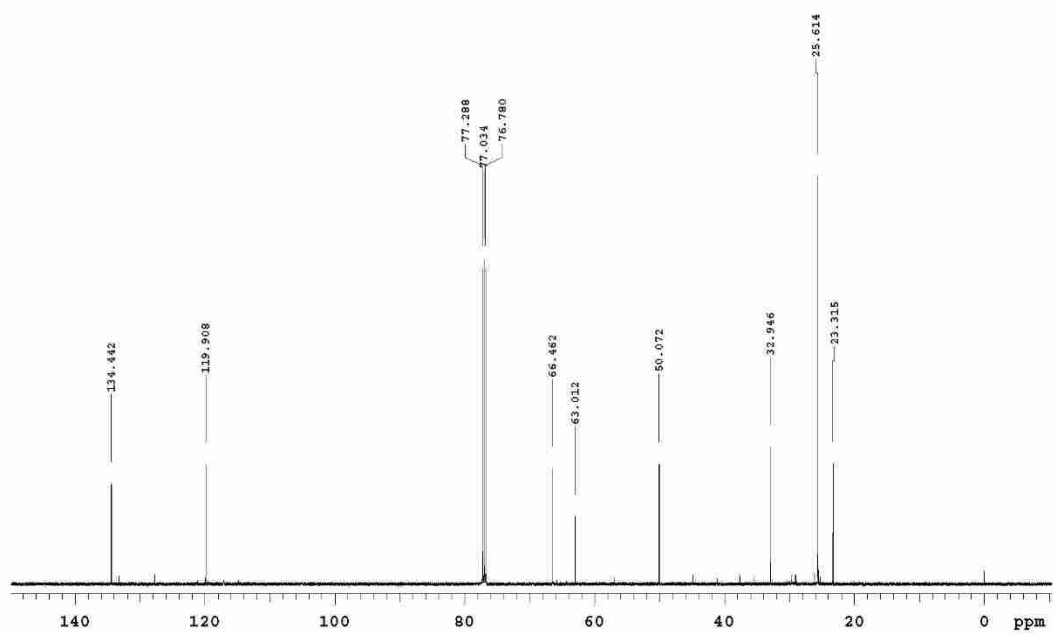
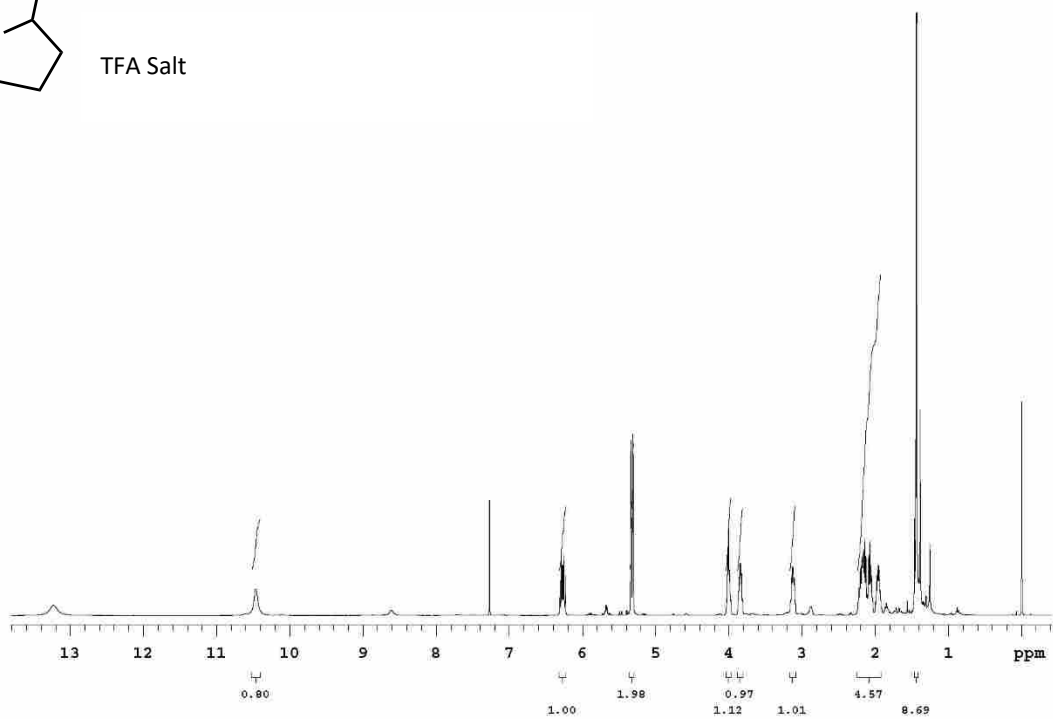
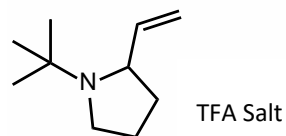
1-cyclohexyl-2-vinylpiperidine TFA Salt (**14c**):



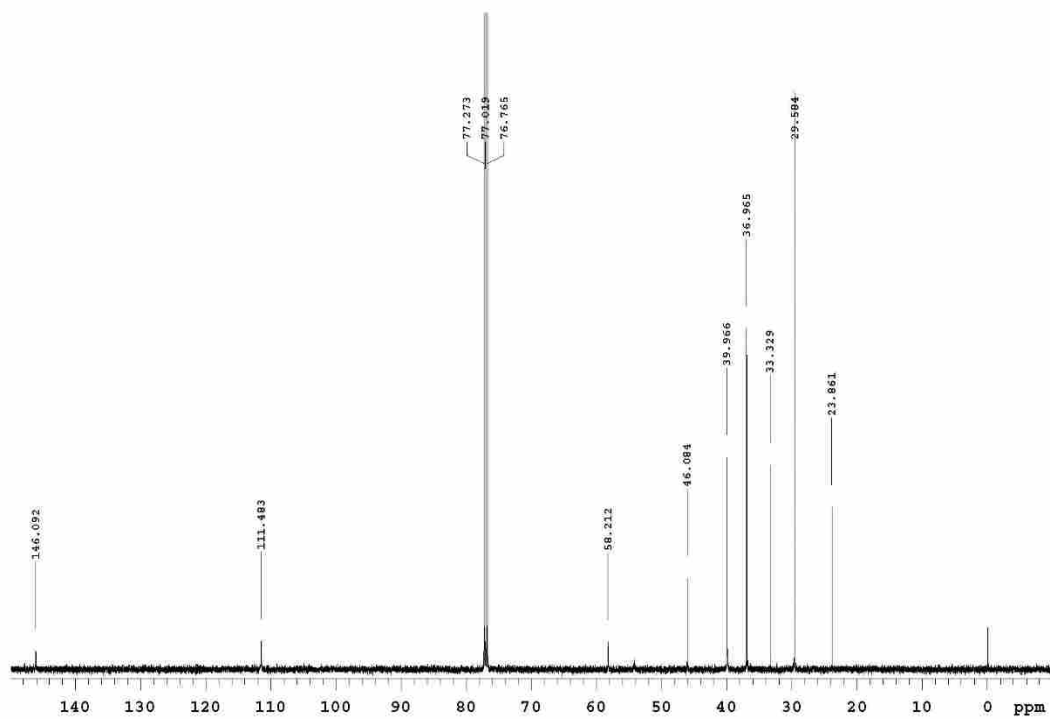
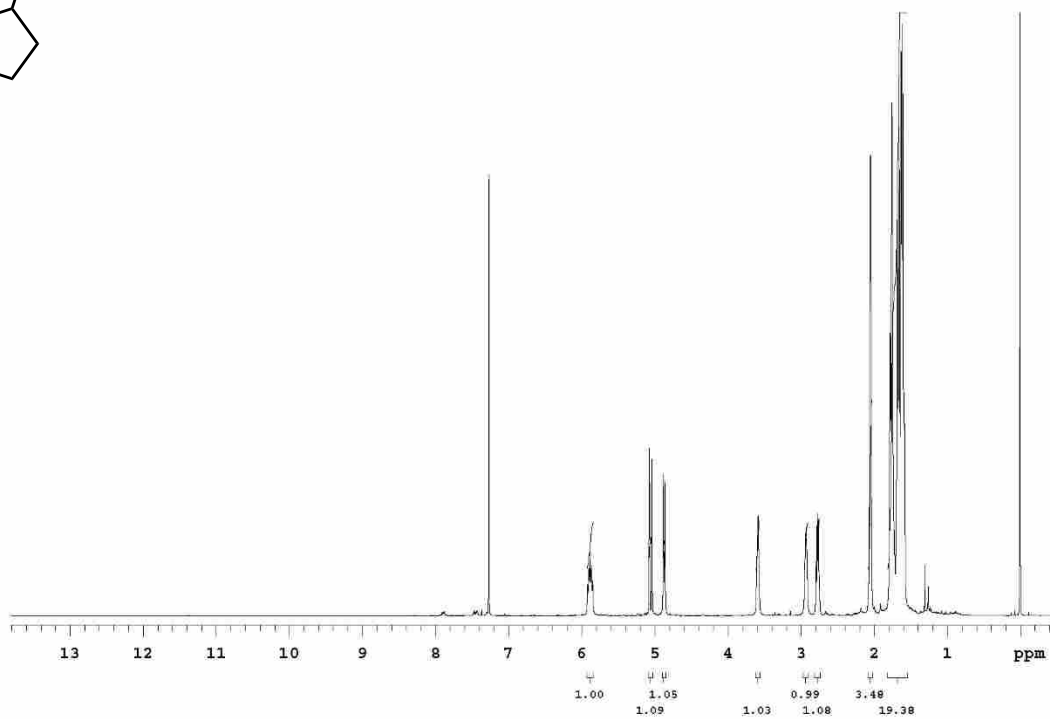
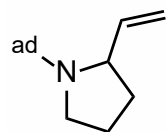
1-(adamantan-2-yl)-2-vinylpiperidine (**14d**):



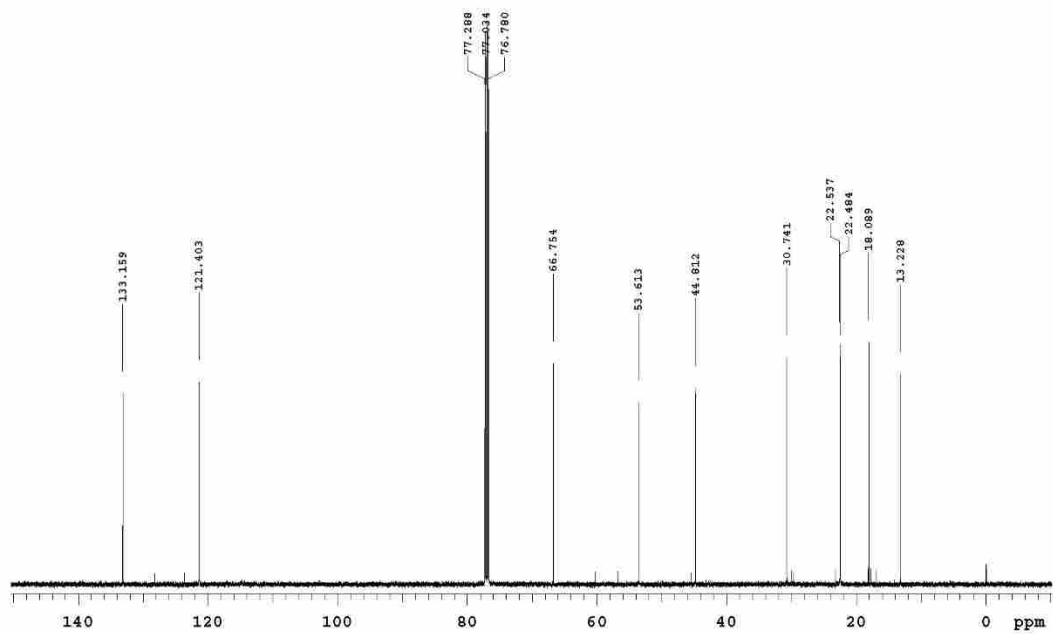
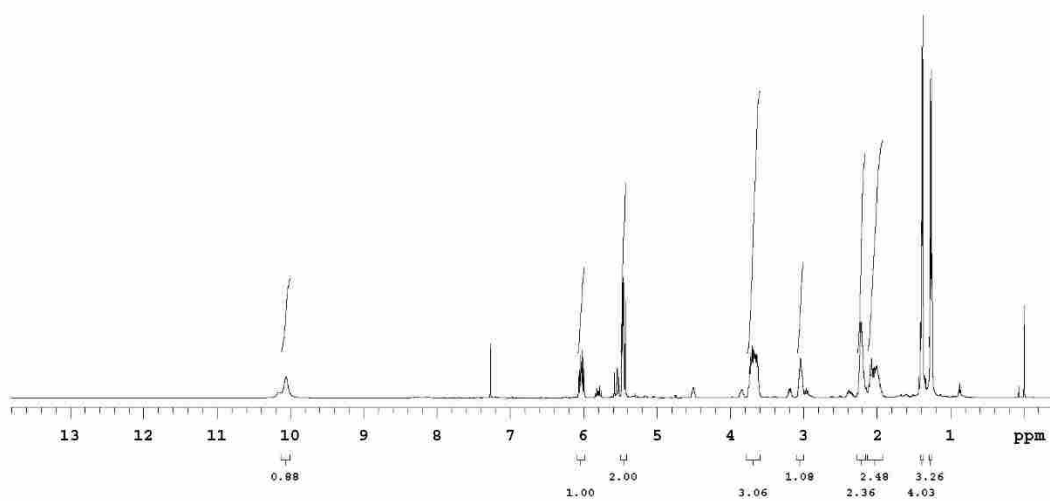
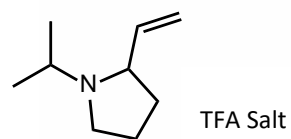
1-(*tert*-butyl)-2-vinylpyrrolidine TFA Salt (**15a**):



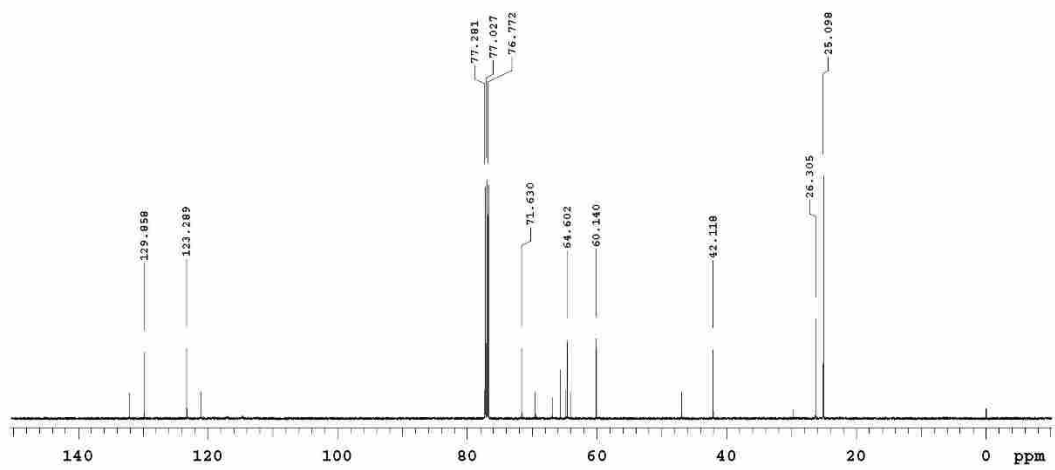
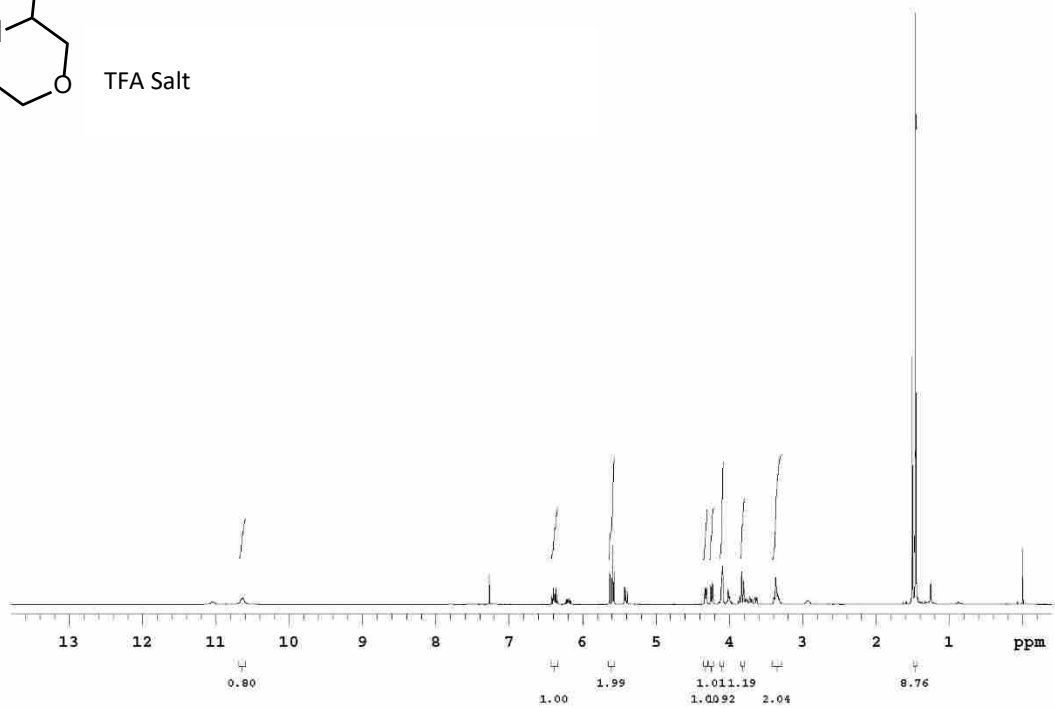
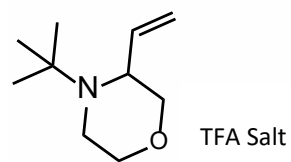
1-(adamantan-2-yl)-2-vinylpyrrolidine (**15b**):



1-isopropyl-2-vinylpyrrolidine TFA Salt (**15c**):



4-(*tert*-butyl)-3-vinylmorpholine TFA Salt (**16**):



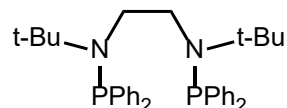
6.2 SUPPORTING INFORMATION FOR CHAPTER 3

6.2.1 General Information

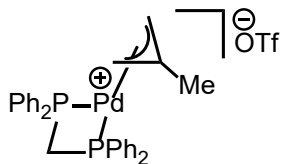
All reactions were carried out in oven-dried glassware with magnetic stirring, unless otherwise indicated. All the reagents were used as obtained unless otherwise noted. All commercially available amines were distilled from calcium hydride under nitrogen and stored over 4Å molecular sieves for at least 12 h before use. Reactions requiring a moisture-free environment were conducted in a nitrogen atmosphere glove box (Innovative Technology, PureLab HE system, double glove box). Analytical thin-layer chromatography was performed with 0.25 mm coated commercial silica gel plates (E. Merck, DC – Plastikfolien, kieselgel 60 F254). Flash Chromatography was performed with EM Science silica gel (0.040-0.063µm grade) Proton nuclear magnetic resonance (¹H-NMR) data were acquired on a Inova-300 (300 MHz) or on a Inova-500 (500 MHz) spectrometer. Chemical shifts are reported in delta (δ) units, in parts per million (ppm) downfield from tetramethylsilane. Carbon-13 nuclear magnetic resonance (¹³C-NMR) data were acquired on a Inova-500 at 125 MHz. Signals are reported as follows: s (singlet), d (doublet), t (triplet), q (quartet), dd (doublet of doublets), qd (quartet of doublets), brs (broad singlet), m (multiplet). Coupling constants are reported in hertz (Hz). Chemical shifts are reported in ppm relative to the center line of a triplet at 77.0 ppm for chloroform-d. Mass spectral data were obtained using ESI techniques (Agilent, 6210 TOF). Heterobimetallic complex **1**⁴ was synthesized as previously described.

⁴ Tsutsumi, H.; Sunada, Y; Shiota, Y; Yoshizawa, K; Nagashima, H. *Organometallics* **2009**, *28*, 1988-1991.

6.2.2 Synthesis of Bisphosphinepalladium methyl triflate Complexes

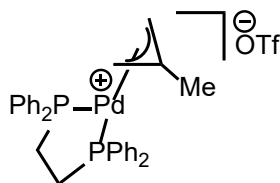


N,N'-di-tert-butyl-N,N'-bis(diphenylphosphino)ethane-1,2-diamine: Into a 5 dram vial containing a stir bar was placed *N,N'*-di-tert-butylethylenediamine (0.50 g, 2.9 mmol), dry toluene (5 ml), chlorodiphenylphosphine (1.04 ml, 5.8 mmol, 2 equiv), then trimethylamine (0.89 ml, 6.38 mmol, 2.2 equiv), the reaction was heated to 75 °C overnight (14 hrs). The reaction was then diluted with 10 ml CH₂Cl₂ and loaded directly onto a short column of silica gel and eluted with 4:1 hexanes:EtOAc. The product was isolated as a white solid, 0.570 g, (36% yield) (M.P. = 148-150 °C). IR (film): ν = 3071, 3052, 2963, 2916, 2849, 1260, 1087, 1019, 798; ¹H NMR (CDCl₃, 500 MHz) δ (ppm): 7.27-7.43 (m, 20 H), 2.78 (apparent s, 4H), 0.94 (s, 18H); ¹³C NMR (CDCl₃, 125 MHz): 139.8 (doublet), 131.9 (doublet), 128.8 (doublet), 127.8, 56.0 (doublet), 50.0 (doublet), 31.1 (doublet); ³¹P NMR (CDCl₃, 202 MHz) δ (ppm): 49.6; HRMS (ESI): C₃₄H₄₃N₂P₂ (M+H) calculated: 541.2901, found 541.2884.



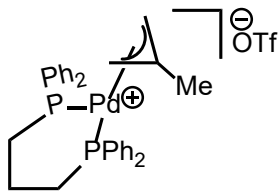
(bis(diphenylphosphino)methane)palladium(η^3 -methyl)triflate (7a): General Procedure: Into a flame dried vial containing a stir bar were placed [η^3 -methyl]PdCl₂ (43.7 mg, 0.111 mmol) and Ag(OTf) (57.0 mg, 0.222 mmol, 1 equiv), and the mixture was dissolved in dry

dichloromethane (4 mL). Acetone (163 μ L, 2.22 mmol, 20 equiv) was added and the solution was allowed to stir 10 minutes. In a separate vial, 1,1-bis(diphenylphosphino)methane (85.3 mg, 0.222 mmol, 2 equiv) was dissolved in dichloromethane (1 mL) and then added to the reaction mixture. The resulting solution was allowed to stir for an additional 30 minutes, the solvent was removed, and the remaining precipitate was dissolved in dichloromethane (2 mL). The solution was then filtered over celite into a 5 dram vial, layered with hexanes, and the product was allowed to crystallize overnight. The product was obtained as tan crystals (125 mg, 81% yield, Melting Point: 235 $^{\circ}$ C (decomp)). 1 H-NMR (500 MHz, CDCl_3): δ (ppm) = 7.47-7.43 (m, 1H), 7.41-7.33 (m, 6H), 7.23 (t, $J=7.62$ Hz, 4H), 7.07 (s, 4H), 6.95 (s, 4H), 4.30 (s, 2H), 4.24 (s, 2H), 3.80-3.71 (m, 1H), 3.54-3.44 (m, 1H) 1.54 (2, 3H); 13 C-NMR (125 MHz, CDCl_3): δ (ppm) = 138.4 (t, $J=2.48$ Hz), 134.1 (t, $J=3.53$ Hz), 131.5 (d, $J=69.74$ Hz), 131.3 (t, $J=3.03$ Hz), 129.7 (dt, $J=92.75$, $J=2.20$ Hz), 78.4 (t, $J=7.18$ Hz), 28.5 (s), 22.5 (s); 31 P-NMR (202 MHz, CDCl_3): δ (ppm) = 9.98 (s). HRMS (ESI): $\text{C}_{29}\text{H}_{29}\text{P}_2\text{Pd}$ calculated: 545.0785, found 545.0703.

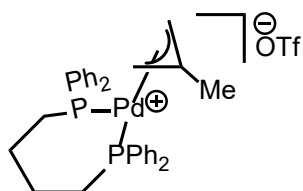


(bis(diphenylphosphino)ethane)palladium(η^3 -methylallyl) triflate (7b): Synthesized according to the general procedure using 88.4 mg 1,2 bis(diphenylphosphino)ethane (0.222 mmol, 2 equiv). The product was obtained as white crystals (136 mg, 86% yield, Melting Point: 245 $^{\circ}$ C (decomp)). 1 H-NMR (500 MHz, CDCl_3): δ (ppm) = 7.65-7.58 (m, 4H), 7.55-7.46 (m, 16H), 4.62 (s, 2H), 3.31-3.26 (m, 2H), 2.89-2.62 (m, 4H), 1.95 (s, 3H); 13 C-NMR (125 MHz, CDCl_3): δ (ppm) = 137.6 (t, $J=5.91$ Hz), 132.5 (q, $J=5.99$ Hz), 132.0 (s), 129.7 (ddt, $J=88.85$ Hz, $J=44.29$ Hz, $J=18.08$ Hz), 129.8 (dt, $J=16.21$ Hz, $J=5.52$ Hz), 70.3 (t, $J=16.86$ Hz), 27.5 (d, $J=22.06$ Hz), 27.3 (d, $J=22.06$ Hz), 24.4 (s);

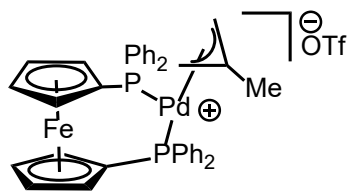
^{31}P -NMR (202 MHz, CDCl_3): δ (ppm) = 52.13 (s). HRMS (ESI): $\text{C}_{30}\text{H}_{31}\text{P}_2\text{Pd}$ calculated: 559.0941, found 559.0838.



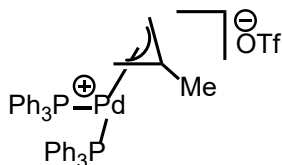
(bis(diphenylphosphino)propane)palladium(η^3 -methylallyl) triflate (7c): Synthesized as previously reported.⁴



(bis(diphenylphosphino)butane)palladium(η^3 -methylallyl) triflate (7d): Synthesized according to the general procedure using 94.7 mg 1,4-bis(diphenylphosphino)butane (0.22 mmol, 2 equiv). The product was obtained as grey crystals (129 mg, 79% yield, Melting Point: 250 °C (decomp)). ^1H -NMR (500 MHz, CDCl_3): δ (ppm) = 7.56-7.44 (m, 16 H), 7.42-7.36 (m, 4H), 3.67 (s, 2H), 3.24-3.20 (m, 2H), 2.83-2.75 (m, 2H), 2.64-2.55 (m, 2H), 1.99-1.87 (m, 2H) 1.86-1.73 (m, 2H), 1.69 (s, 3H); ^{13}C -NMR (125 MHz, CDCl_3): δ (ppm) = 137.4 (t, $J=5.64$ Hz), 133.1 (dt, $J=24.87$ Hz, $J=19.96$ Hz), 132.4 (dt, $J=27.26$ Hz, $J=6.25$ Hz), 131.2 (d, $J=21.88$ Hz), 129.3 (dt, $J=7.15$ Hz, $J=5.26$ Hz), 75.2 (t, $J=16.07$ Hz), 26.6 (d, $J=12.04$ Hz), 26.5 (d, $J=12.04$ Hz), 23.7, 23.3 (t, $J=3.23$ Hz); ^{31}P -NMR (202 MHz, CDCl_3): δ (ppm) = 21.04 (s). HRMS (ESI) $\text{C}_{32}\text{H}_{35}\text{P}_2\text{Pd}$ calculated: 587.1254, found 587.1139.

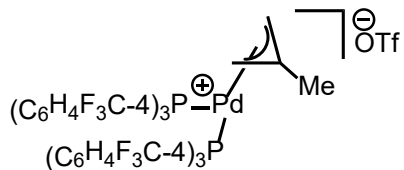


(bis(diphenylphosphino)ferrocene)palladium(η^3 -methallyl) triflate (7e): Synthesized according to the general procedure using 123.1 mg 1,1-bis(diphenylphosphino)ferrocene (0.222 mmol, 2 equiv). The product was obtained as orange crystals (131 mg, 68% yield, Melting Point: 260 °C (decomp)). $^1\text{H-NMR}$ (500 MHz, CDCl_3): δ (ppm) = 7.65-7.58 (m, 4H), 7.58-7.46 (m, 16H), 4.49 (s, 2H), 4.45 (d, $J=13.13$ Hz, 4H), 4.18 (s, 2H), 3.70 (s, 2H), 3.46 (s, 2H), 1.87 (s, 3H); $^{13}\text{C-NMR}$ (125 MHz, CDCl_3): δ (ppm) = 138.2 (t, $J=5.54$ Hz), 133.3 (q, $J=7.52$ Hz), 133.0 (ddt, $J=106.14$ Hz, $J=46.25$ Hz, $J=23.50$ Hz), 131.6 (d, $J=6.13$ Hz), 129.3 (dt, $J=15.50$ Hz, $J=5.38$ Hz), 76.8 (t, buried in CDCl_3 , retaken in CD_2Cl_2 , $\delta=76.1$ (t, $J=15.74$ Hz)), 75.7 (dt, $J=59.34$ Hz, $J=5.91$ Hz), 74.5 (dt, $J=56.62$ Hz, $J=27.18$ Hz), 73.5 (dt, $J=33.40$ Hz, $J=3.58$ Hz), 23.9 (s); $^{31}\text{P-NMR}$ (202 MHz, CDCl_3): δ (ppm) = 24.14 (s). HRMS (ESI) $\text{C}_{38}\text{H}_{35}\text{FeP}_2\text{Pd}$ calculated: 715.0604, found 715.0482.

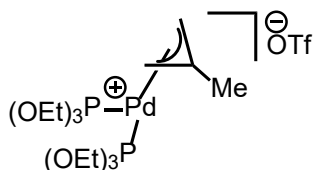


(bis(triphenylphosphino)palladium(η^3 -methallyl) triflate (8): Synthesized according to the general procedure using 116.5 mg triphenylphosphine (0.444 mmol, 4 equiv). The product was obtained as light orange crystals (176 mg, 95% yield, Melting Point: 215 °C (decomp)). $^1\text{H-NMR}$ (500 MHz, CDCl_3): δ (ppm) = 7.39 (t, $J=7.21$ Hz, 6H), 7.32-7.23 (m, 24H), 3.80-3.75 (m, 2H), 3.63 (s, 2H), 1.87 (s, 3H); $^{13}\text{C-NMR}$ (125 MHz, CDCl_3): δ (ppm) = 138.0 (t, $J=5.03$ Hz), 133.5 (t, $J=6.59$ Hz), 131.1 (dt, $J=44.34$ Hz, $J=21.00$ Hz), 131.0 (s), 129.0 (t, $J=5.24$ Hz), 78.7 (t, $J=15.03$ Hz), 23.6

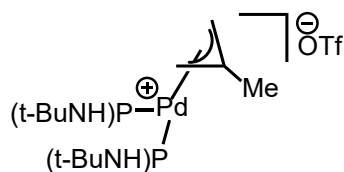
(s); ^{31}P -NMR (202 MHz, CDCl_3): δ (ppm) = 24.00 (s). HRMS (ESI) $\text{C}_{40}\text{H}_{37}\text{P}_2\text{Pd}$ calculated: 685.1411, found 685.1259.



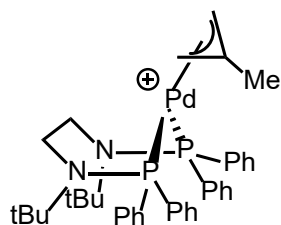
(bis(tris(4-trifluoromethylphenyl))phosphino)palladium(η^3 -methallyl) triflate (9): Synthesized according to the general procedure using 207.0 mg tris(4-trifluoromethylphenyl)phosphine (0.444 mmol, 4 equiv). The product was obtained as white crystals (183 mg, 69% yield, Melting Point: 265 $^\circ\text{C}$ (decomp)). ^1H -NMR (500 MHz, CDCl_3): δ (ppm) = 7.62 (d, $J=7.96$ Hz, 12H) 7.51-7.45 (m, 12H), 4.22-4.17 (m, 2H), 3.84 (s, 2H), 1.92 (s, 3H); ^{31}P -NMR (202 MHz, CDCl_3): δ (ppm) = 22.83 (s). HRMS (ESI) $\text{C}_{46}\text{H}_{31}\text{F}_{18}\text{P}_2\text{Pd}$ calculated: 1093.0654, found 1093.0424.



(bis(triethylphosphite)palladium(η^3 -methallyl) triflate (10): Synthesized according to the general procedure using 76.1 μL triethyl phosphite (0.444 mmol, 4 equiv). The product was obtained as a grey oil. IR (film): ν = 2984, 2937, 2906, 1390, 1272, 1223, 1151, 1098, 1009, 954, 788; ^1H -NMR (500 MHz, CDCl_3): δ (ppm) = 4.42 (s, 2H), 4.11-4.03 (m, 12H), 3.49 (s, 2H), 1.86 (s, 3H), 1.33 (t, $J=6.91$ Hz, 18H); ^{13}C -NMR (125 MHz, CDCl_3): δ (ppm) = 138.5 (s), 71.5 (s), 61.7 (s), 24.1 (s), 16.3 (s); ^{31}P -NMR (202 MHz, CDCl_3): δ (ppm) = 128.52 (s). HRMS (ESI) $\text{C}_{16}\text{H}_{37}\text{O}_6\text{P}_2\text{Pd}$ calculated: 493.1106, found 493.1075.



(bis(*N*-*tert*-butyldiphenylphosphoamido)palladium(η^3 -methallyl) triflate (11): Synthesized according to the general procedure using 114.1 mg *N*-*tert*-butyl-1,1-diphenylphosphanamine (0.444 mmol, 4 equiv). The product was obtained as grey crystals (94 mg, 51% yield, Melting Point: 180 °C (decomp)). $^1\text{H-NMR}$ (500 MHz, CDCl_3): δ (ppm) = 7.64-7.58 (m, 4H), 7.48-7.39 (m, 12H), 7.33 (t, $J=7.36$ Hz, 4H), 3.97-3.91 (m, 2H), 3.44 (s, 2H), 3.36-3.31 (m, 2H), 1.23 (s, 3H), 1.05 (s, 18H); $^{13}\text{C-NMR}$ (125 MHz, CDCl_3): δ (ppm) = 136.8 (t, $J=5.38$ Hz), 135.7 (ddd, $J=159.98$ Hz, $J=24.96$ Hz, $J=21.87$ Hz), 131.9 (td, $J=6.79$ Hz, $J=2.53$ Hz), 130.1 (d, $J=27.01$), 128.3 (q, $J=5.08$ Hz), 75.7 (t, $J=16.78$ Hz), 56.0 (t, $J=6.26$ Hz), 31.9 (t, $J=1.85$ Hz), 22.6 (s); $^{31}\text{P-NMR}$ (202 MHz, CDCl_3): δ (ppm) = 47.94 (s). HRMS (ESI) $\text{C}_{36}\text{H}_{49}\text{N}_2\text{P}_2\text{Pd}$ calculated: 675.2255, found 675.2114.



(*N*, *N'*-di-*tert*-butyl-*N,N'*-bis(diphenylphosphino)ethane-1,2-diamine)palladium(η^3 -methallyl) triflate (6): Synthesized according to the general procedure using 84.5 mg *N,N*-di-*tert*-butyl-*N,N'*-bis(diphenylphosphanyl)ethane-1,2-diamine (0.156 mmol, 2 equiv). The product was obtained as light yellow crystals (116 mg, 87% yield, Melting Point: 175 °C (decomp)). $^1\text{H-NMR}$ (500 MHz, CDCl_3): δ (ppm) = 7.82-7.76 (m, 4H), 7.57-7.46 (m, 12H), 7.45-7.40 (t, $J=7.33$ Hz, 4H), 3.98-3.87 (m, 2H), 3.81-3.69 (m, 2H), 3.11 (s, 2H), 2.76-2.71 (m, 2H), 1.29 (s, 3H), 1.10 (s, 18H); $^{13}\text{C-NMR}$

(125 MHz, CDCl₃): δ (ppm) = 137.7 (t, J=4.64 Hz), 135.4 (dd, J=41.51 Hz, J=28.00 Hz), 131.5 (q, J=7.45 Hz), 130.9 (d, J=28.73 Hz), 128.9 (dt, J=15.04 Hz, J=5.34 Hz), 77.5 (t, buried in CDCl₃, retaken in CD₂Cl₂, δ = 77.5 (t, J=16.82 Hz)), 60.7 (t, J=5.64 Hz), 54.3 (t, J=13.18 Hz), 30.6 (s), 22.2 (s); ³¹P-NMR (202 MHz, CDCl₃): δ (ppm) = 73.15 (s). HRMS (ESI) C₃₈H₄₉N₂P₂Pd calculated: 701.2411, found 701.2506.

6.2.3 Allylic Amination Rate Studies

General procedure for allylic aminations with diethylamine (Table 1): In a glove box: Into an NMR tube was weighed the bisphosphine palladium(η^3 -methallyl) triflate (0.005 mmol, 0.05 equiv) and 1 mL CDCl₃ was added. Diethylamine (103 μ L, 1 mmol, 10 equiv) was then added, followed by methallyl chloride (9.8 μ L, 0.1 mmol) and finally mesitylene (5 μ L, internal standard). The vial was capped, mixed vigorously and ¹H-NMR was taken at several different time intervals. Conversion to product was determined by comparison to the internal standard.

General procedure for allylic aminations with 2,2,6,6-tetramethylpiperidine (Table 2, room temperature): In a glove box: Into an NMR tube was weighed the bisphosphine palladium(η^3 -methallyl) triflate (0.005 mmol, 0.05 equiv) and 1 mL CDCl₃ was added. 2,2,6,6-tetramethylpiperidine (169 μ L, 1 mmol, 10 equiv) was then added, followed by methallyl chloride (9.8 μ L, 0.1 mmol) and finally mesitylene (5 μ L, internal standard). The vial was capped, mixed vigorously and ¹H-NMR was taken at several different time intervals. Conversion to product was determined by comparison to the internal standard.

Procedure for amination at 90 °C with 8 (Table 2): In a glove box: Into a 2 dram vial was weighed the bis(triphenylphosphine)palladium(η^3 -methallyl) triflate (4.28 mg, 0.005 mmol, 0.05 equiv) and 1 mL CDCl₃ was added. 2,2,6,6-tetramethylpiperidine (169 μ L, 1 mmol, 10 equiv) was then added, followed by methallyl chloride (9.8 μ L, 0.1 mmol) and finally mesitylene (5 μ L, internal

standard). The vial was capped with a teflon cap, mixed vigorously and heated to 90 °C for 24 hrs. The contents of the vial were then transferred to an NMR tube and ¹H-NMR was taken. Conversion to product was determined by comparison to the internal standard. Reaction was also run using bis(4-CF₃C₆H₄)₃P)Pd(methallyl)triflate using 6.7 mg (0.005 mmol, 0.05 equiv).

Allylic Amination with complex 12: In a glove box: Into an NMR tube was weighed **12** (4.3 mg, 0.005 mmol, 0.05 equiv) and 1 mL CDCl₃ was added. Diethylamine (103 μL, 1 mmol, 10 equiv) was then added, followed by methallyl chloride (9.8 μL, 0.1 mmol) and finally mesitylene (5 μL, internal standard). The vial was capped, mixed vigorously and ¹H-NMR was taken at several different time intervals. Conversion to product was determined by comparison to the internal standard. The reaction was found to proceed to 51% conversion after 3 hrs.

Intermolecular allylic amination with excess tetrabutylammonium chloride (0.5 M): In a glove box, 9.4 mg (0.01 mmol, 1 mol%) **1** and tetrabutylammonium chloride (277.9 mg, 1.0 mmol, 1 equiv) was added to an NMR tube and 1 mL of CDCl₃ added. 2,2,6,6-tetramethylpiperidine (311 mg, 2.2 mmol, 2.2 equiv) was then added, followed by methallyl chloride (91 mg, 1.0 mmol). The reaction was monitored by ¹H-NMR, and went to completion in 35 min.

Intermolecular allylic amination with methallyl acetate (0.5 M): In a glove box, 23.5 mg (0.025 mmol, 5 mol%) **1** was added to an NMR tube and 1 mL of CDCl₃ added. 2,2,6,6-tetramethylpiperidine (159 mg, 1.1 mmol, 2.2 equiv) was then added, followed by methallyl acetate (57 mg, 0.5 mmol). The reaction was monitored by ¹H-NMR and conversion stalled after 30 minutes at 16% product with respect to starting methallyl acetate.

Intermolecular allylic amination with methallyl trifluoroacetate (0.5 M): In a glove box, 23.5 mg (0.025 mmol, 5 mol%) **1** was added to an NMR tube and 1 mL of CDCl₃ added. 2,2,6,6-tetramethylpiperidine (159 mg, 1.1 mmol, 2.2 equiv) was then added, followed by 1,1,1-trifluoro-4-

methylpent-4-en-2-one (76 mg, 0.5 mmol). The reaction was monitored by $^1\text{H-NMR}$, and went to completion in 5 min.

Intermolecular allylic amination with methallyl chloride (0.5 M): In a glove box, 23.5 mg (0.025 mmol, 5 mol%) **1** was added to an NMR tube and 1 mL of CDCl_3 added. 2,2,6,6-tetramethylpiperidine (159 mg, 1.1 mmol, 2.2 equiv) was then added, followed by methallyl chloride (46 mg, 0.5 mmol). The reaction was monitored by $^1\text{H-NMR}$ and went to completion in 5 min.

6.2.4 Observation of Catalytic Intermediates

Phosphorous NMR was used to track the formation of new intermediates during allylic amination catalysis as follows:

In the following example, 2 equivalents of methallyl chloride were used WRT amine base to ensure that the catalyst remained at the Pd(II) oxidation state at the end of the reaction. In a glove box, 9.4 mg (0.01 mmol, 1 mol%) **1** was added to an NMR tube and 1 mL of CDCl_3 added. 2,2,6,6-tetramethylpiperidine (141 mg, 1 mmol) was then added, followed by methallyl chloride (199 mg, 2.2 mmol, 2.2 equiv). The reaction was allowed to run to completion (20 minutes) and $^{31}\text{P-NMR}$ taken. $^{31}\text{P-NMR}$ (300 MHz, CDCl_3): δ (ppm) major peaks at -16.75, 24.18 were observed.

Addition of tetrabutylammonium chloride to complex **1** was accomplished as follows:

In a glove box, 9.4 mg (0.01 mmol) **1** was added to an NMR tube and 1 mL of CDCl_3 added. Tetrabutylammonium chloride (27.7 mg 0.1 mmol, 10 equiv) was added. A $^{31}\text{P-NMR}$ was then taken. $^{31}\text{P-NMR}$ (300 MHz, CDCl_3): δ (ppm) major peaks at -16.72, 24.20 were observed, suggesting formation of the same intermediates as observed in the catalytic reaction. When attempts were made to isolate any complex formed by addition of exogenous chloride, only complex **1** was

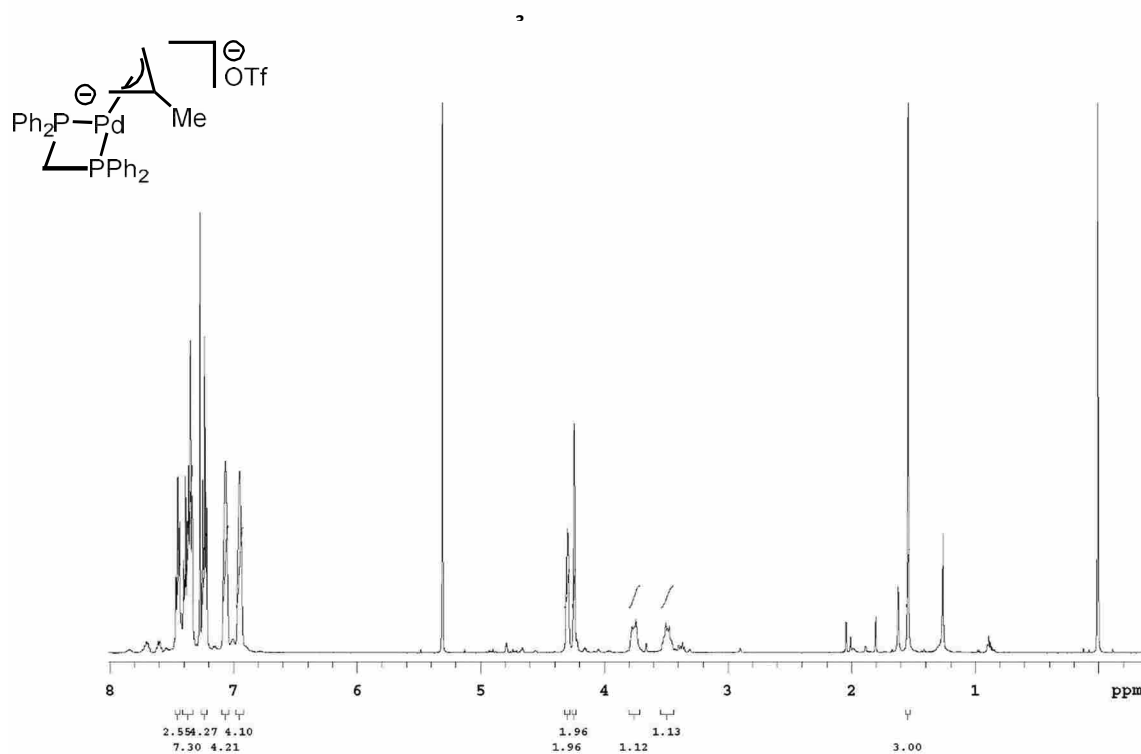
re-isolated (as confirmed via X-ray crystallography of the crystals obtained), suggesting the dynamic and reversible nature of formation of chloride adducts such as **1-Cl**.

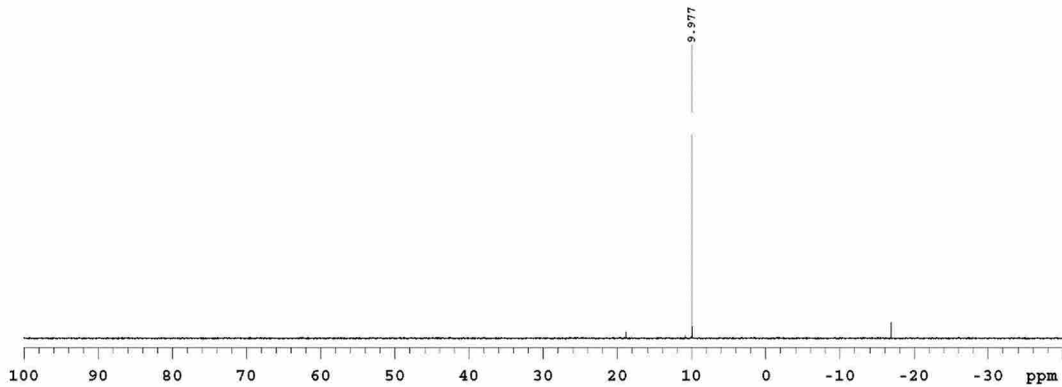
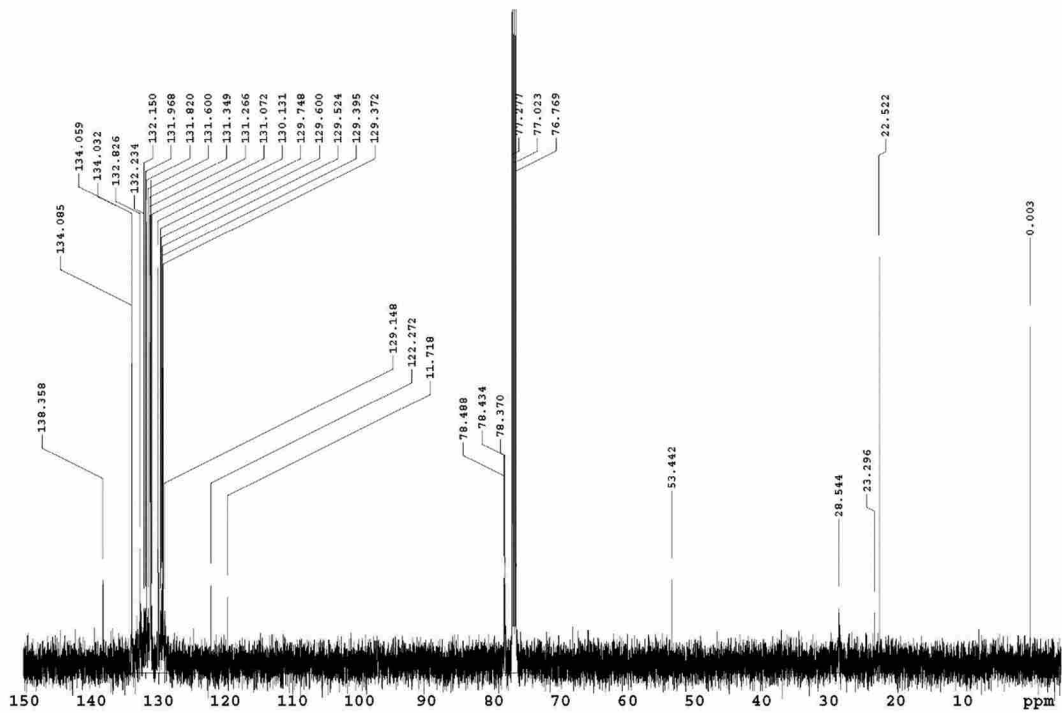
6.2.5 XYZ Coordinates and Absolute Energies

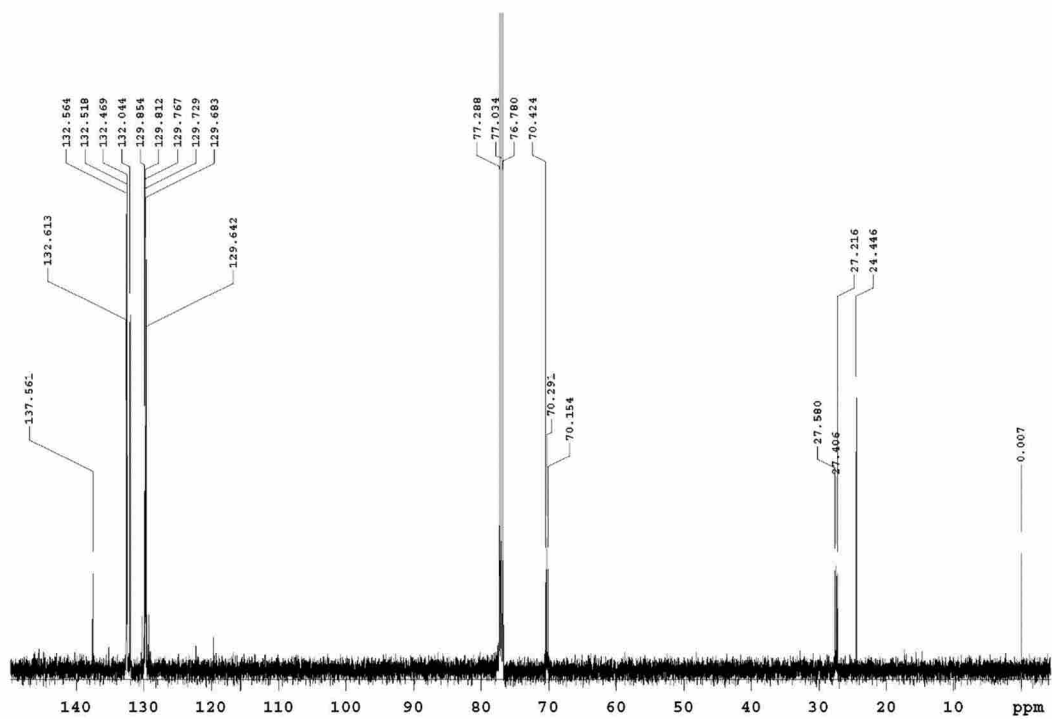
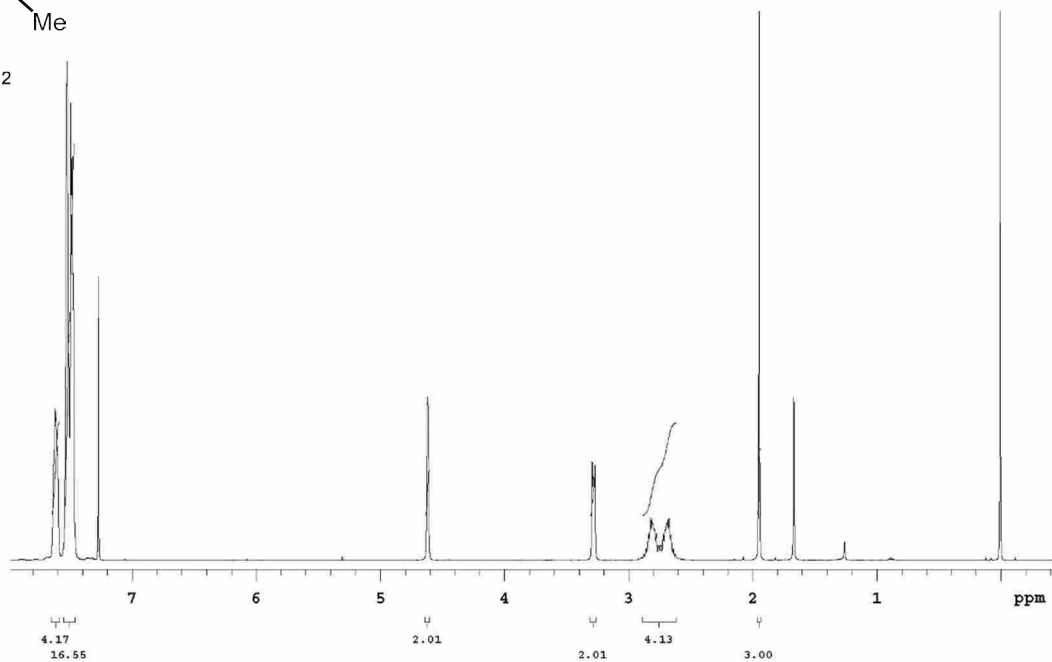
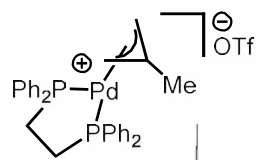
M06/6-31G(d,p)[LANL2DZ] optimized geometries in SMD dichloromethane solvent. For organic compounds, e.g. methallyl chloride, the optimized geometry results from using the 6-31G(d,p) basis set in the route section of Gaussian 09. All other geometries were generated with basis sets specified using the Gen keyword. E large = M06/6-311+G(2d,p)[LANL2TZ(f).

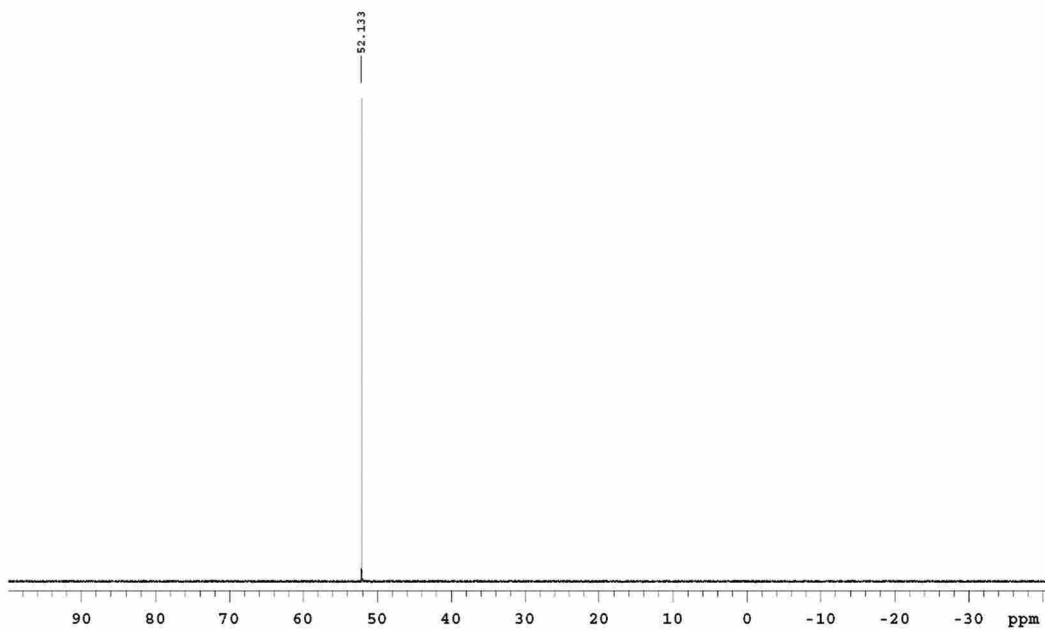
For XYZ coordinates of complexes, please see SI of work DOI: 10.1021/jacs.5b02428

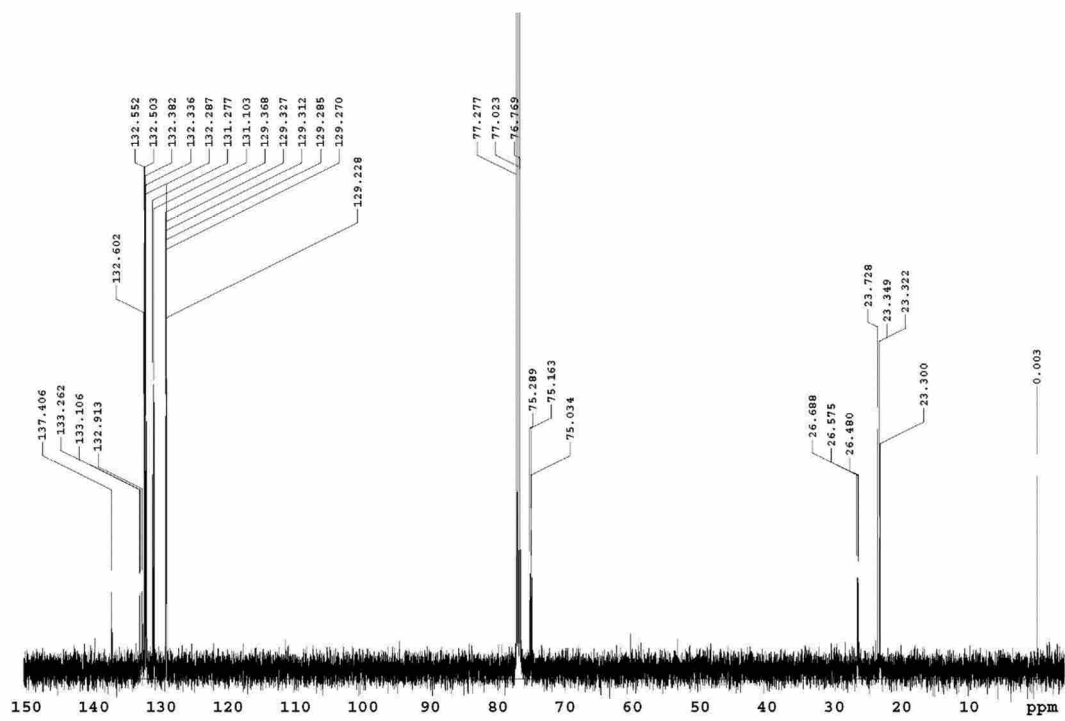
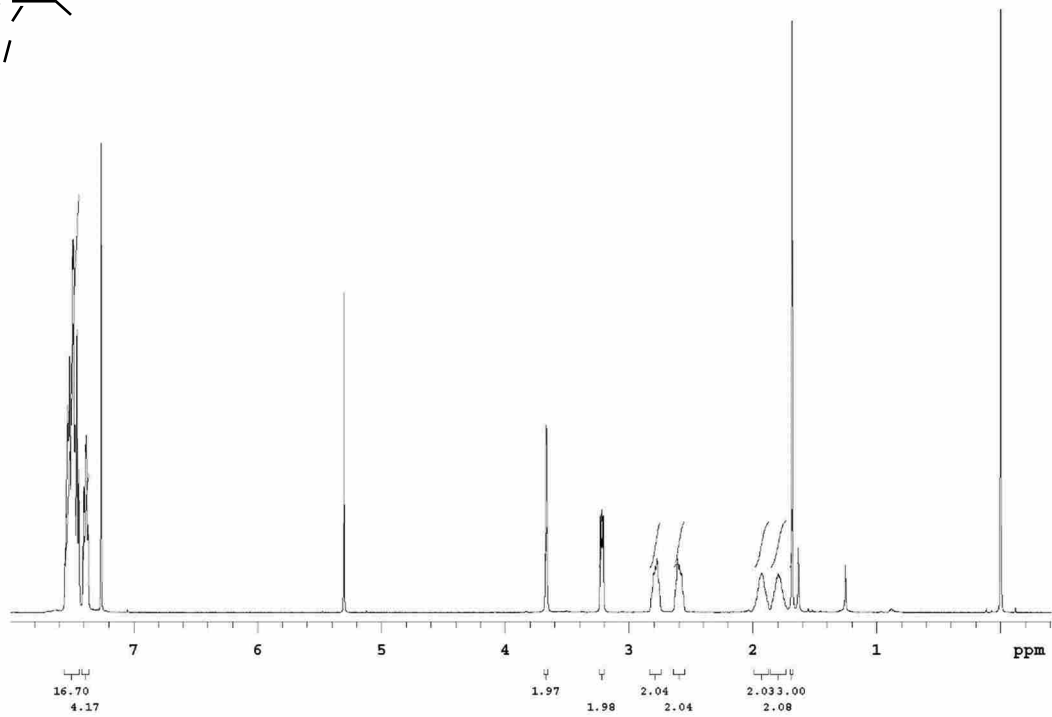
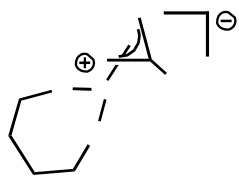
6.2.6 Spectral Images

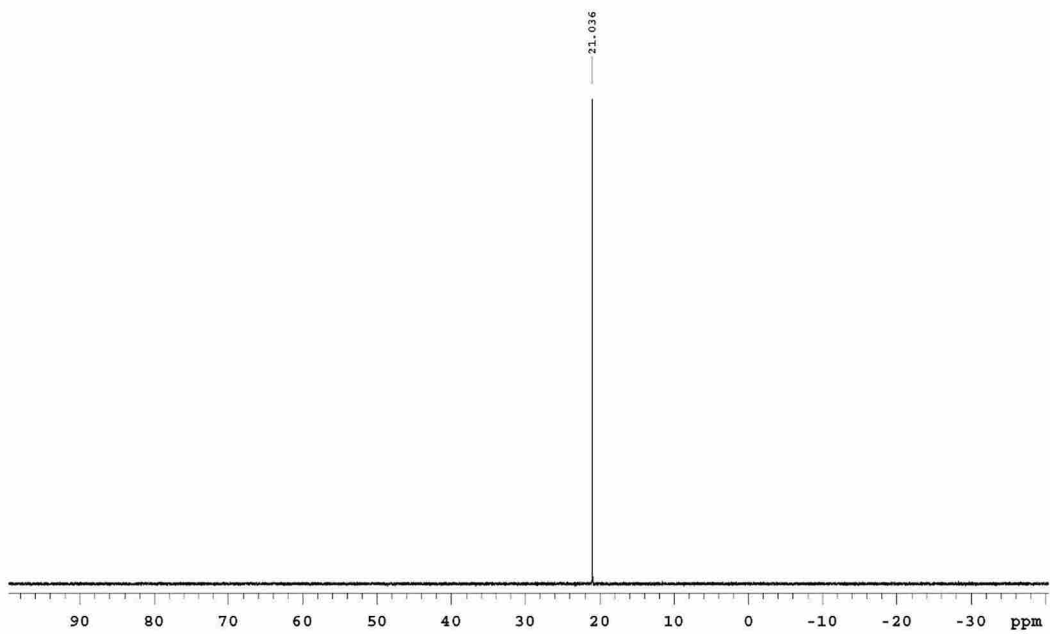


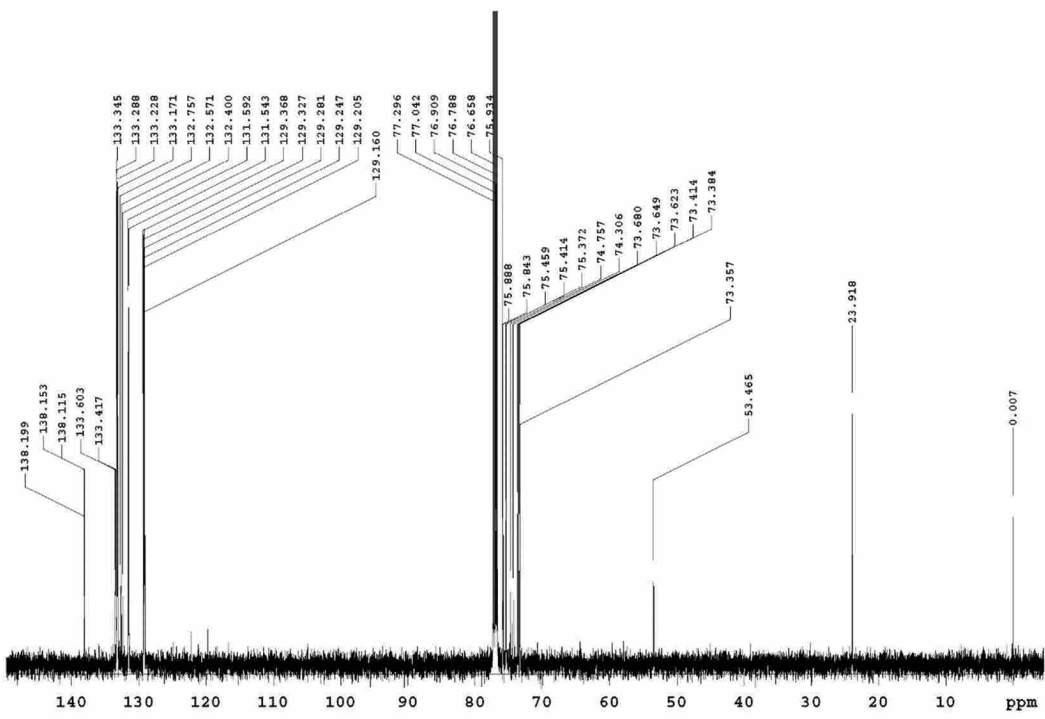
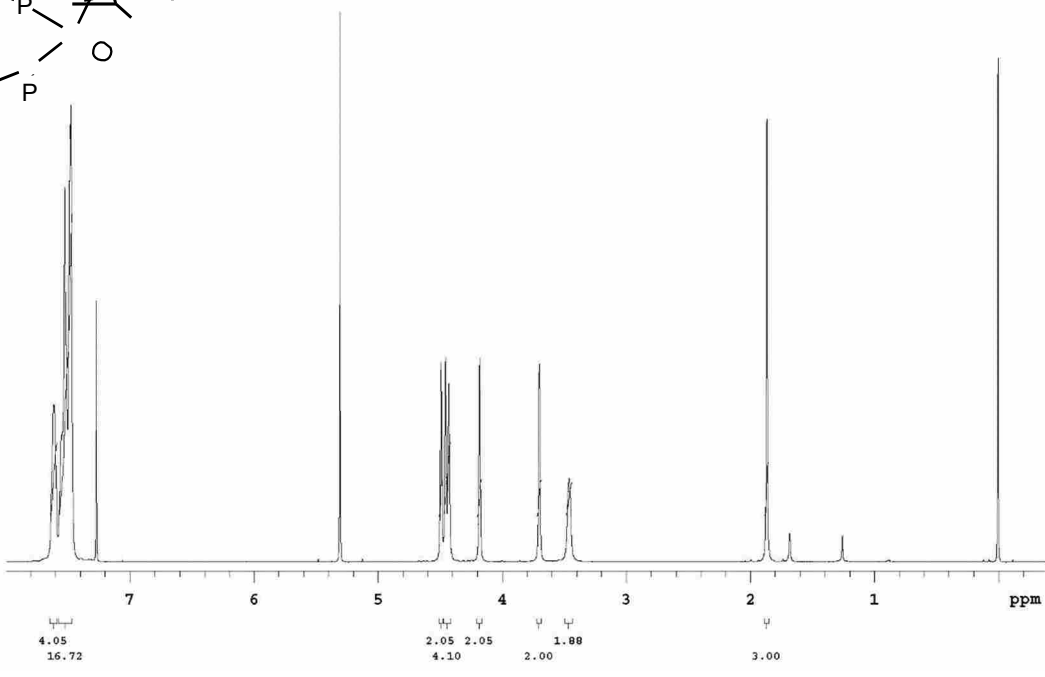
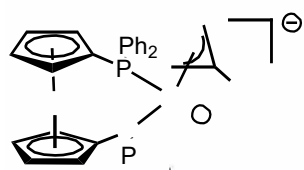


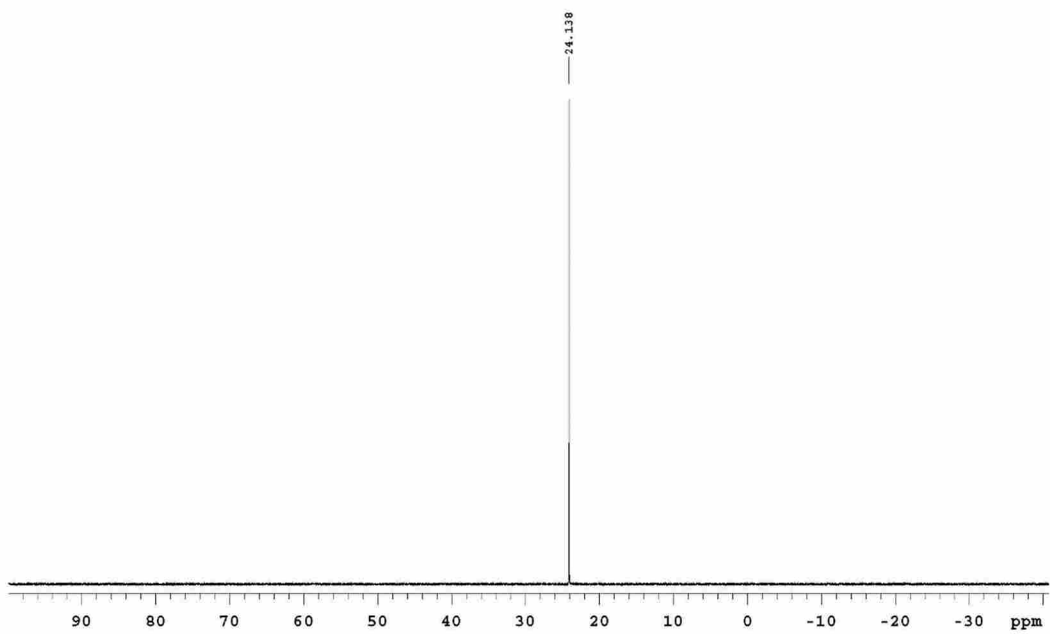


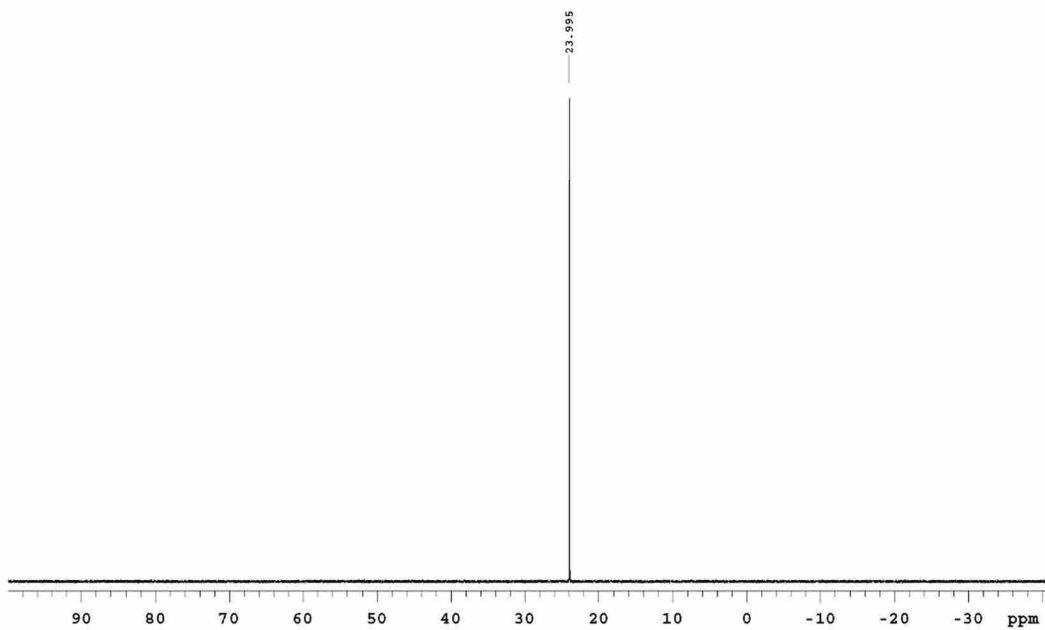


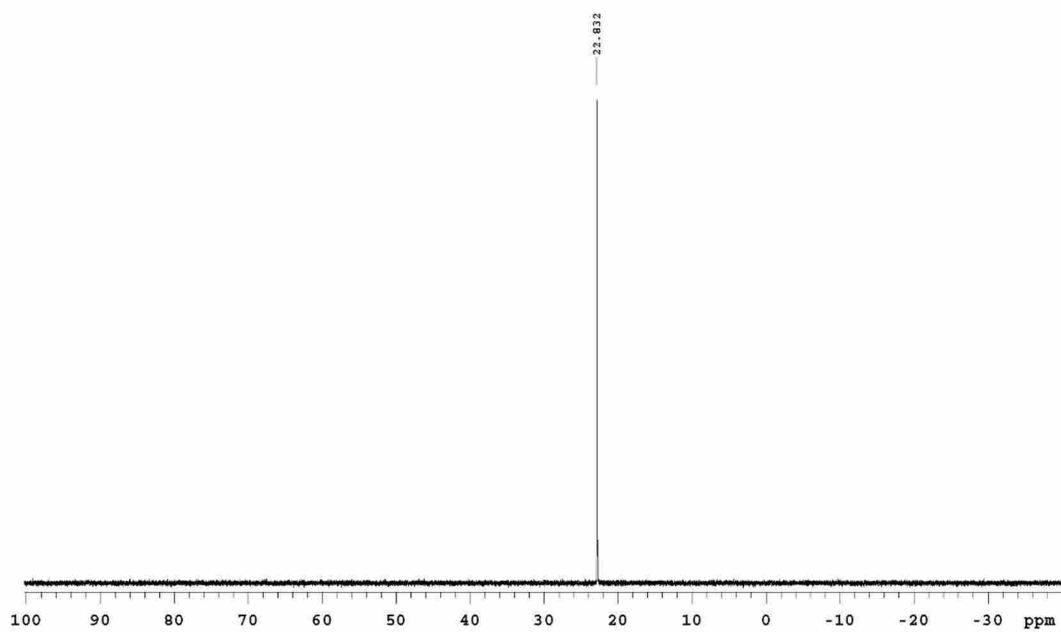
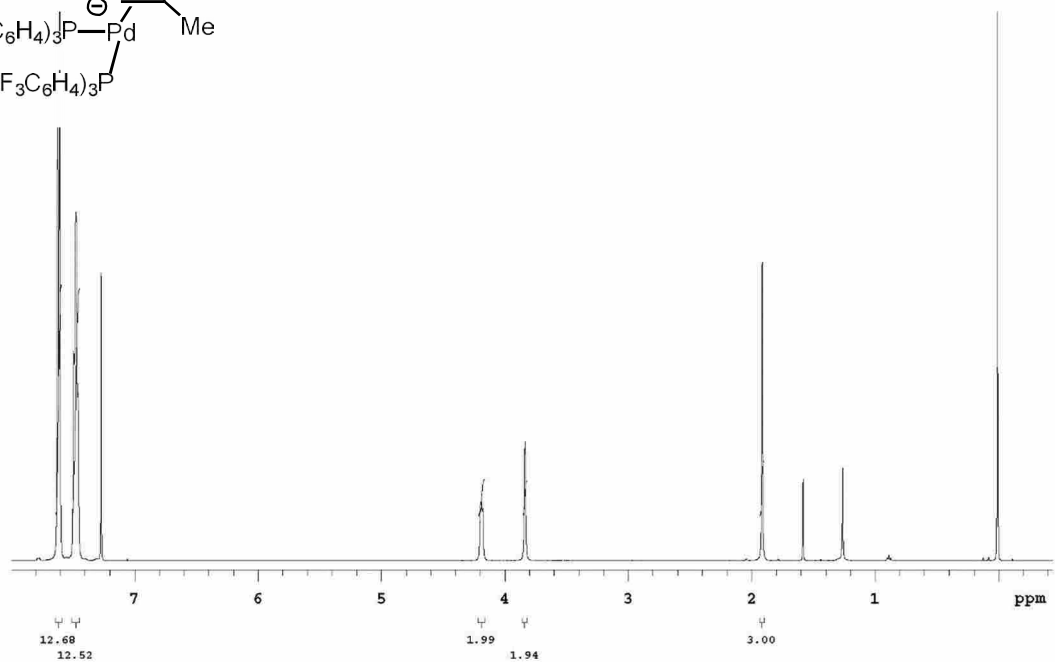
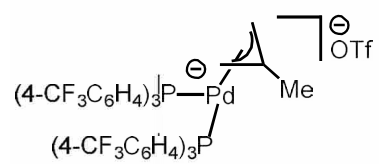


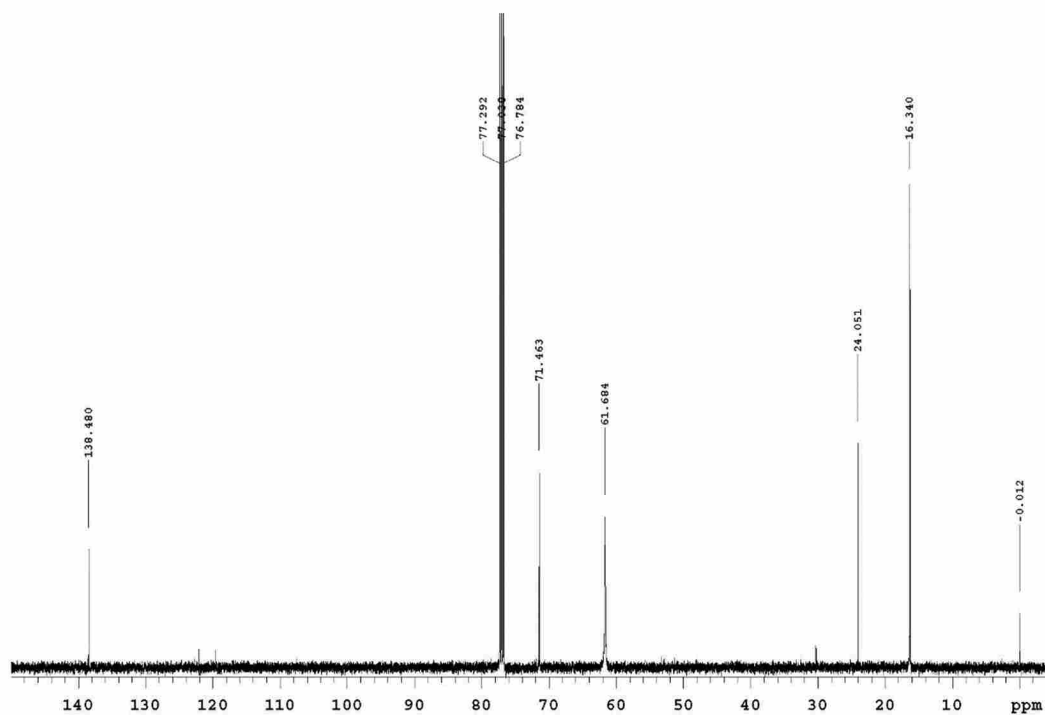
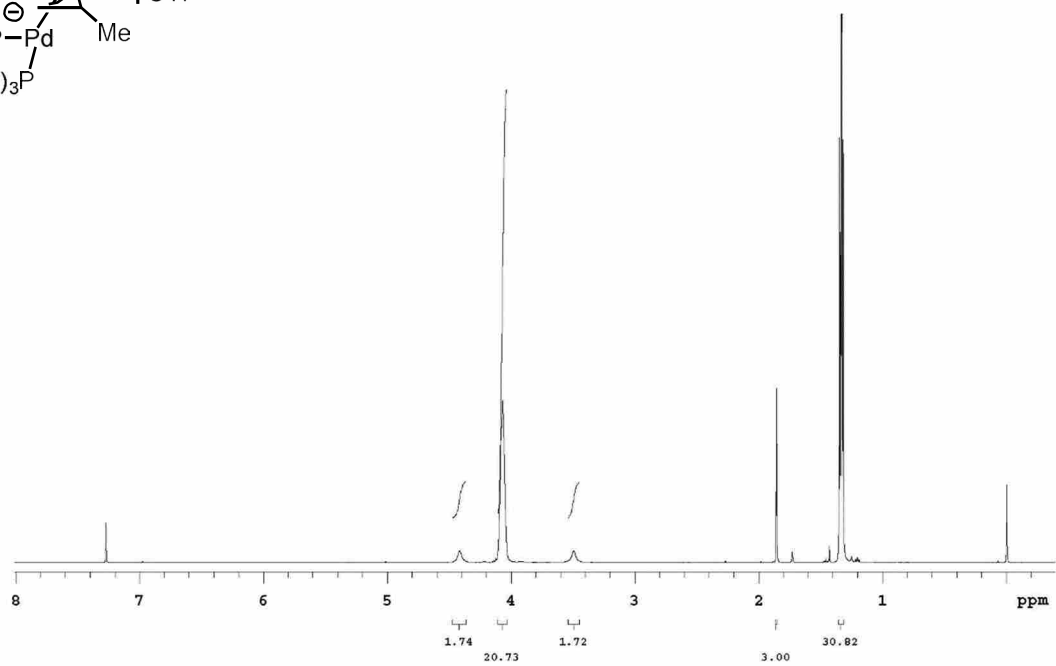
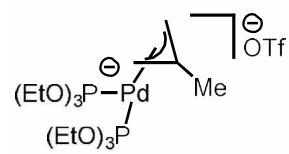


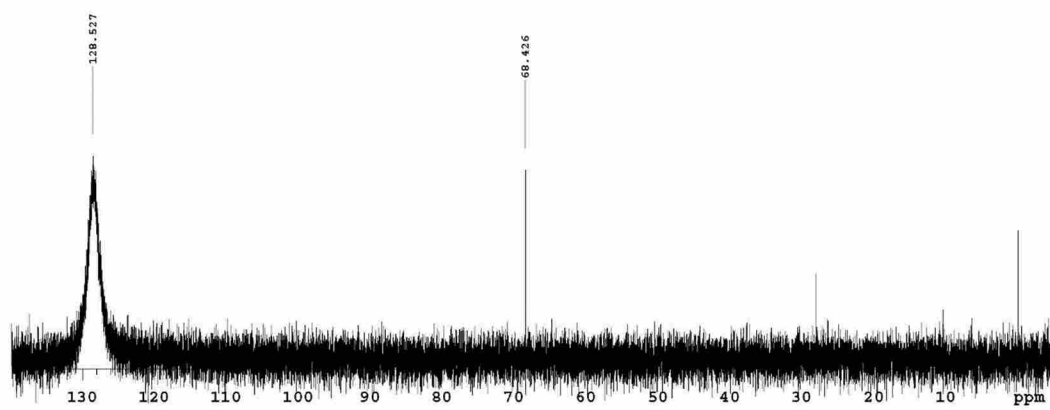


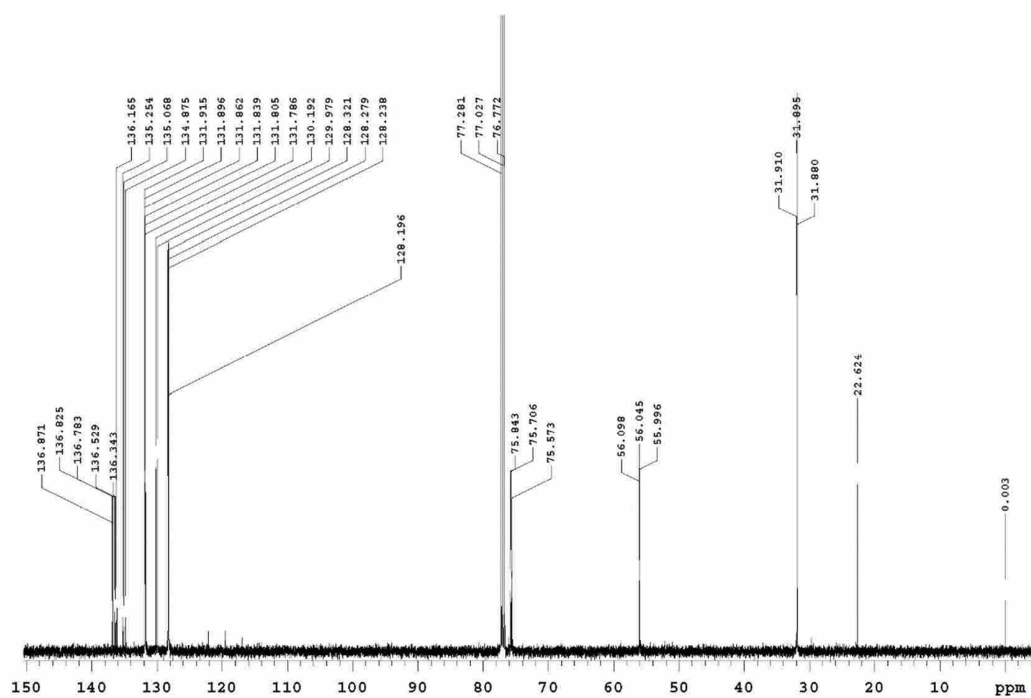
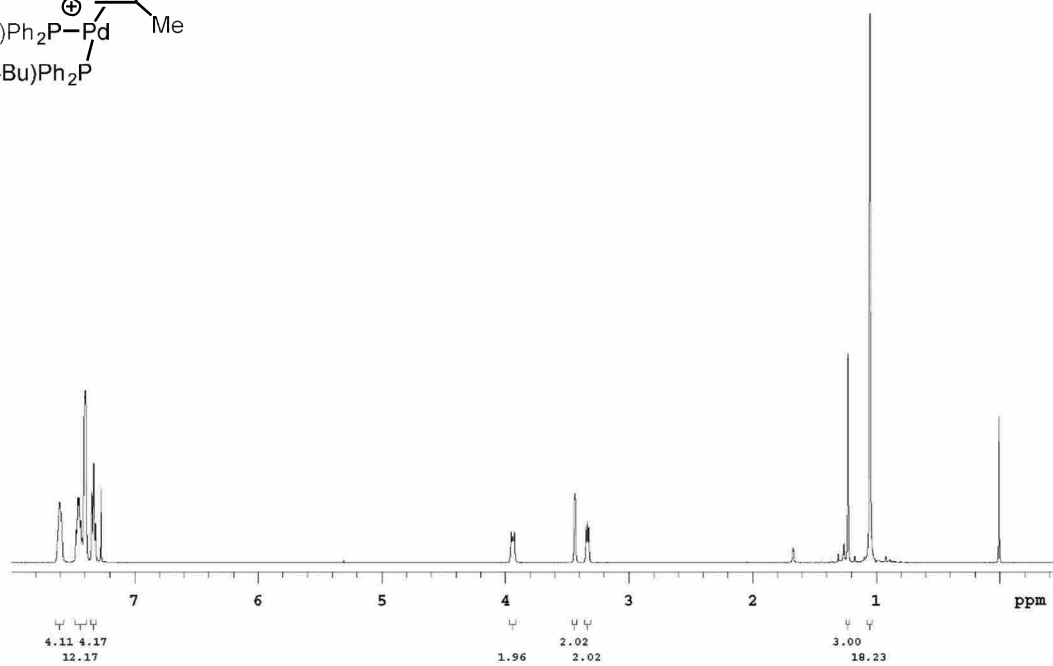
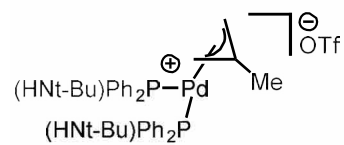


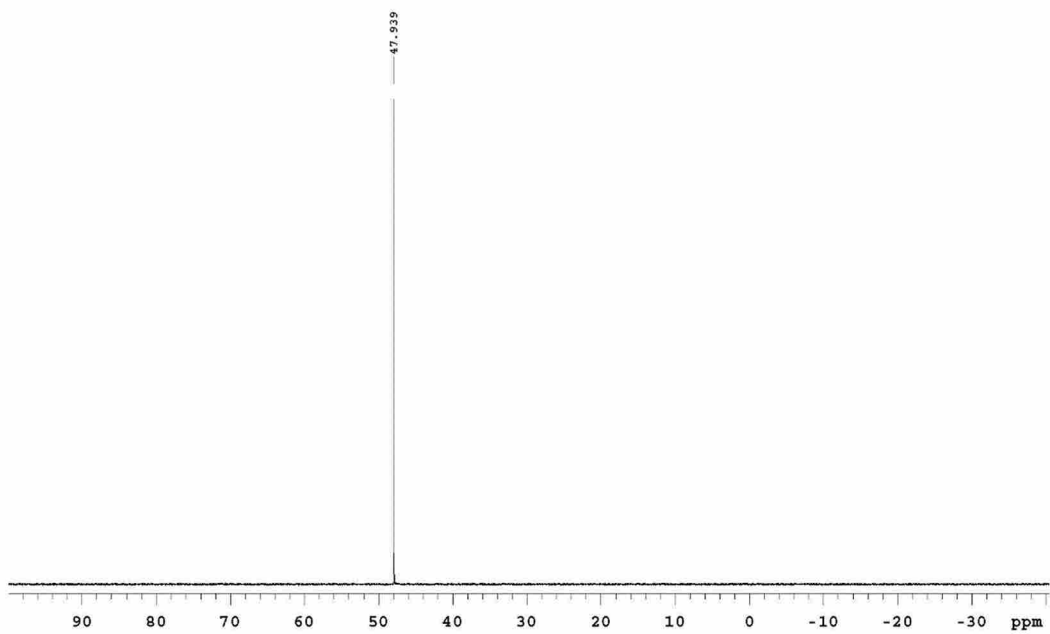


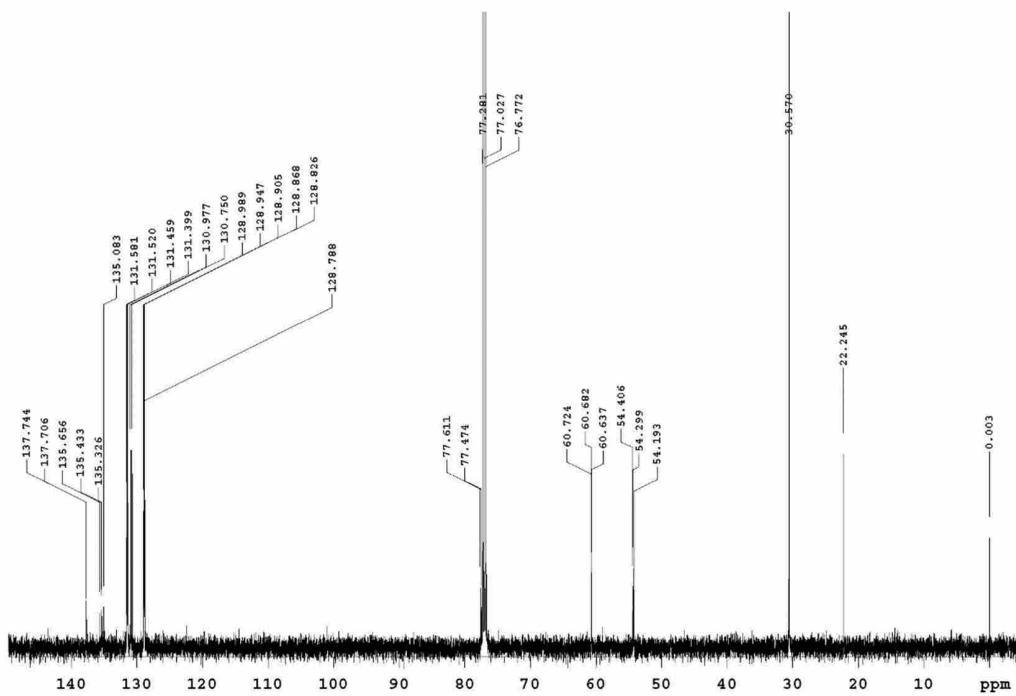
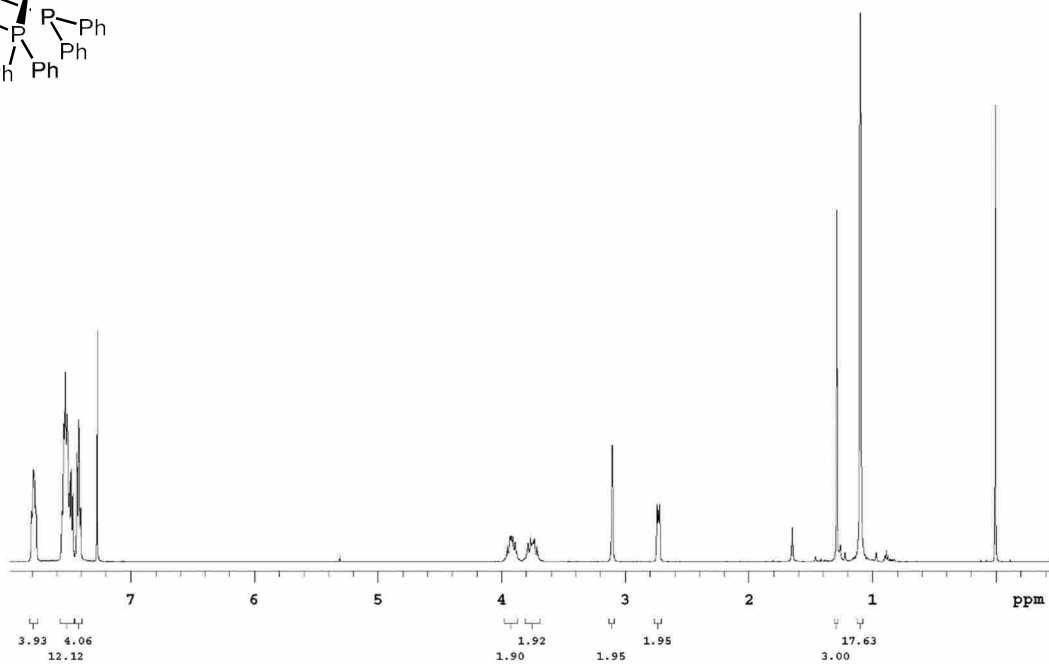
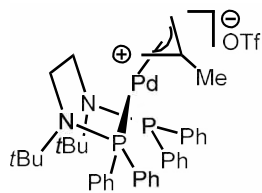


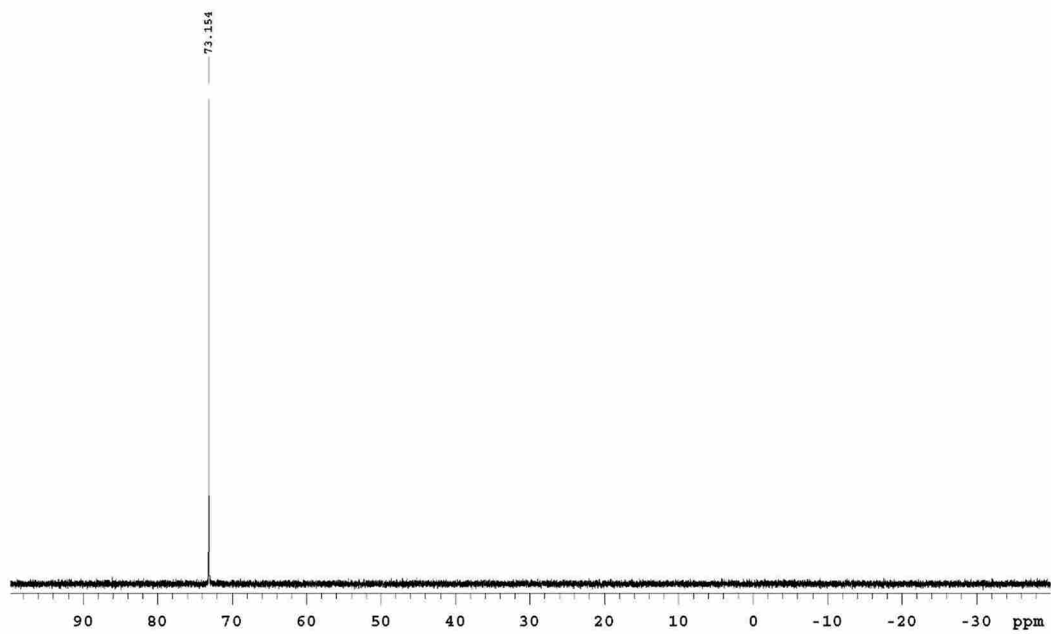


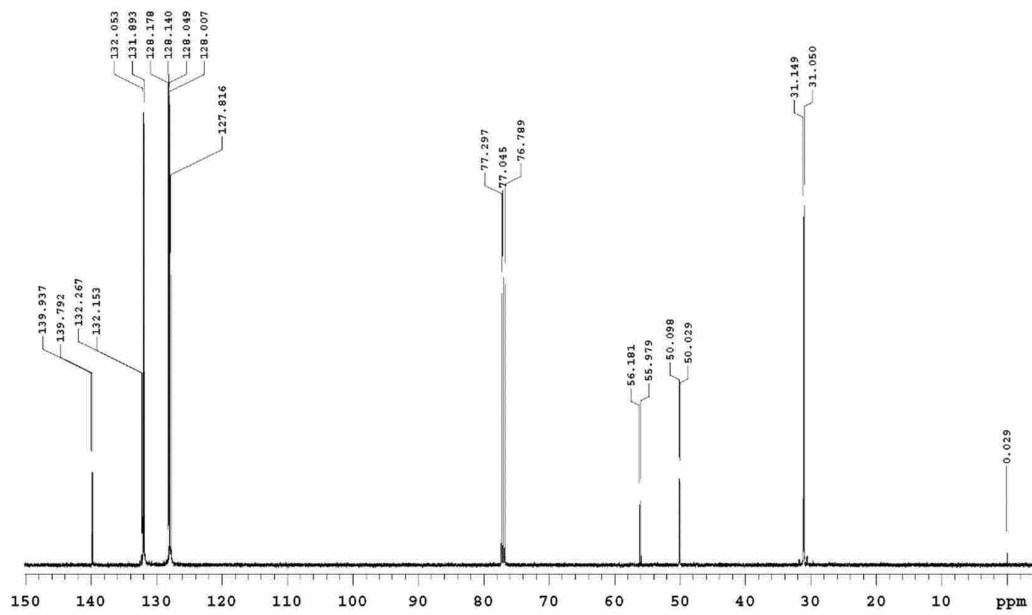
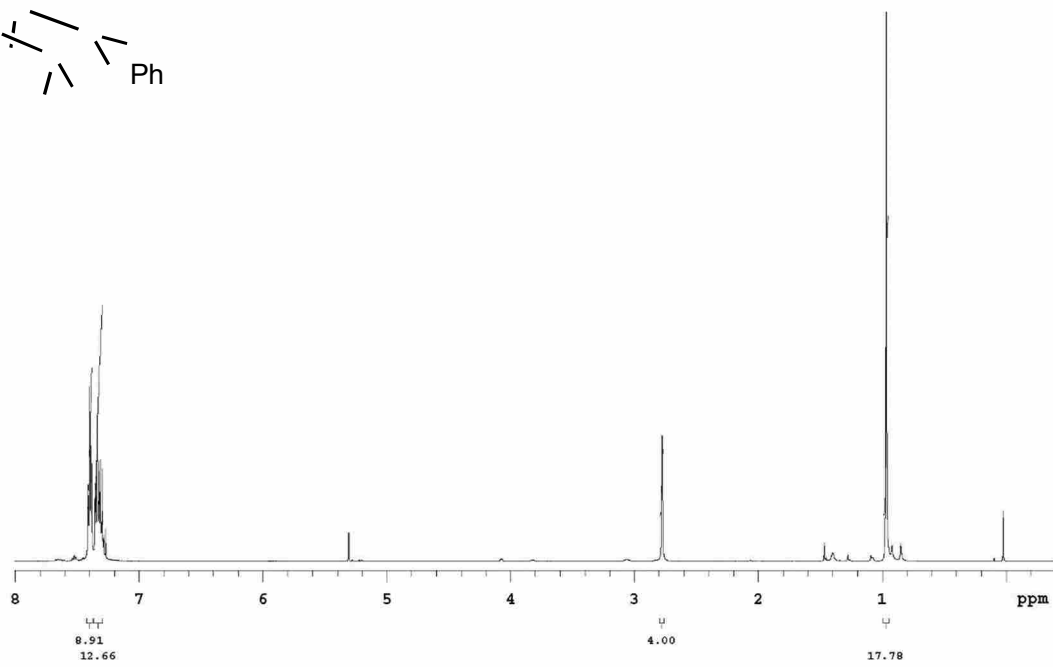
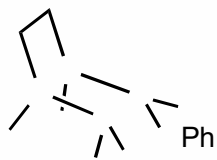


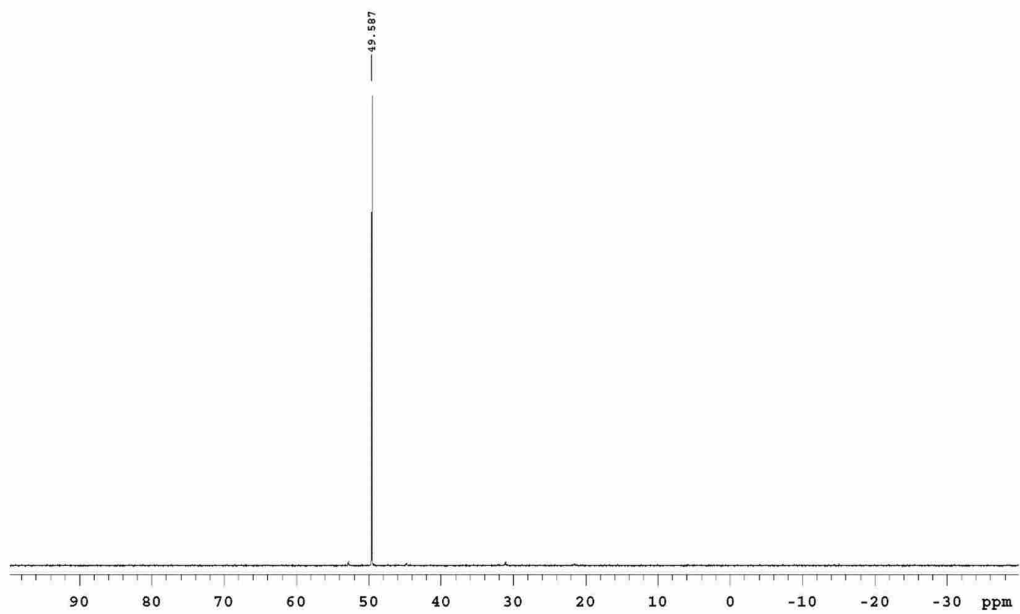












6.3 SUPPORTING INFORMATION FOR CHAPTER 4

6.3.1 *General Information*

All reactions were carried out in oven-dried glassware with magnetic stirring, unless otherwise indicated. Reactions requiring a moisture-free environment were conducted in a nitrogen atmosphere glove box (Innovative Technology, PureLab HE system, double glove box). Solvents were taken from dry solvent system and stored under molecular sieves. Hexanes were distilled with calcium hydride. Analytical thin-layer chromatography was performed with 0.25 mm coated commercial silica gel plates (E. Merck, DC-Plastikfolien, kieselgel 60 F254). Flash Chromatography was performed with EM Science silica gel (0.040-0.063 μm grade). Phosphorous nuclear magnetic resonance (^{31}P -NMR) data were acquired on an Inova-300 (300 MHz). Proton nuclear magnetic resonance (^1H -NMR) data were acquired on an Inova-300 (300 MHz) or on an Inova-500 (500 MHz) spectrometer. Chemical shifts are reported in delta (δ) units, in parts per million (ppm) downfield from the deuterium signal of the NMR solvent. Carbon-13 nuclear magnetic resonance (^{13}C -NMR) data were acquired on an Inova 500 at 125 MHz. Signals are reported as follows: s (singlet), d (doublet), t (triplet), q (quartet), dd (doublet of doublets), qd (quartet of doublets), brs (broad singlet), m (multiplet). Coupling constants are reported in hertz (Hz). Chemical shifts are reported in ppm relative to the deuterium signal of the NMR solvent. Mass spectral data were obtained using ESI techniques (Agilent, 6210 TOF).

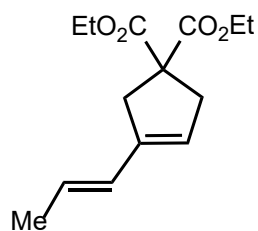
6.3.2 *Synthesis of Trichlorotitanium N-tert-butyl(diphenylphosphino)amide*

In a Schlenk tube, 2.594 g N-tert-butyl-1,1-diphenylphosphanamine (10.038 mmol, 1.1 eq) was dissolved in 2 mL dry Et_2O . Then 16 mL dry hexanes were added. 1 mL TiCl_4 (9.12 mmol, 1 eq) was added and the reaction vessel was sealed. The reaction was heated to 90 $^\circ\text{C}$ for 3 hrs. The

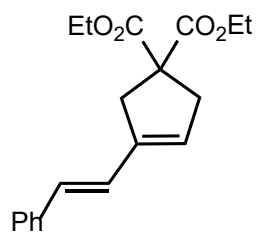
warm reaction was brought into the glovebox, and filtered through a fritted funnel and placed in the fridge (-30 °C) immediately. The product is afforded as dark red crystals: 0.66 g (17.5% yield). Spectra matched previously reported spectra.¹

6.3.3 Experimental Procedures

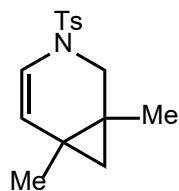
Ligand screen from table 1: In a glovebox, 52 mg (0.206 mmol) of substrate was added to a 3 dram vial with 8.42 mg trichlorotitanium N-tert-butyl(diphenylphosphino)amide (0.0206 mmol, 10 mol%), 5.48 mg PtCl₂ (0.0206 mmol, 10 mol%) and 1 mL toluene. The reaction was stirred and monitored by NMR. At the indicated time (see table 1), a small aliquot was taken from the reaction, diluted in CDCl₃ and the conversion was determined by ¹H-NMR.



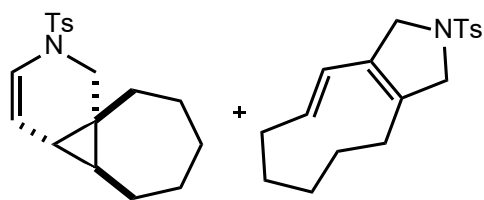
Diethyl (E)-3-(prop-1-en-1-yl)cyclopent-3-ene-1,1-dicarboxylate(2a): General Procedure: In a glovebox, 10 mg (0.040 mmol) **1a** was added to a 25 mL vial with 1.6 mg trichlorotitanium N-tert-butyl(diphenylphosphino)amide (0.0040 mmol, 10 mol%), 1 mg PtCl₂ (0.0040 mmol, 10 mol%) and 0.2 mL toluene. The reaction was stirred and monitored by NMR. Reaction went to completion in 2 hrs. Upon completion, the reaction was filtered through a small silica plug and the silica washed with 20:1 hexane:EtOAc (5 mL). The product was isolated as a colorless oil: 10 mg (>99% yield). Spectra matched previously reported values.²



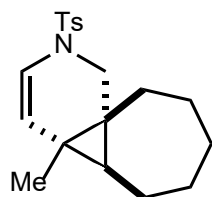
Diethyl (*E*)-3-styrylcyclopent-3-ene-1,1-dicarboxylate (2b): Synthesized according to the general procedure using 64.76 mg **1b** (0.206 mmol), 5.48 mg PtCl₂ (0.0206 mmol, 10 mol%), 8.43 mg trichlorotitanium N-tert-butyl(diphenylphosphino)amide (0.206 mmol, 10 mol%) and 1 mL toluene. Product isolated as a colorless oil: 38.4 mg (58% yield). Spectra matches previously reported spectra.²



1,6-dimethyl-3-tosyl-3-azabicyclo[4.1.0]hept-4-ene (2c): Synthesized according to the general procedure with 57 mg (0.206 mmol) **1c**, 8.42 mg trichlorotitanium N-tert-butyl(diphenylphosphino)amide (0.0206 mmol, 10 mol%), 5.48 mg PtCl₂ (0.0206 mmol, 10 mol%), and 1 mL toluene. Completed in 48 hrs. At 36 hrs 86% conversion was observed. Upon completion of the reaction, the mixture was filtered through a small plug of silica gel and eluted with 20:1 hexane:EtOAc to provide 57 mg recovered of the product as a colorless oil (99% yield). Spectra matches previously reported spectra.⁴



2-tosyl-1,2,3,4,4a,5,6,7-octahydrocyclopenta[f]isoindole (2d) and **(4aR,4bS,9aR)-2-tosyl-2,4a,4b,5,6,7,8,9-octahydro-1H-cyclohepta[1,3]cyclopropa[1,2-c]pyridine (7)**: When conducted according to the general procedure, the product was isolated as a 1:1.3 mixture of diene in 96% total yield. Reaction performed using 65 mg **1d** (0.206 mmol), 5.48 mg PtCl₂ (0.0206 mmol, 10 mol%), 8.42 mg trichlorotitanium N-tert-butyl(diphenylphosphino)amide (0.0206 mmol, 10 mol%) and 1 mL toluene. Completed in 5 hrs and purified on a column of silica gel with 20:1 heaxane:EtOAc to give 27 mg of **2d** (41% yield) and 36 mg of **7** (55% yield); 96% combined isolated yield.



(4aR,4bS,9aR)-4a-methyl-2-tosyl-2,4a,4b,5,6,7,8,9-octahydro-1H-cyclohepta[1,3]cyclopropal[1,2-c]pyridine (2e): Synthesized according to the general procedure with 68.3 mg **1e** (0.206 mmol), 5.48 mg PtCl₂ (0.0206 mmol, 10 mol%), 8.42 mg trichlorotitanium N-tert-butyl(diphenylphosphino)amide (0.0206 mmol, 10 mol%) and 1 mL toluene. Completed in 18 hrs. 59.3 mg recovered. 87% isolated yield. IR (film): ν = 1048.3, 1097.6, 1167.9, 1716.29, 2987.95; ¹H-NMR (500 MHz, CDCl₃): δ (ppm) = 7.66 (d, J=8.05 Hz, 2H), 7.34 (d, J=8.06 Hz, 2H), 6.25 (d, J=7.93 Hz, 1H), 5.23 (d, J=7.93 Hz, 1H), 3.99 (d, J=11.59 Hz, 1H), 2.60 (d, J=11.59 Hz, 1H), 2.43 (s, 3H), 1.87 (m, 1H), 1.71 (m, 5H), 1.37 (m, 3H), 1.06 (m, 1H), 0.70 (m, 1H); ¹³C-NMR

(500 MHz, CDCl₃): δ (ppm) = 14.0, 21.5, 23.0, 25.6, 26.7, 28.3, 28.5, 32.5, 33.3, 37.3, 46.1, 119.7, 120.4, 127.0, 129.7, 135.1, 143.5; (M+H) calculated: 332.1771, found 332.1606.

(4aR,4bS,9aR)-4a-phenyl-2-tosyl-2,4a,4b,5,6,7,8,9-octahydro-1H-

cyclohepa[1,3]cyclopropa[1,2-c]pyridine (2f): Synthesized according to the general procedure with 81 mg **1f** (0.206 mmol), 5.48 mg PtCl₂ (0.0206 mmol), 8.42 mg trichlorotitanium N-tert-butyl(diphenylphosphino)amide (0.0206 mmol, 10 mol%), and 1 mL toluene. 65 mg recovered. Completed in 19 hrs. 80% isolated yield. IR (film): ν = 1048.7, 1100.2, 1170.9, 1710.1, 2956.9; ¹H-NMR (500 MHz, CDCl₃): δ (ppm) = 7.73 (d, J=8.17 Hz, 2H), 7.38 (d, J=7.93 Hz, 2H), 7.25 (m, 3H), 7.0 (d, J=7.08 Hz, 2H), 6.28 (d, J=7.93 Hz, 1H), 5.24 (d, J=7.92 Hz, 1H), 4.17 (d, J=11.84 Hz, 1H), 2.87 (d, J=11.72 Hz, 1H), 2.46 (s, 3H), 1.95 (m, 1H), 1.91 (m, 1H), 1.71 (m, 3H), 1.48 (q, 1H), 1.08 (m, 3H), 0.95 (m, 1H), 0.86 (m, 1H); ¹³C-NMR (500 MHz, CDCl₃): δ (ppm) = 21.6, 26.3, 28.0, 28.2, 30.6, 31.5, 35.3, 39.1, 46.3, 119.1, 120.0, 126.5, 127.1, 128.5, 129.8, 131.2, 135.2, 139.8, 143.7; (M+H) calculated: 394.1936, found 394.1762.

Table 3 product selectivity studies: Table 3, Entry 7: In a 3 dram vial is placed 29.3 mg of **1d**, (0.092 mmol), 2.2 mg Pt(cod)₂Cl₂ (0.0046 mmol, 5 mol%) and 3.2 mg (0.0046 mmol, 5 mol%) **4** and 1 mL CDCl₃. Reaction was heated to 35 °C. The reaction is monitored by ¹H-NMR and went to completion in 24 hrs. ¹H-NMR of the crude reaction mixture showed a 10:1 ratio of cyclopropane:diene products. The reaction mixture was loaded directly loaded onto a column of silica gel and eluted with 20:1 hexane:EtOAc. The product was isolated as a colorless oil (24 mg of **2d**, 4 mg of 7.96% yield total). Spectra matched previously reported values.³

6.3.4 ³¹P NMR Studies

When ligand **5** (2 equiv) is mixed with PtCl_2 in either toluene or CHCl_3 , trace amounts of a new signal at ~ 72 ppm is observed (low solubility of PtCl_2). When the same experiment is conducted with more soluble $\text{Pt}(\text{cod})\text{Cl}_2$, the same peak at 72.7 ppm is initially observed which slowly converts to a new signal at 30.97 ppm after extended reaction times (1 week). Importantly, these new peaks contain Pt satellites, indicating the formation of new Pt-P complexes. These peaks are different from the free phosphinoamide $(\text{tBuNPPh}_2)\text{TiCl}_3$ ligand **5** (-11.0 ppm), the peak for phosphinoamide ligand **6** (22.0 ppm) and the peaks formed when $\text{Pt}(\text{cod})\text{Cl}_2$ is mixed with phosphinoamide ligand **6**. Efforts to isolate either of these intermediates via crystallization have been unsuccessful to date.

Figure S1. ^{31}P NMR mixture of $(\text{tBuNPPh}_2)\text{TiCl}_3$ and $\text{Pt}(\text{cod})\text{Cl}_2$ after 12 h reaction time (in C_6D_6).

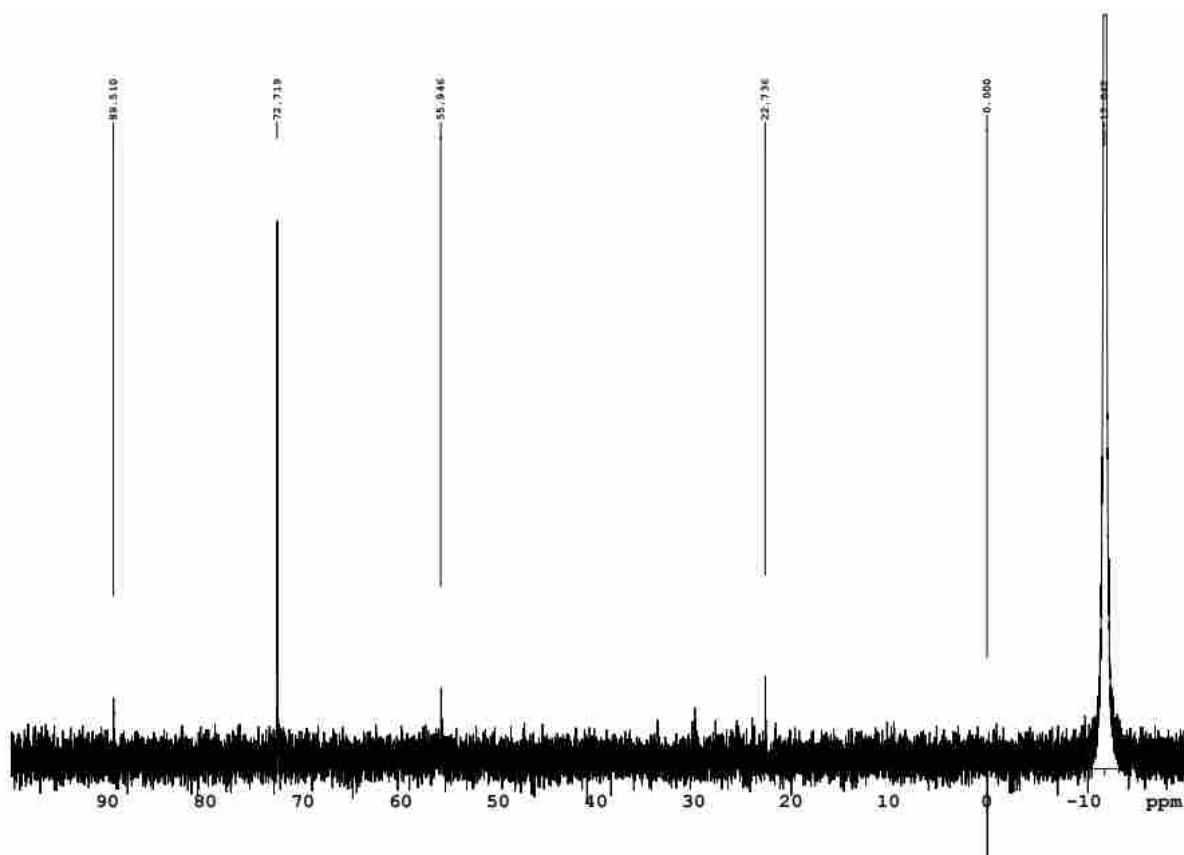


Figure S2. ^{31}P NMR mixture of $(\text{tBuNPPH}_2)\text{TiCl}_3$ and $\text{Pt}(\text{cod})\text{Cl}_2$ after 7 days reaction time (in CDCl_3).

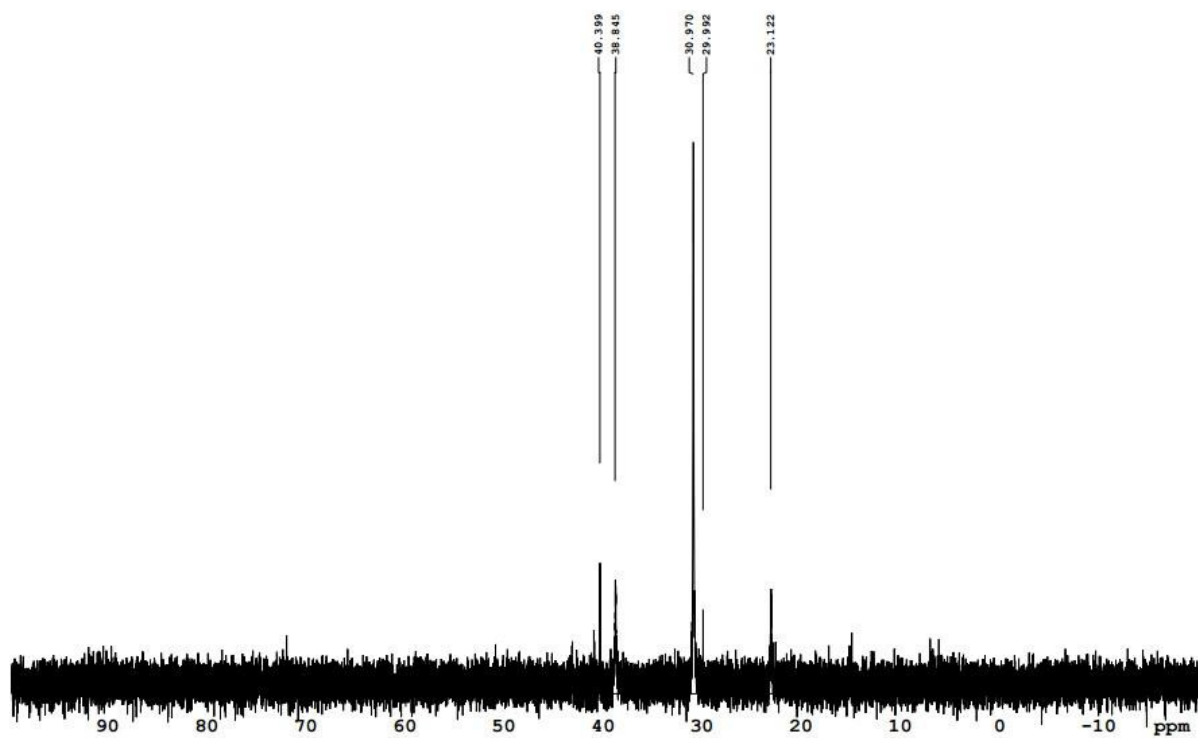


Figure S3. ^{31}P NMR spectrum of $(\text{tBuNPPH}_2)\text{TiCl}_3$ (in CDCl_3).

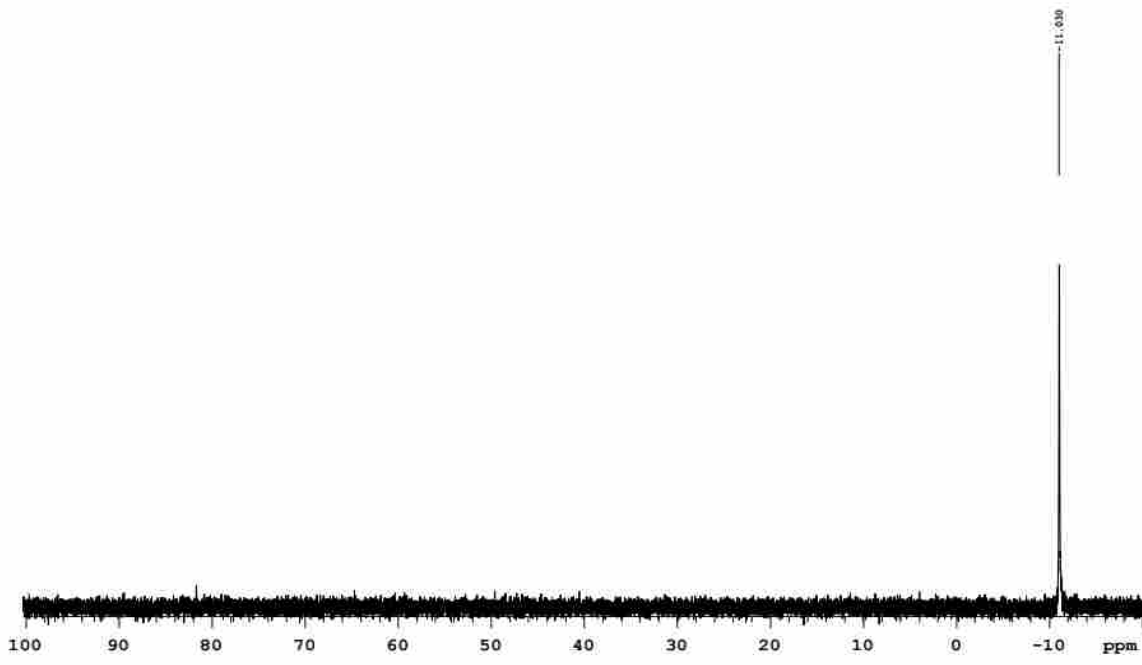


Figure S4. Ligand 6 (*t*BuNHPPH₂) in CDCl₃.

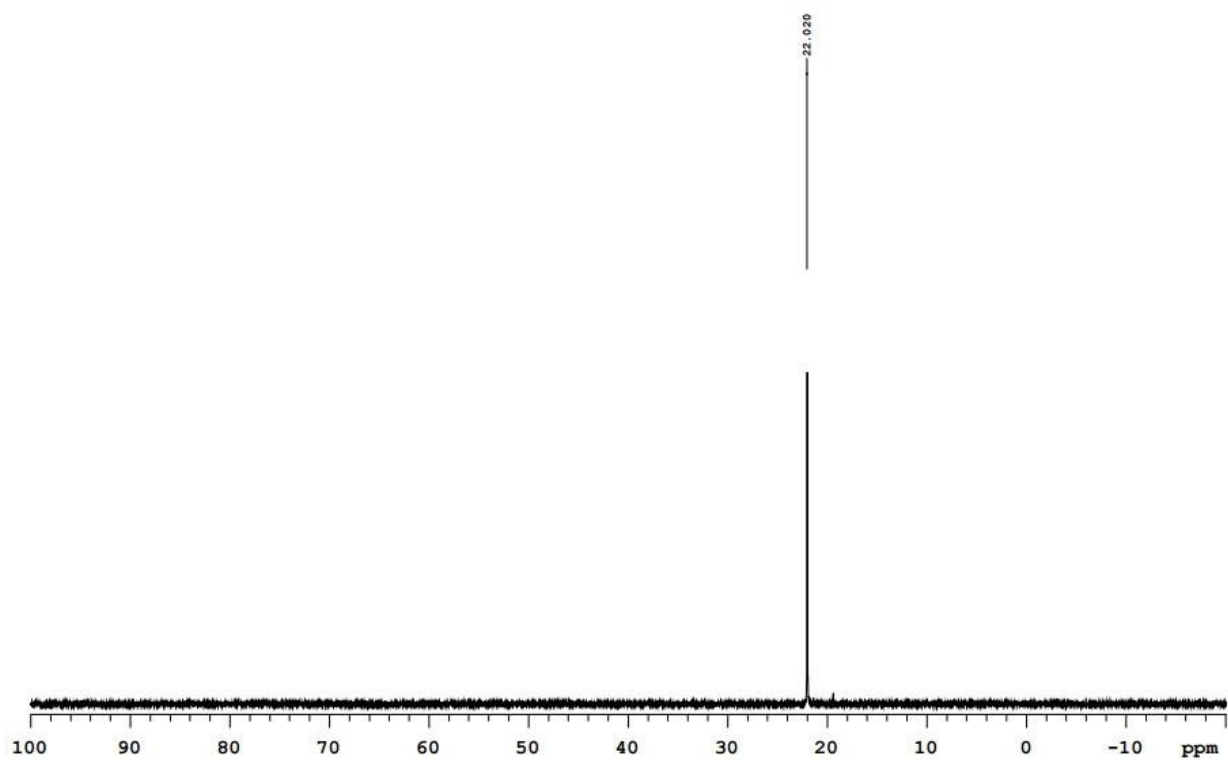
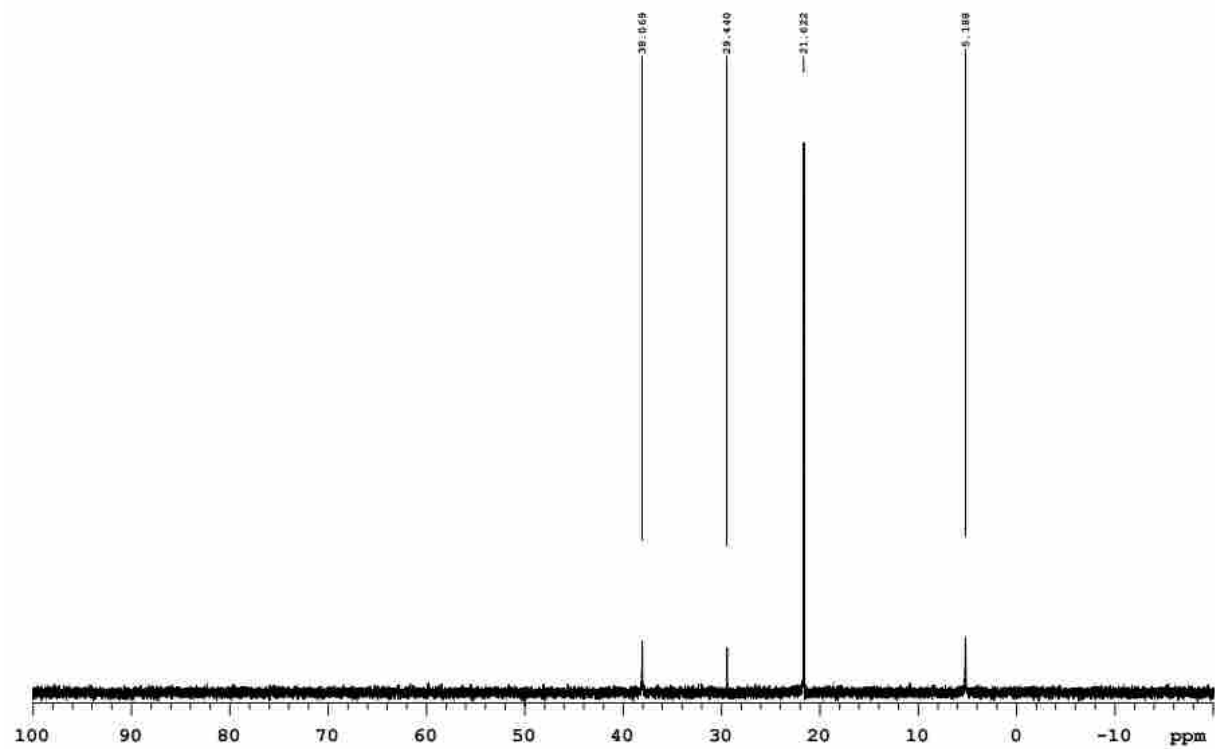
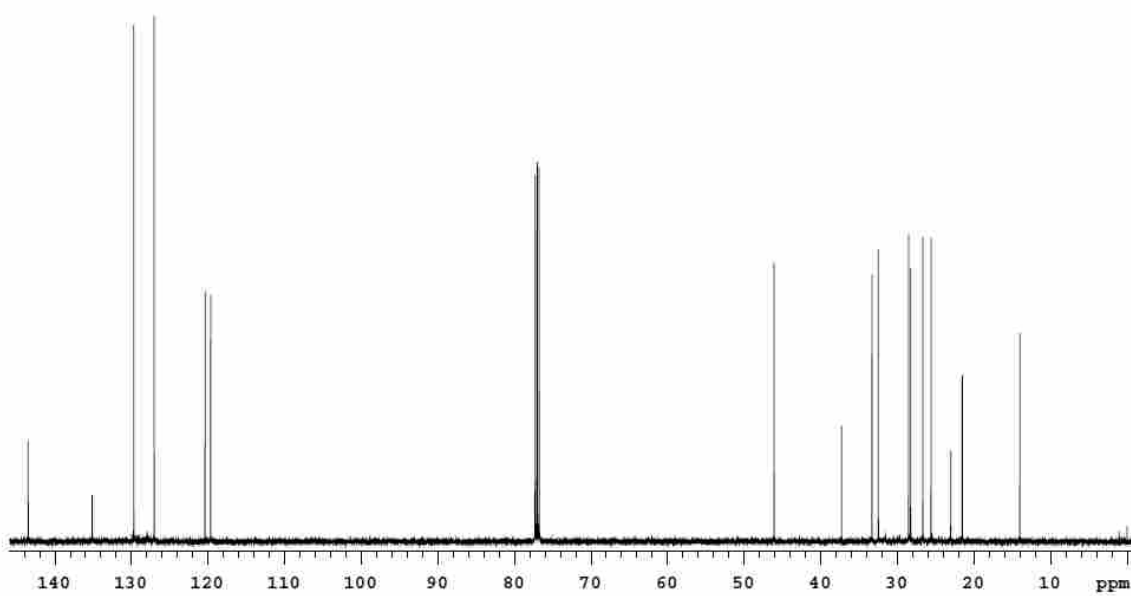
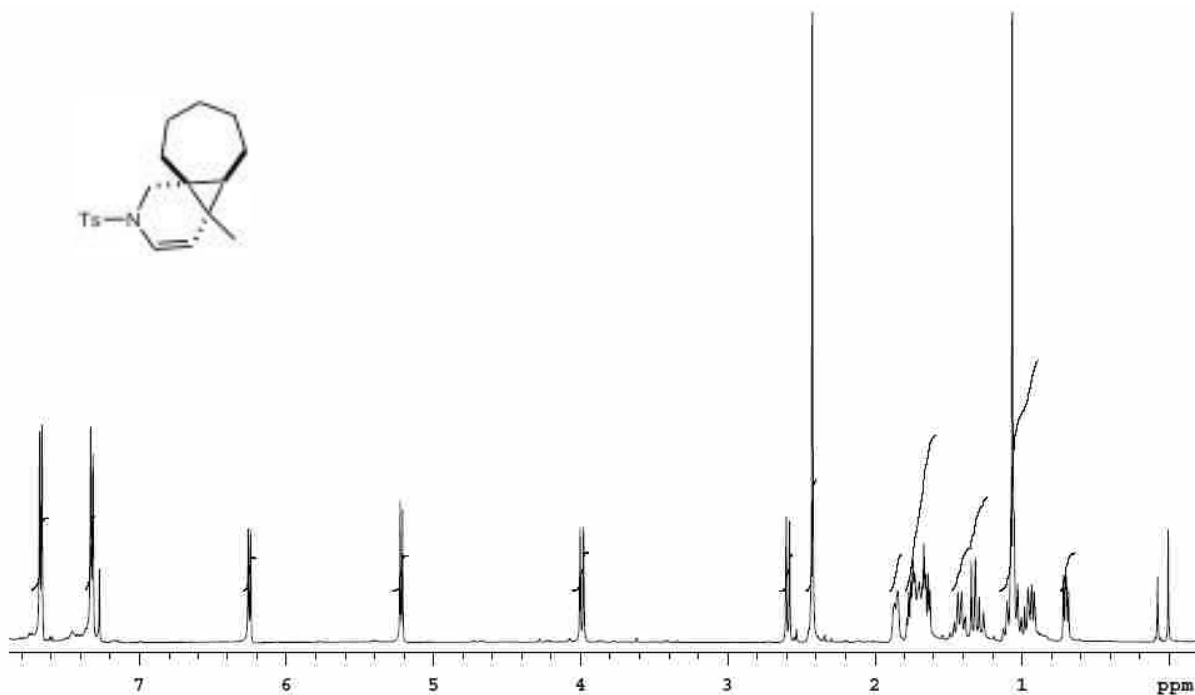
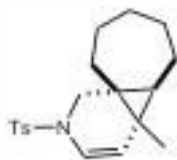


Figure S5. ³¹P NMR mixture of *t*BuNHPPH₂ (**6**) and Pt(cod)Cl₂ after 24 h reaction time (in CDCl₃).



(4aR,4bS,9aR)-4a-methyl-2-tosyl-2,4a,4b,5,6,7,8,9-octahydro-1H-cyclohepta[1,3]cyclopropa[1,2-c]pyridine(2e):



(4aR,4bS,9aR)-4a-phenyl-2-tosyl-2,4a,4b,5,6,7,8,9-octahydro-1H- cyclohepta[1,3]cyclopropa[1,2-c]pyridine(2f):

